International Atomic Energy Agency

INDC(NDS)-342
Distr. FE+G

INDC INTERNATIONAL NUCLEAR DATA COMMITTEE

ACTIVATION CROSS SECTIONS FOR THE GENERATION OF LONG-LIVED RADIONUCLIDES OF IMPORTANCE IN FUSION REACTOR TECHNOLOGY

Texts of Papers presented at the Third and Final Research Coordination Meeting
organized by the International Atomic Energy Agency
in co-operation with the V.G. Khlopin Radium Institute,
St. Petersburg, Russia and held in St. Petersburg
from 19 - 23 June 1995

Compiled by A.B. Pashchenko
IAEA Nuclear Data Section
Vienna, Austria

February 1996

IAEA NUCLEAR DATA SECTION, WAGRAMERSTRASSE 5, A-1400 VIENNA

Reproduced by the IAEA in Austria
February 1996

INDC(NDS)-342
Distr. FE+G

ACTIVATION CROSS SECTIONS FOR THE GENERATION OF LONG-LIVED RADIONUCLIDES OF IMPORTANCE IN FUSION REACTOR TECHNOLOGY

Texts of Papers presented at the Third and Final Research Coordination Meeting
organized by the International Atomic Energy Agency
in co-operation with the V.G. Khlopin Radium Institute,
St. Petersburg, Russia and held in St. Petersburg
from 19 - 23 June 1995

Compiled by A.B. Pashchenko
IAEA Nuclear Data Section
Vienna, Austria

Abstract

The present report contains scientific and technical papers presented at the Third and Final IAEA Research Co-ordination Meeting (RCM) on "Activation Cross Sections for the Generation of Long-lived Radionuclides of Importance in Fusion Reactor Technology" which was hosted by the V.G. Khlopin Radium Institute and held in St. Petersburg, Russia, from 19-23 June 1995. The papers, collected in the report, contain results of measurements, model calculations and evaluations of cross sections for 16 activation reactions of special importance to fusion reactor technology leading to long-lived radionuclides.

February 1996

Contents

FOREWORD

The present report contains scientific and technical papers presented at the Third and Final IAEA Research Co-ordination Meeting (RCM) on "Activation Cross Sections for the Generation of Long-lived Radionuclides of Importance in Fusion Reactor Technology" which was hosted by the V.G. Khlopin Radium Institute and held in St. Petersburg, Russia, from 19-23 June 1995. For a summary report of the meeting containing the technical conclusions and recommendations for specific CRP reactions and the full text of the meeting conclusions and recommendations, agenda and the list of participants see the report INDC(NDS)-340.

Activation of reactor materials due to the neutron field generated by the 14 MeV deuterium-tritium neutrons is a principal issue concerning the development of fusion as a long-term energy source. It will impact the development of reactor technologies relevant to safety, maintenance, and waste disposal. Availability and quality of key activation data are very important for the assessment of solutions to the various activation concerns. Considering the current needs and original requests of the fusion community to meet the design requirement the IAEA formed a Co-ordinated Research Program (CRP) entitled "Activation Cross Sections for the Generation of Long-lived Radionuclides of Importance in Fusion Reactor Technology" with the purpose to obtain reliable information (experimental and evaluated) for 16 long-lived activation reactions of special importance to fusion reactor technology and succeeded in obtaining the participants of 18 laboratories from nine member countries in this very specific task.

The first Research Co-ordination Meeting (RCM) was held in Vienna in November 1991. In April 1993, the second RCM took place in Del Mar, California.

The purpose of this meeting was to report, discuss and evaluate the results of the research carried out by each participating laboratory under this CRP, to review the status of cross sections for 16 activation reactions of special importance to fusion reactor technology leading to long-lived radionuclides and to prepare the Final Report summarizing the results of the CRP to the IAEA.

At the two previous CRP meetings most of the discussion was centered on preliminary values. The most important task of each participant in the St. Petersburg RCM was to provide final values of all the results from measurements and model calculations and prepare the contribution to the Final Report. The texts and final results are being reproduced here directly from the authors' manuscripts with little or no editing, in order in which the presentations were made at the meeting. The Final Report of participants summarizing the results of the CRP to the IAEA will be published separately as INDC(NDS)-344.

Vienna, February 1996 Anatoly Pashchenko

NEUTRON ACTIVATION CROSS SECTIONS FOR COPPER, EUROPIUM, HAFNIUM, IRON, NICKEL, SILVER, TERBIUM AND TITANIUM FROM THE ARGONNE, LOS ALAMOS AND JAERI COLLABORATION *)

J.W. Meadows, D.L. Smith and L.R. Greenwood [a]
Argonne National Laboratory
Argonne, Illinois 60439, USA

R.C. Haight
Los Alamos National Laboratory
Los Alamos, New Mexico 87545, USA

Y. Ikeda and C. Konno
Japan Atomic Energy Research Institute
Tokai-mura, Naka-gun, Ibaraki-ken 319-11, Japan

ABSTRACT

Several fast-neutron activation reactions for copper, europium, hafnium, iron, nickel, silver, terbium and titanium that are important to fusion energy have been investigated in three distinct neutron fields generated by accelerators at Argonne National Laboratory and Los Alamos National Laboratory, USA, and Japan Atomic Energy Research Institute, Tokai, Japan. Final differential cross-sections at 14.7 MeV and integral cross sections for the Be(d,n) thick-target spectrum produced by 7-MeV deuterons are reported here. Data have also been acquired for neutron energies near 10 MeV. However, these latter results will be made available after problems associated with determining the neutron-energy scale and interpreting the quasi-differential cross-sections measured near threshold are resolved.

[a] Present address: Battelle Pacific Northwest Laboratories, Richland, Washington 99352, USA.

*) The complete results from this project are given in the official final report "Measurement of Fast-Neutron Activation Cross Sections for Copper, Europium, Hafnium, Iron, Nickel, Silver, Terbium and Titanium at 10.0 and 14.7 MeV and for the Be(d,n) Thick-Target Spectrum" which was accepted for publication by Annals of Nuclear Energy.

INTRODUCTION

The motivation for undertaking an IAEA Coordinated Research Program (CRP) on "Activation Cross Sections for the Generation of Long-lived Radionuclides of Importance in Fusion Reactor Technology", and the conduct of this extensive international project, are discussed in two conference papers [Von92, SP94]. Argonne National Laboratory (ANL) and Los Alamos National Laboratory (LANL), USA, and Japan Atomic Energy Research Institute (JAERI), Tokai, Japan, joined in a collaboration to examine several neutron-induced reactions under the auspices of this CRP. Progress in this particular collaboration has been reported in three earlier reports [Mea+90, Mea+92, Mea+93]. The purpose of the present report is to provide final cross-section results relevant to those aspects of this work which are considered to be complete, namely, the differential measurements at 14.7-MeV (irradiations at JAERI) and the integral measurements in the Be(d,n) thick-target spectrum produced by 7-MeV deuterons (irradiations at ANL). Data have also been obtained for neutron energies near 10 MeV (irradiations at LANL). However, it has been discovered quite recently that interpretation of these latter results for some of the examined reactions is very sensitive to determination of the energy scale and to detailed definition of the quasi-monoenergetic spectrum from the LANL H(t,n) neutron source reaction. The reason is that for these reactions the incident-neutron energies are rather close to threshold where the differential cross sections vary rapidly and non-linearly with energy.

EXPERIMENTAL PROCEDURE AND DATA ANALYSIS

The experimental procedures and data analysis methods used in this work have been described in the earlier progress reports mentioned above. There have been no fundamental changes in the approach used in analyzing these experimental data. However, much of the preliminary numerical information which appeared in these earlier documents had to be revised due to minor changes in radioactive decay parameters and to recent modifications of the data correction procedures. References to other literature pertinent to this experimental work (e.g., radioactive decay parameters, Q-values, etc.) also appear in the earlier documents so they need not be repeated here. Finally, it is intended to prepare complete documentation of the ANL/LANL/JAERI collaborative project, including all relevant numerical information and comparisons with other work, in the form of a refereed journal article which should be available for publication during late 1995 [Mea+95].

EXPERIMENTAL RESULTS

The tabular information presented here supplants all earlier results appearing in the above-mentioned progress reports from the ANL/LANL/JAERI collaboration. Table 1 lists the reactions which have been examined and Table 2 summarizes the relevant radioactive decay data. The $^{58}Ni(n,p)^{58g,m}Co$ reaction served as a primary reference standard while the $^{93}Nb(n,n')^{92m}Nb$ reaction served as a secondary standard only for the irradiation and data analysis carried out at JAERI. All the measurements utilized elemental samples so the activation cross-section results must be interpreted

accordingly. The integral cross sections obtained from the Be(d,n) spectrum measurements appear in Table 3. The corresponding total errors are reproduced from Table 4 where the various partial error components are exhibited explicitly. Various representations for the Be(d,n) spectrum that are required to interpret these cross-section results are discussed by Meadows et al. [Mea+94]. The 14.7-MeV differential cross sections obtained from the parallel ANL/JAERI measurements and analyses appear in Table 5. The corresponding total errors come from Tables 6 and 7. These tables also show the various partial errors components for these measurements. Not all of the reactions considered are represented in each category of measurements. As discussed in previous progress reports, this is due to the influence of various experimental conditions such as insufficient neutron fluence or interfering (n,γ) reactions. A complete description of these issues will appear in the forthcoming journal article mentioned above.

SUMMARY

The ANL/LANL/JAERI collaboration has provided cross-section results in three distinct neutron fields for several reactions of interest to the CRP. The final values from measurements in two of these irradiation environments (ANL and JAERI) are reported here for consideration during the third coordination meeting of the CRP at St. Petersburg, Russia, June 1995. Results from the LANL measurements will be available later when the above-mentioned problems are resolved and proper interpretation of these data is assured.

ACKNOWLEDGEMENTS

This work has been sponsored in part by the U.S. Department of Energy, Energy Research Programs (Contracts W-31-109-Eng-38 and W-7405-Eng-36) and the International Atomic Energy Agency, Vienna (Research Agreements 5064/CF and 7908/CF). The skilled technical services of the support personnel at the ANL, LANL and JAERI accelerator laboratories during the sample irradiations are appreciated.

REFERENCES

Mea+90 J.W. Meadows, D.L. Smith, L.R. Greenwood, R.C. Haight, Y. Ikeda and C. Konno, "A Search for Long-lived Radionuclides Produced by Fast-neutron Irradiations of Copper, Silver, Europium, Terbium and Hafnium", Proceedings of an IAEA Consultants' Meeting Held at Argonne National Laboratory, Argonne, Illinois, USA, 11-12 September 1989, ed. Wang DaHai, Report INDC(NDS)-232, International Atomic Energy Agency, Vienna, 1990, p. 79.

Mea+92 J.W. Meadows, D.L. Smith, L.R. Greenwood, R.C. Haight, Y. Ikeda and C. Konno, "Measured Fast-neutron Activation Cross Sections of Ag, Cu, Eu, Fe, Hf, Ni, Tb and Ti at 10.3 and 14.8 MeV and for the Continuum Neutron Spectrum Produced by 7-MeV Deuterons on a Thick Be-metal Target", First Meeting of a Co-ordinated Research Programme Organized by the IAEA and Held in Vienna, 11-12 November 1991, ed. Wang DaHai, Report INDC(NDS)-263, International Atomic Energy Agency, Vienna, 1992, p. 53.

Mea+93 J. Meadows, D. Smith, L. Greenwood, R. Haight, Y. Ikeda and C. Konno, "Results from the Argonne, Los Alamos, JAERI Collaboration", Second Research Co-ordination Meeting Organized by the International Atomic Energy Agency, Del Mar, California, USA, 29-30 April 1993, ed. A.B. Pashchenko, Report INDC (NDS)-286, International Atomic Energy Agency, Vienna, 1993, p. 13.

Mea+94 J.W. Meadows, D.L. Smith, L.R. Greenwood, D.W. Kneff and B.M. Oliver, *Annals of Nuclear Energy* 21, No. 3, 1994, p. 155.

Mea+95 To be published.

SP94 D.L. Smith and A.B. Pashchenko, "Investigation of the Generation of Several Long-lived Radionuclides of Importance in Fusion Reactor Technology: Report on a Coordinated Research Program Sponsored by the International Atomic Energy Agency", *Proceedings of an International Conference on Nuclear Data for Science and Technology*, Gatlinburg, Tennessee, ed. J.K. Dickens, American Nuclear Society, LaGrange Park, Illinois, 1994, p. 859.

Von92 H. Vonach, "Report on the IAEA Coordinated Research Program On Activation Cross Sections for the Generation of Long-lived Activities of Importance in Fusion Reactor Technology", *Proceedings of an International Conference on Nuclear Data for Science and Technology*, ed. S.M. Qaim, Springer-Verlag, Berlin, 1992, p. 279.

Table 1: Reactions involved in the present investigation

Reaction	Target Isotope Abundance (%)	Q-Value (MeV)
$^{46}Ti(n,p)^{46g+m}Sc$	8.0±0.1	-1.585,-1.728
$^{47}Ti(n,n'p)^{46g+m}Sc$	7.3±0.1	-10.462,-10.605
$^{54}Fe(n,p)^{54}Mn$	5.9±0.2	0.085
$^{54}Fe(n,\alpha)^{51}Cr$	5.9±0.2	0.844
$^{58}Ni(n,p)^{58g+m}Co$	68.077±0.005	0.401,0.376
$^{60}Ni(n,p)^{60g+m}Co$	26.223±0.005	-2.042,-2.101
$^{61}Ni(n,n'p)^{60g+m}Co$	1.140±0.001	-9.862,-9.921
$^{63}Cu(n,\alpha)^{60g+m}Co$	69.17±0.02	1.715,1.656
$^{93}Nb(n,2n)^{92m}Nb$	100	-8.966
$^{107}Ag(n,2n)^{106m}Ag$	51.839±0.005	-9.627
$^{109}Ag(n,2n)^{108m}Ag$	48.161±0.005	-9.296
$^{151}Eu(n,2n)^{150g}Eu$	47.8±0.5	-7.934
$^{159}Tb(n,2n)^{158g+m}Tb$	100	-8.133,-8.243
$^{176}Hf(n,2n)^{175}Hf$	5.206±0.004	-8.165
$^{179}Hf(n,2n)^{178m2}Hf$	13.629±0.005	-8.546
$^{178}Hf(n,n')^{178m2}Hf$	27.297±0.003	-2.446
$^{180}Hf(n,2n)^{179m2}Hf$	35.100±0.006	-8.493
$^{179}Hf(n,n')^{179m2}Hf$	13.629±0.005	-1.106

Table 2: Decay properties of the radioactive nuclei involved in the present investigation

Activity	Half Life[a]	Decay Mode	Measured γ Ray (MeV)	Relevant γ-ray Branch (%)
^{46g}Sc	83.810±0.010 d	β^-	0.889	99.984±0.001
^{46m}Sc	18.75±0.04 s	IT	NA[b]	NA
^{51}Cr	27.702±0.004 d	EC,(β^+)	0.320	10.08±0.23
^{54}Mn	312.12±0.10 d	EC,(β^+)	0.835	99.976±0.001
^{58g}Co	70.82±0.03 d	EC, β^+	0.811	99.448±0.008
^{58m}Co	9.15±0.10 h	IT	NA	NA
^{60g}Co	5.2714±0.0005 y	β^-	1.333	99.982±0.001
^{60m}Co	10.47±0.04 m	IT,(β^-)	NA	NA
^{92m}Nb	10.15±0.02 d	EC,(β^+)	0.934	99.07±0.04
^{106m}Ag	8.46±0.10 d	EC,(β^+)	0.512	87.7±2.7
^{108m}Ag	418±15 y	EC,IT	0.434	90.5±0.6
^{150g}Eu	35.8±1.0 y	EC,(β^+)	0.334	96±3
^{158}Tb	180±11 y	EC, β^+,β^-	0.944	43.9±1.3
^{158m}Tb	10.5±0.2 s	IT	NA	NA
^{175}Hf	70±2 d	EC	0.343	84.0±0.3
$^{178m2}Hf$	31±1 y	IT	0.325	94.11±0.17
$^{179m2}Hf$	25.1±0.3 d	IT	0.454	68.6±3.6

[a] s (second), m (minute), h (hour), d (day), y (year).
[b] Not applicable.

Table 3: Experimental integral cross sections obtained from the present investigation for the Be(d,n) neutron spectrum

Reaction	Integral Cross Section (millibarns) [a]
$^{46}Ti(n,p)^{46g+m}Sc$	36.3 (±6.6%)
$^{54}Fe(n,p)^{54}Mn$	174 (±7.4%)
$^{54}Fe(n,\alpha)^{51}Cr$	3.52 (±7.9%)
$^{63}Cu(n,\alpha)^{60g+m}Co$	2.11 (±6.9%)
$^{107}Ag(n,2n)^{106m}Ag$	1.01 (±12.9%)
$^{151}Eu(n,2n)^{150g}Eu$	14.8 (±9.3%)
$^{159}Tb(n,2n)^{158g+m}Tb$	27.5 (±12.1%)
$^{176}Hf(n,2n)^{175}Hf$	39.4 (±9.5%)
$^{180}Hf(n,2n)^{179m2}Hf$ + $^{179}Hf(n,n')^{179m2}Hf$	3.08 (±9.9%)

[a] Absolute cross sections based on reference value of 231±14 millibarns for the $^{58}Ni(n,p)^{58g+m}Co$ standard reaction in the Be(d,n) neutron spectrum [Mea+94]. Errors obtained from Table 4.

Table 4: Error sources for the Be(d,n)-spectrum neutron cross-section measurements

Reaction	Estimated Error Component (%) γ-ray Meas.[a]	Half Life	γ-ray Brnch.	Activ. Decay	NSA[b]	Neut. Scat.[c]	Isot. Abun.	(n,γ)[d]	Total Error[e]
^{46}Ti(n,p)$^{46g+m}$Sc	2.1	Neg[f]	Neg	0.1	0.7	0.6	1.3	NA[g]	6.6
^{54}Fe(n,p)^{54}Mn	2.0	Neg	Neg	0.5	Neg	1.2	3.4	Neg	7.4
^{54}Fe(n,α)^{51}Cr	2.5	Neg	Neg	1.4	2.3	0.3	3.4	NA	7.9
^{63}Cu(n,α)$^{60g+m}$Co	2.2	Neg	Neg	0.1	2.3	0.3	Neg	NA	6.9
^{107}Ag(n,2n)^{106m}Ag	2.3	0.1	3.0	4.2	9.8	0.7	Neg	NA	12.9
^{151}Eu(n,2n)^{150g}Eu	4.0	2.8	3.1	Neg	3.9	0.4	1.0	NA	9.3
^{159}Tb(n,2n)$^{158g+m}$Tb	6.8	6.1	3.0	Neg	4.0	0.4	Neg	NA	12.1
^{176}Hf(n,2n)^{175}Hf	2.1	2.9	0.4	Neg	5.3	0.3	Neg	3.4	9.5
^{180}Hf(n,2n)^{179m2}Hf + ^{179}Hf(n,n')^{179m2}Hf	5.5	1.2	5.2	1.0	1.2	0.3	Neg	Neg	9.9

[a] Includes errors due to statistics, detector efficiency and sum-coincidence effects.
[b] Combined error for geometric effects and neutron-source anisotropy.
[c] Includes errors due to perturbation of primary neutron spectrum by scattering and absorption.
[d] Uncertainty in the estimated correction for neutron-capture activation.
[e] Includes an error of 6.1% due to use of the ^{58}Ni(n,p)$^{58g+m}$Co standard for determining neutron fluence.
[f] Negligible (< 0.1%).
[g] Not applicable.

Table 5: Experimental differential cross sections at 14.7 MeV obtained from the present investigation

Reaction	Cross Section (millibarns) [a] ANL [b]	JAERI [c]	Ratio (JAERI/ANL)
$^{46}Ti(n,p)^{46g+m}Sc$ + $^{47}Ti(n,n'p)^{46g+m}Sc$	306 (±5.5%)	311 (±7.5%)	1.02
$^{54}Fe(n,p)^{54}Mn$	280 (±6.4%)	288 (±7.0%)	1.03
$^{54}Fe(n,\alpha)^{51}Cr$	87.9 (±6.5%)	ND [d]	ND
$^{60}Ni(n,p)^{60g+m}Co$	ND	137 (±5.5%)	ND
$^{63}Cu(n,\alpha)^{60g+m}Co$	41.6 (±5.4%)	40.2 (±5.5%)	0.97
$^{109}Ag(n,2n)^{108m}Ag$	628 (±6.7%)	682 (±7.2%)	1.09
$^{151}Eu(n,2n)^{150g}Eu$	1214 (±7.7%)	1258 (±6.9%)	1.04
$^{159}Tb(n,2n)^{158g+m}Tb$	1981 (±9.3%)	2072 (±8.6%)	1.05
$^{176}Hf(n,2n)^{175}Hf$	1915 (±7.0%)	2057 (±6.2%)	1.07
$^{179}Hf(n,2n)^{178m2}Hf$ + $^{178}Hf(n,n')^{178m2}Hf$	ND	7.2 (±9.0%)	ND
$^{180}Hf(n,2n)^{179m2}Hf$ + $^{179}Hf(n,n')^{179m2}Hf$	21.8 (±8.6%)	ND	ND

[a] Absolute cross sections are based on 292±14 millibarns for the $^{58}Ni(n,p)^{58g+m}Co$ standard cross section at 14.7-MeV.
[b] JAERI irradiation. Sample counts and analysis conducted at ANL. Errors obtained from Table 6.
[c] JAERI irradiation. Sample counts and analysis conducted at JAERI. Errors obtained from Table 7.
[d] Not determined in the present investigation.

Table 6: Error sources for the 14.7-MeV neutron cross-section measurements (ANL set)

Reaction	Estimated Error Component (%) γ-ray Meas.[a]	Half Life	γ-ray Brnch.	Activ. Decay	Geom.	Neut. Scat.[b]	Isot. Abun.	(n,γ)[c]	Total Error[d]
$^{46}Ti(n,p)^{46g+m}Sc$ + $^{47}Ti(n,n'p)^{46g+m}Sc$	2.1	Neg[e]	Neg	0.3	0.2	0.7	1.3	NA[f]	5.5
$^{54}Fe(n,p)^{54}Mn$	2.2	Neg	Neg	0.2	0.1	0.4	3.4	NA	6.4
$^{54}Fe(n,\alpha)^{51}Cr$	2.5	Neg	Neg	0.2	0.1	0.2	3.4	NA	6.5
$^{63}Cu(n,\alpha)^{60g+m}Co$	2.2	Neg	Neg	0.2	0.1	0.4	Neg	NA	5.4
$^{109}Ag(n,2n)^{108m}Ag$	2.2	3.6	0.7	0.3	1.3	0.4	Neg	0.7	6.7
$^{151}Eu(n,2n)^{150g}Eu$	2.1	2.8	3.1	0.2	3.4	0.7	1.0	NA	7.7
$^{159}Tb(n,2n)^{158g+m}Tb$	2.1	6.1	3.0	0.2	3.4	0.5	Neg	NA	9.3
$^{176}Hf(n,2n)^{175}Hf$	2.1	2.9	0.4	0.6	3.4	0.3	Neg	0.1	7.0
$^{180}Hf(n,2n)^{179m2}Hf$ + $^{179}Hf(n,n')^{179m2}Hf$	3.1	1.2	5.2	0.5	3.4	0.3	Neg	Neg	8.6

[a] Includes errors due to statistics, detector efficiency and sum-coincidence effects.
[b] Includes errors due to perturbation of primary neutron spectrum by scattering and absorption.
[c] Uncertainty in the estimated correction for neutron-capture activation.
[d] Includes an error of 4.9 % due to use of the $^{58}Ni(n,p)^{58g+m}Co$ standard for determining neutron fluence.
[e] Negligible (< 0.1%).
[f] Not applicable.

Table 7: Error sources for the 14.7-MeV neutron cross-section measurements (JAERI set)

Reaction	Estimated Error Component (%) γ-ray Meas.[a]	Half Life	γ-ray Brnch.	Neut. Scat.[b]	Isot. Abun.	Total Error[c]
$^{46}Ti(n,p)^{46g+m}Sc$ + $^{47}Ti(n,n'p)^{46g+m}Sc$	5.5	Neg[d]	Neg	1.0	1.3	7.5
$^{54}Fe(n,p)^{54}Mn$	2.1	Neg	Neg	3.0[e]	3.4	7.0
$^{60}Ni(n,p)^{60g+m}Co$	2.3	Neg	Neg	1.0	Neg	5.5
$^{63}Cu(n,\alpha)^{60g+m}Co$	2.3	Neg	Neg	1.0	Neg	5.5
$^{109}Ag(n,2n)^{108m}Ag$	3.7	3.6	0.7	Neg	Neg	7.2
$^{151}Eu(n,2n)^{150g}Eu$	2.3	2.8	3.1	Neg	1.0	6.9
$^{159}Tb(n,2n)^{158g+m}Tb$	2.0	6.1	3.0	Neg	Neg	8.6
$^{176}Hf(n,2n)^{175}Hf$	2.4	2.9	0.4	Neg	Neg	6.2
$^{179}Hf(n,2n)^{178m2}Hf$ + $^{178}Hf(n,n')^{178m2}Hf$	6.8	3.2	0.2	Neg	Neg	9.0

[a] Includes errors due to statistics, detector efficiency and sum-coincidence effects.

[b] Includes errors due to perturbation of primary neutron spectrum by scattering and absorption. In the JAERI analysis this is referred to as the correction for low-energy neutrons.

[c] Includes an error of 4.9 % due to use of the $^{58}Ni(n,p)^{58g+m}Co$ standard for determining neutron fluence.

[d] Negligible (< 0.1%).

[e] Error component was not explicitly determined in this work. However, an estimate of 3.0% error is provided to be consistent with the error previously deduced at JAERI for the calculated correction to the $^{58}Ni(n,p)^{58g+m}Co$ reaction yield. These two reactions have similar low thresholds and corresponding sensitivities to low-energy neutrons.

XA9642391

SUMMARY OF ACTIVATION CROSS SECTION MEASUREMENTS AT FNS

Y. Ikeda, C. Konno, A. Kumar* and Y. Kasugai

Japan Atomic Energy Research Institute
Tokai-mura, Ibaraki-ken 319-11 Japan
* University of California, Los Angeles
Los Angeles, CA 90024-1597 U. S. A.

Presented at
Third IAEA-RCM on "Activation Cross sections for the Generation of Long-Lived radionuclides of Importance in Fusion Reactor Technology"

St. Petersburg, Russia,
19-23 June, 1995

Abstract: Neutron activation cross sections around 14 MeV for seventeen reactions have been measured at the FNS facility in JAERI in order to provide experimental data meeting the requirement in the radioactive wastes disposal assessment in the D-T fusion reactor. This report summarize contributing data measured in several phases of experiments to the IAEA-CRP on "Activation Cross sections for the Generation of Long-Lived radionuclides of Importance in Fusion Reactor Technology".

Introduction

Cross sections for the long-lived radioactivity production in structural materials with 14 MeV neutrons are of key importance from the waste management point of view in the D-T fusion reactor development. An endeavor of experimental measurement for long-lived activation cross sections was initiated in an IAEA-CRP[1-3] to respond to the nuclear data requirement, and significant efforts have been devoted to experimental measurements, theoretical predictions and evaluations. However, still there is need to measure more systematic data from the fusion reactor application point of view. In this context, experimental measurements of activation cross sections for reactions of concern at 14 MeV have been conducted at Fusion Neutronics Source (FNS) facility [4] at Japan Atomic Energy Research Institute (JAERI) since 1989. The major objective was to provide experimental data for verifying systematically the induced radioactivity calculation codes and activation cross section data libraries currently available[4-6]. This report summarize the experiments at FNS and gives results for seventeen reactions cross sections around 14 MeV.

Experiment

Decay data were taken from the Table of Radioisotopes.[5] The long-lived radioactivities with half-lives from 5 to more than 10^6 years were studied in this experiment. Only the radioactivities associated with γ-ray emissions were dealt as the objects.

(a) 1989 Irradiation

Samples of Al, ^{61}Ni, Cu, Nb, Mo, Ag, ^{151}Eu, ^{153}Eu, Tb, Dy, Hf, W, Re, and Bi were irradiated with D-T neutrons for 4 days (8 hours irradiation per day), which were generated at FNS [4] by bombarding ^{3}T target with 350 keV deuterium (d^+) beam. It

resulted in 1.7 x 10^{17} neutrons of total neutron yield at the target. Four sets of foil packages were placed at angles of 0°, 45°, 90° and 135° with respect to the incident d^+ beam, the distances of which were about 50 mm from the D-T source. This configuration was assumed to provide cross section data in the energy range from 13.5 to 15.0 MeV. Since the stacked sample package was considerably thick and significant neutron flux depression was expected in the sample, multiple thin Nb foils were inserted between samples for the neutron flux monitor. Neutron flux at each sample was determined with the $^{93}Nb(n,2n)^{92m}Nb$ reaction rate. The neutron fluence at the samples was estimated to be 0.8 -2.0 x $10^{15}/cm^2$.

More than 1.7 year after γ-ray counting was started using a high detection efficiency Ge detector (115% relative to 3" x 3" NaI(Tl)). Gamma-ray spectrum was analyzed by a GENIE system provided by CANBERRA. The detector efficiency was calibrated by several standard γ-ray sources, the uncertainty of which was estimated to be about 3%.

(b) 1992 Irradiation

In response to the further data need in the summary document of the first RCM [2] in November 1991, cross sections for $^{94}Mo(n,p)^{94}Nb$ and $^{95}Mo(n,np)^{94}Nb$, $^{158}Dy(n,p)^{158}Tb$, $^{182}W(n,n'\alpha)^{178m2}Hf$ and $^{187}Re(n,2n)^{186m}Re$ reactions at 14 MeV energy region have been measured by performing a new irradiation experiment in 1991 using enriched isotopes or re-counting of samples which were irradiated in 1989. Although the summary document gave a status for $^{94}Mo(n,p)^{94}Nb$ as adequate and no more data required, contribution of $^{95}Mo(n,np)$ reaction for ^{94}Nb production is of important and no experimental data has been reported so far. In the present measurement aimed at discriminating contributions from both reactions of $^{94}Mo(n,p)^{94}Nb$ and $^{95}Mo(n,np)^{94}Nb$ by using isotopic enriched samples. For the measurement of the $^{182}W(n,n'\alpha)^{178m2}Hf$ reaction, an enriched sample was also used because of low activity yield, the cross section of which was expected to be less than several tens micro barn according to the previous investigation.[2] For the reaction of $^{158}Dy(n,p)^{158}Tb$ and $^{187}Re(n,2n)^{186m}Re$, we have tried to determine the cross sections by counting the samples irradiated in 1989, putting longer cooling time. The longer cooling time more than 3.5 year enabled us to count γ-ray lines from ^{158}Tb decay in the Dy sample sufficiently. The new measurement, however, gave unreasonably large cross section value of more than 500 mb. Possible source of this extremely dubious data was investigated. On the other hand, we found that additional cooling time of 2 to 3 years is still needed for activity measurement of ^{186m}Re in order to reduce interfering radioactivity in the Re sample.

The neutron source of FNS and irradiation configuration in 1989 were described somewhere in detail.[2] The new irradiation in 1991 lasted for 288,000 seconds with total D-T neutron yield of 2.74 x 10^{17} at the target. The Mo samples were placed at 10° and 90° with respect to incident d+ beam direction. The ^{182}W sample was placed at 10°. The neutron flux was monitored by using the $^{93}Nb(n,2n)^{92m}Nb$ reaction with 459 ± 10 mb at 14 MeV region.

(c) 1993 Irradiation

Activation cross sections for the reaction of $^{187}Re(n,2n)^{186m}Re$ [$T_{1/2}$=2.0 x 10^5 y] at 14.9 MeV . and for the reaction of $^{193}Ir(n,2n)^{192m2}Ir$ [$T_{1/2}$=241 y] at 14.9 MeV, were measured by using FNS facility .Commonly for both reaction products, there is strong interfering radioactivities with medium long half-lives. Still after one to two years cooling time, considerably large amounts of γ-rays gives a high background for low energy photon detection. As a framework of activation cross section around 14 MeV at FNS, the cross sections of those reactions were measured to provide the experimental data to meet the initial purpose of the fusion reactor requirement.

As reported previously in the IAEA-CRP meeting [2], these cross sections are of significant difficult to measure due to inherent low decay rates with low energy γ-rays to be detected, and existence of large interference activities. As regard to the importance of

data for fusion applications, efforts have been placed on the reduction of background to emerge weak γ-ray lines incorporated with a Compton suppression γ-ray spectrometer. This paper described the recent results for the activation cross sections of to reactions of concern in the long-lived radioactive nuclides production.

The samples of Re with natural abundance and ^{193}Ir with 98 % enrichment were irradiated with 14 MeV neutrons at FNS facility for 32 h and 40 h, respectively. Neutron fluxes at these samples were derived from the activation rate of monitor reaction, ^{93}Nb(n,2n)^{92m}Nb.

The Compton suppression spectrometer consisting with 11" x 11" NaI(Tl) suppresser and a Ge detector. This detector configuration enabled significant reduction of background in the low energy region of interest. The ordinary first-slow coincidence technique was adopted. The effective suppression ration in the Compton scattering component was around 5 to 8. It was found that for the γ-ray sources with higher energy, the suppression ration increased very much. This was due to the detector arrangement with suppresser covering backward of the main Ge detector. There was, as a result, remarkable suppression of background for the low energy region.

The activities of interest were so weak that the sample had to be placed in the close vicinity of the Ge detector to increase the detector efficiency. Since each radioactivity of interest emits low energetic single γ-rays, there was no need to correct the summing counting loss. However, detector efficiency calibration was essential. For this purpose, several radioactivities, ^{47}Sc, ^{57}Co and ^{99}Mo, which emit low energy g-rays associating with no cascade γ-rays, were prepared by irradiating samples of Ti, Co, Mo. By using these γ-ray sources, the detector efficiency for 120~160 keV was determined.

After 3.7 year and 1.5 year cooling times for Re and Ir samples, respectively, activities were measured with the Compton suppression spectrometer.

The cross sections were derived by using measured decay γ-ray counts, neutron flux and other necessary correction factors. As noticed, the largest experimental error was due to γ-ray counting statistics, being ± 35 %.

1994 Irradiation

One of most interesting reactions are the ^{179}Hf(n,2n)^{178m2}Hf from the model calculation point of view because of high spin state of 16^+ for ^{178m2}Hf. So far, several experimental data were presented and they seemed reasonably consistent each other. There are three reaction channels for ^{178m2}Hf production in Hf, i.e., ^{179}Hf(n,2n), ^{178}Hf(n,n') and ^{177}Hf(n,γ). However, as the data were given as the production cross section in Hf assuming all ^{178m2}Hf are products of the ^{179}Hf(n,2n)^{178m2}Hf reaction. In this irradiation, the enriched isotopes of ^{179}Hf and ^{178}Hf were used to identify the contributions of different reactions. Unfortunately, ^{177}Hf sample was not available, so still there was uncertainty in estimating the ^{177}Hf(n,γ) reaction contribution.

Two set of samples of ^{178}Hf and ^{179}Hf were placed at 0^o and 90^o angles with respect to the incident d^+ beam of FNS. Neutron flux of each sample was determined by the same manner with the ^{93}Nb(n,2n)^{92m}Nb reaction rates. The total neutron fluences were in a range from 4.9 to 7.5 times 10^{15}/cm^2.

Results

The reaction rates of concerned radioisotopes were derived from γ-ray peak counts with necessary corrections, i. e. decay constant, cooling time, collection time, detector efficiency, natural abundance of the target material, γ-ray branching ratio, sample weight, self-absorption of γ-ray, neutron flux fluctuation during irradiation, and so forth.

The cross sections were obtained from the reaction rates divided by neutron flux determined by using a cross section value of 459 mb for ^{93}Nb(n,2n)^{92m}Nb reaction

around 14 MeV. In **Table 1**, experimental data are summarized along with data available in the literature and IAEA-CRP.

^{27}Al(n,2n)^{26}Al

The present data were close to the data reported by Iwasaki [6] and slightly higher than data reported by Sasao [7]. The data in Ref. [9] of ECN evaluation at 14.5 MeV seems lower than other experimental data.

^{61}Ni(n,np)$^{60m+g}$Co

Present measurement gave considerably larger cross sections than data in JENDL-3 [8]. However, from the reaction systematics, our data seemed reasonable.

^{63}Cu(n,α)$^{60m+g}$Co

For the common reaction, many data have been reported. The present data were in a good agreement with the recent measurement by Greenwood [10].

^{93}Nb(n,n')^{93m}Nb

Due to the low threshold energy below 0.1 MeV, a precise evaluation of the reaction cross section has been required. The present measurement is in excellent agreement with a recent evaluation by Odano [11], but is slightly larger than the data by Ryves [12], which were so far the only available experimental data in the 14 MeV region.

^{94}Mo(n,p)^{94}Nb

The contributions of the ^{95}Mo(n,np)^{94}Nb reaction to the ^{94}Nb productions were subtracted even though the enriched isotopes were used. Insufficient γ-ray counting statistics dominated experimental errors for each measurement. This was due to the use of small amounts of samples being about 50 to 60 mg. The uncertainty of half-live (± 6.1 %) was the secondly large error contributor. The present data are in good agreement within experimental errors with data previously reported [13] as shown in **Table 1**. The data measured at FNS are used as the cross sections for ^{95,96,97,98}Mo. The systematic trend support the adequacy of presently measured cross section values. As noted in the last summary document of the RCM, it is confirmed that there is no urgent need for this cross section at 14 MeV.

^{95}Mo(n,np)^{94}Nb

The contributions of ^{94}Mo(n,p)^{94}Nb were subtract from the ^{94}Nb production using isotopic abundance data as in the ^{94}Mo(n,p)^{94}Nb case. Also data other than ^{95}Mo(n,np)^{94}Nb are referred from data at FNS. The large error is due to the γ-ray counting statistics. However, the systematic trend suggests that the present data gives the reasonable range of cross sections. The present results demonstrated that due to the appreciably large cross section at 14.8 MeV, the ^{95}Mo(n,np)^{94}Nb reaction should be taken into account for the long-lived activity production as well as ^{94}Mo(n,p)^{94}Nb.

^{109}Ag(n,2n)^{108m}Ag

No experimental data for the cross section ^{109}Ag(n,2n)^{108m}Ag ($T_{1/2}$=418 y) was reported before IAEA-CRP started. As long as the old half-life of 127 ± 7 year was used, the present experiment gave cross section of 212 ± 11 mb. This value was very close to the other experimental values, whereas it was three times smaller than that of an evaluation by IRK. This large difference between experimental data and the evaluation should be attributed to the wrong half-life data for the deduction of experimental data. After revising half-life of 127 y to 418 y, the experimental data becomes very consistent with the evaluation at IRK. The experimental data at 14.1 and 14.7 MeV along with data at 14.9 MeV are given in **Table 1**.

^{151}Eu(n,2n)^{150m}Eu

Only two cross section data have been reported previously by Qaim [14] and Nethaway [14]. Along with data reported in the first IAEA-CRP[1], the cross section seemed somewhat convergent around 1.2 b. The present data were also in a good agreement within experimental error with those reported.

^{153}Eu(n,2n)$^{152m+g}$Eu

Since the isomeric state of 96 min. de-excites with 100 % isomeric transitions to the ground state, the cross section was obtained for the ^{153}Eu(n,2n)$^{152m+g}$Eu. Only one data was available for this production ($T_{1/2}$=13.2y) by Qaim [14] before IAEA-CRP report appeared. In the report of IAEA-CRP, we found the data of 1,544 mb at 14.77 MeV by Beijing and 1,740 mb at 14.7 MeV by KRI Leningrad. The IRK Vienna gave an evaluation of 1,442 mb at 14 - 15 MeV. These were rather scattered around 1,500 mb.

The present measurement gave cross section about 1.6 being the middle value among the other data. However, the status of the cross section seemed a little bit controversial, because of, as mentioned, rather scattered data different with each other exceeding the experimental errors.

^{158}Dy(n,p)^{158}Tb

After 3.6 year cooling, γ-lines of ^{158}Tb were clearly observed in a g-ray spectrum shown in Fig. 3. The cross section for the ^{158}Dy(n,p)^{158}Tb reaction was derived from the γ-ray peak counts measured. The result however, gave unreasonably large value more than one order of magnitude. From the reaction systematics, the cross section should be around 10 mb. The IRK evaluation also indicated that cross section should be less than 100 mb. The previous measurement at FNS gave cross sections of 100 ± 80 mb. The value was still very tentative because of extremely poor counting statistics. The present new measurement gave much better counting statistics with ± 11 %. We concluded that there must be some error source in the present measurement. This situation could be explained by the impurity of Tb in the Dy sample. Assuming there was some amount of impurity of Tb in a Dy sample and 10 mb for ^{158}Dy(n,p) reaction cross section, al least 200 ppm of Tb should be there to give the ^{158}Tb activity corresponding to the count rate. Unfortunately, there was no data for the impurity composition in the Dy material used. A data of 250 ppm of Tb in Dy, which was available in some literature, was remarkably consistent with the estimation. If the sample constituent is carefully measured by some chemical analysis, we would say that there is no need to have expensive enriched ^{158}Dy sample any more a long as this assumption is true. Nevertheless, it is still recommended to pursue a measurement with enriched sample of ^{158}Dy.

^{159}Tb(n,2n)$^{158m+g}$Tb

Terbium-158 has two states, one isomeric state deexciting 100 % isomeric transition with half-life of 10.5 sec and the ground state decaying with 150 year half-life. The isomer is so short-lived that the cross section is sum of ^{159}Tb(n,2n)$^{158m+g}$Tb.

Two experimental data have been reported by Qaim [14] and Prestwood [16] before IAEA-CRP report. In the IAEA-CRP report, one experimental data and one evaluation were given by IAE Beijing and IRK Vienna, respectively. Those data seemed very close each other to be around 1950 mb. The measurement at FNS through the inter-laboratory collaboration among ANL, LANL and JAERI gave a cross section of 1,600 mb at 14.8 MeV. The value was considerably lower than those previously reported even though the experimental errors were taken into account. Recently, the half-life of 150 y for ^{158}Tb was recommended to be revised to 180 y. According to this revision, the cross section becomes around 1.9 b.

Cross sections of 1944 ± 83, 1932 ± 82, and 1937 ± 82 mb at 14.9, 14.7 and 14.1 MeV were obtained by the measurement at FNS, which are consistent with data reported by other participants of CRP. The energy dependency of the cross section seems flat in the 14 MeV region.

^{178}Hf(n,n')^{178m2}Hf

As noted, two set of isotopically enriched samples of ^{179}Hf and ^{178}Hf were used to identify the each reaction contribution to forming ^{178m2}Hf. The cross sections for the reaction of ^{178}Hf(n,n')^{178m2}Hf were tentatively deduced by solving equations which used in the ^{179}Hf(n,2n)^{178m2}Hf cross section determination. In this study, we neglected the contribution from ^{177}Hf(n,γ)^{178m2}Hf because the abundance of ^{177}Hf was small compared to other isotopes in the samples. Therefore, there is still large uncertainty in the data. Thus note that the present data give an upper limit of cross section.

^{179}Hf(n,2n)^{178m2}Hf

No data has been reported so far before IAEA-CRP summary. In the inter-laboratory collaboration work, the cross section of 6.6 ± 0.3 mb was given. Harwell [1] reported an experimental data of 5.9 ± 0.6 mb at 14.8 MeV. One calculation has been given by Oxford/LANL to be 2.9 mb at 14 MeV.

The final data showed the value of 6.82 ± 0.38 and 5.83 ± 0.36 mb at 14.9 and 14.1 MeV, which was very close to those reported recently.

^{182}W(n,n'α)^{178m2}Hf

Using enriched sample, still very poor counting statistics for the γ-ray line of ^{178m2}Hf. This is simple due to the extremely low reaction cross section being less than 0.1 mb. Nevertheless, slight improvement was achieved in the measurement with the enriched sample in comparison with the last one using sample with natural abundance. The cross sections determined in the present measurement agreed with in experimental error with the previous data.

^{187}Re(n,2n)^{186m}Re

The cross section for ^{187}Re(n,2n)^{186m}Re reaction was obtained for the first time with the direct measurement in this work. The measured cross section of 445 ± 156 mb was compared with a calculation by Yamamuro [17] with SINCROS-II [18] as well as the IRK Evaluation [1]. The measured cross section was agreed within experimental error though it was large with the calculation and the evaluation. As a whole, it could be concluded that there is no serious inconsistency among data. Still more accurate experimental data are strongly requested to give better evaluation.

^{193}Ir(n,2n)^{192m2}Ir

The half-life of 241 year seems not so long for the activation cross section measurement if the emission probability of γ-ray is reasonably large. However, the spin of the second isomeric state of ^{192}Ir is hindering the deexcitement with isomeric transition, resulting in very low γ-ray emission probability. Only one experimental data was reported by China, IAE [3] for this particular reaction. Surprisingly, the data of 147 ± 52 mb measured at FNS was in good agreement with that data of IAE. Although experimental error was reduced significantly in the present experiment, still more accurate data are needed.

^{209}Bi(n,2n)^{208}Bi

Although the error was large, the present measurement gave a data reasonably close to those in currently available evaluated cross sections within the error.

Summary

Under the framework of the IAEA CRP, seventy reaction cross sections of concern were measured in the 14 MeV region at FNS. Some of them were derived by using enriched isotopes to identify the contribution of different reaction channel. In general, it takes considerably long cooling time to reduce interfering activity. Emphasis should be placed on our patient in terms of long waiting time, long counting time. Finally we can cover almost all reactions as far as 14 MeV neutron energy is concerned. We hope that our experimental effort could make a substantial contribution to this CRP.

Acknowledgments

Authors would like to express their sincere thank to the members of the FNS facility for their operation of accelerator. The part of activity was supported by USDOE.

REFERENCES

1. INDC(NDS)-232/L, "Activation Cross Sections for the Generation of Long-Lived Radionuclides of Importance in Fusion Reactor Technology", Proc. of an IAEA Consultants' Meeting, Argonne National Laboratory, 11th - 12th. Sept 1989.

2. Proceedings of the First Meeting of a Coordinated Research Program on Cross Sections for the Generation of Long-Lived Radionuclides of Importance in Fusion Reactor Technology, Vienna, November 11-12, 1991, INDC(NDS)-263, July 1992, Wang DaHai, Ed.

3. Proceedings of the Second Meeting of a Coordinated Research Program on Cross Sections for the Generation of Long-Lived Radionuclides of Importance in Fusion Reactor Technology, Del Mar, California, U. S. A., April 29-30, 1993, INDC(NDS)-288, November 1993, A. B. Pashchenko, Ed.

4. T. Nakamura, H. Maekawa, J. Kusano, Y. Oyama, Y. Ikeda, C. Kutsukake, Shi. Tanaka and Shu. Tanaka, "Present Status of the Fusion Neutron Source(FNS)," Proc. 4th Symp. on Accelerator Sci. Technol., RIKEN, Saitama, 24 - 26 November 1982, pp 155-156.

5. E. Browne and R. B. Firestone, V. S. Shirley, Editor, "Table of Radioactive Isotopes," A Wiley-Interscience Publication, John Wiley & Sons, 1986.

6. S. Iwasaki, J. R. Dumais and K, Sugiyama, Proc. Int'l. Conf. on Nuclear Data for Sci. and K. Sugiyama, Proc. Int'l. Conf. on Nuclear Data for Sci. and Technol., May 30-June 3, 1988, Japan. (Editor S. Igarashi) Saikon Publishing Co. LTD., Tokyo (1988) pp 295-297.

7. M. Sasao, T. Hayashi, K. Taniguchi, A. Takahashi and T. Iida, IPPJ-805, Inst. Plasma Phys., Nagoya Univ. (1987), and Phys. Rev. C 35, 2327 (1987).

8. K. Shibata, T. Nakagawa, T. Asami, T. Fukahori, T. Narita, S. Chiba, M. Mizumoto, A. Hasegawa, Y. Kikuchi, Y. Nakajima and S. Igarashi, "Japanese Evaluated Nuclear Data Library, Version-3 -JENDL-3-", JAERI-1319 (1990).

9. H. Gruppelaar, H. A. J. Van Der Kamp, J. Kopecky and D. Nierop, "The REAC-ECN-3 Data Library with Neutron Activation and Transmutation Cross Sections for Use in Fusion Reactor Technology," ECN -207 (1988).

10. L. R. Greenwood, "Recent Research in Neutron Dosimetry and Damage Analysis for Materials Irradiations", Proc. Symp. on the Effects of Radiation on Materials, June 23-25, 1987 Seattle, Washington, U. S. A.

11. N. Odano, S. Iwasaki and K. Sugiyama, "Evaluation of Cross Sections for the Dosimetry Reactions of Niobium," Presented in this conference. Paper No. C32

12. T. B. Ryves and T. Klokowski, J. Phys. G: Nucl. Phys. 7, 52 (1981).

13. L. R. Greenwood, D. G. Doran and H. L. Heinisch, Phys. Rev. C 35, 76 (1987).

14. S. M. Qaim, Nucl. Phys. A 224, 319 (1974).

15. D. R. Nethaway, Nucl. Phys. A 190, 635 (1972).

16. R. J. Prestwood, D. B. Curtis, D. J. Rokop, D. R. Nethaway and N. L. Smith, Phys. Rev. C 30, 823 (1984).

17. N. Yamamuro, "Activation Cross Section Calculations on the Production of Long-Lived Radionuclides," published in NSE (1994).

18. N. Yamamuro, "A Nuclear Cross Section Calculation System with Simplified Input-Format Version-II (SINCROS-II)," JAERI-M 90-006 (1990).

Table 1 Summary of Cross Sections Measured at FNS/JAERI

Reaction	Data at FNS		References		
	E_n(MeV)	Cross Section(mb)	E_n(MeV)	Cross Section(mb)	
$^{27}Al(n,2n)^{26}Al$	14.8	47 ± 5	14.7	40.6±4.4	6)
	14.5	30 ± 7	14.8	35±7	7)
	14.1	19 ± 10	14.5	16.2	9)
			14.1	19.0	10)
$^{61}Ni(n,np)^{60m+g}Co$	14.8	50.5 ± 8.2	14.5	18	9)
			14.1	17.4	10)
$^{63}Cu(n,\alpha)^{60m+g}Co$	14.8	40.4 ± 2.3	14.8	40.1±1.2	10)
	14.5	43.8 ± 2.5			
$^{93}Nb(n,n')^{93m}Nb$	14.8	43 ± 9	14.1	36±4	12)
	14.5	44 ± 9			
$^{94}Mo(n,p)^{94}Nb$	14.8	54 ± 12	14.8	53.1±5.3	13)
	14.1	58 ± 9			
$^{95}Mo(n,np)^{94}Nb$	14.8	21 ± 9			
	14.1	12 ± 7			
$^{109}Ag(n,2n)^{108m}Ag$	14.8	648 ± 31	14.77	230±7	*-1)
	14.5	621 ± 29	14.56	263±20	*-2)
	14.1	558 ± 26	14 - 15	665±73	*-3)
			14.9	191±7	*-4)
			14.9	208±37	*-5)
$^{151}Eu(n,2n)^{150m}Eu$	14.8	1276 ± 64	14.77	1219±28	*-1)
	14.5	1170 ± 59	14 - 15	1325±94	*-3)
	14.1	1215 ± 53	14.8	1127±55	*-4)
			14.9	1090±84	*-5)
			14.7	1270±149	14)
			14.8	1180±150	16)
$^{153}Eu(n,2n)^{152m2+g}Eu$	14.8	1659 ± 83	14.8	1712±155	*-4)
	14.5	1533 ± 77	14.77	1544±42	*-1)
	14.1	1326 ± 75	14 - 15	1442±60	*-3
			14.9	1740±145	*-5)
			14.7	1542±138	15)
$^{159}Tb(n,2n)^{158m+g}Tb$	14.8	1937 ±82	14.77	1968±56	*-1)
	14.5	1932 ±82	14.8	1600±-88	*-4)
	14.1	1944 ±83	14 - 15	1930±49	*-3)
			14.7	1801	15)
			14.8	1930	16)
$^{158}Dy(n,p)^{158m+g}Tb$	14.8	10 - 20**	14.5	10.7	9)
$^{178}Hf(n,n')^{178m2}Hf$	14.8	0.082± 0.011			
	14.1	0.11 ± 0.03			

Table 1 Continued

$^{179}Hf(n,2n)^{178m2}Hf$	14.8	6.82 ± 0.38	14.8	5.9±0.6	*-6)
	14.1	5.83 ± 0.36	14	2.9	*-7)
			14.9	6.0±-0.3	*-4)
$^{182}W(n,n'\alpha)^{178m2}Hf$	14.8	$(2.6\pm1.3)\times10^{-2}$	14.5	0.176	9)
			14.9	< 0.04	*-1)
$^{187}Re(n,2n)^{186m}Re$	14.8	135 ±65	14.1	693	10)
			14.5	605±258	9)
			14 - 15	591±122	*-3)
$^{193}Ir(n,2n)^{192m2}Ir$	14.8	147 ± 52			
$^{209}Bi(n,2n)^{208}Bi$	14.8	2450 ±260	14.1	2176	10)
			14.5	2340	9)

*Measurement, evaluation or calculation performed for CRP[1]:

*-1); IAE Beijing
*-2); Debrecen
*-3); IRK, Vienna
*-4); ANL/LANL/JAERI
*-5); KRI Leningrad
*-6); Harwell
*-7); Oxford/LANL

**) Estimation assuming 250 ppm Tb impurity in the Dy sample

XA9642392

MEASURED, ESTIMATED AND CALCULATED CROSS SECTIONS FOR THE GENERATION OF LONG-LIVED RADIONUCLIDES IN FAST NEUTRON INDUCED REACTIONS*

J. Csikai
Institute of Experimental Physics, Kossuth University, H-4001 Debrecen, Pf. 105, Hungary

Research Agreement No. 4882/CF

Abstract: Activation crosss sections have been measured in a Geesthacht-Debrecen cooperation for $^{109}Ag(n,2n)^{108m}Ag$, $^{63}Cu(n,\alpha)^{60}Co$, $^{134}Ba(n,2n)^{133}Ba$, $^{134}Ba(n,p)^{134}Cs$, $^{137}Ba(n,p)^{137}Cs$ reactions at (14.5±0.3)MeV neutron energy. Excitation functions of $^{63}Cu(n,p)^{63}Ni$, $^{109}Ag(n,2n)^{108m}Ag$, $^{151}Eu(n,2n)^{150m}Eu$, $^{153}Eu(n,2n)^{152m2+g}Eu$, $^{159}Tb(n,2n)^{158}Tb$ reactions were investigated in the 7-14.7 MeV range in a Jülich-Debrecen collaboration. High purity C, Al, $KHCO_3$, Zn, Cu, Ni, Mo, Si_3N_4, SiO_2, Dy, Hf and Re samples were irradiated with 14.6 MeV neutrons in Debrecen to produce the following long-lived radionuclides: $^{13}C(n,\alpha)^{10}Be$, (1.6×10^6y); $^{14}N(n,p)^{14}C$, (5730y); $^{17,18}O(n,x\alpha)^{14}C$, $^{27}Al(n,2n)^{26}Al$, (7.16×10^5y) ; $^{37}Cl(n,2n)^{36}Cl$, (3×10^5y); $^{39}K(n,p)^{39}Ar$, (269y) ; $^{39}K(n,\alpha)^{36}Cl$, (3×10^5y) ; $^{54}Fe(n,\alpha)^{53}Mn$, (2×10^6 y) ; $^{66}Zn(n,\alpha)^{63}Ni$, (100y); $^{60}Ni(n,2n)^{59}Ni$, (7.5×10^4y); $^{158}Dy(n,p)^{158}Cd$, (180y); $^{187}Re(n,2n)^{186}Re$, (2×10^5y); $^{179}Hf(n,2n) + {}^{177}Hf(n,\gamma) + {}^{178}Hf(n,n') \rightarrow {}^{178m2}Hf$, (31y).

The determinations of the reaction products are in progress by using either the radiochemical separation method or the classical and accelerator mass spectrometry in collaboration with Jülich KFA and Cologne University. Properties of cyclotron D-D neutron sources were studied and the spectrum unfolding methods (PHRS, activation unfolding, Monte Carlo calculation) were improved to increase the precision of the energy determination. In addition, the combination of the threshold detector and the physical integration methods rendered it possible to determine the volume averaged flux density spectra for extended samples. On the basis of a systematic measurement for 30 $\sigma_{n,\alpha}$ and 27 $\sigma_{n,p}$ data at 14.6 MeV bombarding neutron energy in Debrecen the trends were improved and the cross sections for $^{63}Cu(n,p)$, $^{96}Mo(n,\alpha)$ $^{92}Mo(n,p)$, $^{94}Mo(n,p)$, and $^{158}Dy(n,p)$ reactions have been estimated.

Results obtained by experiment for the excitation functions and the energy dependence of the isomeric cross section ratio were compared with the calculated data from the threshold to 16 MeV using the STAPRE and EXIFON codes. Cross sections were calculated around 14 MeV by the EXIFON code for 29 reactions resulting long-lived ($T_{1/2}$>10y) radionuclides.

*This work was supported by the Hungarian Research Foundation (Contract no. 1734/91, T 016713/95) and the International Atomic Energy Agency, Vienna (Research Contract No. 6971/RB, 7687/RB, 4882/CF).

1. Introduction

Measurements, evaluations and calculations of activation cross sections for production of long-lived isotopes at around 14 MeV neutron energy are of primary importance for radioactive waste estimates as well as for testing nuclear reaction models in addition to the cosmochemical investigations. Cross section data available for such reactions are very scarce and contradictory even in the vicinity of 14 MeV. The excitation functions of the dosimetry reactions require more precise data especially between 5 and 12 MeV. A systematic investigation has been started in Debrecen to complete the experimental data between 2 and 15 MeV and to check the different trends in the cross sections. Precise knowledge of the systematics is indispensable for the estimation of the unknown data. The low yields of the long-lived isotopes produced in different reactions require to use extended samples in which the flux density spectra $\Phi(E)$ can change significantly. Therefore, the methods used for the determination of volume averaged $\Phi(E)$ functions should have been improved. This report describes the present status of the results achieved.

2. Experimental procedure

High purity samples (Goodfellow) of different dimensions and oxyde powders pressed in disk-shaped pellets were irradiated with 13.5-14.8 MeV neutrons in a low scattering arrangement at the neutron generators of the Institute of Experimental Physics, Kossuth University, Debrecen. Neutrons were produced via the $^{3}H(d,n)^{4}He$ reaction using 180 keV magnetically analysed deuteron beam. The foil staks were placed at different angles to the D^{+}-beam to change the incident neutron energy. A special irradiation geometry was assured at (14.5 ± 0.3) MeV neutron energy by using the KORONA generator of the GKSS in Geesthacht. Neutrons in the energy range of 5-12.5 MeV were produced by variable energy cyclotrons in Debrecen (MGC-20) and Jülich (CV28) using D_2 gas target. Special attention was paid to the determinations of the average neutron energy, the energy spead, the flux density spectra, the effect of low energy neutrons and to suppress their contribution to the activities of the samples. In the case of absolute interfering (n,γ) and (n,2n) reactions the Cd-difference method was used.

The absolute activity of the irradiated samples was determined by using Ge(Li), HPGe and NaI detectors. The peak area analysis was based on the program ACCUSPEC developed for IBM compatible personal computers.

The neutron flux density and its variation in time were determined by foil activations, a fission chamber, a Pulse Height Response Spectrometer and a BF_3 "long-counter", respectively. For the determination of the flux denstiy spectra of neutrons in extended samples

by activation unfolding method, the cross section curves were taken from the IRDF-90 dosimetry file.

Corrections were made for the following effects; variation of the flux in time, gamma-ray self-absorption, true coincidence, dead-time, irradiation and measuring geometries, neutron attenuation in the sample. The errors of the cross sections contain the following principal sources: counting statistics, detector efficiency, sample masses, decay constants, energy and fluence uncertainties, reference cross sections.

In the case of low threshold reactions e. g. $^{10}B(n,p)$, $^{14}N(n,p)$, $^{17}O(n,\alpha)$, $^{39}K(n,\alpha)$, breakup neutrons produced in both the Coulomb-field and the $^{2}H(d,np)$ reactions are present in the spectrum with a high yield at $E_d \geq 10$ MeV. These neutrons can contribute significantly to the total activity of the sample. In the knowledge of the energy dependence of the reaction rate $[\phi(E)\sigma(E)]$, this contribution can be taken into account. The $\phi(E)$ functions were determined by the activation unfolding method while for $\sigma(E)$ the evaluated data based on previous measurements or on the calculated values have been accepted. For the determination of the cross sections for the $^{2}H(d,n)^{3}He$ monoenergetic neutrons, the reaction rates integrated over the group of low energy neutrons were subtracted from the total value obtained by experiment. Details of the investigations related to the characteristics of neutron fields, the irradiation and measuring procedures have been described elsewhere [1-10].

3. Results and discussion

Details of cross section measurements on $^{109}Ag(n,2n)^{108}Ag^{m}$, $^{151}Eu(n,2n)^{150}Eu^{m}$, $^{153}Eu(n,2n)^{152}Eu^{m+g}$ and $^{159}Tb(n,2n)^{158}Tb$ reactions at different energies are discussed by Qaim [11]. Corrections for the effect of scattered neutrons on the activity of $^{108}Ag^{m}$ produced via the $^{107}Ag(n,\gamma)$ reaction have given consistent results with other experiments. From two sets of measurements a value of (711 ± 44) mb was found at E_n = 14.5 MeV accepting $T_{1/2}$ = 433y.

High purity C, Al, $KHCO_3$, Zn, Cu, Ni, Mo, Si_3N_4 and SiO_2 samples were irradiated with about 5 x 10^{12}n/cm^2 fluence of 14.6 MeV neutrons in Debrecen to produce long-lived radionuclides in fast neutron induced reactions. The sample preparations are in progress at Cologne University for the determination of the production cross sections by using the accelerator mass spectrometry.

Reactions to be studied in the first set of measurements are as follows:

$^{13}C(n,\alpha)^{10}Be$ $^{1.62 \times 10^6}$y ; $^{17}O(n,\alpha)^{14}C$, $^{18}O(n,n\alpha)^{14}C$ 5.73 x 10^3 y ; $^{27}Al(n,2n)^{26}Al$ 7.2x10^5y; $^{39}K(n,\alpha)^{36}Cl$ 3 x 10^5y

Relative data will also be given for the production of ^{10}Be, ^{14}C and ^{36}Cl isotopes using a $KHCO_3$ complex sample for testing the measuring methods.

Precise knowledge of the systematics in the $\sigma(n,\alpha)$ and $\sigma(n,p)$ data [13, 14] at around 14 MeV rendered it possible to estimate some data for production of long-lived isotopes by interpolation and extrapolation methods. These data are indicated in Table 1 together with some measured cross sections. It was found that the effects of (N-Z)/A asymmetry parameter as well as the isotopic, isotonic an odd - even properties of nuclei are present in the (n,α) cross sections especially in the Coulomb sub-barrier region [15, 16].

Studies on the excitation functions of (n,p) and (n,α) reactions can give information on the effect of Coulomb sub-barrier, therefore a systematic investigation on these reactions is recommended.

Excitation functions of neutron induced reactions were calculated for some reactions from the threshold to 18 MeV by the STAPRE and the EXIFON codes. It was found that the STAPRE code can give more realistic results for both the total cross sections and the energy dependence of the isomeric ratio than the EXIFON model [9,19]. It should be noted, however, that in general, the EXIFON code can be used for the estimation of the data for (n,p), (n,α) and (n,2n) reactions around 14 MeV [14, 17, 18]. As indicated in Table 1. a number of reaction cross sections for the generation of long-lived radionuclides were calculated [18] by this model between 13.5-15.0 MeV.

Figure 1. shows typical examples for the measured and calculated energy dependence of the isomeric cross section ratios. The significant change in the σ_m/σ_g-E_n function at around 14 MeV could not be reproduced by model calculation

A comparison of neutron flux density spectra from D_2 gas target determined by different methods is given in Fig. 2. The average energy of the monoenergetic peak is consistant but the relative yields of low energy neutrons depends on the applied method [20].

Table 1. Some measured, estimated and calculated cross sections for the generation of long-lived isotopes

Reaction	$T_{1/2}$	σ(mb)	Remarks
$^{109}Ag(n,2n)^{108m}Ag$	433 y	677±82 716±44	Measured
$^{134}Ba(n,2n)^{133}Ba$	10.54 y	1556±95	
$^{134}Ba(n,p)^{134}Cs$	2.06 y	6±2	
$^{137}Ba(n,p)^{137}Cs$	30 y	5±1	
$^{63}Cu(n,\alpha)^{60}Co$	5.27 y	45±2	
$^{63}Cu(n,p)^{63}Ni$	100.1 y	70±9	Estimated
$^{96}Mo(n,\alpha)^{93}Zr$	1.5×10^6 y	10.6±0.9	
$^{92}Mo(n,p)^{92}Nb$	3.6×10^7 y	97±11	
$^{94}Mo(n,p)^{94}Nb$	2×10^4 y	52±6	
$^{158}Dy(n,p)^{158}Tb$	1.8×10^2 y	10.6±1.2	

Table 1. cont.

$^{27}Al(n,2n)^{26}Al$	7.5×10^{6} y	0 - 75.2	
$^{137}Ba(n,p)^{137}Cs$	30 y	8.2 - 13.3	
$^{209}Bi(n,2n)^{208}Bi$	3×10^{4} y	2118.2 - 2159.9	EXIFON calc. $13.4 \leq En \leq 15.0$ MeV
$^{79}Br(n,p)^{79}Se$	6.5×10^{4} y	40.7 - 42.8	
$^{40}Ca(n,p)^{40}K$	1.28×10^{9} y	485 - 456	
$^{42}Ca(n,\alpha)^{39}Ar$	269 y	138.1 - 147.9	
$^{63}Cu(n,p)^{63}Ni$	100 y	78.4 - 87.4	
$^{63}Cu(n,\alpha)^{60}Co$	5.27 y	61.4 - 73	
$^{50}Cr(n,p)^{50}V$	0.25×10^{14} y	521.6 - 496.4	
$^{113}In(n,p)^{113}Cd$	9.10^{15} y	9.1 -12.1	
	14.6 y		
$^{39}K(n,p)^{39}Ar$	269 y	108.9 - 114.3	
$^{39}K(n,\alpha)^{36}Cl$	3×10^{5} y	310.4 - 308.5	
$^{139}La(n,2n)^{138}La$	1.1×10^{11} y	1496.7 - 1700.2	
$^{92}Mo(n,p)^{92}Nb$	1.7×10^{8} y	197 - 206.4	
$^{94}Mo(n,p)^{94}Nb$	2×10^{4} y	45.8 - 55.7	
$^{14}N(n,p)^{14}C$	5736 y	18.9 - 24.4	
$^{93}Nb(n,p)^{93}Zr$	1.5×10^{6} y	23 - 30	
$^{60}Ni(n,2n)^{59}Ni$	7.5×10^{4} y	246.3 - 557.5	
$^{64}Ni(n,2n)^{63}Ni$	125 y	916 - 1120.2	
$^{17}O(n,\alpha)^{14}C$	5736 y	154.4 - 155.4	
$^{141}Pr(n,\alpha)^{138}La$	1.3×10^{11} y	0.6 - 1.1	
$^{80}Se(n,2n)^{79}Se$	7×10^{4} y	855 - 1133.9	
$^{116}Sn(n,\alpha)^{113}Cd$	9×10^{15} y	2.2 - 4.4	
	14.6 y		
$^{99}Tc(n,2n)^{98}Tc$	1.5×10^{6} y	1231.5 - 1368.3	
$^{51}V(n,2n)^{50}V$	4.8×10^{14} y	388.9 - 751.4	
$^{180}W(n,p)^{180}Ta$	2×10^{13} y	5.6 - 6.7	
$^{66}Zn(n,\alpha)^{63}Ni$	100 y	18.4 - 27.7	
$^{93}Zr(n,\alpha)^{90}Sr$	29 y	12 - 13.1	
$^{94}Zr(n,2n)^{93}Zr$	9×10^{5} y	1459.3 - 1501.8	

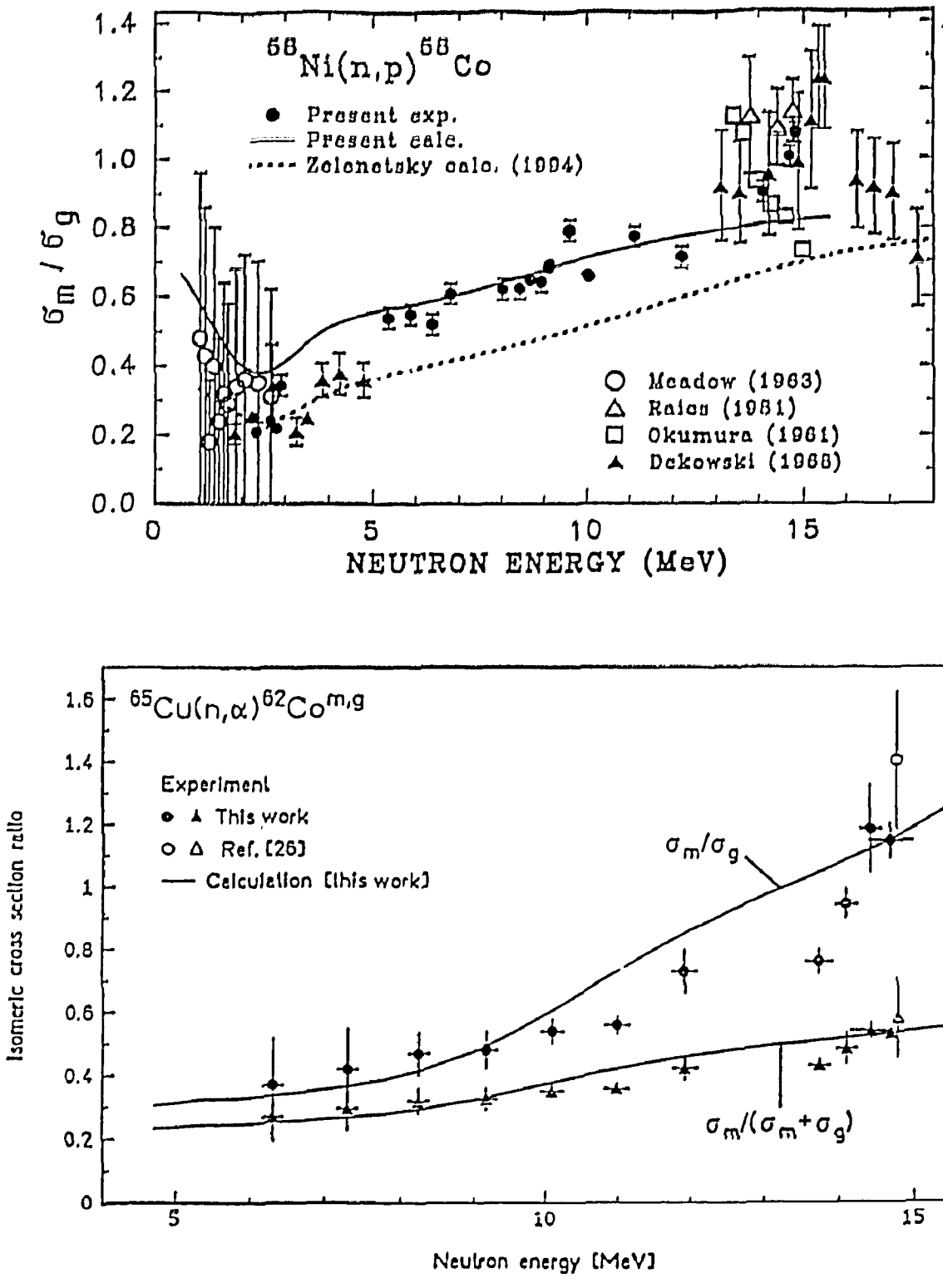

Fig. 1. Measured and calculated isomeric cross section ratios vs. neutron energy for ^{58}Ni(n,p) and ^{65}Cu(n,α) reactions.

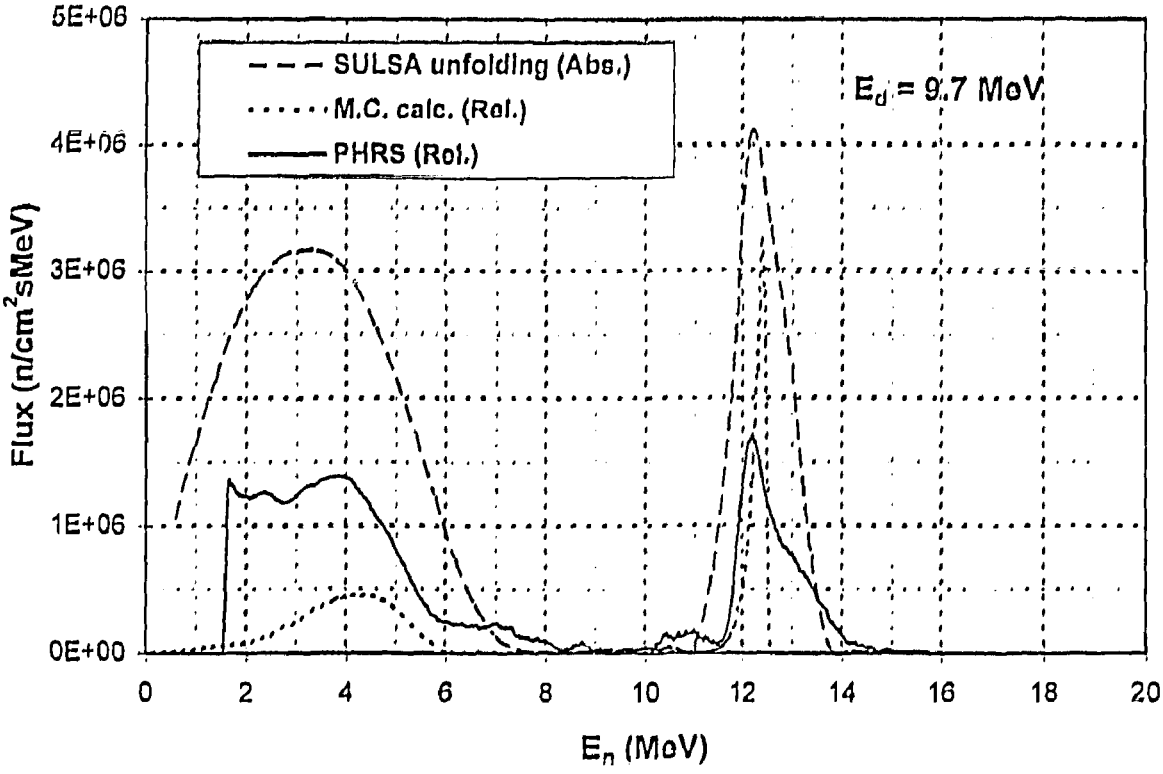

Fig. 2. Spectral yields of neutrons from D_2 gas target at E_d = 9.7 MeV.

References

[1] Á. Grallert, J. Csikai, S.M. Qaim, J. Knieper, Nucl. Instrum. Meth., A334(1993)154-159.

[2] Á. Grallert, J. Csikai, S.M. Qaim, Nucl. Instrum. and Methods A337 (1994) 615-618.

[3] N. V. Kornilov, A. B. Kagalenko, V. Ya. Baryba, S. Daróczy, J. Csikai, Z. Papp, Zs. Schram, Phys. Rev., C39 No. 3. (1989) 789-794.

[4] M. Wagner, G. Winkler, H. Vonach, J. Csikai and Cs. M. Buczkó, Ann. nucl. Energy, 16 (1989) 623-635.

[5] M. Wagner, G. Winkler, H. Vonach, Cs. M. Buczkó and J. Csikai, INDC(NDS)-232/L, IAEA Vienna (1990) p. 17.

[6] J. Csikai, Zs. Lantos, Cs. M. Buczkó and S. Sudár, Z. f. Phys., A-337 (1990) 39.

[7] M. Wagner, G. Winkler, H. Vonach and G. Pető, Ann. nucl. Energy, 15 (1988) 363.

[8] P. Raics, S. Nagy, S. Szegedi, N. V. Kornilov and A. B. Kagalenko, Int. Conf. on Nuclear Data for Science and Technology, (Ed. S. M. Qaim), Springer-Verlag, (1992) p. 660.

[9] Cs. M. Buczkó, J. Csikai, S. Sudár, Á. Grallert, S. A. Jonah, B. W. Jimba, T. Chimoye and M. Wagner, Phys. Rev. C. (in press)

[10] J. Csikai, Á. Grallert, L. Oláh and S. M. Qaim, Int. Conf. on Nuclear Data for Science and Technology, (Ed. J. K. Dickens), ANS Ins. Illinois (USA), (1994) p. 78

[11] S. M. Qaim, F. Cserpák and J. Csikai, IAEA-NDS, CRP Progress Report, (1995)

[12] J. Csikai, Cs. M. Buczkó, R. Pepelnik and H. M. Agrawal, Ann. nucl. Energy, 18 (1991) 1.

[13] Á. Grallert, J. Csikai, Cs. M. Buczkó and I. Shaddad, INDC(NDS)-286, IAEA, Vienna, (1993) p. 131

[14] J. Csikai, JAERI-M 94-019, INDC(JPN)-169/L (1994) p. 408-425.

[15] N. V. Kornilov and A. F. Gurbich, private communication.

[16] A. M. El-Megrab, S. A. Jonah, R. Dóczi, A. D. Majdeddin, A. Fenyvesi, V. Semkova, Cs. M. Buczkó, S. Sudár, S. Szegedi, J. Csikai, to be published.

[17] J. Csikai, INDC(NDS)-286 L. IAEA, Vienna, (1993) p. 5-11.

[18] J. Csikai, INDC(NDS)-263, IAEA, Vienna, (1992) p. 33.

[19] F. Cserpák, S. Sudár, J. Csikai and S. M. Qaim, Phys. Rev., C49(1994)1525-1533

[20] M. Várnagy, L.Oláh, F. Cserpák, A.M.El-Megrab, A.D.Madeddin,J. Csikai (to be published)

Activation Cross Sections for Generation of Long-lived Radionuclides

(Research Agreement No 5060/CF)

Lu Hanlin, Yu Weixiang, Zhao Wenrong
(China Institute of Atomic Energy, P.O.Box 275-3, Beijing 102413)

Wang Yongchang, Yuan Junqian, Kong Xiangzhong
(Lanzhou University, Department of Modern Physics, Lanzhou 730001)

Shi Zhaomin
(Peking University, Beijing 100871)

Xia Yijun, Wang Chunhao, Long Xianguan
(Institute of Nuclear Science and Technology, Sichuan University, Chengdu 610064)

Abstract-This paper is a summation of activation cross section measurements for generation of long-lived radionuclides of importance in fusion reactor technology. The measurements were performed by Institute of Atomic Energy(IAE), Lanzhou University(LU), Peking University(PU) and Sichuan University(SU) in a period from 1989 to 1994. The cross sections were measured for reactions of $^{109}Ag(n,2n)^{108m}Ag$, $^{151}Eu(n,2n)^{150m}Eu$, $^{153}Eu(n,2n)^{152g}Eu$, $^{159}Tb(n,2n)^{158}Tb$, $^{179}Hf(n,2n)^{178m2}Hf$, $^{182}W(n,n'\alpha)^{178m2}Hf$, $^{187}Re(n,2n)^{186m}Re$ and $^{193}Ir(n,2n)^{192m2}Ir$ at 14 MeV, $^{109}Ag(n,2n)^{108m}Ag$, $^{151}Eu(n,2n)^{150m}Eu$, $^{159}Tb(n,2n)^{158}Tb$ and $^{179}Hf(n,2n)^{178m2}Hf$ at 9.5 and 9.9 MeV, and $^{98}Mo(n,\gamma)^{99}Mo(\beta^-)\rightarrow^{99}Tc$, $^{165}Ho(n,\gamma)^{166m}Ho$ and $^{151}Eu(n,\gamma)^{152g}Eu$ in E_n 20-1100 keV. Some of them were calculated by systematic and HFTT code, which was based on the compound nucleus evaporation and the preequilibrium excition model.

1. Introduction

Investigation of activation cross sections needed for waste disposal assessment of fusion reactor materials was presented by E.T.Cheng in the INDC meeting(1987). A list of important reactions selected on long-lived nuclides for fusion technology was given in Research Coordination Meeting, Argonne(1989). For this reason, a cooperation group of CIAE, LU, PU and SU was organized in China. Up to now, a lot of results were obtained by this group and the measurements were greatly improved for the nuclear data used in fusion energy applications.

2. Experiment

The irradiations were carried out using the neutrons from $T(d,n)^4He$, $D(d,n)^3He$, $T(p,n)^3He$ and $^7Li(p,n)^7Be$ reactions in neutron energy ranges ~14 MeV, 9-10 MeV, 200-

1100 keV and 20-250 keV at Intense Neutron Generator(LU), Cockcroft-Walton and Tandem accelerator(IAE) and Van-de-Graaff accelerators(SU and PU).

The activities of the investigated products were determined in four laboratories. And the same standard γ-ray sources were used to calibrate the efficiencies of Ge or Ge(Li) detectors.

Recommended decay parameters for the half-life($T_{1/2}$), photon energy(E_γ) and photon emission probability(I_γ) are given in table 1.

Table 1. Decay data of products

	^{108m}Ag	^{150m}Eu	^{152g}Eu	^{158}Tb	^{178m2}Hf	^{192m2}Ir	^{166m}Ho	^{99}Mo
$T_{1/2}$ (y)	418	35.8	13.54	180	31	241	12000	2.7477d
E_γ (keV)	434	334	344	944	574	316	772	140
I_γ (%)	90.5	94.0	26.6	43	83.8	83*	54.7	90.7**

* from decay of ^{192g}Ir

** with ^{99m}Tc in equilibrium

The ^{93}Nb(n,2n)^{92m}Nb, ^{197}Au(n,2n)^{196}Au and ^{197}Au(n,γ)^{198}Au reactions were used as the neutron fluence monitors. The values of the cross sections were taken from evaluated data of Lu Hanlin[1], H Vonach[2] and ENDF/B-VI.

3. Correction

A main correction came from the contamination of the neutron field. The neutron field of T(d,n)^{4}He source is always contaminated by d-D neutron and scattered neutrons. For example, in the measurements of ^{153}Eu(n,2n)^{152g}Eu reaction, the corrections were about 4-20%, which came from the contribution of ^{151}Eu(n,γ)^{152g}Eu reaction for low energy neutrons.

Using d-D neutron source at 9.5 and 9.9 MeV, there are several kinds of low energy neutrons in the field. They came from breakup neutron, self-buildup solid D target in window and backing, structure material bombarded by deuteron and multi-scattering neutrons. In present work, the ratios of neutron fluence measured by the monitors of ^{58}Ni(n,p)^{58}Co and ^{197}Au(n,2n)^{196}Au are about 2.3 and 1.8 at 9.5 and 9.9 MeV respectively.

In the 20-1100 keV neutron energy range for (n,γ) reaction, the effect of scattering neutrons from target structure and cooling materials, room background is very large. So the sample groups are wrapped by cadmium and gold foils to reduce the influence of low energy neutrons below 0.6 eV and ~5 eV(gold resonant absorption).

For the correction in activity determination, the effect of sum peak was about 47% in the measurements of ^{179}Hf(n,2n)^{178m2}Hf and ^{182}W(n,n'α)^{178m2}Hf reactions.

Other corrections were also made for the fluctuation of neutron flux, γ-ray self-absorption in the sample, impurity activities, which have γ-rays with energies close to the studyed one, the effect of low energy neutrons(which have energies lower than main neutron energy and over threshold), owing to different excitation function shapes of standard and investigated reactions.

4. Results

The cross sections of all reactions were summarized in tables 2-4, performed by IAE, LU, SU and PU. A consistent results were obtained for $^{109}Ag(n,2n)^{108m}Ag$, $^{151}Eu(n,2n)^{150m}Eu$, $^{153}Eu(n,2n)^{152g}Eu$, $^{159}Tb(n,2n)^{158}Tb$ and $^{179}Hf(n,2n)^{178m2}Hf$ reactions at 14 MeV.

The cross sections of $^{182}W(n,n'\alpha)^{178m2}Hf$ and $^{187}Re(n,2n)^{186m}Re$ reactions at 14 MeV appear big scattered and uncertainties. The cross section of $^{187}Re(n,2n)^{186m}Re$ may be improved when the reaction will be measured after another two years cooling.

There are large discrepancies between the data of IAE, and ANL/LA/JAERI, as well as Jülich/Debrecen collaborations, near threshold in the reactions of $^{151}Eu(n,2n)^{150m}Eu$, $^{159}Tb(n,2n)^{158}Tb$ and $^{109}Ag(n,2n)^{108m}Ag$. Therefore, precise measurements are needed for obtaining reliable data.

$^{193}Ir(n,2n)^{192m2}Ir$: The first value of the cross section was 134±80 mb with a large statistical error, about ~50%, the γ-ray of 155 keV with I_γ=0.097%, was measured in 1992. In 6 years later after irradiation, the activities of the short-lived isomer(m1) and the medium-lived ground state(g) of ^{192}Ir decayed to a neglected level relative to that of isomer(m2). The 316 keV γ-ray (I_γ=83%) of ground state, to which isomer m2 state only decays, was measured with a high count rate(about eight hundred times higher than before) and a small statistical error. Therefore the second value of 167±24 mb for this reaction is greatly improved.

5. Work plan in future

A. measurements in progress:

$^{187}Re(n,2n)^{186m}Re$, $^{185}Re(n,\alpha)^{182}Ta$, $^{182}W(n,p)^{182}Ta$, $^{184}W(n,\alpha)^{181}Hf$, $^{192}Pt(n,p)^{192m2}Ir$ at ~14 MeV

$^{187}Re(n,p)^{187}W$, $^{187}Re(n,\alpha)^{184}Ta$ at ~10 MeV

$^{64}Zn(n,p)^{64}Cu$ in the 3-10 MeV region

$^{64}Zn(n,\gamma)^{65}Zn$ in the 150-1100 keV region

$^{191}Ir(n,\gamma)^{192m2}Ir$ at 0.0253 eV

B. A effort will be considered in the neutron energy range of 7-12 MeV. The elements of Mo, Ti, Fe, Co and Ni will be selected to measure first.

C. On-going measurement in 0.03-7 MeV and 14 MeV will continued.

Table 2. Measured Cross Sections (mb) [CIAE]

Reaction	9.5±0.5	9.9±0.5	14.19±0.23	14.28±0.24	14.44±0.26	14.77±0.48	14.83±0.34
$^{109}Ag(n,2n)^{108m}Ag$		45.1±4.1	737±20	707±38	734±34	757±24	767±24
$^{151}Eu(n,2n)^{150m}Eu$	307±35	496±40	1190±27		1215±36	1219±28	
$^{153}Eu(n,2n)^{152g}Eu$						1560±70	
$^{159}Tb(n,2n)^{158}Tb$	491±61	803±76	1980±56			1968±58	
$^{179}Hf(n,2n)^{178m2}Hf$		0.32±0.09	6.6±0.6			7.0±0.6	
$^{182}W(n,n'\alpha)^{178m2}Hf$			0.016±0.10				
$^{193}Ir(n,2n)^{192m2}Ir$			167±24				
$^{187}Re(n,2n)^{186m}Re$						340±192	

Table 3. Measured Cross Sections (mb) [LU]

Reaction	13.54	13.64	13.72	13.79	14.03	14.33	14.35	14.60	14.80
$^{109}Ag(n,2n)^{108m}Ag$		733±23		733±59	747±66	737±26		763±26	777±23
$^{151}Eu(n,2n)^{150m}Eu$	1227±47		1238±48				1165±44	1168±44	1170±44
$^{159}Tb(n,2n)^{158}Tb$			2077±277				2144±112	1909±85	1922±89
$^{179}Hf(n,2n)^{178m2}Hf$								6.04±0.32	

Table 4. Measured Cross Sections (mb) [SU, CIAE]

En (keV)	$^{98}Mo(n,\gamma)^{99}Mo$-^{99}Tc	$^{165}Ho(n,\gamma)^{166m}Ho$	En (keV)	$^{151}Eu(n,\gamma)^{152g}Eu$
29±8.9	74.2±6.4		22±16	2822±170
59±20.6	43.6±3.8		36±30	1999±174
121±33	33.8±2.9		57±25	1734±110
196±28	29.8±2.6		160±40	1040±65
203±30		37.4±5.6	173±40	994±63
215±43	30.6±2.6		175±55	953±66
230±12	29.4±2.5		230±40	860±54
376±101	28.2±2.4		318±33	681±43
655±144	30.1±2.1		376±116	641±40
676±114		12.1±2.4	465±110	480±36
962±121	20.2±1.5		817±167	348±23
974±126		10.9±3.1	1100±80	284±19
1100±68	16.3±1.2		1120±80	265±20

References

[1] Zhao Wenrong, Lu Hanlin, Yu Weixiang, "Compilation of measurements and evaluations of nuclear activation cross sections for nuclear data applications", INDC(CPR)-16, p55,59, 1989

[2] H.Vonach et al., "Evaluation der wirkungsquerschnitte der recktionen $^{197}Au(n,2n)^{196}Au$, $^{59}Co(n,2n)^{58}Co$ und $^{93}Nb(n,2n)^{92m}Nb$", Diplomarbeit, die zur Erlangung des akademischen Grades, Wien April, 1990

Cross Sections of $^{109}Ag(n,2n)^{108m}Ag$, $^{151}Eu(n,2n)^{150m}Eu$, $^{159}Tb(n,2n)^{158}Tb$ and $^{179}Hf(n,2n)^{178m2}Hf$ Reactions at 9.5 and 9.9 MeV

Yu Weixiang, Zhao Wenrong, Cheng Jiangtao and Lu Hanlin
(China Institute of Atomic Energy, P.O.Box 275(3), Beijing 102413)

Abstract-The cross sections for the formation of long-lived products $^{108m}Ag(6^+,433y)$, $^{150m}Eu(5^-,36.9y)$, $^{158}Tb(3^-,180y)$ and $^{178m2}Hf$ are measured in the (n,2n) reaction on the elements of ^{109}Ag, ^{151}Eu, ^{159}Tb and ^{179}Hf at neutron energies of 9.5 MeV and 9.9 MeV, respectively. The neutron fluence is obtained through $^{197}Au(n,2n)^{196}Au$ reaction. The $D(d,n)^3He$ reaction is used as neutron source at the tandem accelerator of CIAE, Beijing. The present results are compared with the values of averaged theoretical cross sections and the experimental data.

1 INTRODUCTION

The Nuclear Data Section of International Atomic Energy Agency (IAEA) established a Coordinate Research Programme (CRP) on activation cross sections for the generation of long-lived radionuclides of importance in fusion reactor technology in 1988. Five years later, about 20 laboratories from 9 countries participated in this CRP. Since then, great progress has been made in experimental measurements, theoretical calculations and evaluations[1,2,3]. However, all the theoretical calculations[4] are larger than the experimental data below neutron energy 11 MeV, measured by Julich-Debrecen[5] collaboration and Argonne-Los Alamos[6] collaboration recently. Dr. M.B. Chadwick, et al.[4] suggested that the large discrepancies between theory and experimentnear threshold in the $^{151}Eu(n,2n)^{150m}Eu$, $^{159}Tb(n,2n)^{158}Tb$, $^{179}Hf(n,2n)^{178m2}Hf$ and $^{109}Ag(n,2n)^{108m}Ag$ reactions should be understood.

2 EXPERIMENT

Irradiation:

The irradiations were carried out at CIAE tandem accelerator (HI-13). Approximately monoenergetic neutrons of 9.5 and 9.9 MeV were produced by the $D(d,n)^3He$ reaction using a gas target, which had a length of 3.5 cm and a pressure of 0.75-0.80 MPa. The entrance window of the target box is a 50 μm Mo foil and borne 4-5.5 μA deuteron current. The neutron energy and resolution were determined by calculations and

measurements using time-of-flight method. The sample packet of 2 cm in diameter and 1.45 cm in thickness was placed on the beam line at zero degree and irradiated for about 34 and 21 hours respectively for each run. The target-sample distances were 0.8 cm and 1.2 cm, respectively. The samples for irradiation were arranged in the following order(shown in Fig.1). Au(0.1 mm, 1.5 g), Ag(0.5 mm, 1.5 g), Au, HfO_2(5.1 mm, 8.2 g), Au, Tb_2O_3(2.0 mm, 2.58 g), Au, Eu_2O_3(2.45 mm, 2.2 g), Au, Ni(0.2 mm, 0.5 g), Al(0.4 mm, 0.34 g), Au, Ni, Re(0.1 mm, 0.6 g), Ni, Zn(0.45 mm, 1.0 g), Ni. The powder of Eu_2O_3, Tb_2O_3 and HfO_2 was pressed into tablets and packed by nylon film. The Au foils were placed in different positions in the sample packet to measure the total neutron fluence gradients, and the neutron fluence as a function of reaction threshold was obtained by the monitor reactions of $^{59}Ni(n,p)^{58}Co$, $^{27}Al(n,\alpha)^{24}Na$ and $^{197}Au(n,2n)^{196}Au$.

The neutron fluences were determined by the monitor reactions of $^{197}Au(n,2n)^{196}Au$($T_{1/2}$=6.183 d, Eγ=355.6 keV, Iγ=87%), $^{59}Ni(n,p)^{58}Co$($T_{1/2}$=70.916 d, Eγ=810.8 keV, Iγ=99.5%) and $^{27}Al(n,\alpha)^{24}Na$($T_{1/2}$=14.965 h, Eγ=1368 keV, Iγ=99.9936%). The average cross section values of $^{197}Au(n,2n)^{196}Au$ are 991.4 mb at 9.9 MeV and 706 mb at 9.5 MeV, which were taken from the evaluated data of H.Vonach[7] and Lu Hanlin[8]. The accumulated neutron fluences at the sample area are $(0.71\text{-}1.61)\times10^{13}$ at 9.5 MeV and $(0.82\text{-}1.47)\times10^{13}$ at 9.9 MeV, respectively.

The activities of investigated products were determined with a well calibrated Ge(Li) spectrometer system. The activities of ^{150m}Eu, ^{108m}Ag, ^{158}Tb and $^{178m2}Hf$ were measured in about 2-12 months after the irradiations. The measurements lasted 3-15 days for each sample.

Effect of low energy neutrons:

When the $D(d,n)^3He$ reaction is used as a neutron source, there are several kinds of low energy neutrons in the neutron spectrum. They beam stop, from the breakup neutron of deuteron, from the A(d,n)B reaction when the target structure materials are irradiated by the d beam and from the multi-scattering of the main neutrons. The effect of the low energy neutrons depends on the irradiation time, detection distance, detection angle, incident d beam energy, size of beam spot and strongly depends on the threshold of the specific reaction. In the present work, differences of 130% at 9.5 MeV and 80% at 9.9 MeV were found between the lowest and the highest neutron fluences measured by the monitors with different threshold, as shown in Table 1. And similar results can also be found in J. W. Meadows' report[9]. For activation cross section measurement of long-lived radionuclides, the monitor reaction selected must be nearly the same in threshold and be of very similar shape in excitation function with the investigated reaction. In this way, the effect of the low energy neutrons can be reduced strongly. Our cross sections for the $^{109}Ag(n,2n)^{108m}Ag$, $^{151}Eu(n,2n)^{150m}Eu$, $^{159}Tb(n,2n)^{158}Tb$ and $^{179}Hf(n,2n)^{178m2}Hf$

reactions were derived from the neutron fluence of the $^{197}Au(n,2n)$ monitor reaction, because they have a similar threshold and a similar shape of excitation function.

Table 1. Measured fluence by monitors (10^{13} neutron per sample area)

Monitor reactions	9.5 MeV	9.9 MeV
$^{58}Ni(n,p)^{58}Co$	1.61	1.47
$^{27}Al(n,\alpha)^{24}Na$	1.05	1.07
$^{197}Au(n,2n)^{196}Au$	0.715	0.818

3 RESULTS

The cross sections of the (n,2n) reaction for ^{109}Ag, ^{151}Eu, ^{159}Tb and ^{179}Hf at neutron energies of 9.5±0.5 and 9.9±0.5 MeV are summarized in Table 2 and plotted in Figs 2-5 The figures show that the average theoretical values calculated by M. B. Chadwick agree with our measured results.

The uncertainties of the measured cross sections were as follows. the monitor(±6%), the effect of low energy neutrons (+6%, -3%, ±2%, +8%), the γ yield(1.6-25%), the half-life(3.5%, 2.4%, 6.1%, 3.2%), the γ branch(0.6%, 3.1%, 3.0%, 2.0%), the effect by the (n,γ) reaction(<1%, 0, 0, <0.1%), the irradiation geometry (0.1%, 1%, 1%, 3%), and the purity and weight for the Ag, Eu, Tb and Hf samples(0.1%, 0.5%, 0.5%, 0.5%) The total uncertainty is about 8-28%

Table 2. Measured cross sections below 14 MeV (mb)

Authors	Presentwork		J.W.Meadows	S.M Qaim*			M.B.Chadwick**		
En. MeV	9.5±0.5	9.9±0.5	10.3	9.63	10.10	10.59	9.5	10.0	10.5
$^{109}Ag(n,2n)^{108m}Ag$		45.1±4.1	38.5±10.6				7.5	77.17	152
$^{151}Eu(n,2n)^{150m}Eu$	307±35	496±40	215±17	185±26	270±30	380±37	384.6	562.8	732
$^{159}Tb(n,2n)^{158}Tb$	491±61	803±76	575±57	373±36	588±65	943±113	680.9	1059	1345
$^{179}Hf(n,2n)^{178m2}Hf$		0.32±0.09					0.12	0.33	0.62
$^{197}Au(n,2n)^{196}Au$	706±42	991±60							

* Cross sections normalized to the new half-life of 180 y for ^{158}Tb

** Averaged theoretical cross sections (from Chadwick, Ignatyuk, Meadows, Gardner and Yamamuro)

Reference

[1] Wang Dahai, "Proceedings of an IAEA consultants Meeting on Activation Cross Sections for the Generation of Long-lived Radionuclides of Importance in Fusion Reactor Technology," Report INDC(NDS)—232/L, ANL, USA(1989)

[2] Wang Dahai, "Proceedings of an IAEA Research Co-ordination Meeting (RCM—1) on Activation Cross Sections for the Generation of Long-lived Radionuclides of Importance in Fusion Reactor Technology," Report INDC(NDS)-263, IAEA, Vienna(1991)

[3] A. B. Pashchenko, "Proceedings of an IAEA RCM—2 on Activation Cross Sections for the Generation of Long-lived Radionuclides of Importance in Fusion Reactor Technology," Del Mar, California, USA(1989)

[4] M. B. Chadwick, O. T. Grudzevich, J. W. Meadows et al., Contributed paper in Ref. 3 P. 123

[5] S. M. Qaim, F. Cserpak, J. Csikai, Contributed paper in Ref. 2 P. 31

[6] J. W. Meadows, R. C. Haight, Y. Ikada et al., Contributed paper in Ref. 3 P. 13

[7] H. Vonach, "Evaluation der Wirkungsquerschnitte der Reaktionen $^{197}Au(n,2n)^{196}Au$, $^{59}Co(n,2n)58Co$ und $^{93}Nb(n,2n)^{92m}Nb$" Diplomarbeit, die zur Erlangung des akademischen Grades. Wien April 1990

[8] Lu Hanlin, "Compilation of Measurements and Evaluations of Nuclear Activation Cross Sections for Nuclear Data Applications", INDC(CPR)—16; P. 59, 1989

[9] J. W. Meadows, R. C. Haight, Y. Ikada et al., Contributed paper in Ref. 1 P. 7

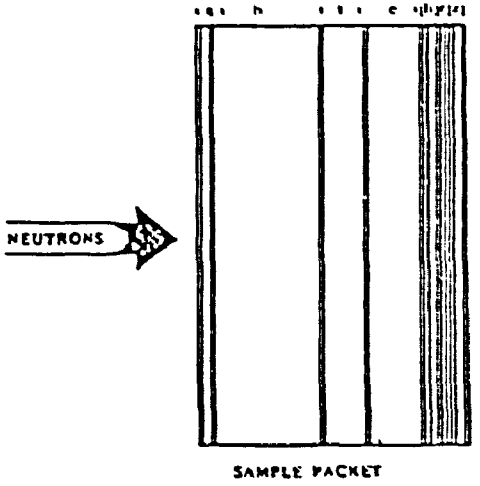

Fig. 1 The samples materials are as follows: i = Au, s = Ag, h = HfO_2, t = Tb_2O_3, e = Eu_2O_3, j = Ni, l = Al, r = Re, z = Zn. The oxide samples are contained in nylon capsules.

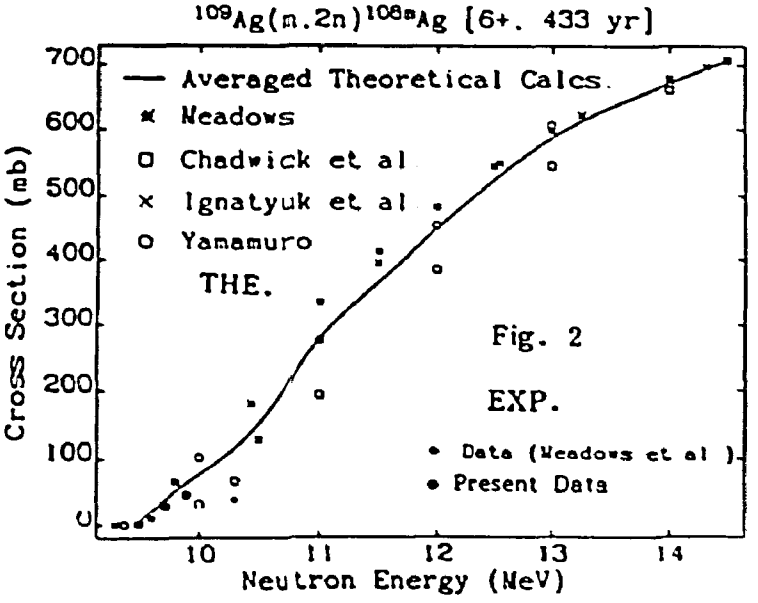

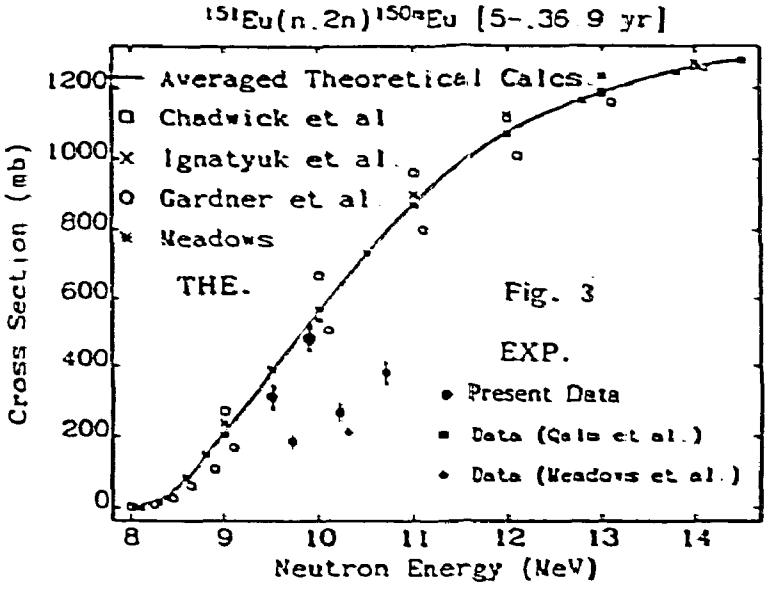

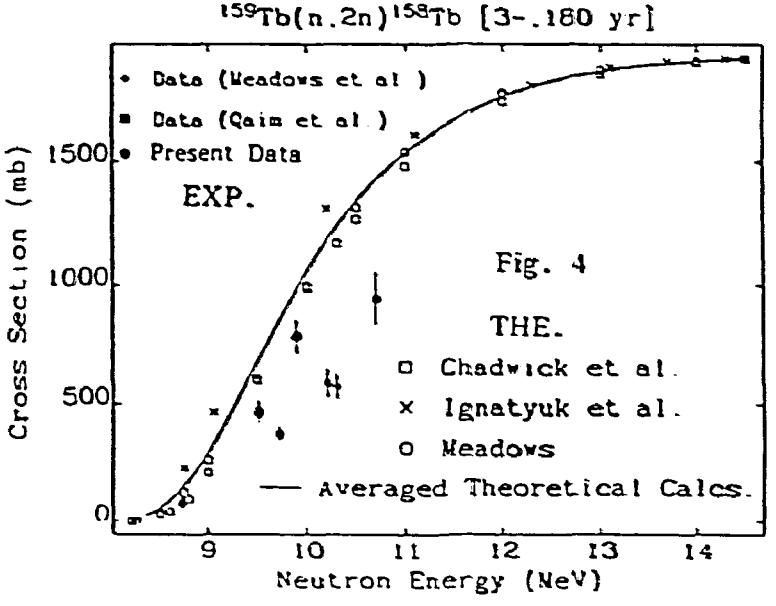

Figs. 2-4 Cross sections calculated and measured

Progress Report on Measurement of Cross Sections for the Formation of some Long-lived Activation Products in Fast Neutron Induced Reactions

S.M. Qaim[1], F. Cserpák[2] and J. Csikai[2]
[1]Institut für Nuklearchemie, KFA Jülich, Germany
[2]Institute of Experimental Physics, Kossuth University,Debrecen. Hungary

Within the last two years following nuclear reactions were investigated.

$^{109}Ag(n,2n)^{108m}Ag$ [$T_{1/2}$ = 433 y; γ_S: 434 keV (90.5%), 614 keV (89.8%, 723 keV (90.8%)]

Highly enriched ^{109}Ag (99.26%) powder was pressed at 10 t cm^{-2} to obtain a thin pellet of 13 mm diameter (wt. ≈ 160 mg). Three such pellets were prepared. Each pellet was sandwiched between two Al monitor foils and irradiated for about 25 h with neutrons from a dd gas target at the variable energy compact cyclotron CV 28 at KFA Jülich. In one case the primary deuteron energy was 8.25 MeV and in the other 9.62 MeV. The third sample was irradiated with background neutrons (E_d = 8.94 MeV and gas cell evacuated).

The radioactivity was determined via γ-ray spectrometry using a stable low background HPGe detector system. Each sample was counted for about three weeks. The areas under the above mentioned three peaks were determined (and agreed within ≈ 8%). The activation through background neutrons was found to be < 5%, i.e. within the error limits of the measured peak areas. The ϕ_{th} was determined via the $^{109}Ag(n,\gamma)^{110m}Ag$ process and amounted to < 1% of ϕ_{fast}. The interference from the $^{107}Ag(n,\gamma)^{108m}Ag$ process to the $^{109}Ag(n,2n)^{108m}Ag$ reaction was found to be < 0.5%.

The measured results are given in Table 1 and the excitation function in Fig. 1. Besides our own data, the evaluated value at 14.5 MeV [Ref. 1] and a recent experimental value (Weixiang et al. [Ref. 2]) in the low energy region are also shown. The averaged calculated curve [Ref. 3] is reproduced for comparison. The experimental and theoretical data appear to agree well.

Table 1. **Measured cross sections near reaction thresholds**

$^{109}Ag(n,2n)^{108m}Ag$†		$^{151}Eu(n,2n)^{150m}Eu$†		$^{159}Tb(n,2n)^{158}Tb$†	
E_n (MeV)	σ (mb)	E_n (MeV)	σ (mb)	E_n (MeV)	σ (mb)
		9.18±0.14	164±23*	9.18±0.14	333±32*
		9.60±0.14	250±28*	9.60±0.14	547±60*
		10.10±0.14	335±32*	10.10±0.14	828±99*
10.86±0.27	276±36	10.83±0.30	849±102	10.83±0.30	1410±145
		11.20±0.20	952±142		
12.17±0.30	451±58	12.14±0.30	982±127		

† New measurements, unless otherwise stated.
* Recalculated neutron energies and cross sections.

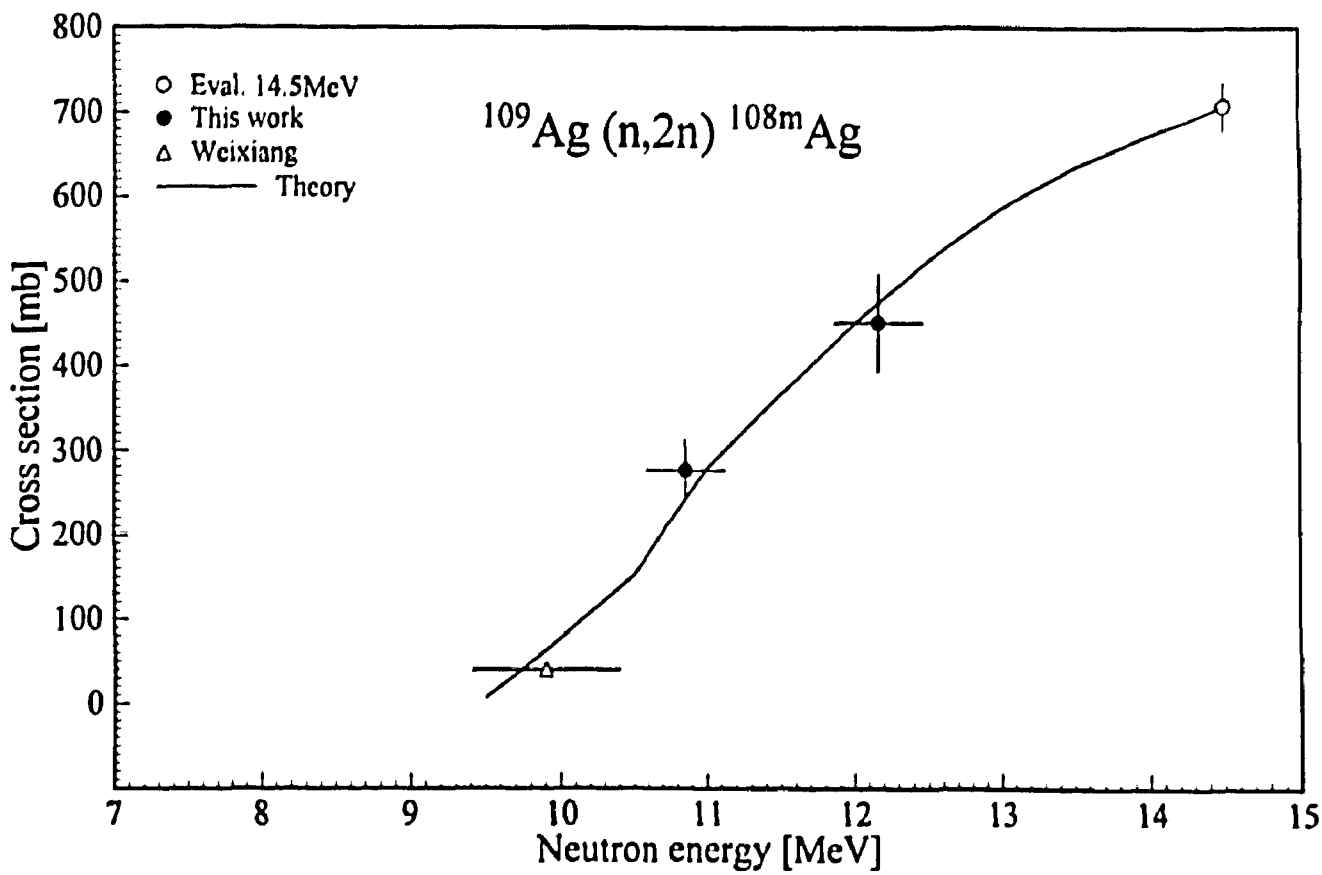

Fig. 1 Excitation function of $^{109}Ag(n,2n)^{108m}Ag$ process

$^{151}Eu(n,2n)^{150m}Eu$ [$T_{1/2}$ = 36.9 y; γ_S: 334 keV (96.0%), 439 keV (80.3%)]

This reaction was investigated by us previously near its threshold [Ref. 4]. However, there appeared to be some discrepancy between the experimental and theoretical data. Since the primary deuteron energies at the compact cyclotron CV 28 were recently redetermined, we recalculated the older data and the results are given in Table 1. In addition, three new Eu_2O_3 samples in the form of 2 cm ∅ x 0.4 cm thick pellets, each placed in an Al-capsule and sandwiched between two Al foils, were irradiated for about 25 h with neutrons produced via deuteron beams from the cyclotrons CV 28 at Jülich and MGC-20 at Debrecen. The radioactivity of ^{150m}Eu was determined via γ-ray spectrometry. In the present case, it was easier to measure the activity since the samples had better dimensions than the previously used extended samples [4]. The results of these new measurements are also given in Table 1. All the recent experimental results in the energy region up to 12 MeV (this work and [Ref. 2]) as well as the evaluated value at 14.5 MeV [Ref. 1] are reproduced in Fig. 2 together with the averaged calculated curve [Ref. 3]. There is still some disagreement between the experimental and theoretical data in the low energy region but, in general, now there appears to be no serious discrepancy.

$^{159}Tb(n,2n)^{158}Tb$ [$T_{1/2}$ = 180 y; γ: 944 keV (43.9%)]

This reaction was also investigated by us previously [Ref. 4]. However, similar to the $^{151}Eu(n,2n)^{150m}Eu$ reaction discussed above, there was some uncertainty in the primary deuteron energy, resulting in some discrepancy between the experimental and theoretical cross section data. The older data, except the lowest energy point, were therefore recalculated and the results are given in Table 1. The lowest energy point had such an increased error that it appeared meaningless to include it in the present evaluation. In addition to the reappraisal of the older measurements, a new Tb_4O_7 sample in the form of a 2 cm ∅ x 0.4 cm thick pellet was placed in an Al-capsule and sandwiched between two Al foils. Irradiation was done for about 26 h with neutrons using a primary deuteron energy of 8.25 MeV. The measurement of radioactivity via γ-ray spectrometry was again easier than in the case of extended samples used earlier [Ref. 4]. The result of the new measurement is also given in Table 1. All the recent experimental results in the energy region up to 12 MeV (this work and [Ref. 2]) as well as the evaluated value at 14.5 MeV [Ref. 1] are reproduced in Fig. 3 together with the averaged calculated curve [Ref. 3]. The experimental and theoretical data appear to be in good agreement, though below 10 MeV some deviation still exists.

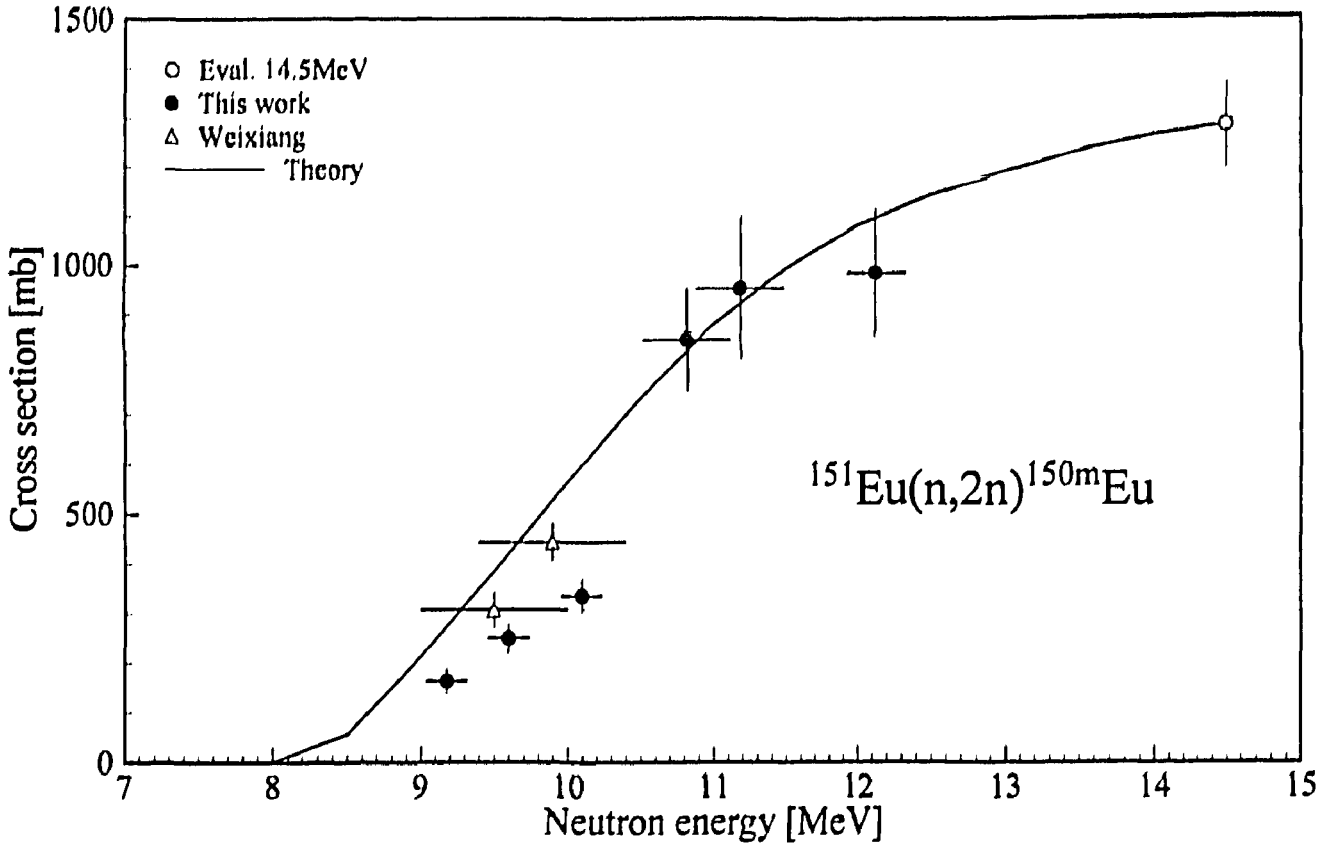

Fig. 2 Excitation function of $^{151}Eu(n,2n)^{150m}Eu$ process

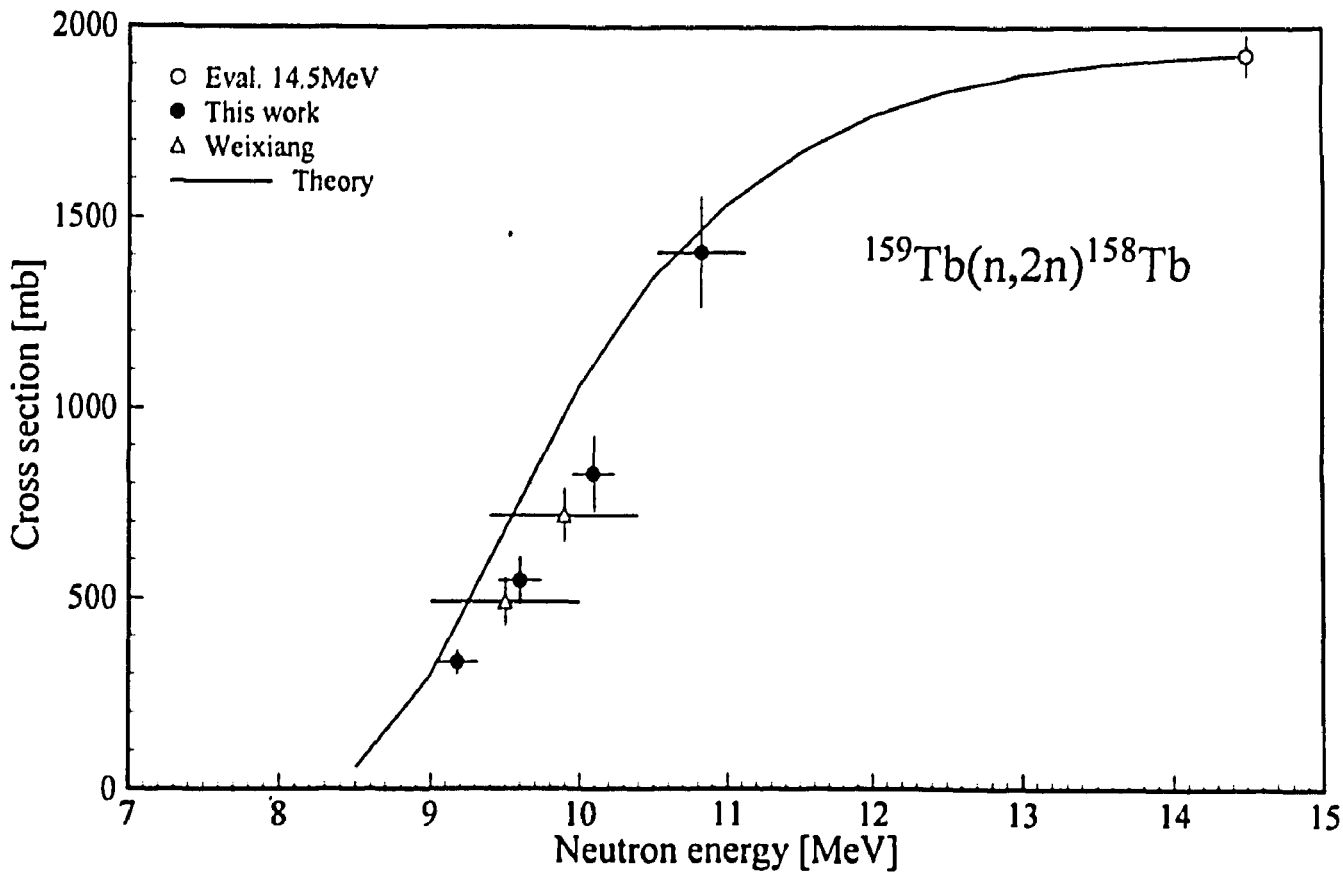

Fig. 3 Excitation function of $^{159}Tb(n,2n)^{158}Tb$ process

$^{63}Cu(n,p)^{63}Ni$ [$T_{1/2}$ = 100 y; E_{β^-} = 66 keV, I_{β^-} = 100%]

Thick Cu-samples irradiated with 7 - 10 and 14.7 MeV neutrons were chemically processed and low-level β^- counting is in progress. However, more time is needed to complete these measurements.

References

[1] H. Vonach and M. Wagner, Proc. 2nd Research Coordination Meeting, Del Mar, 1993, page 67.

[2] Yu Weixiang, Zhao Wenrong, Cheng Jiangtao and Lu Hanlin, Beijing, PR China, Preprint, October 1994.

[3] M.B. Chadwick, M. Gardner, D. Gardner, O.T. Grudzevich, A.V. Ignatyuk, J.W. Meadows, A. Pashchenko, N. Yamamuro and P.G. Young, Preprint UCRL-JC-115239, September 1993.

[4] S.M. Qaim, F. Cserpák and J. Csikai, Appl. Radiat. Isot. 43, 1065 (1992).

XA9642376

Presented at 3rd IAEA RCM on "Activation Cross Sections for the Generation of Long-Lived Radionuclides of Importance in Fusion Reactor Technology", St. Petersburg, Russia, 19-23 June 1995

MEASUREMENT OF CROSS SECTIONS OF SOME REACTIONS OF IMPORTANCE IN FUSION REACTOR TECHNOLOGY

M.V.Blinov*, S.V.Chuvaev, A.A.Filatenkov, V.A.Jakovlev, A.A.Rimski-Korsakov

V.G.Khlopin Radium Institute, St.Petersburg, 194021, Russia

Abstract

The Ag-109(n, 2n)Ag-108m, Eu-151(n, 2n)Eu-150 and Eu-153(n, 2n)Eu-152 cross sections have been measured in the neutron energy interval of 13.7 - 14.9 MeV. The measurements were performed at the neutron generator NG-400 of the Radium Institute using (D-T) neutrons. At the same facility, the W-182(n, n'α)Hf-178m2, Bi-209(n, 2n)Bi-208 and Bi-209(n, 3n)Bi-207 cross sections have been measured at the neutron energy 14.8 MeV. The isomeric ratios for the reactions Eu-151(n, 2n)Eu150m,g, Eu-153(n,2n)Eu-152m,g and Re-185(n,2n)Re-184m,g were obtained at neutron energies around 14 MeV. Neutron capture of the Mo-98 that lead ultimately to the production of the long-lived Tc-99 has been studied at neutron energies 0.7 - 2.0 MeV. For these purposes, the Van de Graaf accelerator (EG-5) was employed that produced monochromatic neutrons in the (p-T) reaction. Both at EG-5 and NG-400 measurements, special efforts were made to minimize neutron spectrum impurities. The neutron spectra inside the samples were calculated taking into account the real geometry of the experiment.

* This work was carried out under IAEA scientific agreement No. 5677

1.Introduction

A growing social thrill for ecological problems demands an especial attention to the disposal of radioactive waste, among which long-lived radionuclides are of great importance [1]. Recently, an IAEA CRP was established that is devoted to calculations and measurements of long-lived radioactivity produced in the fusion reactor. In view of the high complexity of similar investigations, the needed data were extremally poor up to the last time [2].

One of the main experimental difficulties is the necessity to work with rather weak activities hidden usually in a much more intensive background. For measurements of corresponding cross sections, high power neutron sources seem to have an obvious advantage because they spare the time of sample irradiation and activity measurement, and besides, allow to diminish to some extent uncertainties caused by finite sizes of samples and detectors.

However, high power neutron sources, as a rule, generate neutrons of spectra which are studied not so well as, for example, spectra of neutrons produced by conventional neutron generators. So in the cases when the cross sections to be measured change rapidly in the covered neutron energy interval, this may lead to somewhat ambiguous results (e.g. in region near the reaction threshold). An additional uncertainty emerges when the measured or interfering cross sections have a much higher value at the lower neutron energies (e.g. the (n, γ)-reaction), where scattered neutrons can produce considerable effects which are difficult to correct for. In the similar situation, the low current accelerators should be prefered where rather pure neutron fields can be generated.

Among the cross sections measured by us in the frame of this agreement, two were expected to have high sensitivity to contaminations of neutron spectra, namely, the Eu-153(n, 2n)Eu-152 and Mo-98(n, γ)Mo-99 cross sections. To measure them correctly, we used thin wall constructions and air cooling of the target. The special computer codes were created to calculate real parameters of the neutron field during irradiation.

2.Experimental proceedures

2.1. Sample preparation

In our measurements we used various forms of samples assembled in packages of several types. In the Mo-98(n, γ) reaction study, metallic disks of the natural molybdenum 0.3 mm thick and 14.1 mm in diameter were used. Each of them was installed in the middle of an assembly which also contained pairs of the Au- and In-foils used as neutron flux monitors. The total thickness of the assembly was 1.5 mm.

The Ag-109(n, 2n)Ag-108m cross section were measured with two types of sample packages. The first used the enriched Ag-109 (99.4%). This was a metallic powder encapsulated in a lavsan packet and arranged in a thin-wall plastic tube together with two similar packets containing the enriched europium isotopes (see below). In front and in the back of the packets, the niobium foils were mounted to determine the neutron flux. Typically, such a sample package was 14.5 mm in diameter and 7 mm in hight.

The other type of samples used in the Ag-109(n, 2n) experiment was a metallic foil of natural silver sandwiched between the niobium foils. This sandwich was 0.7 mm thick and 14.1 mm in diameter.

For the Eu-151(n, 2n)Eu-150 and Eu-153(n, 2n)Eu-152 cross section measurement, also two variants of samples were prepared. The first contained oxides of the enriched Eu-151 (97,5%) and Eu-153 (99.2%) as well as the enriched metalic Ag-109 (see above). Three packets with distinct isotopes were placed in a plastic tube parallel to each other. The common neutron flux was determined by the niobium foils framing the packages.

In the second variant, the oxide of the natural europium was thoroughly mixed with the niobium oxide. The use of a homogeneous mixture of the studied and reference nuclei reduced considerably the uncertainties connected with the geometrical factor in irradiation and activity measurement. Each sample weighed about 1 g. The ratios of the Eu-153-, Eu-151- and Nb-93-nuclei were 4.63 : 4.24 : 1.

Since the W-182(n, n'α)Hf-178m2 cross section was expected to be very small, the close geometries of irradiation and measurement are highly desirable. Therefore, a homogenious mixture of tungsten acid and niobium oxide was used initially.The total weight of this sample was 12.9 g, and it contained 14.4 nuclei of W-182 per a Nb-93 nucleus.

As before, another type of sample package was used for this cross section measurement too. Ten metallic foils of the natural tungsten were placed close to the neutron target. The eleventh foil was sandwiched between two niobium foilsand distanced from the target at 42 mm. This was used to obtain in the same experiment the W-182(n, 2n)W-181 cross section, relative to which the W-182(n, n'α) cross section could be determined most convenient. The size of each W-foil was 11 mm *0.1 mm.

The Re-187(n, 2n)Re-186m and other reactions on the Re-isotopes were measured with samples prepared by pressing the powder of the K_2ReCl_6 salt under the pressure of 200 atmosphere. This procedure was used also for preparation the Bi-samples from the oxide Bi_2O_3. The samples were 14.1 mm in diameter an about 2 mm in thickness.

2.2. Irradiation conditions

The Mo-98(n, γ)Mo-99 reaction was studied in the 0.7 - 2.0 MeV neutron energy range. Irradiations were conducted using monochromatic neutrons of the $^{3}H(p, n)^{3}He$ reaction. The proton beam diameter of the Van de Graaf accelerator was about 2 mm. During irradiation the beam was rotated drawing a circle with the diameter up to 8 mm on the titanium-tritium target. Since the target was cooled by an air jet, the beam current was restricted by the magnitude of 8 μA.

The sample package contained the Mo-, Au- and In-foils was located at 0 deg with respect to the incident beam direction and 23 mm from the target. The irradiations were performed at proton energy of 1.6, 2.1, 2.3, 2.6 and 2.8 MeV that corresponded to the mean neutron energy of 0.74, 1.26, 1.46, 1.76 and 1.97 MeV. The neutron energy spread (FWHM) resulted from proton slowing-down in the target and angular dependence of neutron energy was 0.12, 0.11, 0.10, 0.10 and 0.09MeV, respectivelly. These quantities were calculated using the recommended c.m.s. data on the (p-T)-reaction kinematics [1] and the sheets of charged particle energy losses in materials [2].

The samples were irradiated usually 12 hours, accumulating neutron fluence (3 - 5)*10^{12} n/cm^2. Small neutron flux variations were registered by means of a long counter.

The Ag-109(n, 2n)Ag-108m, Eu-151(n, 2n)Eu-150, Eu-153(n, 2n)Eu-152, W-182(n, n'α)Hf-178m2, Re-187(n, 2n)Re-186m and Bi-209(n, 2n)Bi-208 cross sections were measured at the neutron generator NG-400 using the H-3(d, n)He-4 reaction neutrons.Irradiations were carried out at the accelerating voltage varied from 220 to 280 kV. The mean neutron energy determined mainly by the angle relative to the deuteron beam line was ranged from 13.6 to 14.9 MeV.

At the study of the Ag-109(n, 2n), Eu-151(n, 2n) and Eu-153(n, 2n) reactions, sample packages were placed at different angles at the distance of 3 - 4 cm from the target. The total neutron fluence collected by a sample was (2 - 5)*10^{12} n/cm^2.

In the case of the W-182(n, n'α), Re-187(n, 2n)Re-186m and Bi-209(n, 2n)Bi-208 cross section measurement, the samples occupied a position close to the target at 0 degrees relative to the beam. The water cooling of the target was used. The mean value of the neutron fluence recieved by the sample was ~ 10^{14} n/cm^2.

2.3. Activity measurement

The induced gamma-activities were measured with a Ge(Li)-detector having the energy resolution 2.7 keV and peak efficiency 7.9% at 1332.5 keV gamma-ray energy. A computer DVK-3M fitted for on line data acquisition was provided with a program set adapted for gamma-activation analysis.

The gamma-spectrometer efficiency was determined by means of standard gamma-sources, activities of which were attestated with error of 1.5 - 2.0% at the confidence probability of 0.99. The calibrations were periodically repeatet showing constancy of the efficiency value in bounds of 0.5% for the gamma-ray energy range 200-3000 keV.

Corrections for gamma-ray self-absorbtion and the change of the effective distance between the sample center and the detector center were measured experimentally. Besides, we were able to deduce these corrections using the code aimed to the volume gamma-activity measurement that yielded fairly close results. Typically, those were of order of several percent, though in individual cases they could exceed 40% (the large homogenious tungsten sample).

2.4. Neutron field calculation

In work [5], an exact analytical expression of the geometrical efficiency of a parallel disk neutron producing target and sample system has been deduced. In this work the expression is presented in more geometrically clear form with the further simplifications

$$\frac{d\Omega}{d\theta}(\theta) = \frac{d\Omega_0}{d\theta}(\theta) \cdot \frac{S_{t\text{-}s}}{S_t}, \qquad [sr/rad] \tag{1}$$

where $\frac{d\Omega_0}{d\theta}(\theta) = 2\pi \sin\theta$ is the geometrical efficiency for the point target geometry; $S_{t\text{-}s}$ is the area of covering surface of the target and sample circles when one of them shifted from the central axis by the distance equal to $r = h \cdot tg\theta$ and projected on the opposite plane (a schematic drawing of the geometry for parallel-disk coaxial target and sample system is shown in Fig. 1.).

The expression (1) can be used for a more common case of the non-coaxial position of sample. In this case, the geometrical efficiency is expressed as

$$\frac{d\Omega}{d\theta}(\theta) = \int_{\alpha_{min}}^{\alpha_{max}} \frac{d^2\Omega}{d\theta d\alpha}(\theta,\alpha) \cdot \Phi(\alpha) d\alpha \tag{2}$$

where $\Phi(\alpha)$ is the part of the circle with the radius R_s intercepted by the sample disk (see Fig. 2).

Using the differential cross section of neutron producing reaction it can be written as

$$\frac{d\sigma}{dE_n}(E_n) = \frac{d\sigma_{cm}}{d\Omega_{cm}}(\theta_{cm}) \cdot f_{ls}^{cm}(\theta) \cdot \frac{d\Omega}{d\theta}(\theta) \cdot \frac{d\theta}{dE_n}, \tag{3}$$

where $f_{ls}^{cm}(\theta)$ is the factor for transferring cm-cross-section into ls-one. Parameters in equation (3) as function of E_n and E_d can be deduced with the well-known relations of the relativistic kinematics.

Modeling the realistic primary neutron spectra it is necessary to take into account the depth distribution of neutron producing nuclei in target layer, the processes of slowing down and scattering (straggling) of initiate particles depending, in turn, on the depth composition of the target layer.

The depth distribution of tritium in the absorption layer of the target was studied in works [6,7]. The dependence of tritium distribution on depth, x, was approximately the same in both works for the layer thickness from 0.5 to 1.1 mg/cm^2 and was proportional to $x^3 \cdot e^{-x}$ with the maximum at $x \approx 0.3$ of the total thickness of absorbing layer.

In recent time the stopping power tables of Andersen-Ziegler [8] and Northcliffe-Schilling [9] are widely used at the slowing down calculations. The stopping power data from these tables are quite good compatible in the proton energy range more than several MeV. However, at the projectile energy less than 0.5 MeV, the discrepancy of these data large. So, the stopping power values from [8] are higher than values from [9] in several times for hydrogen and on 30% for titanium.

The energy and angle straggling dispersions in dependence on depth, x, were calculated in frame of the transport theory [10]

$$\sigma_{E_d}^2(x) = E_d^{o2} \cdot \frac{m_e}{m_d} \cdot \frac{1-(1-\xi)^2}{2(1-\xi)} \cdot \frac{1}{L_{ion}} \tag{4}$$

and

$$\sigma_\theta^2(x) = \pi^2 \cdot \ln\frac{1}{1-\xi} - \sqrt{\frac{m_e}{\pi m_d L_{ion}}} \cdot \frac{\xi}{1-\xi} \cdot \sqrt{\frac{\xi}{2-\xi}} \tag{5}$$

where E_d^0 is deuteron energy on the target surface; m_e and m_d are masses of electron and deuteron, respectively; $\xi = x/R_d$, R_d is deuteron range in absorption layer of the target; L_{ion} is the ionization logarithm (in this work it is deduced with tables from [8,9] and well-known Bethe formula for stopping power); $\varkappa^2 \approx (Z+1)\cdot\frac{m_e L_k}{m_d L_{ion}}$; $L_k \approx \ln\left[210\cdot(A\cdot Z)^{-1/6}\right]$ is the Coulomb logarithm.

On the basis of calculations of neutron spectra from the T(d,n)^{4}He reaction made with a SPECTRON computer code we can do following conclusions:

1) the depth distribution of tritium essentially influences on shape of neutron spectra;

2) if different tables are used for the stopping power then the average value of neutron fluence is changed only (the difference between the average neutron energy is less than 5 keV for to the 0^0 and 180 sample position);

3) taking into account of the relativistic effects gives about 50 keV decreasing of neutron energy;

4) straggling effects lead to the smal increasing of the low (high) energy "tail" of neutron spectra if the sample position is $<90^0$ ($>90^0$).

2.5. Cross section computation

Experimental data were processed by an IBM PC using GAMANAL and ACTICS codes. The last was specially written to treat the neutron activation information. It included various libraries, such as energies and yields of the induced gamma-activity, geometries and histories of the conducted irradiations, masses and sizes of the available samples, etc. The cross sections were calculated by the formulas taking into account two generations of the induced radioactivity:

$$\overline{A_B} = \frac{N_{B0}\cdot\lambda_B}{t_2^c - t_1^c}\cdot\int_{t_1^c}^{t_2^c} dt^c \cdot \frac{\int_{t_1^i}^{t_2^i}\Phi_n(t)\cdot e^{-\lambda_B t}\left[1+\frac{\sigma_B}{\sigma_{B^m}}\cdot\frac{\lambda_B}{\lambda_B-\lambda_{B^m}}\left(e^{-\lambda_{B^m}t}-e^{-\lambda_B t}\right)\right]\cdot dt}{\int_{t_1^i}^{t_2^i}\Phi_n(t)\cdot dt}, \quad (6)$$

where N_{B0} - the total number of B nuclei produced during the irradiation; λ_B and λ_{B^m} are decay constants of B and B^m nuclei, respectively; (t_1^c, t_2^c) - the counting interval; (t_1^i, t_2^i) - the irradiatio

n one; Φ_n - integrated fluence of neutrons; σ_B and σ_{B^m} are cross sections of nuclear reactions A(n, x)B and A(n, x)B^m, respectively.

In order to decrease the errors due to poor statistics of the treated gamma-spectra, the mean weighted values of the cross sections were obtained using data on all the observable gamma-peaks. The main errors of the experimental results were the following: the uncertainties of the fluence measurement - (2 - 5)% and the uncertainties of the induced activity determination (2 - 40)%.

3. Results

The following reactions were studied in the present work:

Reaction	Neutron energy
$^{98}Mo(n, \gamma)^{99m}Mo$	0.74 - 1.97
$^{109}Ag(n, 2n)^{108m}Ag$	13.70 - 14.90
$^{151}Eu(n, 2n)^{150g}Eu$	13.52 - 14.90
$^{151}Eu(n, 2n)^{150m}Eu$	13.52 - 14.90
$^{153}Eu(n, 2n)^{153g}Eu$	13.52 - 14.90
$^{153}Eu(n, 2n)^{153m}Eu$	13.52 - 14.90
$^{182}W(n,n'\alpha)^{178m2}Hf$	14.74
$^{185}Re(n, 2n)^{184g}Re$	14.74
$^{185}Re(n, 2n)^{184m}Re$	14.74
$^{187}Re(n, 2n)^{186g}Re$	14.85
$^{187}Re(n, \alpha)^{184}Ta$	14.85
$^{187}Re(n, 2n)^{187}W$	14.85
$^{209}Bi(n, 2n)^{208}Bi$	14.74
$^{209}Bi(n, 3n)^{207}Bi$	14.74

The reference data on the studied reactions and associated decay data of products are presented in Table 1. The results of the cross section measurements are given in Fig. 1 - 6 and in Tables 2 - 5.

References

1. E.Cheng, Proc. IAEA Advisory Group Mtg. on Nucl Data for Fusion Reactor. Techn. FRG 1986. IAEA TECDOC-457 IAEA Vienna p.16 (1988).
2. E Cheng, Nucl. Data for Science and Technology (Proc. of the Intern. Conf. MITO 1988, JAERI 1988 p.187.
3. M.Drosg, O.Schwerer, In: Handbook on Nuclear Activation Data Techn. rep. ser. N273 IAEA Vienna (1987).
4. L.C.Northcliffe, R.F.Shilling, NDT A7 (1970) p. 233.
5. V.A. Jakovlev. Analytical Expression of the Fast Neutron Energy Spectrum at the Finite Geometry of Experiment. Preprint ĐÉ-211, Moscow, TsNIIatominform, 1988, 12 p.
6. E.M. Gunnersen, G. James, Nucl. Instr. Meth. 8, 173 (1960).
7. S.M. Kabir, Nucl. Instr. Meth. 109, 533 (1973).
8. H.H. Andersen, J.F. Ziegler. Hydrogen Stopping Powers and Ranges in All Elements (Pergamon Press, New York. 1977).
9. L.C. Northcliffe and R.F. Schilling. Range and Stopping Power Tables for Heavy Ions. Nucl. Data Tables A7, 233 (1970).
10. V.S. Remizovich, D.B. Rogozkin and M.I. Riazanov. Fluctuation of Charged Particle Ranges. Moscow, Energoatomizdat, 1988, 240 p.

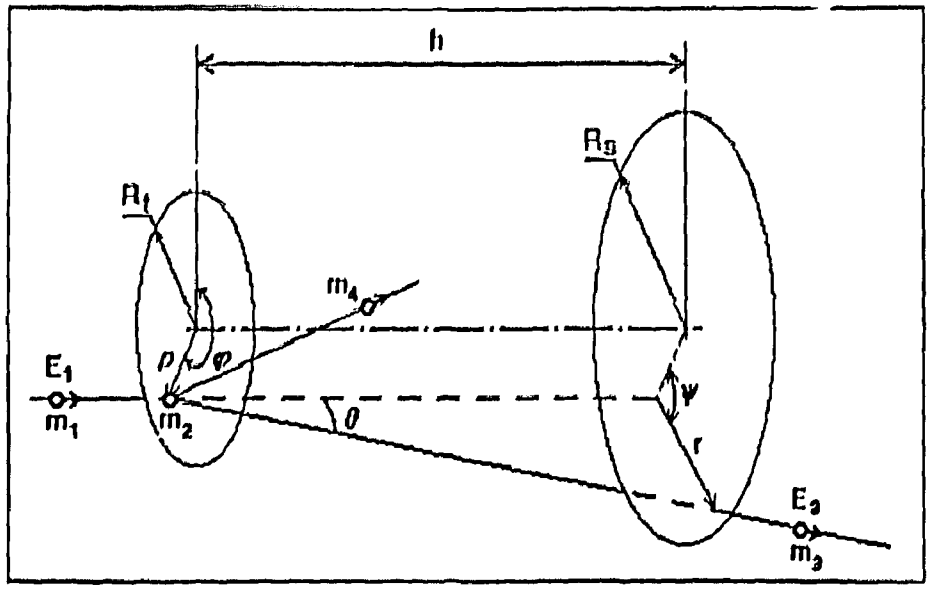

Fig 1. Geometry for coaxial parallel-disk target and sample system.

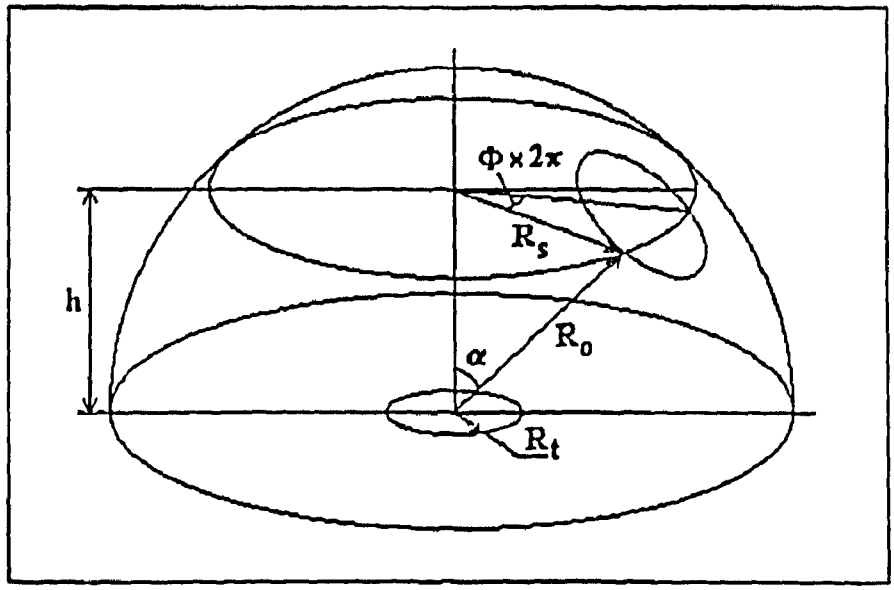

Fig 2. Geometry for non-coaxial disk target and sample systen.

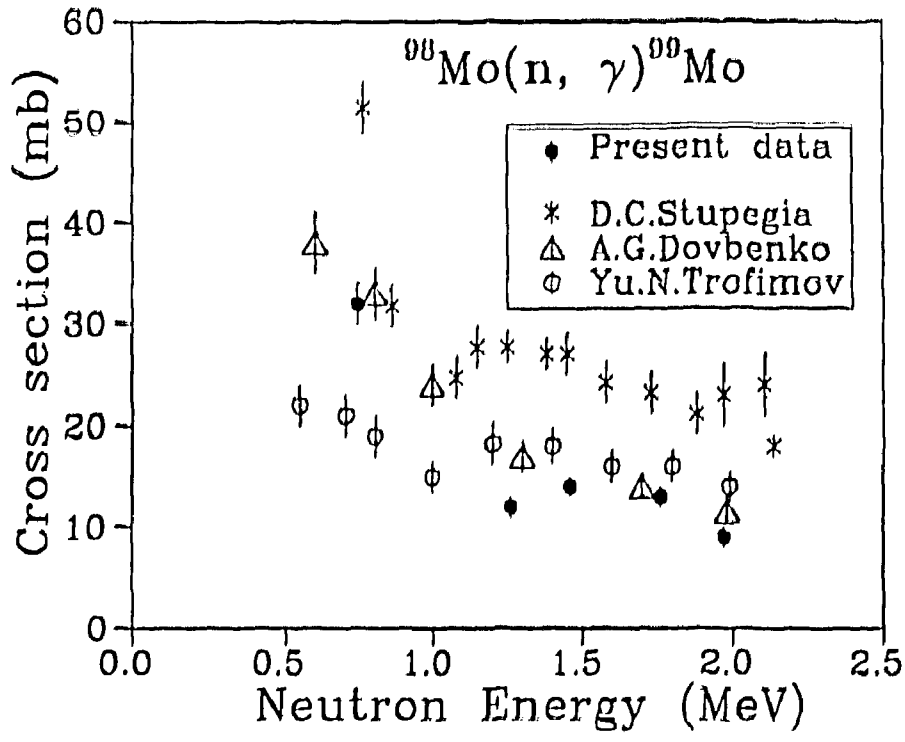

Fig. 3. Cross-section data for ^{98}Mo(n, γ)^{99}Mo.

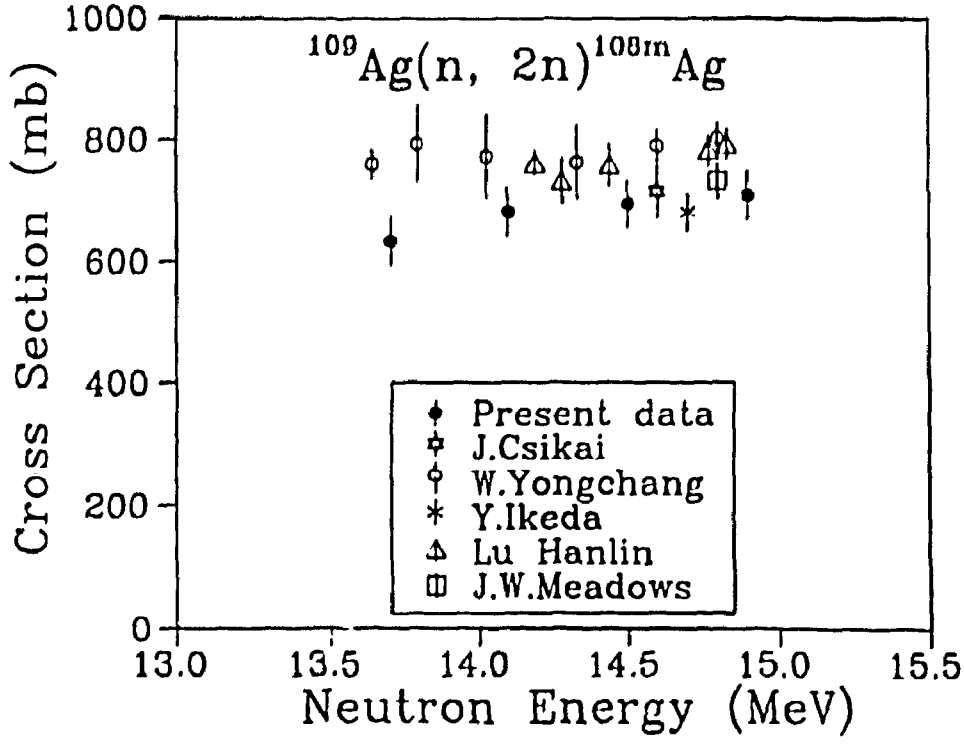

Fig. 4. Cross-section data for ^{109}Ag(n, 2n)^{108m}Ag.

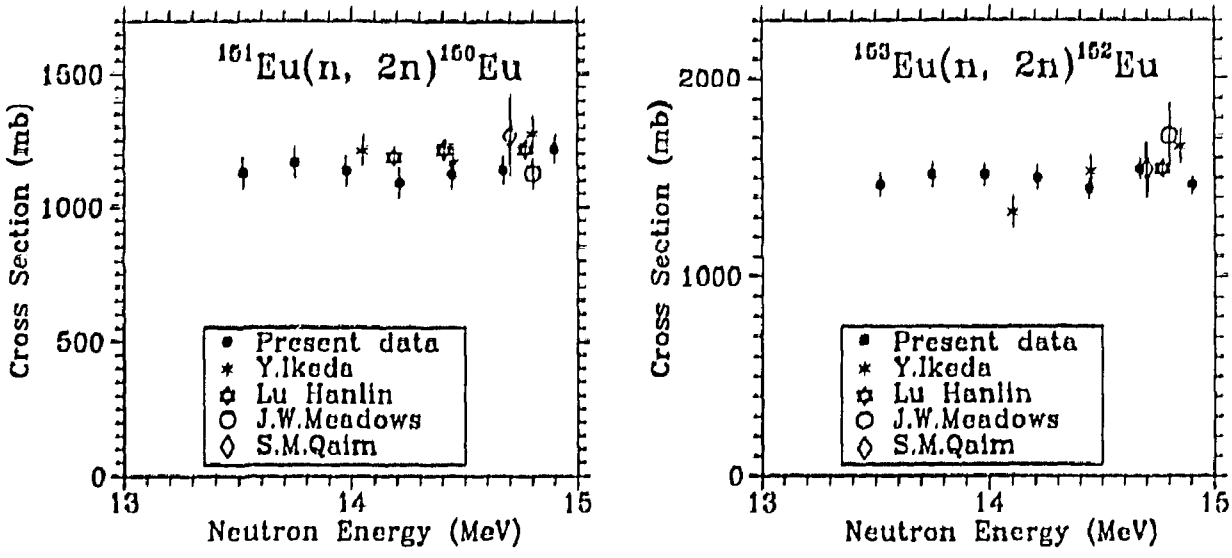

Fig. 5. Excitations functions of the ^{151}Eu(n, 2n)^{150}Eu and ^{153}Eu(n, 2n)^{152}Eu reactions in the 14 MeV region.

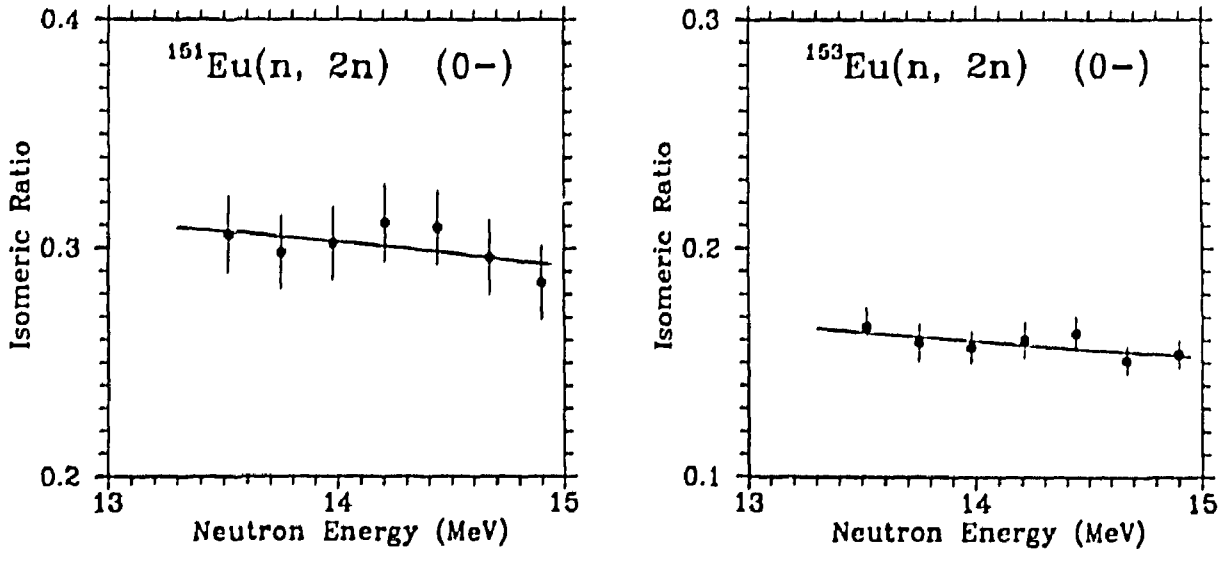

Fig. 6. Isomeric ratios for the 0$^-$ states of the Eu-isotopes. The straight lines were drawn through the data by means of the least square method. Their parameters are:

IR(Eu-151)=0.435-0.00947*E_n[MeV];
IR(Eu-153)=0.264-0.00745*E_n[MeV].

Table 1. Decay data used in this work.

Nuclear reaction	Q-value (MeV)	Init. spin	Final spin	Half-life	E_γ (keV)	Brancing ratio(%)
$^{98}Mo(n, \gamma)^{99}Mo$	+5925.	0^+	$1/2^+$	65.94(1)h	140.5	89.4(2)
$^{109}Ag(n, 2n)^{108m}Ag$	-9.186	$1/2^-$	6^+	433(15)y	433.9	90.5(6)
					614.3	89.8(19)
					722.9	90.8(19)
$^{151}Eu(n, 2n)^{150}Eu$	-7.935	$5/2^+$	5^-	35.80(10)y	334.0	96.0(30)
					439.4	80.4(34)
$^{153}Eu(n, 2n)^{152m2+g}Eu$	-8.553	$5/2^+$	3^-	13.54(1)y	121.8	28.40(23)
					244.7	7.51(7)
					344.3	26.58(19)
					778.9	12.96(7)
					1112.1	13.54(6)
					1408.0	20.85(8)
$^{182}W(n, n\alpha)^{178m2}Hf$	-1.773	0^+	16^+	31(1)y	325.6	94.1(18)
					426.4	96.9(20)
					495.0	71.4(22)
					574.2	89.1(20)
$^{209}Bi(n, 2n)^{208}Bi$	-7.453	$9/2^-$	5^-	368000(4000)y	2614.5	100.0
$^{209}Bi(n, 3n)^{207}Bi$	-14.35	$9/2^-$	$9/2^-$	32.2(9)y	569.7	97.8(4)
					1063.7	74.08(25)
$^{185}Re(n, 2n)^{184m}Re$	-7.87	$5/2^+$	8^+	165(5)d	104.7	13.3(4)
					161.3	6.64(22)
					536.7	3.37(11)
					920.9	8.30(30)
$^{185}Re(n, 2n)^{184g}Re$	-7.68	$5/2^+$	3^-	38.0(5)d	111.2	17.1(7)
					641.9	1.94(5)
					894.8	15.6(4)
$^{187}Re(n, 2n)^{186g}Re$	-7.371	$5/2^+$	1^-	90.64(9)h	137.2	8.6(3)
$^{187}Re(n, \alpha)^{184}Ta$	7.102	$5/2^+$	5^-	8.7(1)h	414.2	73.9(9)
$^{187}Re(n, p)^{187}W$	-0.529	$5/2^+$	$3/2^-$	23.9(1)h	479.6	21.1(9)
					685.7	26.4(11)

Table 2. Cross sections data for the $^{98}Mo(n, \gamma)^{99}Mo$ reaction.

E_n (MeV)	Cross Section (mb)
0.74	32(2)
1.26	12(1)
1.46	14(1)
1.76	13(1)
1.97	9(1)

Table 3. Cross sections data for the $^{109}Ag(n, 2n)^{108m}Ag$ reaction.

E_n (MeV)	Cross Section (mb)
13.7	634(39)
14.1	682(40)
14.5	695(40)
14.9	709(41)

Table 4. Activation cross sections and isomeric ratios for the $^{151}Eu(n2n)^{150}Eu$ and $^{153}Eu(n2n)^{152}Eu$ reactions.

E_n (MeV)	Cross Section (mb)	
	$^{151}Eu(n2n)^{150}Eu$	$^{153}Eu(n2n)^{152}Eu$
13.52	1127(66)	1464(54)
13.75	1167(63)	1515(59)
13.98	1139(65)	1516(53)
14.21	1092(67)	1500(61)
14.44	1126(60)	1445(52)
14.67	1140(57)	1545(49)
14.90	1218(56)	1460(44)

E_n (MeV)	Isomeric Ratio	
	$^{151}Eu(n,2n)$ (0^-)	$^{153}Eu(n,2n)$ (0^-)
13.52	0.316(20)	0.166(4)
13.75	0.307(20)	0.159(8)
13.98	0.312(20)	0.157(7)
14.21	0.321(20)	0.160(8)
14.44	0.318(20)	0.163(7)
14.67	0.305(20)	0.151(6)
14.90	0.295(20)	0.154(6)

Table 5. Other activation cross sections measured in this work.

Reaction	Half-life	Cross section (mb)	E_n (MeV)
$^{182}W(n, n\alpha)^{178m2}Hf$	31(1)y	0.010(6)	14.74
$^{209}Bi(n, 2n)^{208}Bi$	368000(4000)y	2280(370)	14.74
$^{209}Bi(n, 3n)^{207}Bi$	32.2(9)y	0.55(5)	14.74
$^{185}Re(n, 2n)^{184m}Re$	165(5)d	356(33)	14.74
$^{185}Re(n, 2n)^{184g}Re$	38.0(5)d	1484(90)	14.74
$^{187}Re(n, 2n)^{186g}Re$	90.64(9)h	1670(100)	14.85
$^{187}Re(n, \alpha)^{184}Ta$	8.7(1)h	0.59(7)	14.85
$^{187}Re(n, p)^{187}W$	23.9(1)h	3.96(43)	14.85

Analysis of evaluations for Al-27(n,2n), Cu-63(n,p), Dy-158(n,p),W-182(n,n'α) and Ho-165(n,γ)Ho-166m, Ir-191(n, γ)Ir-192m2 Reactions

A.V.Ignatyuk

Institute of Physics and Power Engineering, Obninsk, Russia

O.T.Grudzevich, A.V.Zelenetsky

Institute of Nuclear Power Engineering, Obninsk, Russia

A.B.Pashchenko

International Atomic Energy Agency, Vienna, Austria

Report to the IAEA CRP Meeting on Activation Cross Sections for the Long-Lived Radionuclides Important in Fusion Reactor Technology

S.Petersburg, Russia, 19-23 August 1995

INTRODUCTION

A recent interest in low-activation materials for fusion reactor technology has stimulated the development of activation data libraries with a large number of nuclei and reaction types included. The development of Russian Activation Data Library (ADL) includes the following steps:

1) The first version of ADL-1 (1988) was based on semiempirical description of the threshold reaction excitation functions normalized to experimental data or cross section systematics for 14.5 MeV neutrons. The cross sections for about 3000 threshold reactions were included in this library.

2) The Weiskopf-Ewing approach with a phenomenological account of direct and pre-equilibrium processes was used for calculations of the reaction cross sections for the second version of ADL-2 (1991). The calculated cross sections were fitted to experimental data available. For the most important reactions the Hauser-Feshbach approach was used for cross section calculations and

the neutron capture cross sections based on BROND or EAF-2 evaluations were added to the library. This version contained more than 5000 reactions.

3) It was shown through the activation cross section intercomparision that most of the old evaluations based on simplified approaches like the THRESH do not guarantee a require accuracy of recommended cross sections. We found that many evaluations based on the Weiskopf-Ewing model are not rather accurate too. So the new version ADL-3 was produced on the basis of the consistent Hauser-Feshbach approach. The neutron induced reaction cross sections for all stable and unstable nuclei with half-life exceeding ,5 day were evaluated. The total number of reactions included in ADL-3 is above 33000. The catalog of this library is published in Ref. /1/

In this report the ADL-3 evaluations for the reactions included in the CRP program are considered and compared with other evaluations available.

MAIN FEATURES OF ADL-3 EVALUATIONS

To take into account the angular momentum conservation on all steps of the particle emission we used the modified version of the STAPRE code /2/ in which the phenomenological description of the direct inelastic processes was included /3/.The optical model (SCAT2 code) was used to calculate the transmission coefficients for both incident and emitted particles. The optical potential parameters were adopted to reproduce the available experimental data on the elastic and total cross sections properly.

The gamma-ray transmission coefficients were defined by means of Brink-Axel approach in which for the strength functions of the E1 transitions the standard two-hump Lorentzian was used for deformed nuclei and the generalized Lorentzian of Kopecky-Uhl was adopted for spherical ones /4/. In addition to the E1 radiation, the M1 and E2 transitions were also included with the strength functions recommended by Kopecky-Uhl.

For the level density description the generalized superfluid model was used with parameters obtained from the analysis of the observed density of neutron resonances and the cumulative numbers of low-lying nuclear levels /5/.

For the last years the statistical approach has been applied to the isomer yield calculations by many authors /6-9/. The main uncertainties of such calculations are connected with the description of gamma-transitions between the low- lying levels. As a rule we do not have enough experimental information on all branching ratios for the first twenty or more levels which are crucial for a computation of isomer yields.

To overcome this problem we must prepare more complete schemes of possible gamma-transitions based on theoretical models or realistic empirical systematics of gamma-transitions in neighboring nuclei. The number of levels which have to be added to the observed ones is especially large for the odd-odd nuclei where the long-lived isomers exist as a rule. The important condition of such level schemes is the correspondence of the cumulative number of levels and their spin distribution to the well known level density laws. The branching ratios for all constructed levels may be calculated on the basis of the same model of the radiative strength functions that are used for the description of gamma-transition in continuum. We understand that such an approach does not guarantee the correct description of the individual transition between discrete levels but we hope it could be accurate enough for calculations of gamma-transition integrated characteristics which define the isomer yields. The models proposed in Refs./6-9/ give generally very similar schemes of gamma transitions and the discrepancies between the models mainly relate to different approximations of the Ml and E2 gamma-transition probabilities for the constructed discrete levels.

The typical differences of the reaction cross sections for the ADL-3, EAF-2(3), JENDL-3 and ENDF/B evaluations are demonstrated in Figs. 1 - 11. The agreement of our evaluations and other ones is rather good only for reactions with the adequate experimental data. For the reactions with inadequate experimental data or without any data differences of evaluated cross sections can be very large. Uncertainties of evaluations are especially big for the isomer production cross sections (Figs. 6, 8, 10).

SUMMARY

We suppose that ADL-3 evaluations based on the consistent statistical calculations would be reliable predictions of the reaction cross sections required. A normalizing of the theoretical curves to new experimental data could be very useful for a reduction of uncertainties available.

REFERENCES

1. Grudzevich O.T., Zelenetsky A.V.,.Ignatyuk A.V., Pashchenko A.B. Voprosy Atomnoi Nauki i Tekhniki. Ser. Nuclear Constants, 1993, No 3-4.
2. Uhl M., Stromaier B. Report IRK-76/01, Vienna, 1976.
3. Grudzevich O.T. et al. In: Methods for Calculations of Neutron Nuclear Data for Structural Materials. INDC(NDS)-193/L, Vienna, 1988, p.81.
4. Kopecky Yu., Uhl M. Phys.Rev., C42 (1990) 1941.

5. Grudzevich O.T. et al. In: Nucl.Data for Science and Technolody (Mito, 1988).JAERI, 1988, p.767.
6. Gardner M., Gardner D., Hoft R. Proc. V Symposium on Capture Gamma- Ray Spectroscopy and Related Topics, Knoxville, TN, September 10-14, 1984.
7. Chadwick M.B., Young P.G., Nucl.Sci.and Eng., 108, 117 (1991).
8. Grudzevich O.T.,Zelenetsky A.V., Ignatyuk A.B., Pashchenko A.B. Inter.Conf.on Nucl.Data for Science and Technology (Gatlinburg, 1994). Ed.J.K.Dickens, ORNL, 1994, p.433
9. Qaim S.M. Inter.Conf.on Nucl.Data for Science and Technology (Gatlinburg, 1994). Ed.J.K.Dickens, ORNL, 1994, p.186.
10. Kopecky Yu., Nierop D. Contents of EAF-2. Report ECN-1-91-053, 1991.
11. Nakajima Y. JENDL Activation Cross Section File. Report JAERI-M-032 (1991).

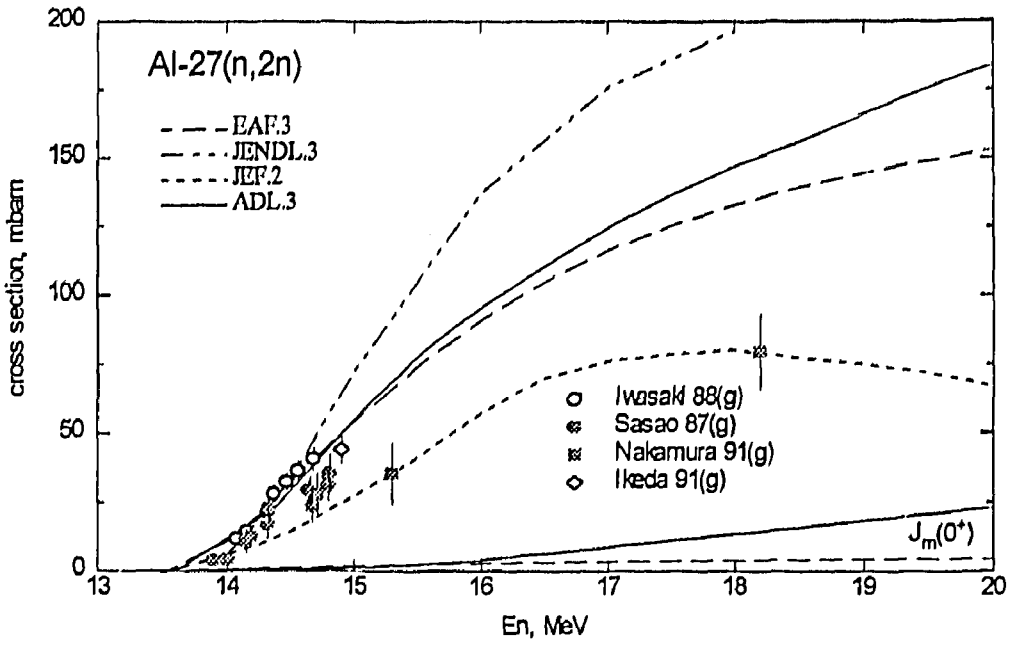

Fig. 1. Evaluations available for the ^{27}Al(n,2n) cross sections in comparision with experimental data.

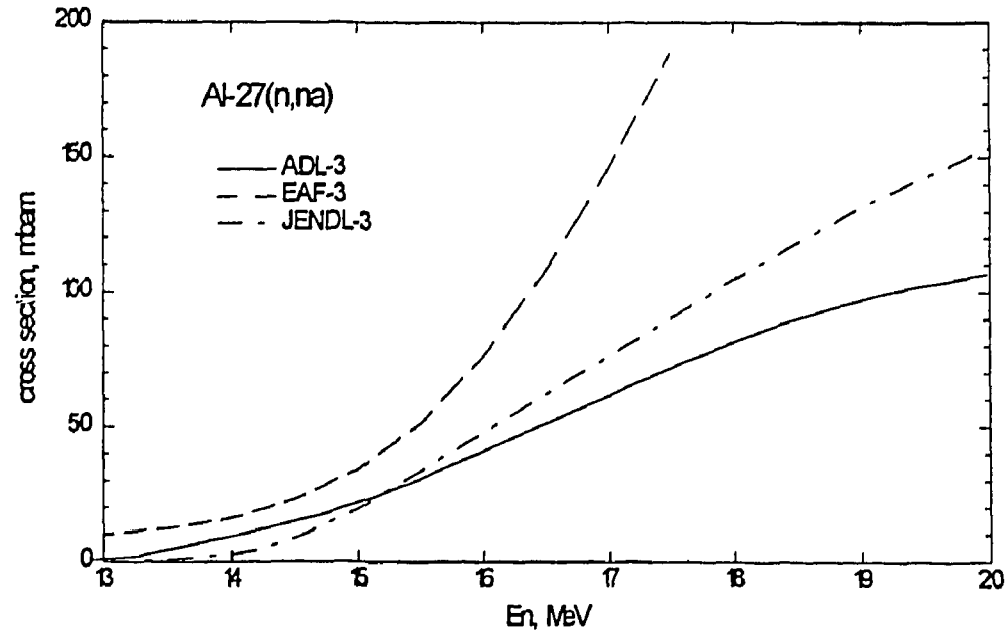

Fig. 2. Evaluations available for the ^{27}Al(n,nα) cross sections.

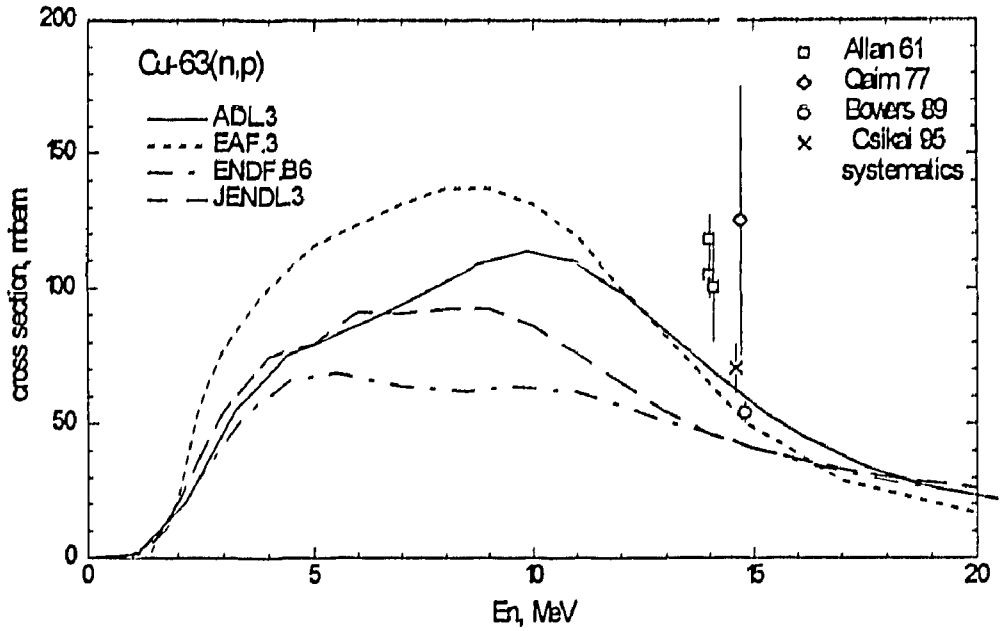

Fig. 3. Evaluations available for the ^{63}Cu(n,p) cross sections in comparision with experimental data.

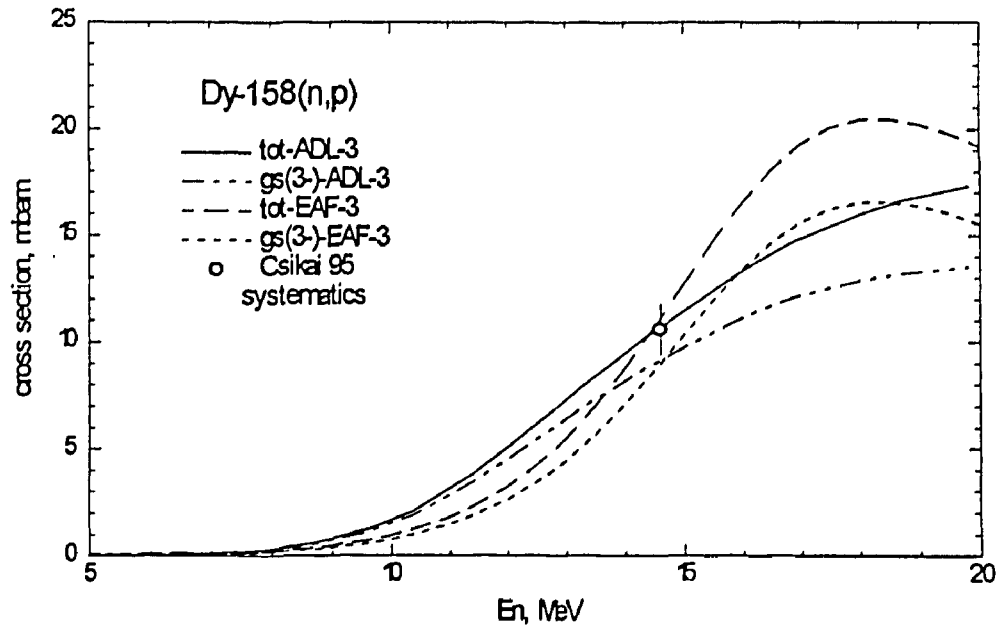

Fig. 4. Evaluations available for the ^{158}Dy(n,p) cross sections.

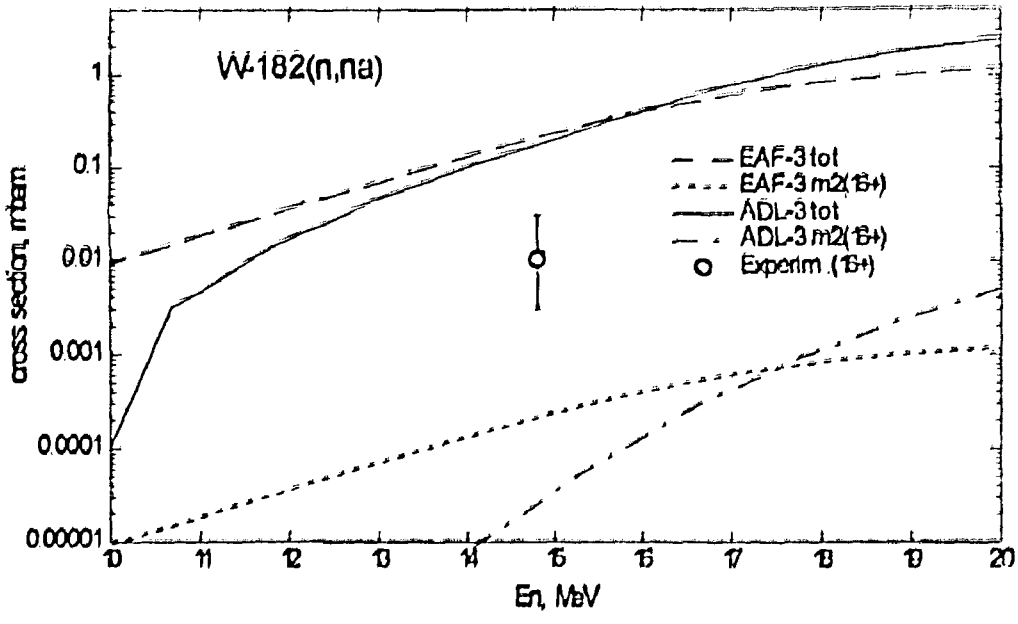

Fig. 5. Evaluations available for the $^{182}W(n,n\alpha)$ cross sections.

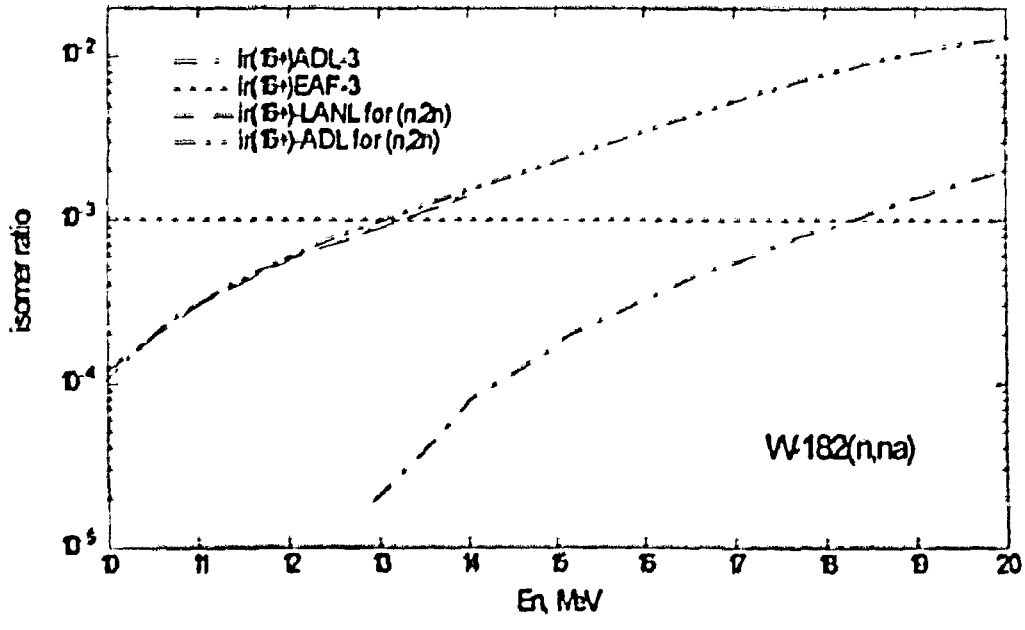

Fig. 6. Evaluations available for the isomer ratios of $^{182}W(n,n\alpha)$-reaction

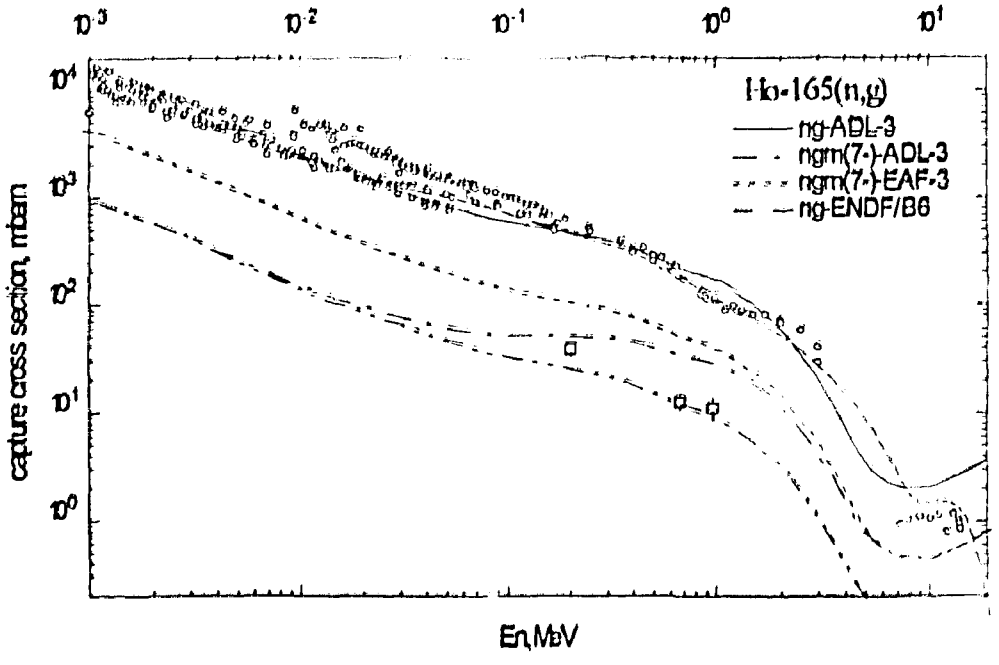

Fig. 7. Evaluations available for the ^{165}Ho(n,γ) cross sections in comparision with experimental data.

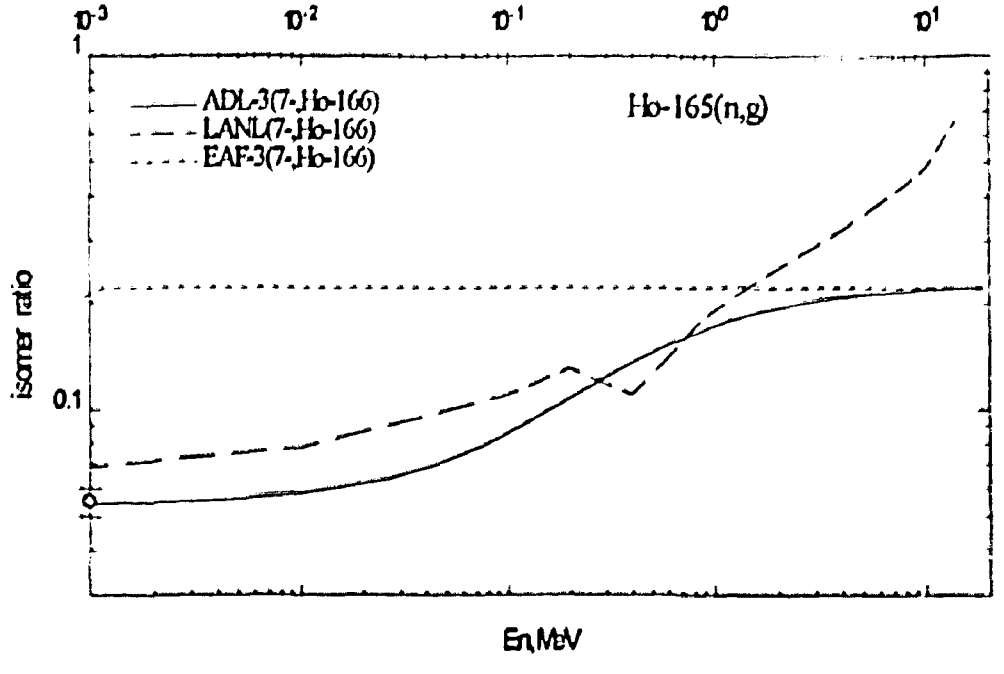

Fig. 8. Evaluations available for the isomer ratios of ^{165}Ho(n,γ) reaction

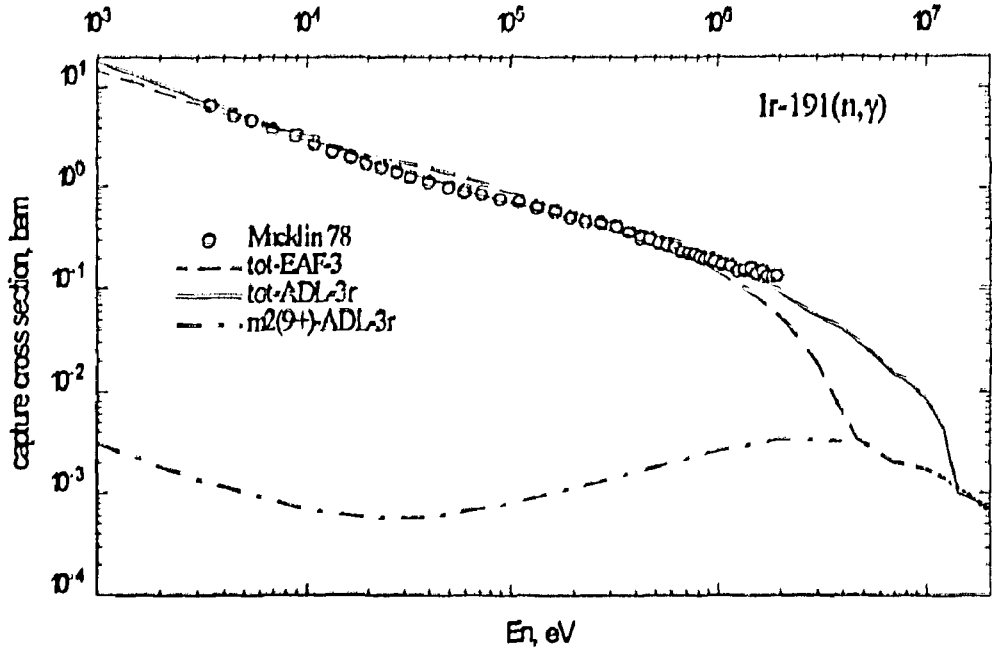

Fig. 9. Evaluations available for the ^{191}Ir(n,γ) cross sections in comparision with experimental data.

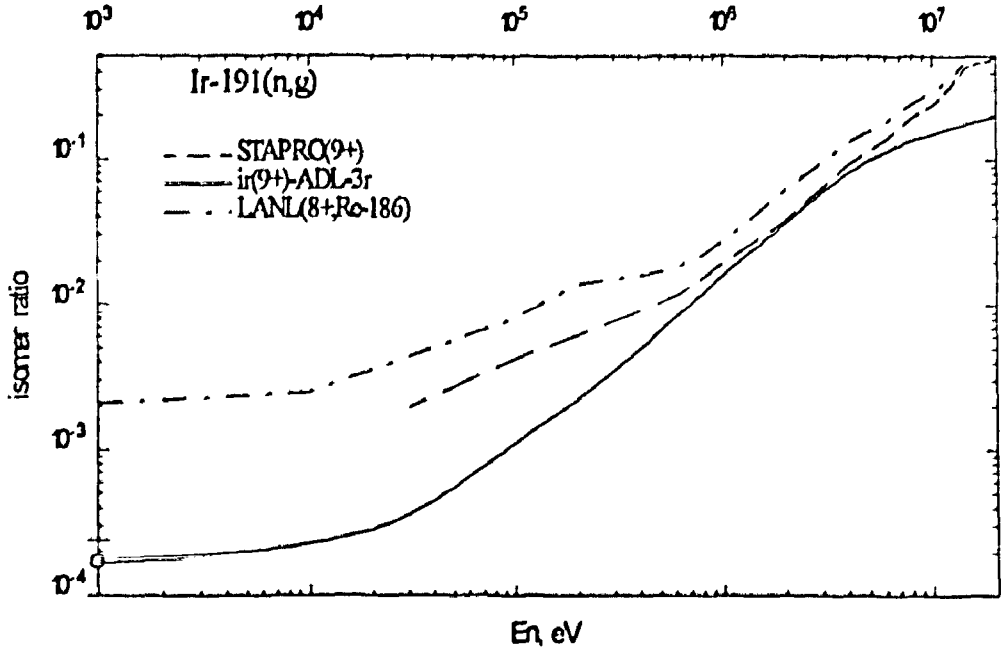

Fig. 10. Evaluations available for the isomer ratios of ^{191}Ir(n,γ) reaction

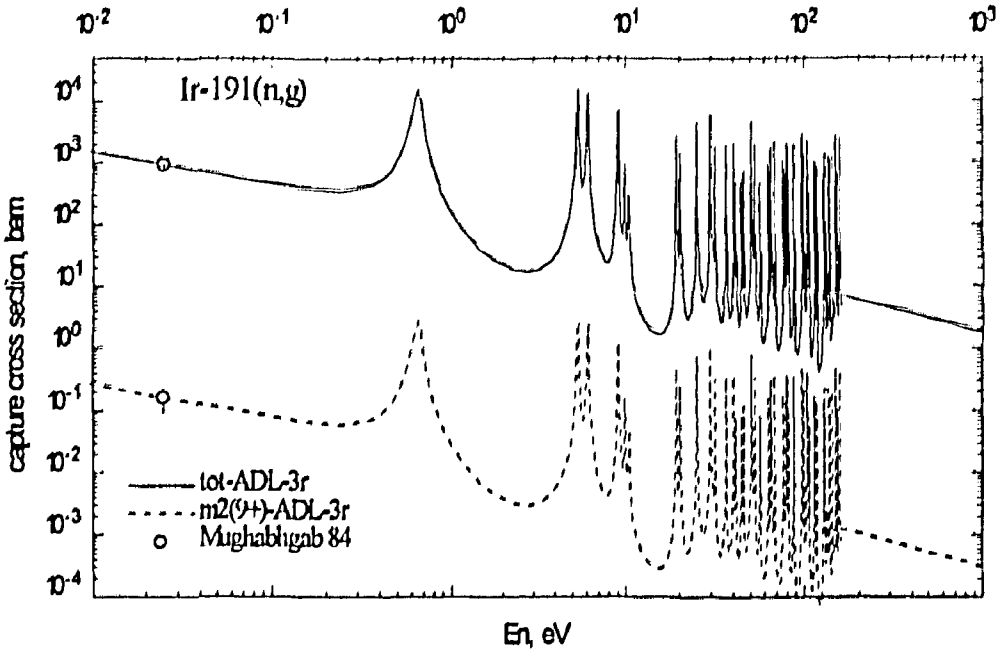

Fig. 11. Evaluation of the ^{191}Ir(n,γ) cross sections for the resonance region.

Calculated excitation functions of neutron induced reactions on ^{63}Cu, ^{94}Mo, ^{158}Dy, and ^{159}Tb from 1-20 MeV incident energy.

H. Marshall Blann
Nuclear Data Group
Lawrence Livermore National Laboratory
P.O. Box 808, L-294
Livermore, CA 94551

Abstract

We use the ALICE code to calculate excitation functions for the ^{63}Cu (n, p) ^{63}Ni, ^{94}Mo (n, p), ^{94}Zr, ^{158}Dy (n, p) ^{158}Tb, and ^{159}Tb (n, 2n) ^{158}Tb reactions. The example of the ^{159}Tb (n, 2n) excitation function folded over a calculated t(^{1}H, ^{3}He)n neutron spectrum for nominal 10 MeV neutrons is used to discuss differences between calculated and experimental results, in particular for incident energies near reaction thresholds. The importance of an accurate knowledge of the incident neutron spectrum in this regime is emphasized.

Introduction

At earlier meetings of the IAEA-CRP on activation cross sections of importance to fusion reactor materials, measurements at 14.7 MeV neutron energies were reported for a dozen or so reactions.[1-3] Several measurements were also reported for incident neutron energies below 14 MeV, and calculated excitation functions were provided by several authors using several codes.

One point of concern was a very significant difference between measured and calculated ^{159}Tb (n, 2n) cross sections at incident neutron energies below 11 MeV. In this work we calculated these excitation functions over a fine energy mesh. We then investigated the relationship of an experimental yield measured with a beam which is distributed over a fairly broad interval and calculated yields. We will present these results and discuss them with respect to the experimental/calculational differences observed. We also present calculated excitation functions for ^{63}Cu (n, p), ^{94}Mo (n, p) and ^{158}Dy (n, p) reactions, and compare these with the experimental results presented at earlier meetings of this CRP.[1-3]

Results and discussion

The calculated excitation functions and measured cross sections are summarized in tables 1-5. In particular, table 5 gives the ^{159}Tb (n, 2n) cross sections calculated in 0.1 MeV increments from 8.1 to 10.2 MeV. All results were run with the ALICE code with default parameters except inverse cross sections were calculated using the nuclear optical model subroutine. The experimental yields reported at earlier meetings of this CRP are included in the tables 1-4. The extremely large discrepancies between the ^{159}Tb (n, 2n) calculated and experimental yields are obvious for incident neutron energies below 14 MeV. Values reported at 14.7 MeV are in reasonable agreement for all four excitation functions.

One point which needs to be addressed, particularly for yields near threshold, is that the experimental neutron beams will always have a distribution in energies, while calculated results are generally made at a single energy. In fig.1 we reproduce the energy spectra calculated by Haight and Garibaldi[4] for the ^{1}H (t, n) reaction cell used for the ANL/LANL measurement reported at 10.3 MeV in the Del Mar meeting summary.[2,3,5] The largest solid angle in fig.1 is for the case of a 6 mm displacement from the beam axis at a 20 mm distance behind the gas cell. (see fig.1) We took the results given in Table 5, and folded them over a beam weighted according to the y = 0.6 cm distribution of fig.1 (which has been reproduced from ref. (4)). If this is done, the nominal 1702 mb yield calculated at 10.3 MeV becomes 1311 mb. If, to demonstrate sensitivity to mean energy, we assume that the experimental energy distribution is actually 0.5 MeV lower than the calculated result of fig.1, then the calculated yield, averaged over the distribution of incident energies, would be 850 mb, just one-half of the nominal 10.3 MeV incident energy value.

The calculated excitation functions presented by Chadwick in the earlier CRP were re-normalized to a 1930 mb evaluated yield at 14.7 MeV [6]. If we do this, the nominal calculated 10.3 MeV yield is 1410 mb; the result using the y = 0.6 cm distribution of fig. 1 is 1086 mb, and if the neutron distribution is shifted downward by 0.5 MeV, the 'effective' calculated cross section, renormalized, is 704 mb. This result is not in good agreement with the 528 ± 73 mb of 5), but it is acceptable.

We have also investigated sensitivity of results to parameter changes in the ALICE code. If the level density parameter is changed from the default $a = \frac{A}{9}$ to $a = \frac{A}{11}$, the (n, 2n) cross sections decrease at most by 20%. Similarly if the geometry dependent hybrid model option is used to slightly increase precompound decay, the result is at most a 20% decrease in the (n, 2n) yields near threshold. It is very difficult to attribute the huge differences between 'nominal energy' calculated and experimental cross sections at 14 MeV to model parameter uncertainties.

For ^{63}Cu (n, p) and ^{94}Mo (n, p) reactions, the agreement between calculated and measured cross sections at 14.7 MeV (see Tables 1 and 2) is excellent. This is near the peak of the excitation functions, where beam energy spread would have a minimal effect. Even so, the cross sections of around 50 mb are but 2.5% of the reaction cross section. Small branches of this magnitude are difficult to calculate accurately, and this degree of agreement is rather surprising to us.

Conclusions

We have presented calculations of some neutron induced reaction excitation functions using the ALICE code. Large discrepancies were observed for the ^{159}Tb (n, 2n) excitation function for incident neutron energies below 14.7 MeV, i.e. below the peak of the excitation function. These discrepancies could not be attributed to uncertainties in calculational parameters. If calculated results were averaged over estimates of the incident neutron spectra, much of the discrepancy could be resolved. The sensitivity of the calculated cross section to the incident neutron spectrum makes clear that comparisons between calculation and experiment, especially near threshold, require a good knowledge of the incident spectrum. The calculation must be appropriately weighted for the comparison to be valid. This is not a new conclusion, but a point which sometimes needs to be refreshed.

Acknowledgments

The author is grateful to Dr. Donald Smith for many helpful comments and suggestions, without which this work would not have been concluded.

Table 1. Neutron induced reactions on ^{63}Cu; ALICE calculations vs. experimental results.

elab (mev)	exc (mev)	res (mb)	^{63}Cu (n, p) 28 63	(n, p) exptl	(n, pn) 28 62	(n, α) 27 60
1.0	8.9	2346	—		—	—
2.0	9.9	2150	1.0		—	—
3.0	10.9	1947	8.4		—	—
4.0	11.9	1857	22		—	—
5.0	12.8	1812	37		—	0.46
6.0	13.8	1779	57		—	3.3
7.0	14.8	1750	66		—	9.4
8.0	15.8	1718	80		0.001	17
9.0	16.8	1687	93		0.14	25
10.0	17.8	1661	96		107	28
11.0	18.7	1632	90		449	33
12.0	19.7	1607	81		798	40
13.0	20.7	1588	65		834	43
14.0	21.7	1575	53		713	42
14.7	22.4	1567	48	54 ± 4 [a] ~120 [b]	572	37
15.0	22.7	1564	46		502	35
16.0	23.7	1553	41		478	26
18.0	25.6	1529	35		439	12
20.0	27.6	1494	29		375	5.1

a) ANL (Greenwood)/INCD (NDS)-288, p18 (1993)
b) Jülich (new measurement in progress), INDC (NDS)-288 p18 (1993)

Table 2. Neutron induced reactions on ^{94}Mo; ALICE calculations vs. experimental results.

elab (mev)	exc (mev)	^{94}Mo (n, p) 42 res (mb)	(n, p) (mb)	(n, p) expt (mb)	(n, pn) (mb)
1.0	8.4	2605	0.0		0.0
2.0	9.3	2427	0.0		0.0
3.0	10.3	2381	0.0		0.0
4.0	11.3	2260	0.0		0.0
5.0	12.3	2160	0.12		0.0
6.0	13.3	2098	1.3		0.0
7.0	14.3	2061	3.8		0.0
8.0	15.3	2038	7.7		0.0
9.0	16.3	2010	12		.0.0
10.0	17.3	1979	20		0.0
11.0	18.3	1951	25		.001
12.0	19.2	1920	33		.005
13.0	20.2	1894	40		3.2
14.0	21.2	1873	44		7.8
14.7	21.9	1866	45	50 ± 18 [a] 56± 11 [a] 50.1 ± 5.3 [b]	12
15.0	22.2	1863	45		14
16.0	23.2	1854	45		24
18.0	25.2	1832	42		49
20.0	27.6	1802	38		76

a) JAERI/INDC (NDS)-288, p18 (1993)
b) ANL(Greenwood) INDC (NDS)-288 p18 (1993)

Table 3. Neutron induced reactions on ^{159}Tb; ALICE calculations vs. experimental results.

exc (mev)	elab (mev)	^{159}Tb 65 res (mb)	(n, n') 65 159	(n, 2n) 65 158	(n, 2n) expt
15.0	8.7	2606	2329	275	77 ± 30 a)
15.8	9.5	2565	1426	1136	491 ± 61 c)
16.0	9.9	2555	1239	1314	374 ± 36 a)
16.2	9.9	2547	1078	1466	718± 68 c)
16.5	10.2	2535	880	1651	589 ± 65 a) 528 ± 73 b)
17.0	10.7	2520	647	1870	944 ± 113 a)
17.3	11.0	2514	548	1962	
18.3	12.0	2493	351	2136	
19.3	13.0	2474	263	2203	
20.3	14.0	2457	216	2228	
21.0	14.7	2440	194	2230	1930 ± 49 d) 2037 ± 160 e) 2042 ± 190 c) 1968 ± 56 c)
21.3	15.0	2432	186	2229	
22.3	16.0	2404	164	2129	
24.3	18.0	2359	132	1299	
26.3	20.2	2336	110	714	

a) Qaim et al, Jülich; see ref. 7.
b) ANL/LANL e 10.3 MeV nominal, INDC (NDC)-288 p.20 and 5).
c) Beijing; Weixiang, Hanlin and Zhao, from 5)
d) IRK evaluation (1989), INDC (NDS)-288 p18 (1993)
e) JAERI/ANL, INDC (NDS)-288 p.18 (1993)

Table 4. Neutron induced reactions on ^{153}Dy; ALICE calculations vs. experimental results.

elab (mev)	exc (mev)	$^{158}_{66}Dy$ res (mb)	(n, p) $^{65}_{158}$	(n, 2n) expt	(n, pn) $^{65}_{157}$
1.0	7.8	3320	—		—
2.0	8.8	3009	—		—
3.0	9.8	2860	—		—
4.0	10.8	2776	—		—
5.0	11.8	2706	—		—
6.0	12.8	2682	—		—
7.0	13.8	2660	0.1		—
8.0	14.8	2619	0.47		—
9.0	15.8	2568	1.29		—
10.0	16.8	2520	2.8		—
11.0	17.8	2488	5.0		—
12.0	18.8	2465	8.2		—
13.0	19.7	2447	12		1.15
14.0	20.7	2431	16		2.01
14.7	21.4	2418	19	<100 [a]	2.8
15.0	21.7	2411	20		3.0
16.0	22.7	2385	24		4.4
18.0	24.7	2338	28		13
20.0	26.7	2310	30		27

a) IRK evaluation /INDC (NDS)-288

Table 5. ^{159}Tb (n, 2n) calculated excitation function with fine mesh.

exc (mev)	elab (mev)	rcs (mb)	(n, 2n) 65 158
14.4	8.1	2640	0.
14.5	8.2	2634	0.
14.6	8.3	2629	0.
14.7	8.4	2623	40
14.8	8.5	2617	103
14.9	8.6	2612	183
15.0	8.7	2606	275
15.1	8.8	2601	380
15.2	8.9	2595	487
15.3	9.0	2590	600
15.4	9.1	2585	713
15.5	9.2	2579	825
15.6	9.3	2574	934
15.7	9.4	2569	1038
15.8	9.5	2565	1136
15.9	9.6	2560	1228
16.0	9.7	2555	1314
16.1	9.8	2551	1393
16.2	9.9	2547	1466
16.3	10.0	2543	1533
16.4	10.1	2539	1595
16.5	10.2	2535	1651
16.6	10.3	2531	1702
16.7	10.4	2530	1751

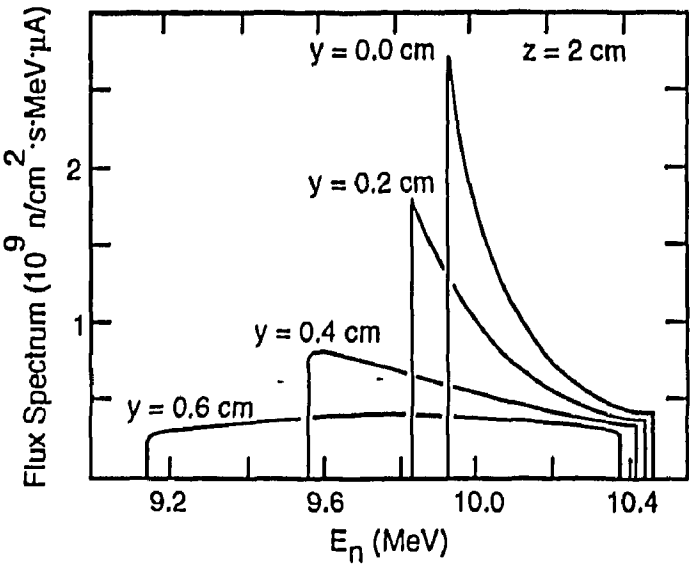

Fig.1. Calculated neutron energy spectrum 2 cm behind the Haight-Garibaldi gas cell for lateral positions (*y*) from the beam axis; the ^{1}H (*t*,*n*) reaction is assumed with the cell pressurized to 1.0 Mpa (from R. Haight and J. Garibaldi, NS & E 106, 296-298, (1990)).

References

1) Activation Cross Sections for the Generation of Long Lived Radionuclides of Importance in Fusion Reactor Technology, INDC (NDS) 263, July 1992, compiled by Wang Da Hai.

2) INDC (NDS)-286, compiled by A.B. Pashchenko, IAEA Nuclear Data Section, Nov. 1993.

3) INDC (NDS)-288, Ed. by A. B, Pashchenko, IAEA Nuclear Data Section, Nov. 1993

4) R. Haight and J. Garibaldi, Nuclear Science and Engineering 106, 296 (1990).

5) Private communication, D. Smith, May 1995.

6) M. B. Chadwick et al, INDC (NDS) - 286 (1993) p123.

7) S. Qaim, Int. J. App. Rad. and Isotopes 43 9, 1065 (1992).

Summary of nuclear model calculations for the IAEA Coordinated Research Programme on activation cross sections for fusion reactor technology *)

M.B. Chadwick[1] and P.G. Young[2]

[1] *Lawrence Livermore National Laboratory, Livermore, CA 94550, USA*

[2] *Los Alamos National Laboratory, Los Alamos, NM 87545, USA*

We describe research performed for the International Atomic Energy Agency (IAEA) Coordinated Research Programme on activation cross sections for fusion reactor technology. Using the GNASH nuclear modeling code, we have investigated: (1) production cross sections of isomeric states, and isomer ratios, for the reactions ^{94}Mo(n,p)^{94}Nb, ^{109}Ag(n,2n)^{108m}Ag, ^{151}Eu(n,2n)^{150m} Eu, ^{153}Eu(n,2n)$^{152g+m2}$Eu, ^{159}Tb(n,2n)^{158}Tb, ^{187}Re(n,2n)^{186m}Re, ^{179}Hf(n,2n)^{178m2}Hf, ^{193}Ir(n,2n)^{192m2}Ir.; (2) systematical dependence of isomeric ratios on isomer spin and incident-energy; (3) preequilibrium spin effects on calculated isomer production; and (4) intercomparison and evaluation of nuclear model excitation functions of isomer production cross sections.

*) presented by M. Blann

1. INTRODUCTION AND SUMMARY OF TASKS PERFORMED

The International Atomic Energy Agency (IAEA) Nuclear Data Section has established a Coordinated Research Programme (CRP) on activation cross sections for the generation of long-lived radionuclides of importance in radioactive waste problems in fusion reactor technology. A number of reactions of particular importance were selected, and the CRP organized both experimental and theoretical efforts to determine production cross sections for these reactions. The first Research Coordination Meeting (RCM) was held in Vienna in November 1991 and experimental and theoretical results were presented. On the basis of this first meeting, priorities for future work were established. Further measurements and calculations were presented at the second RCM of the CRP, held at Del Mar, California, April 29-30, 1993. The final RCM was held in St Petersburg, June 19-23, 1995.

In this report we summarize the nuclear theory and model calculations performed for the CRP using the GNASH code, for the reactions ^{94}Mo(n,p)^{94}Nb, ^{109}Ag(n,2n)^{108m}Ag, ^{151}Eu(n,2n)^{150m} Eu, ^{153}Eu(n,2n)$^{152g+m2}$Eu, ^{159}Tb(n,2n)^{158}Tb, ^{187}Re(n,2n)^{186m}Re, ^{179}Hf(n,2n)^{178m2}Hf, ^{193}Ir(n,2n)^{192m2}Ir. Below we list the areas we studied:

Calculated isomer productions Using the GNASH modeling code, we calculated isomer production cross sections and isomer ratios for numerous reactions of importance in reactor technology. See Refs. [1-5].

Evaluated theoretical excitation functions We normalized the theoretical results from a range of calculations to the evaluated experimental data at 14.5 MeV, and took their average. This yields averaged theoretical excitation functions for the production of the various radionuclides at neutron energies ranging from threshold to 14.5 MeV. Our theoretical results may be used in conjunction with experimental data to produce evaluated radionuclide production cross sections for neutron energies lower than 14.5 MeV. See Ref. [3]

Systematics of isomer ratios By calculating isomer ratios for a range of reactions we were able to investigate the validity of the Kopecky and Gruppelaar systematics [2, 11].

Investigated theoretical spin-effects We investigated the role of angular momentum conservation in semiclassical and quantum mechanical preequilibrium models, and its influence on isomer production [4, 5].

In the following sections we describe the GNASH nuclear modeling code, and we give brief descriptions of our results from each of the above areas of study. Further details of our work can be found in Refs. [1-5].

II. DESCRIPTION OF GNASH MODEL CALCULATION

The GNASH nuclear theory code [7] is based on the Hauser-Feshbach statistical theory with full angular momentum conservation, with preequilibrium corrections calculated with the exciton model of Kalbach, or with the quantum mechanical multistep theory of Feshbach, Kerman, and Koonin [8]. Transmission coefficients for deformed nuclei are obtained from the coupled-channel code ECIS [9], and for spherical nuclei from SCAT2 [10]. The optical potentials used to obtain the transmission coefficients depended on the reaction considered. In some cases, potentials were obtained for a particular target nucleus by fitting experimental elastic and nonelastic data, and in other cases global optical potentials were utilized. Transmission coefficients for gamma-ray emission are usually obtained from the generalized Lorentzian model of Kopecky and Uhl [6], normalized to experimental values of $2\pi\Gamma_\gamma/D_0$ for s-wave neutrons.

The level density model of Ignatyuk, or in some cases Gilbert and Cameron, was used and matched on to the cumulative number of experimental levels at low energies. In the case of the hafnium calculations, where the isomeric level is at a very high excitation energy (2.447 MeV), a discrete band of rotational levels was built onto this state and embedded into the continuum-described states [1, 2].

III. SYSTEMATICS OF ISOMER RATIOS

The systematics of neutron-induced isomeric cross section ratios at 14.5 MeV have been studied by Kopecky and Gruppelaar [11]. They used a simplified version of the GNASH code to determine the ratio of cross section to the isomeric state and ground state in (n,n'), (n,p), (n,t), (n,α), and $(n,2n)$ reactions, replacing the realistic nuclear level structure by two discrete states (the ground state and the isomeric state) plus a continuum of statistically-described states. Their approach is, therefore, considerably simpler than our calculations and so we have compared our results with the Kopecky-Gruppelaar systematics.

In Ref. [2] we showed that while such systematics are very useful, in many cases a full calculation (with a realistic description of nuclear structure) is important in accurately determining isomer ratios. Also, Kopecky and Gruppelaar point out that their calculation is particularly sensitive to the simple model parameters that they adopt for the $(n,2n)$ reaction. Our investigations into an analogous simple model confirmed this, and indicate that for certain reactions one should be wary of using simple systematics predictions.

Our calculations generally support predictions from the systematics at 14 MeV, except for isomer spins above about 12. The agreement is not as good for (n,n') reactions, though the systematics may still be good enough to be of use when developing large activation libraries. We also provided theoretical results for isomeric ratios in neutron capture reactions, where experimental results are scarce.

Full details of these investigations can be found in Ref. [2]

IV. PHYSICS OF SPIN EFFECTS

A proper treatment of angular momentum conservation in preequilibrium and equilibrium reaction processes is important when determining the production cross sections of isomers, which are often of high-spin.

To assess the production of the 16+ ^{178m2}Hf isomer in the ^{179}Hf$(n,2n)^{178m2}$Hf reaction, both experimental measurements and theoretical calculations have been performed. In 1990 we performed calculations of this isomer [1] with the GNASH nuclear model code before experimental measurements were made, and obtained results which agreed to within a factor of two with the later measurement by Patrick *et al.* [12]. Taking into account the very small cross sections for isomer production (due to the high spin), and the uncertainties in the theoretical modeling (particularly in the nuclear structure and optical potentials) our results were very encouraging. Since then, more measurements [13] have been made which have verified Patrick *et al.*'s initial result. Furthermore, a number of developments to the GNASH code have been made which led us to recalculate isomer production cross section. Even though experimental data exists at 14 MeV, they do not at lower energies, and thus theoretical calculations are of importance since they can be normalized to the measurements at 14 MeV and used to provide cross sections for lower neutron energies.

We applied the improved GNASH code system to calculate 14 MeV neutron reactions on ^{179}Hf to both the 16$^+$ isomer in ^{178}Hf and the 12.5$^-$ isomer in ^{179}Hf. Two calculations were compared which utilize different modifications to the code: firstly, the exciton model preequilibrium calculation was modified so that the spin distribution of residual nuclei after preequilibrium decay is obtained from the exciton spin-dependent level density [13], and not from the compound-nucleus spin distribution; and secondly, a version of the code, FKK-GNASH [5], which uses the quantum mechanical Feshbach-Kerman-Koonin (FKK) [8] preequilibrium model.

With the recent modifications to the exciton model calculations in GNASH we obtained high-spin isomer production cross sections that are in good agreement with measurements, and agree more closely with measurements than those we published in 1991 [1]. However, our calculations which utilize the FKK theory yield smaller high-spin-transfer transitions than found with the exciton model, and underpredict high-spin isomer production. We doubt that this underprediction represents a failure of the basic physics of the FKK theory, but rather the inadequacy of its present implementation. Our formalism for implementing the FKK theory has been successful in describing nucleon emission cross sections and angular distributions, and this investigation is the first to be sensitive to the transfer of large angular momenta.

For further details, see Refs. [4, 5].

V. INTERCOMPARISON OF VARIOUS MODEL CALCULATIONS

A number of different groups have performed theoretical cross section calculations, and at the 1993 IAEA Del Mar meeting a recommendation was made to perform an

intercomparison of the theoretical works. This intercomparison was performed at Lawrence Livermore National Laboratory.

A comparison of theoretical calculated cross sections for the production of radionuclides should play a number of useful roles: it identifies cases where discrepancies exist between calculations and therefore stimulates further theoretical work to understand (and hopefully remove) differences; the comparison yields spreads in theoretical calculations which can be interpreted as uncertainties in the calculations; and the averaged theoretical results can be used, with data where it exists, to provide evaluated cross sections at energies lower than 14.5 MeV.

As there is often only sparse experimental information on production cross sections of radioactive nuclides at energies lower than 14.5 MeV, theoretical calculation of the shape of the excitation functions for the production of these nuclides can be very useful. Such calculations are often normalized to the experimental value at 14.5 MeV, and then used to obtain cross sections at lower incident neutron energies. To facilitate this procedure, we compare all theoretical calculations for the excitation functions of the various reactions considered in this RCM and determine averaged theoretical excitation functions for each reaction. For some reactions there does exist experimental data at lower neutron energies. Apart from commenting on how the calculations compare with the data, we do not include this information in our work. Thus, in cases where there is data at neutron energies lower than 14.5 MeV, further evaluation work is needed before a recommended excitation function for fusion technology applications can be provided.

The various groups who have calculated radionuclide production cross sections are as follows: M.B. Chadwick and P.G. Young (GNASH code system); A.V. Ignatyuk, O.T. Grudzevich, and A. Pashchenko (STAPRE code system); N. Yamamuro (SINCROS-II code system); J.W Meadows (GNASH code system); and M. Gardner and D. Gardner (STAPLUS code system). All these calculations are based on Hauser-Feshbach compound nucleus theory with preequilibrium emission, and in some cases include direct reactions with a DWBA or coupled-channels approach.

Various groups have determined the radionuclide production cross sections with differing methods, and consequently obtain differing results. We decided to combine these calculations by normalizing each calculation to the evaluated 14.5 MeV value, and determine their average. This produces an average theoretical excitation function for each of the reactions, from threshold to 14.5 MeV. One could examine the various assumptions made in the calculations (optical potentials, level densities, preequilibrium models, etc) and assess the accuracy of each calculation. This would be a useful task to perform in the future. But for the moment we have used equal weightings for all calculations when obtaining the average. Our procedure is thus:

- Normalize theoretical calculations to the 14.5 MeV evaluated values of Vonach *et al.* [13, 14].
- Produce splined fits of each set of calculated excitation functions and obtain

theoretical values on a common 0.5 MeV-spaced grid

- Average the various theoretical curves on this same common grid of energy values

In figures 1-8 we show the various theoretical calculations and the averaged theoretical value, for the production cross sections of the various radionuclides. In cases where experimental data exists at energies below 14.5 MeV, we include these measurements in the figures. The averaged theoretical values are shown in numerical form in Table.1.

On the basis of these comparisons we make the following observations:

1. Whilst there are some reactions for which the various theoretical calculations agree closely, in many cases agreement between calculations is poor. Calculations vary considerably for the reactions ^{109}Ag(n,2n) ^{108m}Ag, ^{153}Eu(n,2n)$^{152g+m2}$Eu, ^{187}Re(n,2n)^{186m}Re, ^{193}Ir(n,2n)^{192m2}Ir (Figs. 2,4,6,8).

2. Experimental data below 10.7 MeV neutron energy has been recently measured by the Julich-Debrecen [15] collaboration, for the reactions ^{151}Eu(n,2n)^{150m}Eu and ^{159}Tb(n,2n)^{158}Tb. Furthermore, experimental data has recently been obtained at 10.3 MeV neutron energy for these two reactions, as well as for the reaction ^{109}Ag(n,2n)^{108m}Ag by the Argonne-Los Alamos-JAERI collaboration [16]. In all these cases the theoretical calculations consistently exceed the measurements. M. Blann addresses possible experimental uncertainties in these measurements in his contribution to the 1995 IAEA Petersburg meeting.

3. It is interesting to note the very different shape of the ^{179}Hf(n,2n)^{178m2}Hf compared to the other (n,2n) excitation functions. This is due to the extremely high spin (16+) of the isomer, and the calculations of Chadwick *et al.* and Ignatyuk *et al.* agree closely.

The theoretical calculations of production cross sections of the radionuclides described can be used to obtain evaluated cross sections for neutron energies below 14.5 MeV.

VI. ACKNOWLEDGMENTS

This work was performed under the auspices of the U.S. Department of Energy by Lawrence Livermore National Laboratory under contract No. W-7405-Eng-48, and under the International Atomic Energy Agency Research Agreement No. 5062/CF.

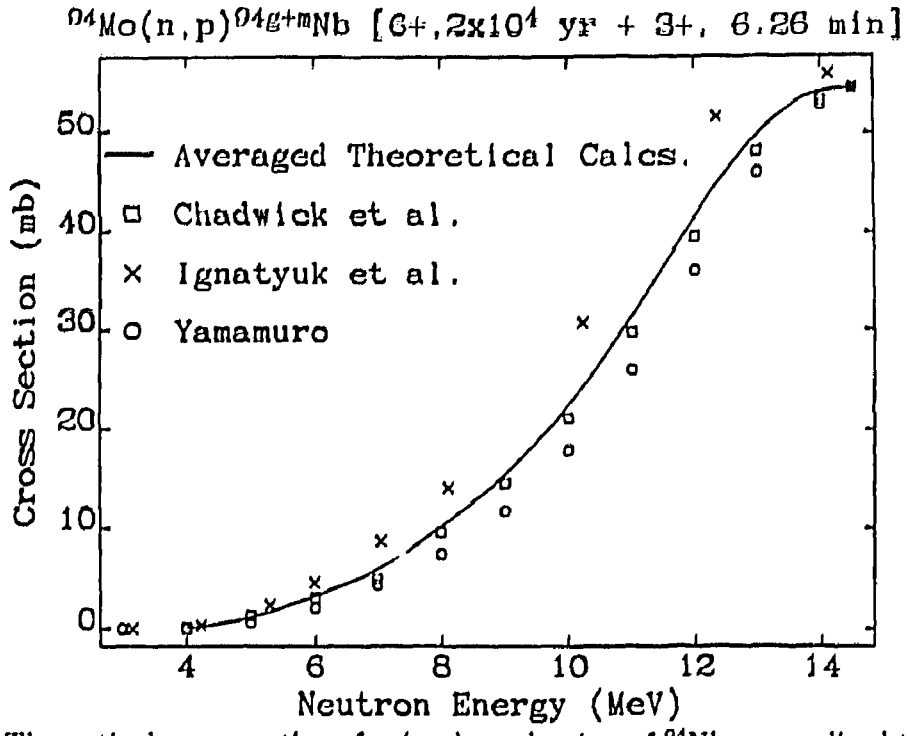

Fig. 1. Theoretical cross sections for (n,p) production of ^{94}Nb, normalized to a value of 54.5 mb at 14.5 MeV [13].

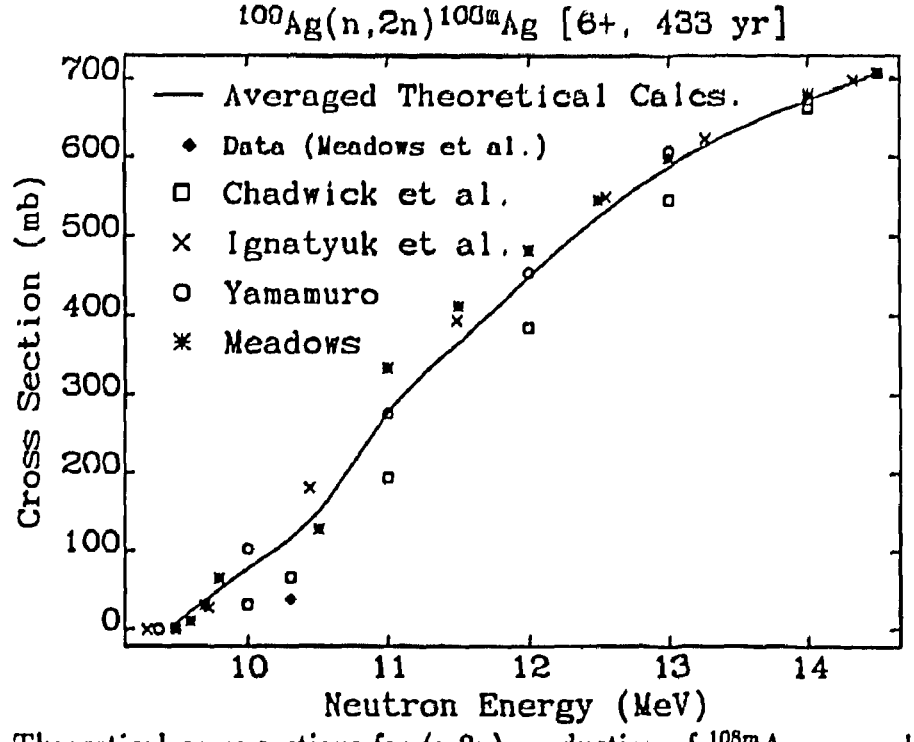

Fig. 2. Theoretical cross sections for (n,2n) production of ^{108m}Ag, normalized to a value of 708 mb at 14.5 MeV [13]. Also shown is the experimental result from the Argonne-Los Alamos-JAERI collaboration [16].

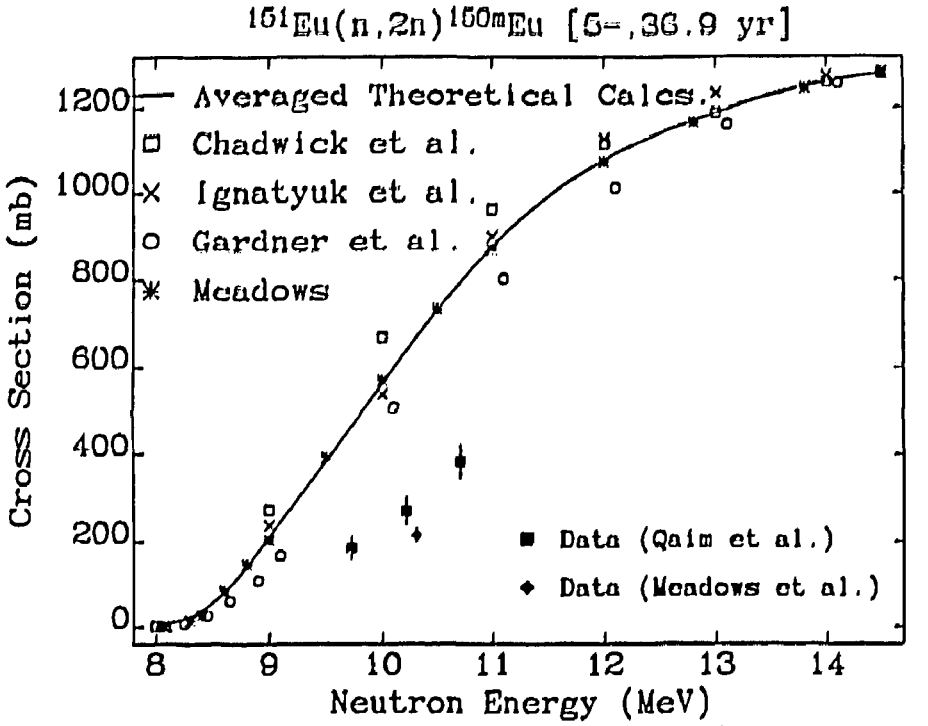

Fig. 3. Theoretical cross sections for (n,2n) production of ^{150m}Eu, normalized to a value of 1282 mb at 14.5 MeV [13]. Also shown are experimental results from the Argonne-Los Alamos-JAERI [16] and Julich-Debrecen [15] collaborations.

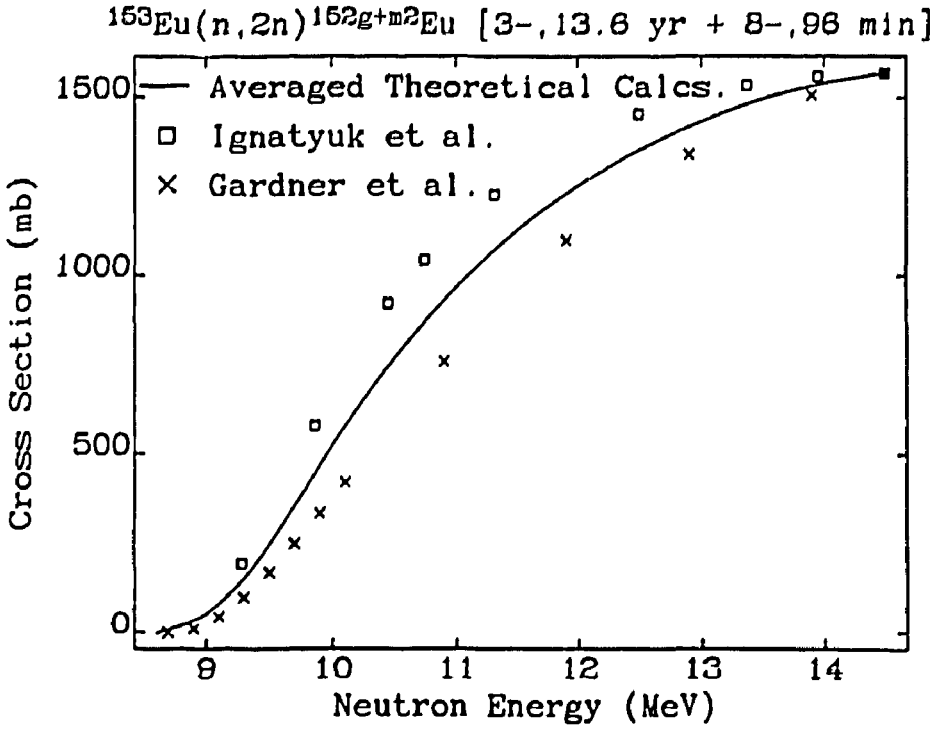

Fig. 4. Theoretical cross sections for (n,2n) production of $^{152g+m2}$Eu, normalized to a value of 1568 mb at 14.5 MeV [13].

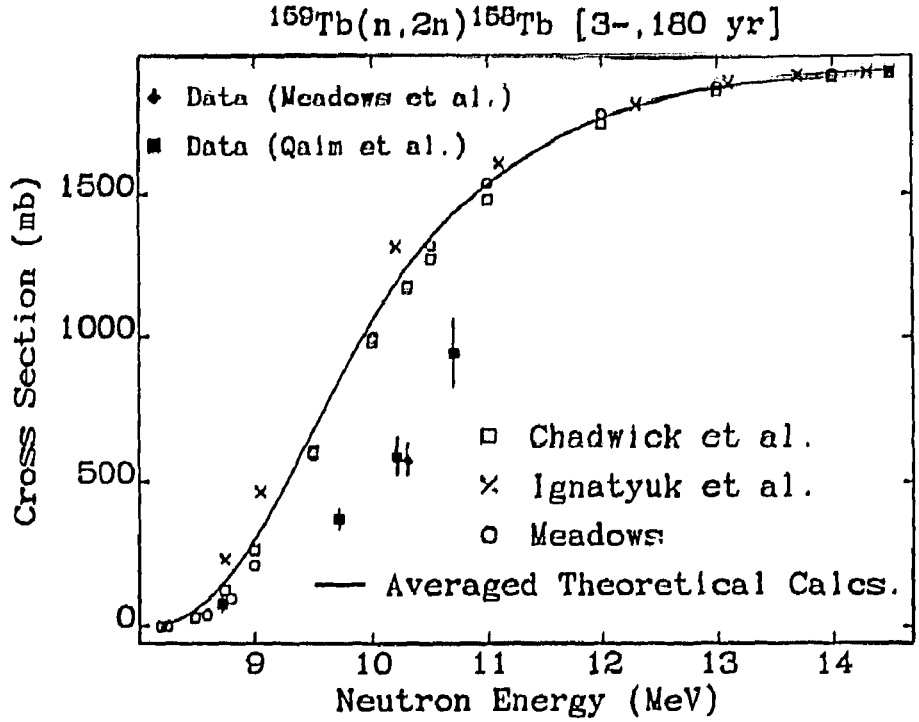

Fig. 5. Theoretical cross sections for (n,2n) production of ^{158}Tb, normalized to a value of 1929 mb at 14.5 MeV [13]. Also shown are experimental results from the Argonne-Los Alamos-JAERI [16] and Julich-Debrecen [15] collaborations.

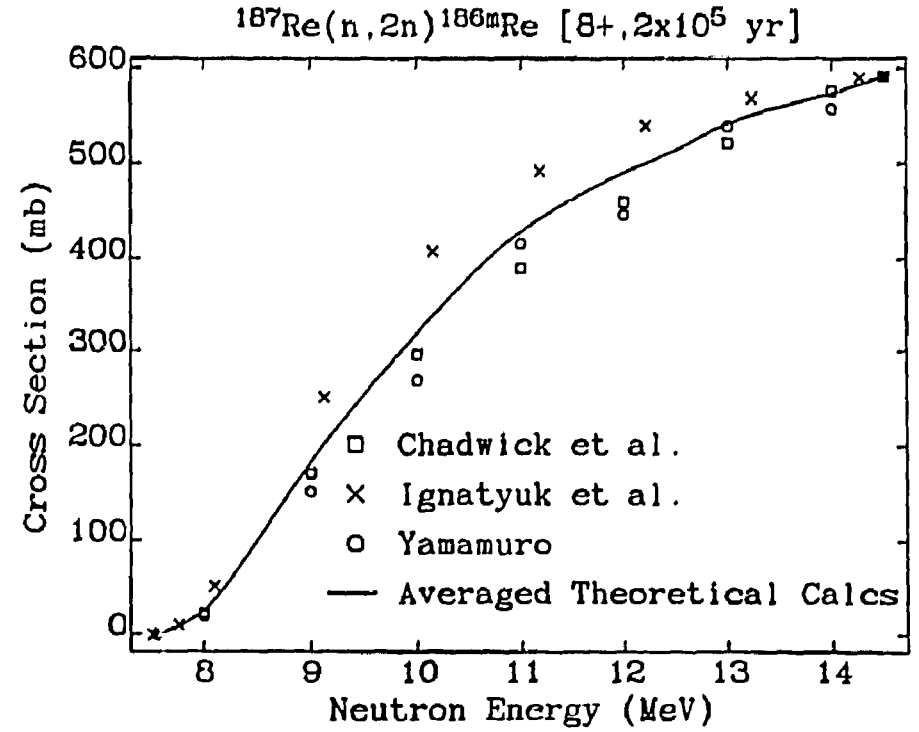

Fig. 6. Theoretical cross sections for (n,2n) production of ^{186m}Re, normalized to a value of 592 mb at 14.5 MeV [14].

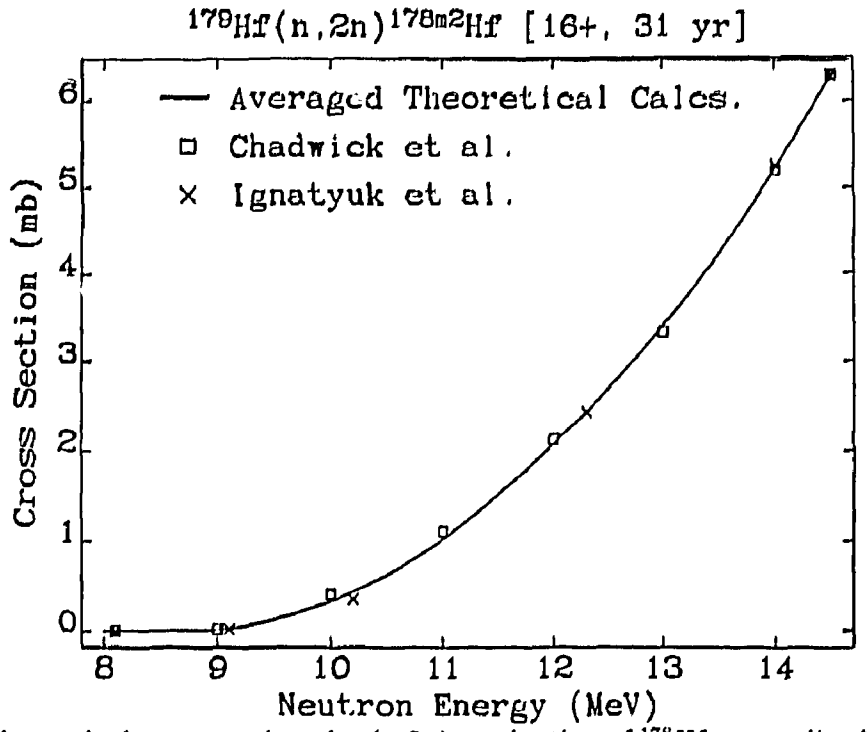

Fig. 7. Theoretical cross sections for (n,2n) production of ^{178}Hf, normalized to a value of 6.29 mb at 14.5 MeV [13].

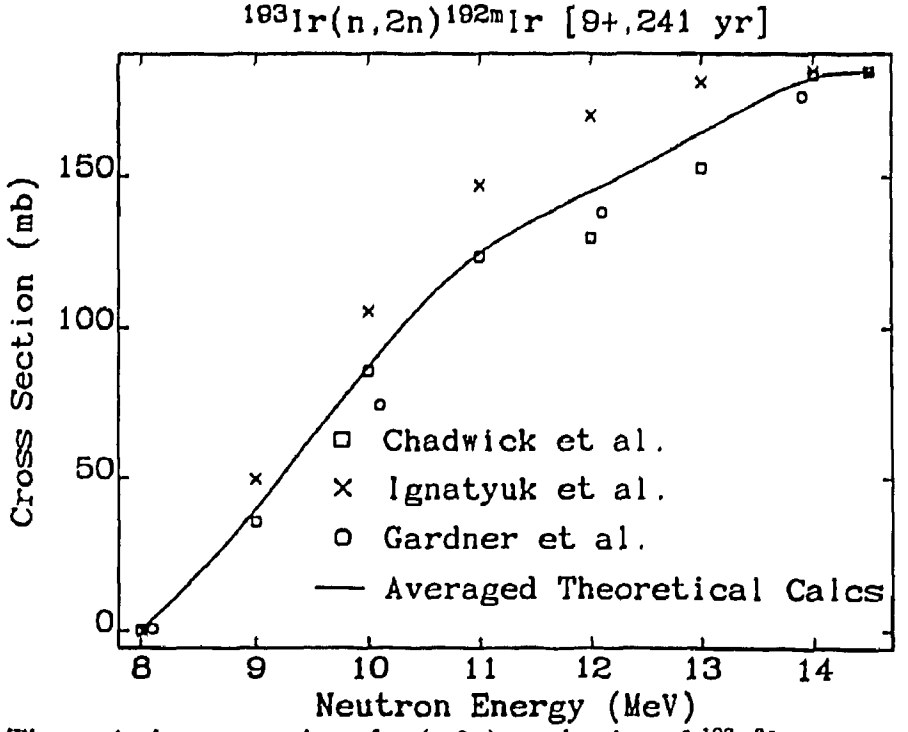

Fig. 8. Theoretical cross sections for (n,2n) production of ^{192m2}Ir, normalized to a value of 184 mb at 14.5 MeV [14].

Table I. Numerical values for averaged theoretical cross sections (mb).

Table 1:

E (MeV)	#1	#2	#3	#4	#5	#6	#7	E (MeV)	#8
8.0	-	1.16	-	-	26.60	-	3.24	4.0	0.08
8.5	-	57.69	-	57.87	100.00	-	18.70	5.0	0.95
9.0	-	212.81	55.19	300.93	183.00	0.01	39.60	6.0	2.66
9.5	7.50	384.60	247.74	680.94	254.00	0.12	63.50	7.0	4.71
10.0	77.17	562.80	525.28	1059.02	319.00	0.33	87.10	8.0	8.56
10.5	152.22	732.02	771.46	1344.51	380.00	0.62	109.00	9.0	13.13
11.0	277.54	876.89	965.89	1535.48	429.00	1.01	125.00	10.0	19.51
11.5	366.04	990.99	1125.82	1672.44	463.00	1.51	136.00	11.0	27.85
12.0	448.87	1075.60	1251.26	1768.89	491.00	2.07	145.00	12.0	37.77
12.5	524.63	1138.42	1354.75	1834.48	515.00	2.69	154.00	13.0	47.03
13.0	586.93	1187.13	1433.15	1876.92	542.00	3.40	164.00	14.0	53.03
13.5	634.37	1229.44	1495.87	1901.99	560.00	4.24	174.00	14.5	54.50
14.0	672.60	1261.49	1539.78	1917.43	574.00	5.23	182.00		
14.5	708.00	1282.00	1568.00	1929.00	592.00	6.29	184.00		

Reactions are labelled as follows:-

#1 $^{109}Ag(n,2n)^{108m}Ag$ (6+)

#2 $^{151}Eu(n,2n)^{150m}Eu$ (5-)

#3 $^{153}Eu(n,2n)^{152g+m2}Eu$ (3 ,8-)

#4 $^{159}Tb(n,2n)^{158}Tb$ (3-)

#5 $^{187}Re(n,2n)^{186m}Re$ (8+)

#6 $^{179}Hf(n,2n)^{178m2}Hf$ (16+)

#7 $^{193}Ir(n,2n)^{192m2}Ir$ (9+)

#8 $^{94}Mo(n,p)^{94}Nb$ (6+)

REFERENCES

[1] M.B. Chadwick and P.G. Young, "Calculations of the Production Cross Sections of High-Spin Isomeric States in Hafnium", Nuclear Science and Engineering, **108**, 117 (1991).

[2] M.B. Chadwick and P.G. Young, in "Proceedings of an IAEA Consultant's Meeting on Activation Cross Sections for the Generation of Long-Lived Radionuclides of Importance in Fusion Reactor Technology," Report INDC(NDS)-263/L, IAEA, Vienna (1992).

[3] M.B. Chadwick, M.A. Gardner, D.G. Gardner, O.T. Grudzevich, A.V. Ignatyuk, J.W. Meadows, A.B. Pashchenko, N. Yamamuro, and P.G. Young, in "Proceedings of an IAEA Consultant's Meeting on Activation Cross Sections for the Generation of Long-Lived Radionuclides of Importance in Fusion Reactor Technology," Report INDC(NDS)-286/L, IAEA, Vienna (1993) p. 123.

[4] M.B. Chadw k and P.G. Young, in "Proceedings of an IAEA Consultant's Meeting on Activation Cross Sections for the Generation of Long-Lived Radionuclides of Importance in Fusion Reactor Technology," Report INDC(NDS)-286/L, IAEA, Vienna (1993) p. 75.

[5] M.B. Chadwick, P.G. Young, P. Oblozinsky, and A. Marcinkowski, Physical Review C 49, R2885 (1994).

[6] J. Kopecky and M. Uhl, "Test of Gamma-Ray Strength Functions in Nuclear Reaction Model Calculations", Phys. Rev. C42, 1941 (1990).

[7] P.G. Young, E.D. Arthur, and M.B. Chadwick, "Comprehensive Nuclear Model Calculations: Introduction to the Theory and Use of the GNASH code", Los Alamos Report LA-12343-MS (1992).

[8] H. Feshbach, S. Koonin, A. Kerman, Annals of Physics (N.Y.) **125**, 429 (1980).

[9] J. Raynal, "Optical Model and Coupled-Channel Calculations in Nuclear Physics", SMR-9/8, International Atomic Energy Agency (1972).

[10] O. Bersillon, "SCAT2 - A Spherical Optical Model Code', in Progress Report of the Nuclear Physics Division, Bruyeres-le-Chatel (1977), CEA-N-2037, p.111 (1978).

[11] J. Kopecky and H. Gruppelaar, "Systematics of Neutron-Induced Isomeric Cross Section Ratios at 14.5 MeV", ECN Report ECN-200 (1987).

[12] B.H. Patrick, M.G. Sowerby, C.G. Wilkins and L.C. Russen, "Measurements of 14-MeV Neutron Cross Sections for the Production of Isomeric States in Hafnium Isotopes," presented at the Specialist's Meeting on Neutron Activation Cross Sections for Fission and Fusion Energy Applications, Argonne, Illinois, September 13-15, 1989. IAEA Report INDC(NDS)-232/L, p.69 (1990), Vienna.

[13] H. Vonach and M. Wagner, in "Proceedings of an IAEA Consultant's Meeting on Activation Cross Sections for the Generation of Long-Lived Radionuclides of

Importance in Fusion Reactor Technology," Report INDC(NDS)-286/L, IAEA, Vienna (1993) p. 67.

[14] H. Vonach, in "Proceedings of an IAEA Consultant's Meeting on Activation Cross Sections for the Generation of Long-Lived Radionuclides of Importance in Fusion Reactor Technology," Report INDC(NDS)-263/L, IAEA, Vienna (1992).

[15] S. Qaim, F. Cserpak and J. Csikai, "Cross Sections for $^{151}Eu(n,2n)^{150m}Eu$ and $^{159}Tb(n,2n)^{158}Tb$ Reactions Near Their Thresholds", Appl. Radiat. Isot. **43**, 1065 (1992); also see S. Qaim, contributed paper in present proceedings.

[16] J. Meadows, D. Smith, R. Haight, Y. Ikeda, and C. Konno, in in "Proceedings of an IAEA Consultant's Meeting on Activation Cross Sections for the Generation of Long-Lived Radionuclides of Importance in Fusion Reactor Technology," Report INDC(NDS)-286/L, IAEA, Vienna (1993) p. 13.

EVALUATION OF SOME ACTIVATION CROSS-SECTIONS FOR FORMATION OF LONG-LIVED ACTIVITIES IMPORTANT FOR FUSION TECHNOLOGY *)

H. Vonach and Maria Wagner

Institut für Radiumforschung und Kernphysik,
Universität Wien,
Vienna, Austria

Abstract: The cross-sections for the reactions $^{94}Mo(n,p)^{94}Nb$, $^{109}Ag(n,2n)^{108m}Ag$, $^{151}Eu(n,2n)^{150m}Eu$, $^{153}Eu(n,2n)^{152g+m2}Eu$, $^{159}Tb(n,2n)^{158}Tb$, $^{179}Hf(n,2n)^{178m2}Hf$, $^{182}W(nn'\alpha)^{178m2}Hf$, $^{187}Re(n,2n)^{186m}Re$ and $^{193}Ir(n,2n)^{192m2}Ir$ were evaluated at E_n = 14.5 MeV. Evaluated cross-sections and their uncertainties were derived as weighted averages of all accepted and if necessary renormalized experimental data. Correlations between different results due to use of common decay data were taken properly into account.

Introduction

Following the recommendations of the International Nuclear Data Committee (INDC) the IAEA Nuclear Data Section has established a Coordinated Research Programme ((CRP) on activation cross-sections for the generation of long-lived radionuclides of importance for radioactive waste problems in future fusion reactor technology. Fifteen reactions of special importance for this purpose were identified by the INDC and selected as the main task of the CRP. For a part of the reactions this task had been solved already at the time of the 1. Research Coordination Meeting (RCM) in Vienna in November 1991 in the sense that several reliable mutually consistent measurements had been performed by CRP participants /Wang Da Hai 1992/. In order to obtain final results for the user community it was decided at that meeting to combine these measurements by means of a careful evaluation into a set of unique recommended cross-section values and corresponding uncertainties for each reaction for the important neutron energy range around 14 MeV. This work was done at IRK Vienna and is presented in the following. A preliminary evaluation covering the data obtained until 1993 has already been published in the proceedings of the last RCM /Vonach 93/. At the last CRP - meeting in St. Petersburg 1995 a number of participants presented slight revisions of their previous data and new results which allow to extend the evaluation to two additional reactions. For this reason the whole evaluation was repeated and thus this work supersedes and replaces the evaluation /Vonach 93/.

Evaluation Method

The evaluation was done in the following steps
1) Selection of data
2) Renormalization of data to a common set of decay data and reference cross-sections and to a nominal neutron energy of 14.5 MeV
3) Calculations of the evaluated cross-sections and their uncertainties from the renormalized input data.

In detail the following procedures were used.
Experimental results were obtained from the CRP-participants in form of formal papers preprints and private communications. In addition the data compilations CINDA and EXFOR were searched for additional measurements. From this data base a few results were not included into the evaluation because they deviated strongly from the mutually consistent bulk of the data or because experimental conditions seemed unsatisfactory. Thus the result of /Ikeda 92/ for the reaction $^{153}Eu(n,2n)^{152g+m2}Eu$ was not used as the result suggests that it contains an appreciable contribution

*) was presented after completion of the meeting and distributed by 8 August 1995.

from the $^{151}Eu(n,\gamma)^{152m2+g}Eu$ reaction due to moderated source neutrons. The cross-section data for all accepted experiments are given in table 1.

All cross-sections have been measured by γ-spectroscopy, that is by determination of the intensity of specific γ-lines of the long-lived activities formed in the studied reactions. Neutron fluence has been determined from the γ-activities formed in monitor foils by means of reactions with accurately known cross-sections.

Accordingly all experimental results were renormalized to the most recent decay data (half-lives and emission probabilities for the γ-lines used in the measurements) and cross-section values for the monitor reactions. The decay data used in the present evaluation are shown in table 2. In generally they were taken from the most recent issue of Nucl.Data Sheets, in a few cases, where recent results of precision measurements became available the latter have been used. The most important case in this respect is the half-life of ^{109m}Ag which is given as 125 years in the Nuclear Data Sheets, whereas a recent measurement at PTB Braunschweig /Schrader 93/ resulted in a half-life of 433 ± 15 years. Use of this latter value removed the earlier large discrepancy between experimental and theoretical values for the $^{109}Ag(n,2n)^{108m}Ag$ cross-sections. For the half-life of ^{150m}Eu the new result of 36.9 ± .9 years /Thompson 93/ was used. For ^{152g}Eu the careful recent evaluation of decay-data performed within a CRP on X-ray and gamma ray standards for detector calibration was used /IAEA 91/. The monitor reactions used in the various experiments are listed in table 3. Most cross-sections were measured relative to the cross-sections for the reactions $^{58}Ni(n,p)^{59}Co$ and $^{93}Nb(n,2n)^{92m}Nb$. For the $^{58}Ni(n,p)^{59}Co$ the experiments were renormalized to the precision results of Pavlik et al. /Pavlik 85/, for $^{93}Nb(n,2n)^{92m}Nb$ the cross-section is known to be constant to better 1% in the 13.5 - 15 MeV range. Therefore a value of 460 ± 5 mb, the result of the careful evaluation of T.B. Ryves /Ryves 89/ at E_n = 14.7 MeV was used for all neutron energies.

The existing cross-section measurements were performed for neutron energies in the range 13.7 - 14.8 MeV (see table 1) whereas the evaluations refer to one specific neutron energy chosen as 14.5 MeV. Thus in principle it is necessary to renormalize all cross-sections to this energy. Actually this was only necessary for the reaction $^{109}Ag(n,2n)^{108m}Ag$. For this reaction the results of Blinov 91, Lu Hanlin 90 and Wang 91 do show a small, but well established increase of the cross-sections with neutron energy and all cross-sections were renormalized from the measured cross-sections using the average value of the slope (45 mb/MeV) derived from the three mentioned experiments. For all other reactions the energy dependence was neglected as for the remaining (n,2n) reaction we are in the flat region of the maximum of the excitation function, where any change of the cross-section with neutron energy is much smaller than the reported cross-section uncertainties. For the $^{94}Mo(n,p)^{94}Nb$ reaction the two reported measurements are inconclusive even concerning the sign of the slope of the excitation function in the 14 - 15 MeV range, thus - as also supported by theoretical calculations - we are probably also in the maximum of the excitation function and thus also the energy dependence of this cross-section was neglected. For the $^{182}W(nn'\alpha)^{178m2}Hf$ reaction the gradient of the cross-section is probably quite large, however very badly known. On the other hand all measurements were performed in the narrow neutron energy range 14.8 - 14.9 MeV. Therefore in this case no attempt was made to renormalize the data to 14.5 MeV and in this one case a neutron energy of 14.85 MeV is assigned to the evaluated cross-section (see table 4). The correlations due to use of common reference cross-sections were neglected as they are very small due to the very low uncertainties of these standards (1 - 2%). By means of the described procedures all cross-section values have been renormalized to common nuclear data and a common neutron energy of 14.5 MeV. For those experiments giving results for several neutron energies these renormalized cross-sections were further combined to one value by simple averaging all cross-sections and corresponding uncertainties of the respective data set. This procedure is somewhat conservative as it assumes that the uncertainties within each data sets are mostly systematic and thus highly correlated. Probably our procedure thus overestimates somewhat the uncertainties of the final renormalized cross-sections for those data sets giving several cross-sections.

The final results of the described procedures one renormalized cross-section value for the nominal energy of 14.5 MeV for each data set are also shown in table 1.

The uncertainties of these renormalized cross-section values include all the uncertainties except those of the decay data.

Evaluated cross-sections were calculated as weighted averages of the renormalized input cross-sections given in the last column of table 1.

Both the external and the internal error of the uncertainty of the evaluated cross-sections were calculated and the larger of the two is used as evaluation results, that is in cases of slight inconsistency all uncertainties were increased until a value of chi-square equal to unity was reached. Finally the uncertainties of the decay data (see table 2) were added quadratically to the uncertainties calculated before as they are common to all measurements.

Evaluation and results

The results of the evaluation are shown in table 4. The second column shows the evaluated cross-sections derived from the experimental data given in table 1 and their uncertainties, column 3 shows the chi-square values per degree of freedom, indicating satisfactory consistency between the different experiments. In parenthesis (in column 3) also the uncertainties are given which result from the uncertainties of the decay data. As the table shows, this is now the largest source of uncertainty for the ^{109}Ag(n,2n)^{108m}Ag, ^{151}Eu(n,2n)^{150m}Eu and ^{159}Tb(n,2n)^{158}Tb cross-sections. In column 4 we give for comparison results derived by a completely other method. In his contribution to the 1989 CPR Vonach derived cross-section values for most of the (n,2n) reactions as difference between total (n,2n) cross-sections taken from systematics and measured cross-sections for the short-lived isomer /Vonach 89/. As the table shows, there is good agreement between the two results for the ^{109}Ag(n,2n)^{108m}Ag, ^{153}Eu(n,2n)$^{152g+m2}$Eu, ^{159}Tb(n,2n)^{158}Tb, ^{187}Re(n,2n)^{186m}Re and ^{193}Ir(n,2n)^{192m2}Ir reactions, whereas for only one reaction, ^{151}Eu(n,2n)$^{150g+m2}$Eu, a discrepancies on the 2σ level exists. Finally in the last column the results from the direct and indirect method are combined to a final evaluation result.

Literature

BLINOV+ 91: Private communication

BLINOV+ 95: M.V. Blinov, Contribution to this meeting

CSIKAI 93: Private communication giving revised values for the ^{109}Ag(n,2n)^{108m}Ag cross-sections

GREENWOOD 87: L.R. Greenwood et al., Phys.Rev.C35, 76 (1987)

IAEA 91: X-ray and Gamma-ray Standards for Detector Calibration , IAEA-TECDOC 619, IAEA, Vienna 1991

IKEDA 91: Y. Ikeda et al., Proc.Int.Conf. on Nuclear Data for Science and Technology, Jülich, May 1991, ed. S.Qaim, Springer 1992, p. 364

IKEDA 95: Y. Ikeda, Contribution to this meeting

LU HANLIN 95: Lu Hanlin et al., Contribution to this meeting

MEADOWS 95: J. Meadows et al., Contribution to this meeting

NETHAWAY 72: D.R. Nethaway, Nucl.Phys. A190, 635 (1972)

PAVLIK 85: A. Pavlik et al., Nucl.Sci.Eng. 90, 186, (1985)

PATRICK 90: B.H. Patrick et al., Report INDC(NDS)-232/L, (1990) IAEA, Vienna, p. 69 and private communication

PRESTWOOD 84: R.J. Prestwood et al., Phys. Rev. C30, 823 (1984)

QAIM 74: S. Qaim et al., Nucl.Phys. A224, 319 (1974)

RYVES 89: T.B. Ryves, A simultaneous Evaluation of Some Important Cross-Sections at 14.7 MeV, European App.Res.Rep., Nucl.Sci.Technol. Vol. 7, 1241 (1989)

SCHRADER 93: H. Schrader, PTB Braunschweig, private communication

THOMPSON 93: J.L. Thompson and A.R. Cartwright, I.Applied Rad.Isot. 44, 707 (1993)

VONACH 89: H. Vonach, Contribution to CRP-Meeting on Activation Cross-Sections for the Generation of long-lived Radionuclides of Importance in Fusion Reactor Technology, Argonne 1989 (unpublished)

WANG DA HAI 92: Report INDC(NDS)-263, IAEA, Vienna 1992, ed. Wang Da Hai

VONACH 93: H. Vonach and M. Wagner, Report INDC(NDS)-286, IAEA, Vienna (1993), p. 67

+ deceased

Table 1: Input data used for the evaluation

Reaction	Reference	Measured Cross-Section E_n(MeV)	σ(mb)	Renormalized C.S. at E_n = 14.5 MeV (mb)
$^{94}Mo(n,p)^{94}Nb$	GREENWOOD 87	14.55	57.2 ± 5.7	54.3 ± 5.00
		14.78	53.1 ± 5.3	
	IKEDA 91	14.1	44 ± 18	50.6 ± 18.9
		14.5	48 ± 20	
		14.8	58 ± 17	
	IKEDA 95	14.1	58 ± 12	56 ± 10
		14.8	54 ± 9	
$^{109}Ag(n,2n)^{108m}Ag$	BLINOV 95	13.7	634 ± 39	695 ± 40
		14.1	682 ± 40	
		14.5	695 ± 40	
		14.9	709 ± 41	
	MEADOWS 95	14.7	628 ± 42	666 ± 26
		14.7	682 ± 49	723 ± 33
	LU HANLIN 95	14.19	737 ± 20	767 ± 29
		14.28	707 ± 38	
		14.44	734 ± 34	
		14.77	757 ± 24	
		14.83	767 ± 24	
		13.64	733 ± 23	783 ± 35
		13.79	733 ± 59	
		14.03	747 ± 66	
		14.33	737 ± 26	
		14.60	763 ± 26	
		14.80	777 ± 23	
	CSIKAI 93	14.50	716 ± 44	716 ± 44
		14.50	667 ± 82	667 ± 82
$^{151}Eu(n,2n)^{150m}Eu$	NETHAWAY 72	14.8	1180 ± 150	1123 ± 135
	QAIM 74	14.7	1270 ± 149	1230 ± 145
	LU HANLIN 95	14.19	1190 ± 27	1220 ± 30
		14.44	1215 ± 36	
		14.77	1219 ± 28	

Table 1 (continued): Input data used for the evaluation

Reaction	Reference	Measured Cross-Section E_n(MeV)	σ(mb)	Renormalized C.S. at E_n = 14.5 MeV (mb)
$^{151}Eu(n,2n)^{150m}Eu$	BLINOV 95	13.52	1127 ± 66	1178 ± 61
		13.75	1167 ± 63	
		13.98	1139 ± 65	
		14.21	1092 ± 67	
		14.44	1126 ± 60	
		14.67	1140 ± 57	
		14.90	1218 ± 56	
	BLINOV 91	13.70	1050 ± 80	
		14.10	1177 ± 85	
		14.50	1150 ± 90	
		14.90	1070 ± 83	
	LU HANLIN 95	13.54	1227 ± 47	1180 ± 45
		13.72	1238 ± 48	
		14.35	1165 ± 44	
		14.60	1168 ± 44	
		14.80	1170 ± 44	
	MEADOWS 95	14.70	1214 ± 93	7278 ± 65
		14.70	1258 ± 87	1325 ± 50
	IKEDA 95	14.10	1215 ± 53	1232 ± 59
		14.50	1170 ± 59	
		14.80	1276 ± 64	
	IKEDA 93 A	14.70	1214 ± 7.7	1287 ± 40
	SMITH 93		1258 ± 6.9	1288 ± 53
	MEADOWS 92	14.80	1282 ± 74.7	1161.8 ± 76.2
$^{153}Eu(n,2n)^{152(m2+g)}Eu$	QAIM 74	14.7	1614 ± 132	1763.6 ± 144.5
	LU HANLIN 90	14.77	1560 ± 70	1560 ± 70
	BLINOV 90	13.7	1580 ± 120	1578 ± 118.7
		14.1	1659 ± 130	
		14.5	1480 ± 114	
		14.9	1514 ± 116	
	IKEDA 91	14.1	1326 ± 75	1577.4 ± 81.3
		14.5	1533 ± 77	

Table 1 (continued 2) Input data used for the evaluation

Reaction	Reference	Measured Cross-Section E_n(MeV)	σ(mb)	Renormalized C.S. at E_n = 14.5 MeV (mb)
$^{153}Eu(n,2n)^{152(m2+g)}Eu$	IKEDA 91	14.8	1659 ± 83	
	BLINOV 93	13.52	1464 ± 54	1493 ± 52
		13.75	1515 ± 59	
		13.98	1516 ± 53	
		14.21	1500 ± 61	
		14.44	1445 ± 52	
		14.67	1545 ± 49	
		14.90	1460 ± 44	
$^{159}Tb(n,2n)^{158}Tb$	PRESTWOOD 84	14.8	1930 ± 135	1897 ± 61
	LU HANLIN 95	14.19	1980 ± 56	1934 ± 57
		14.70	1968 ± 586	
	QAIM 74	14.70	1801 ± 117	1969 ± 138
	MEADOWS 95	14.70	1981 ± 184	2026 ± 99
			2072 ± 178	2120 ± 74
	LU HANLIN 95	13.72	2077 ± 277	1951 ± 97
		14.35	2144 ± 112	
		14.60	1909 ± 85	
		14.80	1922 ± 89	
	IKEDA 95	14.10	1937 ± 82	1899 ± 82
		14.70	1932 ± 82	
		14.90	1944 ± 83	
$^{179}Hf(n,2n)^{178m2}Hf$	PATRICK 90	14.8	5.91 ± 0.64	5.91 ± 0.60
	IKEDA 91	14.80	6.30 ± 0.60	6.30 ± 0.60
	MEADOWS 95	14.70	7.20 ± 0.65	7.36 ± 0.66
	LU HANLIN 95	14.19	7.00 ± 0.60	6.8091 ± 0.60
		14.77	6.60 ± 0.60	
	IKEDA 95	14.10	5.80 ± 0.40	6.30 ± 0.40
		14.80	6.80 ± 0.40	
	LU HANLIN 95	14.60	6.04 ± 0.32	6.04 ± 0.32
$^{182}W(n,n'\alpha)^{178m2}Hf$	LU HANLIN 95	14.19	0.016 ± 0.010	0.016 ± 0.010
	IKEDA 95	14.80	0.026 ± 0.013	0.026 ± 0.013
	BLINOV 95	14.74	0.010 ± 0.006	0.010 ± 0.006

Table 1 (continued 3) Input data used for the evaluation

Reaction	Reference	Measured Cross-Section E_n(MeV)	σ(mb)	Renormalized C.S. at E_n = 14.5 MeV (mb)
$^{182}W(n,n'\alpha)^{178m2}Hf$	IKEDA 91	14.80	0.014 ± 0.008	0.014 ± 0.008
$^{187}Re(n,2n)^{186m}Re$	IKEDA 95		445 ± 156	541 ± 189
	LU HANLIN 95		340 ± 192	340 ± 192
$^{193}Ir(n,2n)^{192m2}Ir$	IKEDA 95		147 ± 52	147 ± 52
	LU HANLIN 95		167 ± 24	167 ± 24

Table 2: Decay data used for the evaluation

Activation Product	Half-life (years)	E_γ (keV)	I_γ (%)
^{94}Nb	$(2.03 \pm .16).10^4$	702.63	98 ± 2
		871.10	100
^{108m}Ag	433 ± 15	434.0	90.5 ± 0.9
^{150m}Eu	36.9 ± 0.9	334	96 ± 3
		439.4	80.35 ± 3
$^{152g+m2}Eu$	13.56 ± 0.03	121.78	28.37 ± 0.13
		344.28	26.57 ± 0.11
		778.90	12.97 ± 0.06
		964.13	14.63 ± 0.06
		1408.01	20.85 ± 0.09
^{158}Tb	180 ± 11	944	43.9 ± 1.3
		184.4	72.6 ± 0.9
^{166m}Ho	$(1.2 \pm 0.18).10^3$	711.7	55.3 ± 0.65
		810.3	58.1 ± 0.68
$^{178m2}Hf$	31 ± 1	325.56	94.1 ± 0.3
		574	83.8
		495	68.9
^{186m}Re	$(2.0 \pm 0.5).10^5$	137**	8.22 ± 0.25
$^{192m2}Ir$	241 ± 9	316*	82.8 ± 0.4
		155.16	0.00097

* from subsequent decay of ^{193g}Ir
** from subsequent decay of ^{186g}Re

Table 3: Neutron Fluence Monitor used in the various experiments

Experiment	Fluence Monitor
NETHAWAY 72	$^{27}Al(n,\alpha)^{24}Na$
QAIM 74	various
PRESTWOOD 84	$^{169}Tm(n,2n)^{168}Tm$
GREENWOOD 87	$^{93}Nb(n,2n)^{92m}Nb$
PATRICK 90	various
BLINOV 91	$^{93}Nb(n,2n)^{92m}Nb$
IKEDA 91	$^{93}Nb(n,2n)^{92m}Nb$
CSIKAI 93	$^{93}Nb(n,2n)^{92m}Nb$
BLINOV 95	$^{93}Nb(n,2n)^{92m}Nb$
LU HANLIN 95	$^{93}Nb(n,2n)^{92m}Nb$
MEADOWS 95	$^{58}Ni(n,p)^{58}Co$
IKEDA 95	$^{93}Nb(n,2n)^{92m}Nb$

Table 4: Evaluation Results, Cross-Sections at E_n = 14.5 MeV

Reaction	Eval.Cross-Section from direct exp. (mb)		Chi-squ.	Eval.Cross-S.[3] from indirect det. (mb)	Final Eval. Cross-S. (mb)
$^{94}Mo(n,p)^{94}Nb$	54.4 ± 6.2	(4.4) [1]	0.07	-	54.4 ± 6.2
$^{109}Ag(n,2n)^{108m}Ag$	721 ± 31	(26)	1.83	665 ± 73	712 ± 29
$^{151}Eu(n,2n)^{150m}Eu$	1219 ± 52	(48)	1.05	1385 ± 63	1287 ± 84
$^{153}Eu(n,2n)^{152g+m2}Eu$	1547 ± 34	(-)	0.90	1585 ± 66	1554 ± 30
$^{159}Tb(n,2n)^{158}Tb$	1965 ± 140	(136)	1.14	1917 ± 57	1924 ± 53
$^{179}Hf(n,2n)^{178m2}Hf$	6.33 ± 0.28[2]	(0.20)	0.90	-	6.33 ± 0.28
$^{182}W(nn'\alpha)^{178m2}Hf$	0.014 ± 0.004	(0.0004)	0.43	-	0.014 ± 0.004
$^{187}Re(n,2n)^{186m}Re$	443 ± 174	(110)	0.57	514 ± 78	502 ± 71
$^{193}Ir(n,2n)^{192m2}Ir$	164 ± 23	(6)	0.12	184 ± 44	168 ± 20

1) Uncertainty contributions from decay data

2) Cross-section at E_n = 14.85 MeV

3) Values from /Vonach 89/ except for $^{153}Eu(n,2n)^{152g+m2}Eu$ and $^{187}Re(n,2n)^{186m}Re$, where the results of /Vonach 89/ were updated.

Isomeric Ratio for the Reaction $^{27}Al(n,2n)^{*)}$

G. Reffo
E.N.E.A., Bologna, Italy

*) was presented at the meeting orally

Report to Third Research Co-ordination Meeting on
"Activation cross sections for the Generation of Long-lived
Radionuclides of Importance in Fusion Reactor Technology."
St. Peterburg , 19 to-23 June 1995.

Evalution of $^{27}Al(n,2n)^{26}Al$ reaction cross section. *)

V.N.Manokhin.

In this work the systematics and systematical trends in behaviour of (n,2n)-reaction cross sections were used for evaluation of $^{27}Al(n,2n)^{26}Al$ reaction as far as available experimental data are scanty, measured near the reaction threshold and do not allow to make reliable extrapolation on high energy region.

Analysis of a great amount of experimental data /1/shows that (n,2n)-reaction cross section in the maximum of excitation functions(if $Q_{n,2n}<Q_{n,np}$) depends as follows:

$$\sigma^{max} = 64.4A^{2/3} \text{ mb } (A=50+210) \qquad (1)$$

A further analysis showed that this dependence takes place also in the mass number region A=35-50.

For $Q_{n,2n}>Q_{n,np}$ the cross sections of (n,2n) - reaction in the maximum of excitation functions lie below and the difference is equal to contribution of the (n,np) - reaction.

From the relation (1) the $^{27}Al(n,2n)^{26}Al$ cross section must be~590 mb. The data for the (n,np) - reaction cross sections on ^{27}Al (see Fig.) are contradictary, however a great (n,p) - cross section on ^{27}Al (~100 mb) makes preferable for the (n,np) reaction cross section the values, measured by S.Grimes/ 2 /(~400 mb) or R Glover/ 3 /(~300 mb) at 14.8 MeV,as far as these values give more great (n,np) - reaction cross section, that is typical for $Q_{n,2n}>Q_{n,np}$.

This means that the $^{27}Al(n,np)$ - reaction cross section can be evaluated at ~20 Mev neutron energy about 450-500 mb (close to ADL-3 evaluation) and the $^{27}Al(n,2n)$ reaction cross section - within 100-150 mb. The value 100 mb is close to JEF-2 evaluation, 150 mb - to the ADL-3 evaluation.

For more reliable conclusions one can pay attention on the following systematic trend in behaviour of (n,2n) reactions for ^{23}Na, ^{27}Al, ^{31}P, ^{35}Cl, ^{39}K, having the same (N-Z). An analysis and comparison of the reaction thresholds for (n,2n) and (n,np) reactions shows that the difference between them increases practically linearly with increase of A (3,6 MeV for ^{23}Na and 6,4 MeV for ^{39}K). That explains a clearly observed decrease of the maximum of (n,2n) - reaction cross sections in the chain of isotopes mentioned above. The ^{23}Na (n,2n) - reaction cross section near the maximum of excitation function is about 110-120 mb, the (n,2n) - reaction cross sections (also at the

*) presented by A.V. Ignatyuk

maximum of excitation function) can be evaluated about (70-80) mb for ^{31}P, - within ~(50-60) mb for ^{35}Cl and - ~(40 - 50)mb for ^{39}K. Having in mind this trend one can estimate the $^{27}Al(n,2n)$ - reaction cross section within (90 - 110)mb.

In the works / 1,4 / it was showed that the (n,2n) - reaction excitation functions normalized to maximum cross section are similar in the neutron energy region from reaction threshold up to the energy at which maximum cross section lies. Calculations made on the base of using the normalized (n,2n)-reaction excitation function give more low cross sections in comparison with experimental data of S.Iwasaki et al/ 5 /(results of which are in agreement with the ADL-3 evalution).

As a result of all those considerations the value 100 mb at the maximum excitation function(at ~20-22 MeV) one should consider as a low limit. In any case there are no strong arguments to evaluate the $^{27}Al(n,2n)$-reaction cross section in the maximum of excitation function more than ~150 mb. It is possible to use the ADL-3 evaluation but more preferable to renormalized it to the value ~100 mb at 20 MeV.

Problem of cross section to isomer state is more difficult because of lack of reliable experimental data but it seems that cross sections for ground state in ADL-3 and EAF-3 are too high. Available data of the work by M.Sasao et al / 6 /shows more low cross sections.

The experimental data by Nakamura at al , reported at Juelich (1991) conference / 7 /, give maximum value of $^{27}Al(n,2n)^{26g}Al$ reaction cross section below 90 mb at 20 MeV. It leads to conclusion that the $^{27}Al(n,2n)^{26m}Al$ - reaction cross section is within 10-20 mb at 20 MeV.This is reasonable value having in mind high spin of gound state(5+).The ADL-3 evaluation may be recommended.

References.

1. V.N.Manokhin, VANT, Ser.Yadernye Konstanty, 1(1994) 18.
2. S.Grimes Nucl.Sci.Eng.,62 (1977) 187.
3. R.Glover et al., Nucl.Phys. 24(1961)630.
4. H.Vonach, Proc.of the 19th Jnt. Symp. on Nuclear Physics,.Gaussig, Germany, 1989
5. S.Iwasaki et al. Proc. of Jnt.Conf. on Nuclear Data, Mito, 1988.p.295.
6. M.Sasao et al., Phys.Rev., 35 (1987) 2327.
7. T.Nakamura at al Proc. of Jnt. Conf. on Nuclear Data, Juelich, Germany, 1991.

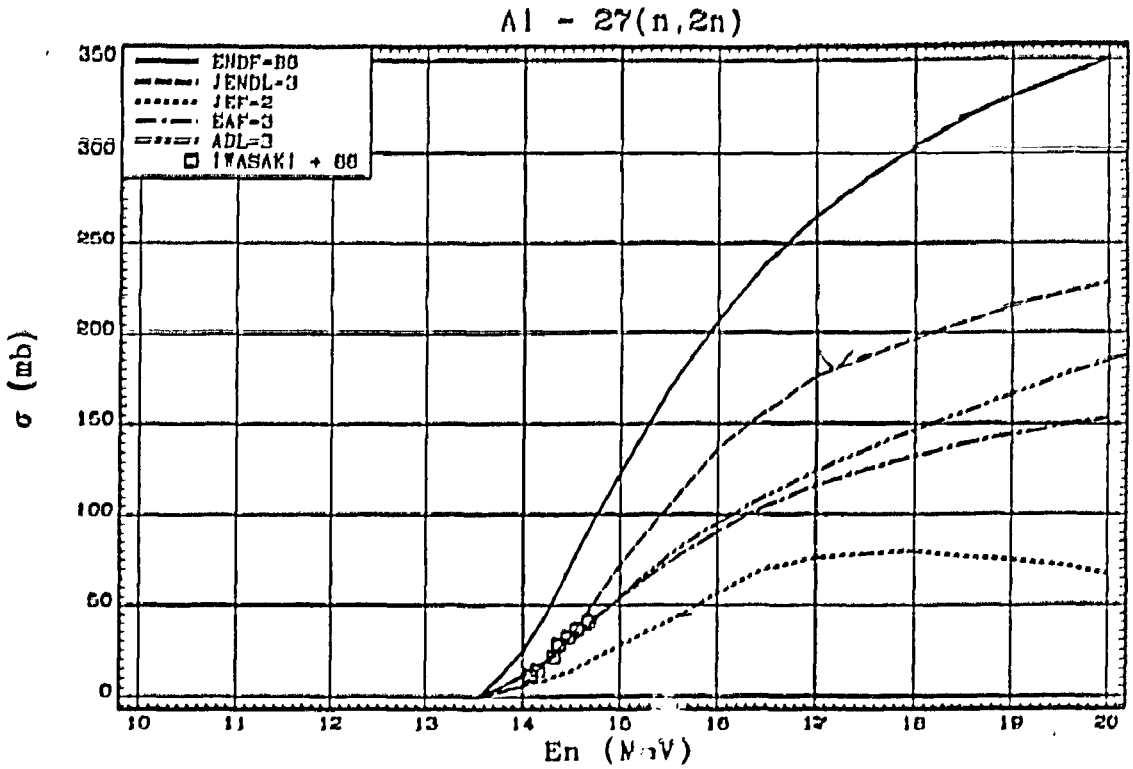
Al - 27(n,2n)
ENDF-B6
JENDL-3
JEF-2
EAF-3
ADL-3
IWASAKI + 88
σ (mb)
En (MeV)

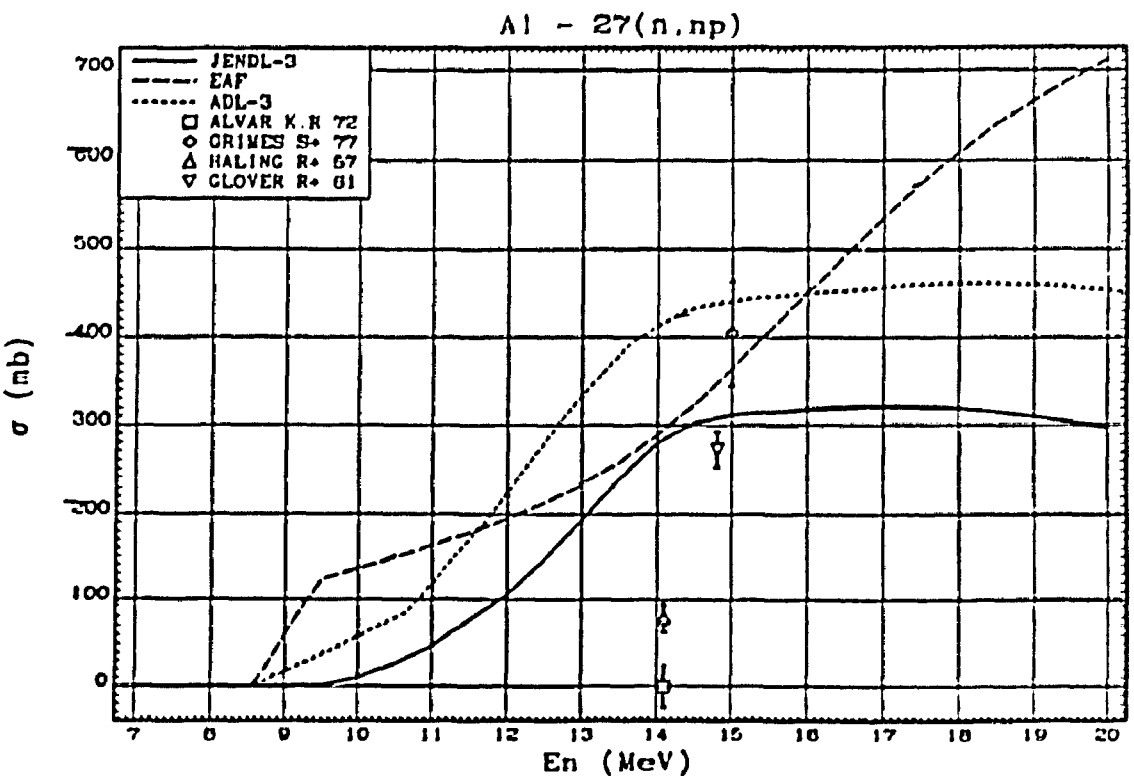
Al - 27(n,np)
JENDL-3
EAF
ADL-3
ALVAR K.R 72
GRIMES S+ 77
HALING R+ 67
CLOVER R+ 61
σ (mb)
En (MeV)

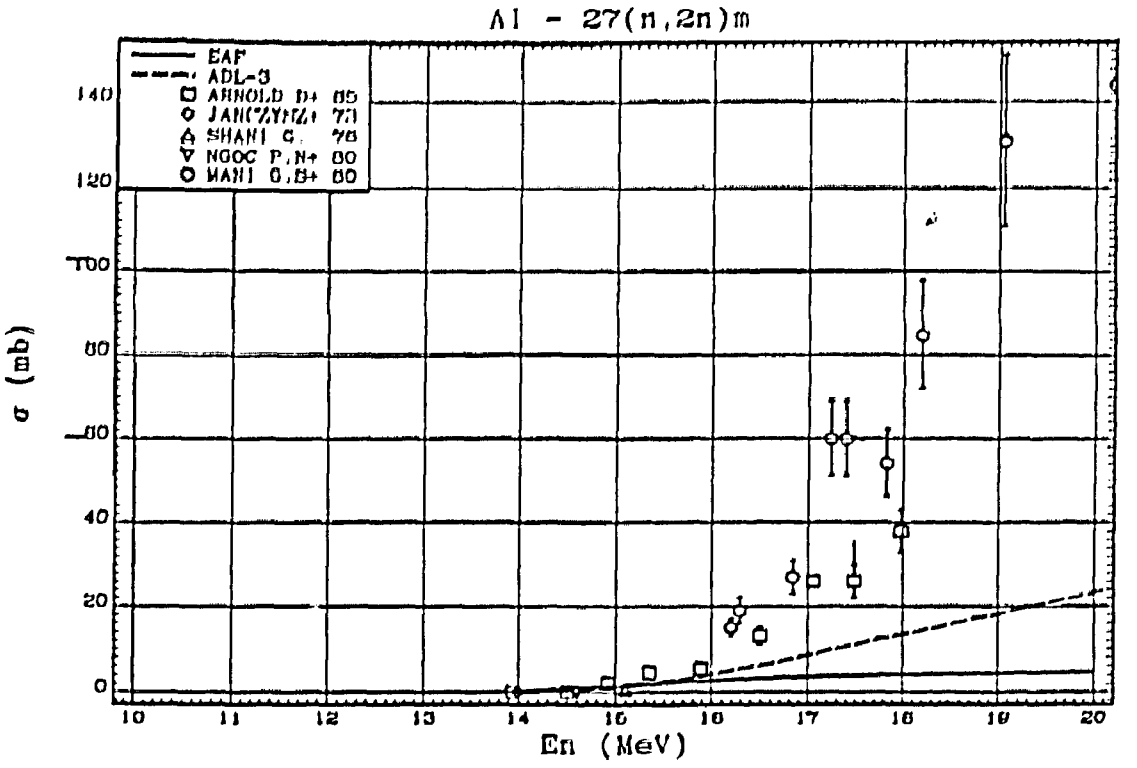
Al - 27(n,2n)m
EAF
ADL-3
ARNOLD D+ 85
JANCZYNZ+ 73
SHANI G. 76
NGOC P.N+ 80
MANI G.S+ 80
σ (mb)
En (MeV)

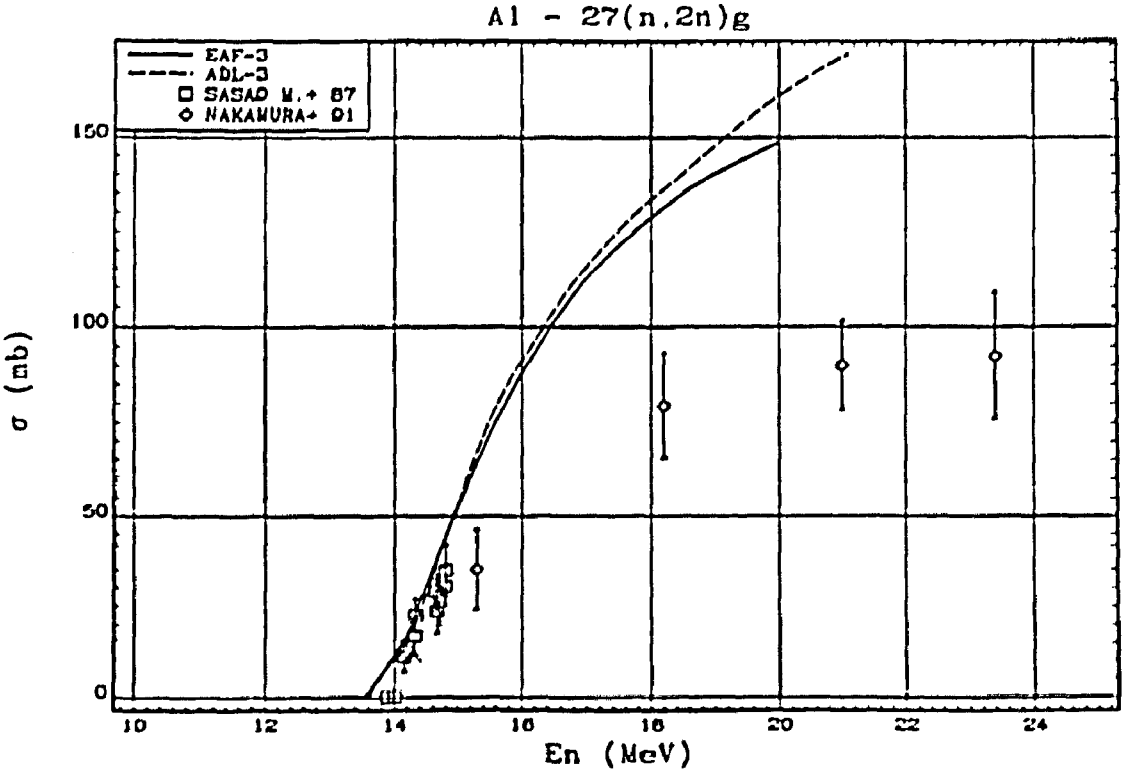
Al - 27(n,2n)g
EAF-3
ADL-3
SASAO M.+ 87
NAKAMURA+ 91
σ (mb)
En (MeV)

Report to Third Research Co-ordination Meeting on
"Activation cross sections for the Generation of Long-lived
Radionuclides of Importance in Fusion Reactor Technology,
St.Peterburg,19 to 23 June 1995. ,25-27 June 1995.

Evalution of ^{63}Cu (n,p) ^{63}Ni reaction cross section.*)

V.N.Manokhin.

It is very difficult to evaluate the ^{63}Cu (n,p)^{63}Ni reaction cross section using experimental data as far as there are only two experimental points at about 14,5 MeV, which differ by factor more two. Available calculated data from the libraries ENDF-6, JENDL-3, EAF-3 and ADL-3 in the region of maximum of the excitation function essentionally differ as well (by factor 2).

In this case to evaluate this reaction cross section one should use the systematics of maximum cross sections of (n,p) - reactions. An analysis of experimental data shows that the (n,p)-reaction cross sections in the maximum of excitation functions (at least for A = 10-100) for isotopes of a given element decreases exponentionally as a function of (N-Z) or A. In Fig.1 the dependences of $\ln\sigma^{max}$(n,p) for isotopes of Ca, Ti, Cr, Fe, Ni and Zn are given as a function of (N-Z).One can see the linear dependences within uncertainties determined from the spread of experimental data in the region of maximum of excitation functions. These lines are practically parallel and equidistant.

The same conclusion was made many years ago by D.Gardner /1/ for the 14 MeV energy region.

The value $\ln\sigma^{max}$ (n,p) increases also practically linearly for isotopes with the same (N-Z).

These trends allow to evaluate ^{63}Cu(n,p) - reaction cross section in the maximum of the excitation function on the base of (n,p)-reaction cross section dependences for Ni and Zn. Parallel and equidistant extrapolation from $\ln\sigma^{max}$ for ^{65}Cu(n,p) reaction to that for ^{63}Cu(n,p) gives (105 ±10) mb for σ^{max} of ^{63}Cu(n,p) reaction. For ^{65}Cu(n,p) - reaction cross section the value (23 ±2)mb was used. Evaluation of this value was based on experimental data.

Concerning excitation function it is recommended to accept the JENDL-3 or ADL-3 evaluations, renormalized to the value 105 mb.

Reference.

1. D.Gardner.Nucl.Physics,20(1962)373.

*) Presented by A.V. Ignatyuk

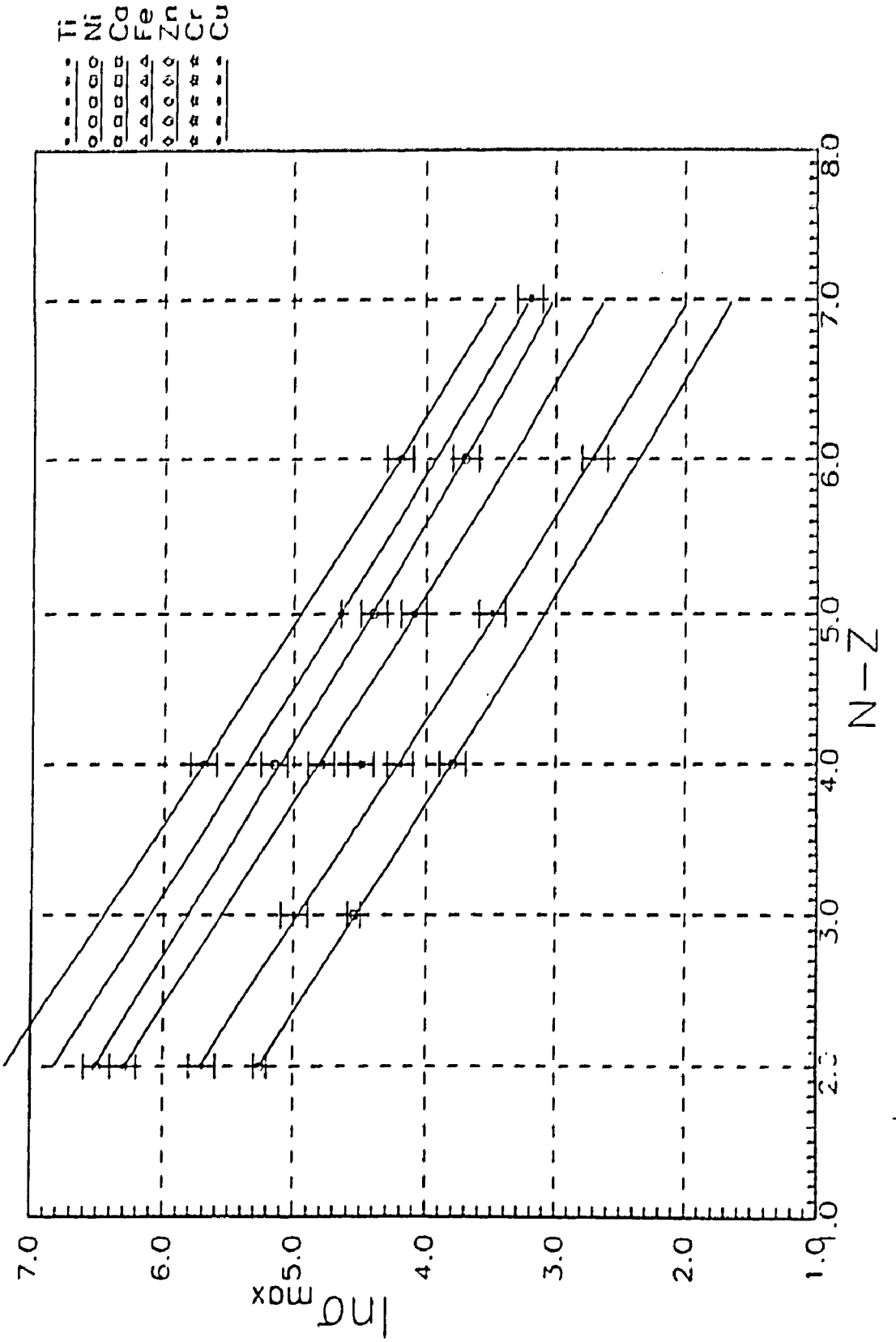

Fig. 1.

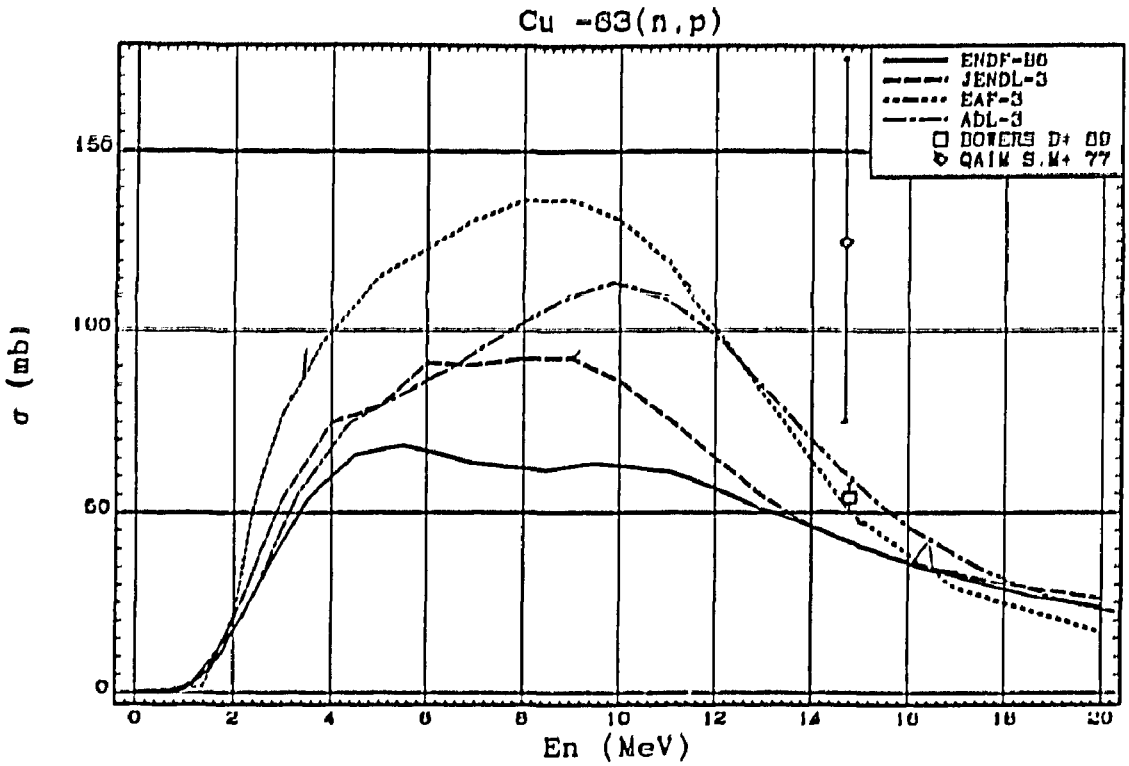

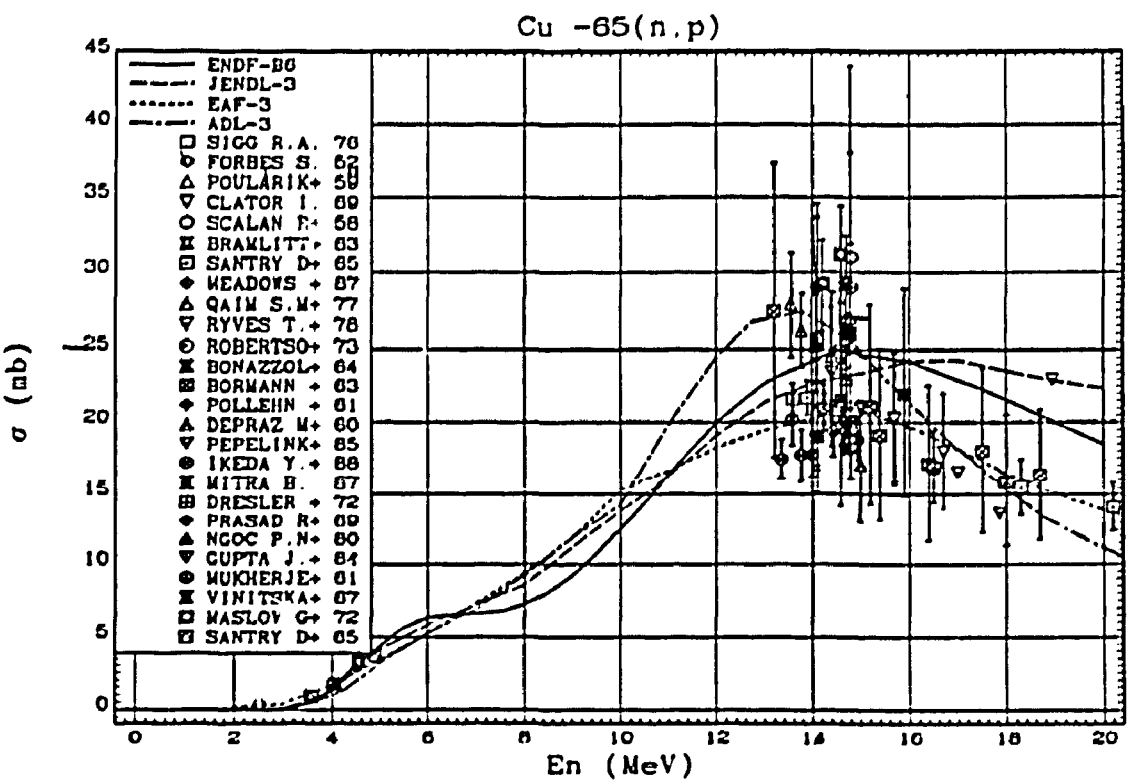

NEXT PAGE(S) left BLANK

Activation Concerns and Cross Section Data Needs for Fusion Reactor Technology*

by

E.T. Cheng
TSI Resrarch, Inc.
225 Stevens Avenue
Solana Beach, California
U.S.A. 92075

Presented at
the third IAEA RCM on Activation Cross Sections for the Generation of Long-lived Radionuclides of Importance in Fusion Reactor Technology
Saint Petersburg, Russia
19-23 June 1995

* Work supported by the U.S. Department of Energy, Office of Fusion Energy, under Grant No.: DE-FG03-92ER54137.

Activation Concerns and Cross Section Data Needs for Fusion Reactor Technology*

by
E.T. Cheng
TSI Resrarch, Inc.
Solana Beach, California
U.S.A.

Abstract

Activation of reactor materials due to the neutron field generated by the 14 MeV deuterium-tritium neutrons is a major issue concerning the development of fusion as a long-term energy source. It will impact the development of reactor technologies relevant to safety, maintenance, and waste disposal. Availability and quality of key activation data are very important for the assessment of solutions to the various activation concerns. Review of the activation data base is necessary to identify deficiencies. A list of neutron reactions for which cross section measurements are needed is presented based on recent reviews.

1. Introduction

A tokamak based, deuterium-tritium (D-T) fueled, international thermonuclear experimental reactor (ITER)[1], which is being designed by an international cooperation effort, is proposed to be constructed and operational at the beginning of the 21st century. Prototype D-T fusion power plants based on the tokamak concept are being investigated aiming at the demonstration of fusion power in the early half of the next century. Due to the presence of 14 MeV neutrons, which are produced in the D-T fusion reaction and carry about 80% of the released energy, blanket and shield components are needed, respectively, to extract the nuclear power and breed tritium, and to protect the superconducting magnet against radiation damage. To design the blanket and shield components, and to assess the performance of these components, nuclear data plays a very important role. With the required design details and demands, it becomes a necessity to make available more accurate nuclear data base.

As the first step to secure an accurate nuclear data base, it is necessary to generate as much as possible experimental data and to perform evaluations for the needed cross sections. During the past few decades, the nuclear laboratories worldwide have produced numerous cross section measurements. The regional nuclear data centers have also collected the respective most up-to-date evaluations needed for the design of fusion power plants. To efficiently improve the nuclear data base in order to meet the design requirement, it is important that all these experimental data and evaluations be made available to all concerned parties. For the design of ITER, it is also desirable to use an

* Work supported by the U.S. Department of Energy, Office of Fusion Energy, under Grant No.: DE-FG03-92ER54137.

internationally acceptable nuclear data library for all transport and activation analyses. There have been a number of coordination activities to support the measurements of fusion specific cross sections and the establishment of an international nuclear data library since the early 1980s. Two of the notable activities, by far the most successful, are (1) coordinated research program on the measurements of activation cross sections leading to the production of long-lived radionuclides of importance to fusion reactor technology,[2] and (2) international fusion evaluated nuclear data library (IFENDL),[3,4] both are under the coordination of the International Atomic Energy Agency.

This paper discusses the role of activation cross sections in fusion reactor technology. It summarizes the results obtained from recent reviews of the activation data base, in which deficiencies were identified. Based on these reviews, a list of needed cross section measurements is presented.

II. Activation Concerns

Activation of reactor materials due to the neutron fluxes induced by the 14 MeV D-T neutrons is one of the most important issues relevant to the development of fusion energy. It plays a key role in the decision of making fusion an ultimate energy source for mankind. It dictates the choice of reactor materials. The activation characteristics of chosen reactor materials are important in determining proper reactor technologies to be develped for future power plants.

Activation of fusion reactor materials, particularly those for the first wall, blanket, and shield components, causes concerns in the following areas:[5-7]

(1) Safety - Release of radiologically hazardous materials during reactor operation and after shutdown;

(2) Maintenance - Exposure of gamma radiation from induced radioactive materials during normal and off-normal maintenance scenarios; and

(3) Waste Management - Storage, transportation, and disposal of radioactive materials in decommissioned reactor components.

Key neutron activation reactions have been identified from candidate fusion materials which were chosen as results of a number of reactor studies in the past. Activation analyses were performed for these candidate materials to identify the dominating radionuclides for safety, maintenance, and waste management concerns.[5-8] From these investigations, it was found that the induced radionuclides of concern to safety and maintenance are generally those with shorter half-lives, such as Fe-56 (half-life 2.6 h), Fe-54 (312 d), Co-58 (70.8 d), Co-57 (272 d), and Cr-51 (27.7 d) for stainless steels, and Sc-48 (43.7 h), Sc-47 (3.35 d), Sc-46 (83.8 d), Cr-51, and Ca-47 (4.54 d) for V-Ti-Cr alloy, and Na-24 (15 h), Al-28 (2.24 m), Al-29 (6.56 m), Mg-27 (9.46 m), and Mg-28 (20.9 h)

for SiC.[8] On the other hand, long-lived radionuclides are considered important for the long-term disposal of waste materials. Activation cross sections leading to the generation of long-lived radionuclides are a subject of coordinated research program sponsored by the IAEA, as mentioned previously.[2] Medium-lived radionuclides such as Co-60 (5.27 y), however, may play a very important role during the storage and transportation phases of the waste management scenario, and in some cases for safety and maintenance assessment.

III. Recent Reviews and Activation Data Needs

Accurate assessment of the various activation concerns is very important during the reactor development stage, and depends mainly on the availability of reliable key neutron activation cross sections. Several reviews of the status of cross sections for the activation reactions were performed recently, and deficiencies in the activation data base were identified.[3,9,10,11] Based on these reviews, a list of neutron reactions for which cross section measurements are needed is presented in Table 1. Energy range requested for these measurements is generally from threshold to 14 MeV for the threshold reactions, and thermal to 1 MeV for the neutron capture reactions. The required accuracy is 20%, in general.

The reactions shown in Table 1 can be further broken into the following areas of concern:

1. Safety and maintenance related concerns:

   PbLi based blanket

   Pb activation: Pb-204(n,p)Tl-204 and Pb-204(n,t)Tl-202

   SiC blanket

   Si activation:
   [Si-28(n,n'p)Al-27]Al-27(n,n'α)Na-23 [Na-23(n,2n)Na-22]

   Tritium production in Si: Si-29(n,t)Al-27

2. Waste manegement related concerns:

   Storage, transportation, and materials recycle

   Co-60 production reactions in Fe and Ni: Fe-58(n,γ)Fe-59(β-)Co-59(n,γ)Co-60, Ni-60(n,p)Co-60, and Ni-61(n,n'p)Co-60

   Recycle of V-alloy: V-50(n,2n)V-49

Waste Classification

Alloying elements in structural materials, Impurities in structural and breeder materials, MHD coating materials for liquid metal blanket, and magnet:
N-14(n,p)C-14, Si-28(n,n'p)Al-27(n,2n)Al-26, Ti-48(n,α)Ca-45(n,α)Ar-42, Ni-63(n,α)Fe-60, Ni-64(n,2n)Ni-63, Cu-65(n,t)Ni-63, Mo-94(n,p)Nb-94, W-182(n,n'α)Hf178m2, W-186(n,n'α)Hf-182, Sn-120(n,γ)Sn-121, and Sn-125(n,γ)Sn-126

3. Other Concerns:

Reactor design

Nuclear heating in the superconducting magnet (copper stabilizer):
Cu-63(n,γ)Cu-64 and Cu-65(N,γ)Cu-66

316SS and Inconel 625 decay heat in the ITER shielding blanket and vacuum vessel: Mn-55(n,γ)Mn-56 and Ta-181(n,γ)Ta-182

Neutron Diagnostics

Dosimeter cross section: Zn-64(n,p)Cu-64 (5% accuracy)

References:

1. ITER Joint Central Team, "The Impact of Materials Selection on the Design of the International Thermonuclear Experimental Reactor (ITER)," Journal of Nuclear Materials, 212-215 (1994), pp. 3-10.

2. D.L. Smith and A.B. Pashchenko, "Investigation of the Generation of Several Long-lived Radionuclides of Importance in Fusion Reactor Technology: Report on a Coordinated Research Program Sponsored by the International Atomic Energy Agency," Proc. Intl. Conf. Nuclear Data for Science and Technology, Gatlinburg, TN, May 9-13, 1994, p. 859.

3. D.C. Larson, et al., "Status of Nuclear Data for ITER Applications," ibid., p. 831.

4. S. Ganesan, "Improved Evaluation and Integral Data Testing for FENDL, Summary of the IAEA Advisory Group Meeting, Garching near Munich, Germany, 12-16 September 1994" INDC(NDS)-312, IAEA Nuclear Data Section report, Vienna, December 1994.

5. E.T. Cheng, "Activation Cross Sections for Safety and Environmental Assessment of Fusion Reactors," Proc. Specialists' Meeting on Neutron Activation Cross Sections for Fission and Fusion Energy Applications, ANL, U.S.A., 13-15 September 1989, p.29.

6. S. Piet, et al., "Initial Investigation of Accident Safety, Waste Management, Recycling, Effluent, and Maintenance Considerations for Low-activation Materials," Fusion Technology, 19 (1991) pp. 146-161.

7. E.T. Cheng and G. Saji, "Activation and Waste Management Considerations of Fusion Materials," Journal of Nuclear Materials, 212-215 (1994), pp. 621-627.

8. E.T. Cheng, "Activation Products from Fusion Materials," TSI Research report, TSIR-37, May 1995 (revised).

9. E.T. Cheng and D.L. Smith, "Nuclear Data Needs and Status for fusion reactor technology," Proc. Intl. Conf. Nuclear Data for Science and Technology, 13-17 May 1991, Juelich, Germany, S.M. Qaim (ed.), Springer-Verlag (1992); p. 237.

10. R. Forrest, "Nuclear Data for Fusion Applications," Proc. Intl. Conf. Nuclear Data for Science and Technology, Gatlinburg, TN, May 9-13, 1994, p. 854.

11. E.T. Cheng, R.A. Forrest, J. Kopecky, F.M. Mann, "List of Neutron Activation Reactions Important for Fusion Power Plant Technology," BU Nuclear Energy, EAF-Doc-004, ECN Report, Petten, Holland, March 1994.

Table 1
List of Neutron Reactions for Which Cross Section Measurements are Needed

- Experimental data needed with 20% accuracy unless otherwise specified

1. N-14(n,p)C-14
Energy range: 10 - 15 MeV
Comment: Waste disposal concern for nitrogen containing structural materials. Measured data above 10 MeV very sparse.

2. Ti-48(n,α)Ca-45(n,α)Ar-42
Energy range: 10 - 15 MeV
Comment: Multi-step reactions to produce Ar-42. Waste disposal concern for the V-Cr-Ti alloy.

3. V-50(n,2n)V-49
Energy range: Threshold - 15 MeV
Comment: Materials recycling concern for the V-alloy.

4. Fe-58(n,γ)Fe-59
Fe-59 (β-) → Co-59(n,γ)Co-60
Energy range: Thermal - 1 MeV
Comment: Waste storage and transportation concerns for structural materials. Note that Fe-59 decays into Co-59 which produces Co-60 via neutron capture reactions.

5. Ni-63(n,α)Fe-60
Energy range: 10 - 15 MeV
Comment: Waste disposal concern for structural materials copper magnet.

6. Ni-64(n,2n)Ni-63
Energy range: Threshold - 15 MeV
Comment: Waste disposal concern for structural materials.

7. Cu-65(n,t)Ni-63
Energy range: 10 - 15 MeV
Comment: Waste disposal concern for first wall (plasma facing) component and copper magnets.

8. Zn-64(n,p)Cu-64
Energy range: 5 - 15 MeV; 5%
Comment: Dosimeter cross section.

Table 1 (cont.)
List of Neutron Reactions for Which Cross Section Measurements are Needed

9. Mo-94(n,p)Nb-94
Energy range: 10 - 15 MeV
Comment: Waste disposal concern for structural materials. Satisfied - IAEA CRP Reports.

10. W-182(n,n'α)Hf178m2
Energy range: 10 - 15 MeV
Comment: Waste disposal concern for tungsten. Measurements performed. Preliminary results reported (IAEA-CRP).

11. W-186(n,n'α)Hf-182
Energy range: 10 - 15 MeV
Comment: Waste disposal concern for tungsten. Measurements performed. Preliminary results reported (IAEA-CRP).

12. Pb-204(n,p)Tl-204
Energy range: 10 - 15 MeV
Comment: Decay heat and radiological hazard concerns in lead.

13. Pb-204(n,t)Tl-202
Energy range: Threshold to 14 MeV
Comment: Decay heat and radiological hazard concerns in lead.

14. Al-27(n,n'α)Na-23
Na-23(n,2n)Na-22/Na-23(n,γ)Na-24
Energy range: Threshold - 15 MeV
Comment: Safety and maintenance concerns for structural materials containing Al.

15. Si-29(n,t)Al-27
Energy range: Threshold - 15 MeV
Comment: Tritium production in SiC.

16. Ti-48(n,α)Ca-45(n,α)Ar-42
Energy Range: Threshold to 14 MeV
Comment: Radioactive target. Waste disposal concern for the V-Cr-Ti alloy.

17. Sn-120(n,γ)Sn-121
Energy range: Thermal - 1 MeV
Comment: Waste disposal concern for the superconducting magnet.

Table 1 (cont.)
List of Neutron Reactions for Which Cross Section Measurements are Needed

18. Sn-125(n,γ)Sn-126
Energy range: Thermal - 1 MeV
Comment: Waste disposal concern for the superconducting magnet.

19. Cu-63(n,γ) and Cu-65(n,γ)
Energy range: thermal - 1 MeV (10% accuracy)
Comment: Needed for ITER and future power reactors to determine the nuclear heating rate in the superconducting toroidal field magnet.

20. Mn-55(n,γ)Mn-56
Energy range: thermal - 1 MeV (10% accuracy)
Comment: Needed for ITER to determine the decay heat in the shielding blanket.

21. Ta-181(n,γ)Ta-182
Energy range: thermal - 1 MeV (10% accuracy)
Comment: Decay heat in ITER blanket and vacuum vessel.

22. Ni(n,x)Co-60
[Ni-60(n,p) and Ni-61(n,n'p)]
Energy range: Threshold - 15 MeV
Comment: Needed to determine the required cooling time for the decommissioned reactor components before transporting to the waste burial/recycling site.

23. Si(n,x)Al-27(n,2n)Al-26
[Si-28(n,n'p)Al-27]
Energy range: Threshold - 15 MeV
Comment: Needed for the determination of waste classification for SiC.

Presented at 3rd IAEA RCM on 'Activation Cross Sections for the Generation of Long-lived Radionuclides of Importance in Fusion Reactor Technology', St. Petersburg, Russia, 19-23 June 1995

Development of EASY to include sequential charged particle reactions and examples of its use with realistic materials

R.A. Forrest
UKAEA Government Division, Fusion
Culham, Abingdon, Oxfordshire OX14 3DB, UK
(UKAEA/Euratom Fusion Association)

Introduction

The European Activation System (EASY) includes the European Activation File (EAF) and the inventory code FISPACT. A new version (4.0) has recently been developed, and one of the main new features is the ability to calculate the effect of sequential charged particle reactions (SCPR). Such reactions have been shown in the past to be significant when considering pure materials. A question has remained over the importance of the effect in realistic alloys which contain representative impurities. This paper describes the new features in EASY4 and reports results of calculations on a series of fusion relevant materials.

Development of EASY4

The FISPACT inventory code has been developed for neutron activation calculations of fusion devices. Details of the use of this code and background about the approach used to solve the set of differential equations are given in the User Manual[1]. FISPACT uses external libraries of reaction cross sections (*e.g.* the European Activation File[2] EAF) and decay data for all relevant nuclides to calculate an inventory of nuclides produced as a result of the irradiation of a starting material with a flux of neutrons.

The actual output quantities include the amount (number of atoms and grams), the activity (Bq), α-, β- and γ-energies (kW), γ dose-rate (Svh^{-1}), ingestion and inhalation doses (Sv), legal transport limits (A_2 value) and the half-life for each nuclide. Amounts and heat outputs are also given for the elements and the γ-ray spectrum for the material is listed as well as various summed quantities, such as total activity and total dose rate. At the end of each time interval the dominant nuclides (in terms of activity, heat, γ dose rate and biological hazards) and the pathway data for the production of these nuclides can be shown. The uncertainties in the five total radiological quantities can be calculated and output. As an option, data files can be produced for subsequent use by other programs to plot graphs of the activity, heat output, γ dose rate and biological hazards as a function of the cooling time and selected blocks of output may also be written to external data files.

An important goal of the current work is to ensure that FISPACT 4.0 remains compatible with the EAF 4.0 library developed by ECN Petten. It is vital that the cross section library, decay data library, associated libraries (biological hazard and legal transport) and the code constitute an integrated package for use in the calculation of fusion activation.

Sequential charged particle reactions

The inventory code FISPACT used for calculations of activation in fusion devices is mainly concerned with the interaction of neutrons with materials. This mode of activation is the dominant process in materials exposed to the high neutron fluxes found in D-T

fusion devices. However, it was pointed out some years ago[3] by workers at FZK Karlsruhe that an additional mechanism of activation would involve the interaction of charged particles (resulting from the primary neutron interactions) with the material; possibly leading to a new set of radionuclides. This mechanism is described as the effect of 'sequential charged particle reactions' and considerable work to determine its importance to fusion devices has been carried out at FZK[4]. This work has involved the production of libraries of data describing the energy distribution of the charged particles (p, α, d, t, h) produced in the neutron interactions, the range of these charged particles in materials and the cross sections for the reactions of the charged particles with nuclei.

For a particular neutron spectrum it is then possible to use these libraries to calculate 'pseudo cross sections' which describe the two-step process of the production of charged particle and the subsequent reaction of it with the material. These pseudo cross sections can be used in a similar way to the effective (or 'collapsed') cross sections used in FISPACT. The code developed by FZK to calculate these pseudo cross sections (PCROSS) works in conjunction with FISPACT, however to make full use of calculations involving this mechanism it is advantageous to fully incorporate this in FISPACT and access it as an additional option.

Changes to the decay data library

The inclusion of sequential charged particle reactions on the target nuclides considered in EAF 3.1 leads to production of a set of nuclides that are not produced by any neutron induced reactions. An example is ^{7}Be (53.3 days) which was not considered in EAF 3.1 but can be produced by (p,n) reactions on ^{7}Li. It is found that an additional 231 new nuclides are required in the decay data library, bringing the total to 1867 (including stables). Evaluated files for these nuclides have been used wherever possible from JEF2.2, otherwise files from ENSDF, or files based on references such as Browne and Firestone[5] have been created.

Changes to the cross section library

EAF4.0 contains data for five additional targets that can be formed by sequential charged particle reactions. The five new nuclides that have been included as targets are: ^{7}Be, ^{48}Cr, ^{76}Kr, ^{86}Zn and ^{211}Rn.

Changes to the other data libraries

The 231 new nuclides introduced in the decay data library also need to have entries in the biological hazard and A_2 libraries. These enlarged libraries have also been constructed for use in EASY.

Modifications to FISPACT

The modifications to FISPACT to allow the inclusion of sequential charged particle reactions have included the addition of new subroutines to FISPACT, broadly based on subroutines taken from PCROSS but with different common blocks. These subroutines are called from other FISPACT subroutines rather than from the organisational subroutine in PCROSS. There is a new code word 'SEQUENTIAL' which activates the option. The COLLAPX and ARRAYX files remain unchanged, so that there is compatibility with previous versions of FISPACT; the new pseudo cross sections are calculated and merged

with the existing collapsed cross sections in the main storage array A(), but they are not stored in a file. This approach is necessary as the pseudo cross sections need to be recalculated either for each time interval with the flux value greater than zero or for each subinterval if the LEVEL parameter N is greater than 1.

In order to follow the calculational method of PCROSS as closely as possible it is necessary to know the density of the material. If the user has included this information in the input file then this value is used for all calculations (note that it is assumed that the density of the material remains unchanged during exposure and transmutation). If the density is not input then the density is estimated using the input masses and the elemental densities.

These modifications are included in FISPACT 4, and similar results to those found by FZK for exposure of various elements have been found. The pathway analysis method works with very few changes (new reaction labels for the two step processes are defined) since this relies only on the parent and daughter identifiers.

There are further modifications that can be considered in the future; these include the treatment of uncertainty data since the sequential charged particle reactions libraries contain no uncertainty information. At present it is assumed that the uncertainty for these two-step processes is zero, but this will need to be improved in the future if the effect of SCPR is significant. Another omission in the current charged particle library is the splitting of cross sections between ground states and isomers. At present only the ground state nuclide is produced.

Calculations on realistic materials

Earlier calculations have shown that the effect of SCPR on single elements can be dramatic. The largest effects were found in the light elements N, F, Na and V although effects were also seen in Au and Pt. In materials containing these elements it is possible that similar effects would also be seen.

Table 1. Elemental composition of studied materials.

Material	Impurities (ppm)
Li_4SiO_4	Al 1580, C 1040, Ca 200, K 200, Na 850
Be	Cu 50, Cr 50, O 4500, Si 300, Al 200, Fe 600, Ni 90, Zn 600, Pb 200, Mn 50, Sb 60
316 stainless steel	Ta 500, Nb 100, Cu 2000, Ti 50, Al 50, Co 900, Ag 400, Sb 10, Sn 10
Manet 2	Cu 100, Al 100, Co 50, Ag 50, As 100, Sb 4, Sn 10
OPTSTAB	Ni 50, Mo 20, Nb 0.2, Cu 100, Ti 10, Al 10, Co 10, Ag 0.5, Sn 10
Inconel 600	Mo 100, C 60, Nb 300, Sn 100, Co 500, Cu 600, Mg 300, Pb 10, N 50
V-5Ti	Si 400, Al 50, Fe 10, Ni 1, Co 0.1, N 180, Mo 1, C 60, W 232, Nb 50, Hf 1, Ag 0.01, Cu 0.3
V-3Ti-1Si	Al 30, Fe 2, Ni 1, Mo 1, C 50, Ta 1, Nb 4, Na 20
V-4Cr-4Ti	Si 200, Al 200, Fe 40, Ni 4, N 50, Mo 10, C 50, W 2, Ta 10, Nb 4, Cu 2, Na 20
Lead	Cu 20, Sn 70, Al 1, Ca 1, Fe 20, Ag 6, Bi 100, Pd 1
EP305 +R Glass	Cu 32, La 12, Ga 13, Ba 160, Ce 32, As 10, Sb 0.8
CuCrZr	Sn 2, Si 1, Al 3, Fe 10, Ag 915, Ni 10, Zn 15, As 5, Bi 1, Pb 2, Mn 2, Sb 5

Material	Impurities (ppm)
FLiBe	Fe 166, Ni 26, Cr 19, S 5, Mo 1
SiC	O 39800, N620, Au 558, Cl 308, Fe 130, Al 25, Ni 18, Na 11.5, K 8, Ti 8, Zn 3.77, Cu 3.25, Mn 2.88, W 0.488, Pb 0.413, Co 0.088, Sb 0.053, As 0.014, La 0.01, Cr 0.003

To test this a set of materials relevant to fusion technology are chosen. The materials and the details of the impurities considered for each material are listed in Table 1. Most of the elemental compositions are taken from an ITER study[6]; where not available, other sources[7,8] are used.

For each material four FISPACT runs were carried out. These are described as:

- No impurity, no SCPR
- No impurity, with SCPR
- Impurity, no SCPR
- Impurity, with SCPR

By comparing the runs with and without SCPR the effect of the charged particles can be seen. A first wall spectrum calculated previously for a European Safety and Environmental[9] study was used for all FISPACT calculations. The effect of the SCPR is expected to be most noticeable in such a hard neutron spectrum where high energy charged particles will be produced. For this survey the exact details of the irradiation conditions are not important, a flux of 1.0 10^{15} ncm^{-2}s^{-1} for a time of 2.5 years is assumed.

The percentage difference between the runs with and without SCPR are calculated at each time interval. At most times the differences are small, and for ease of presentation only the maximum difference over the time range from 10^{-3} to 10^{6} years is summarised in Table 2.

Table 2 shows that in the case of Li_4SiO_4, vanadium alloys and FLiBe the effect of SCPR is very significant in materials with no impurities. However, when the representative impurities listed in Table 1 are included, the effects of SCPR are largely masked by the impurity contribution. To illustrate the SCPR contribution further, graphs are plotted for V-3Ti-1Si and FLiBe. Figures 1 and 2 focus on the time region of greatest difference and it can be seen that although there is a difference between the impurity curves with and without SCPR, the difference is well within the estimated uncertainty (due to errors in the neutron induced cross sections) of the curve without SCPR.

Table 2. Maximum percentage difference between runs with and without SCPR at cooling times from 10^{-3} to 10^{6} years.

Material	Activity No impurities	Activity With impurities	Heat No impurities	Heat With impurities	Dose rate No impurities	Dose rate With impurities
Li_4SiO_4	0.13	0.01	0.17	0.03	7883	5.96
Be	0	0	0	0	0	0
316	0.01	0.01	0.18	0.15	0.23	0.19
Manet 2	0.01	0.01	0.35	0.34	0.41	0.40
OPTSTAB	0.04	0.04	0.07	0.07	0.09	0.09
Inconel 600	0.06	0.06	0.03	0.03	0.04	0.04
V-5Ti	95	0.70	76	0.45	350	1.03
V-3Ti-1Si	1.28	0.80	1.21	1.11	650	20.26
V-4Cr-4Ti	5452	1.59	4120	0.93	112	5.0
Lead	0.04	0.02	2.0	0.3	4.11	0.37
EP305	0	0	0.05	0.05	0.11	0.10
CuCrZr	0.07	0.07	1.63	1.03	3.49	2.11
FLiBe	0	0	0.03	0.03	$4.75\ 10^{8}$	25.41
SiC	0.01	0	0.1	0.04	0.67	0.1

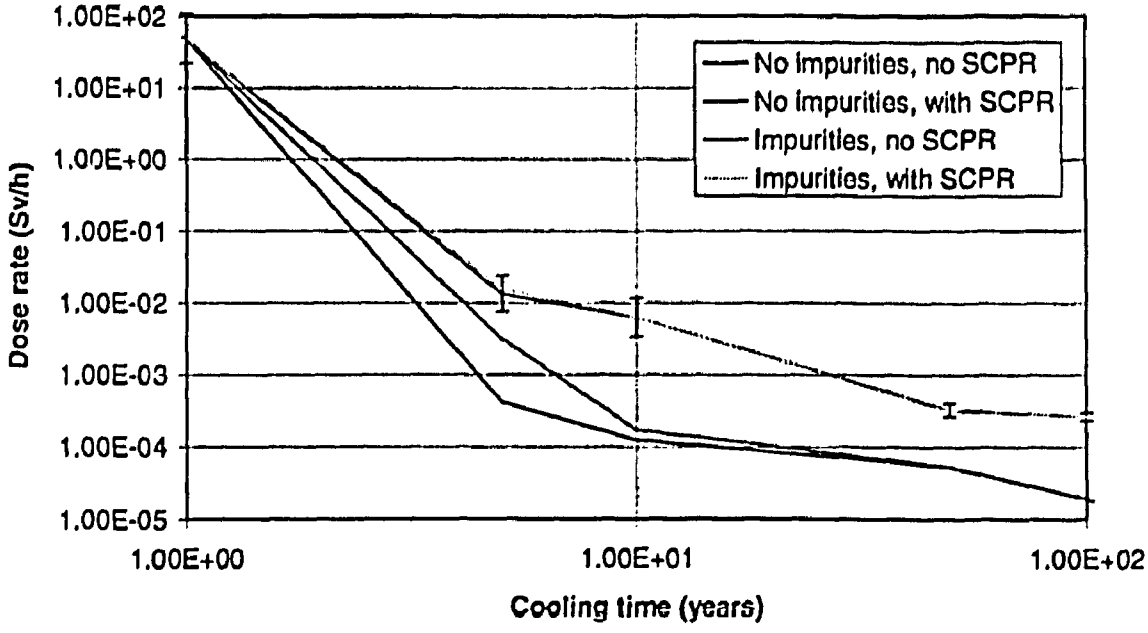

Figure 1. Detail of dose rate cooling curve for V-3Ti-1Si.

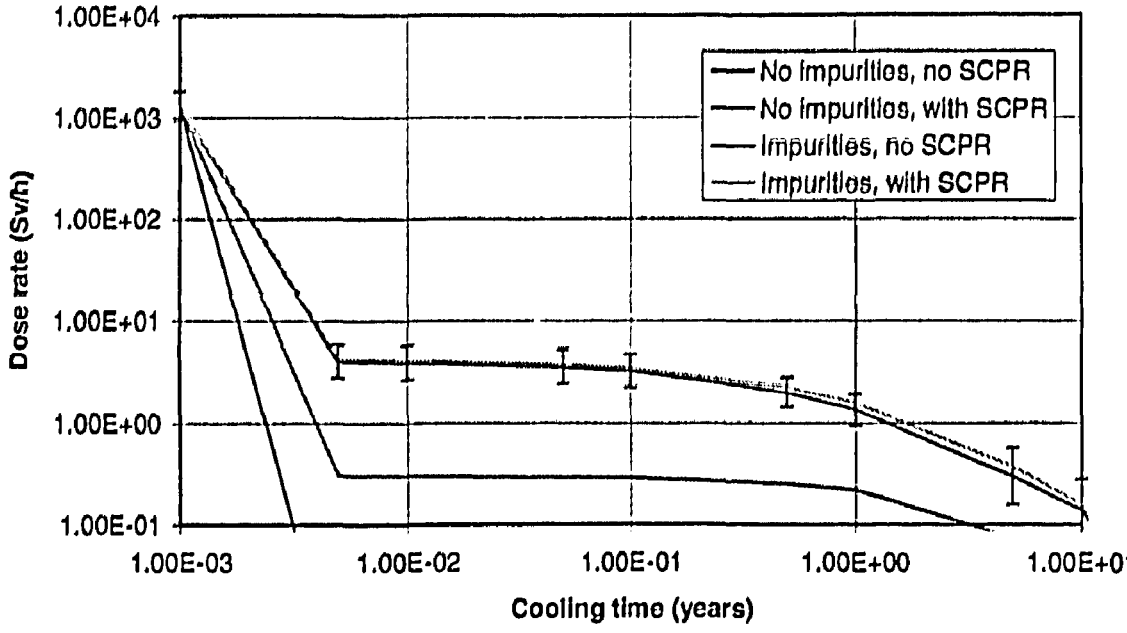

Figure 2. Detail of dose rate cooling curve for FLiBe.

The SCPR effect is most noticeable in FLiBe, and as it possible to reduce impurity levels if special care is taken in materials processing, two additional runs were carried out in which the impurity levels were reduced. In the first the amount of Fe was reduced from 177 ppm to 17 ppm and in the second the amount of Ni was reduced from 26 ppm to 3 ppm. The results are shown in Figures 3 and 4 and in the case of reduced Ni impurity it can be seen that the SCPR contribution is larger than the estimated uncertainty between cooling times of 1 - 10 years.

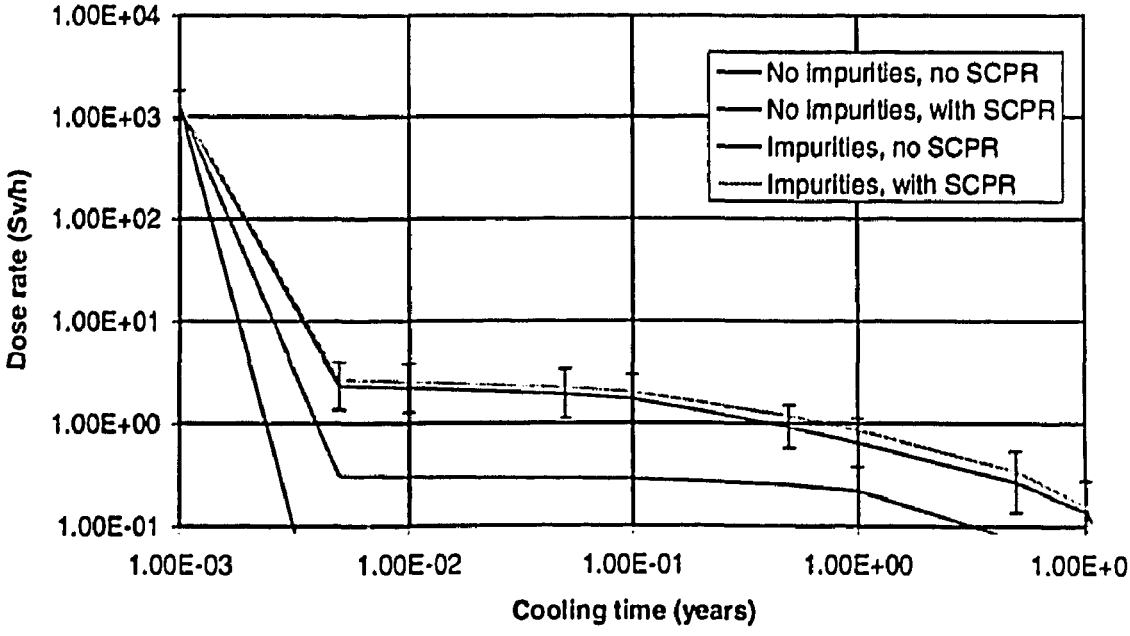

Figure 3. Detail of dose rate cooling curve for FLiBe with reduced iron impurity.

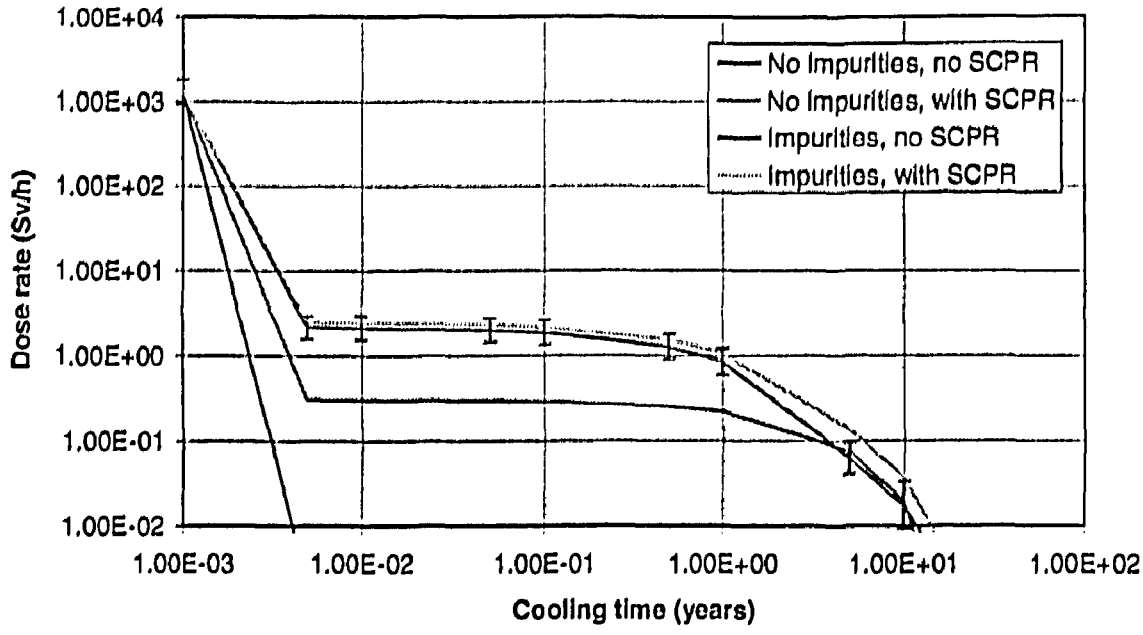

Figure 4. Detail of dose rate cooling curve for FLiBe with reduced nickel impurity.

The graphs illustrate the point that even if all impurities could be reduced in materials the dose rate would be reduced, not to the extremely low level without SCPR, but to the higher value with the SCPR contribution. The results in Table 2 for 316 stainless steel, Manet 2 and OPTSTAB show that with or without impurities the contribution from SCPR is negligible.

The conclusions from this survey can be summarised as:

- It is essential to specify correct impurity levels in materials when considering activation properties.
- For the realistic fusion relevant materials studied here the effect of SCPR is unimportant compared to the estimated uncertainties on the dose rate.
- If special care were to be taken with impurity control in structural materials such as vanadium alloys and breeding materials such as FLiBe then it would necessary to include SCPR in inventory calculations for accurate predictions.
- In the case of iron based alloys the contribution from SCPR is negligible even when no impurities are included.

Acknowledgements

This work was funded jointly by the UK Department of Trade and Industry and Euratom.

References

1. R.A. Forrest and J.-Ch. Sublet, *'FISPACT4 - User Manual'*, UKAEA FUS 287, 1995.
2. J. Kopecky, H. Gruppelaar and R.A. Forrest, *'European Activation File for Fusion'*, S.M. Qaim (editor), Int. Conf. Nuc. Data Sci. Tech., Jülich, Germany, May 1991, p 828, Springer-Verlag, 1992.

3. S.W. Cierjacks and Y. Hino, *'The Importance of sequential (x,n) reactions on element activation of fusion reactor materials'*, J. Nuc. Mat., **170**, 134, 1990.
4. S.W. Cierjacks, P. Oblozinsky, S. Kelzenberg and B. Rzehorz, *Fus. Tech.*, **24**, 277, 1993.
5. E. Browne and R.B. Firestone, *'Table of Radioactive Isotopes'*, John Wiley and Sons, New York, 1986.
6. J-Ch. Sublet, *'Elemental compositions of candidate structural materials including impurities and tramp elements, and their effects on activation characteristics'*, **UKAEA/NID-4d/SEP1-1/1(94)**, Revision 0, July 1994.
7. J.P. Holdren et al., *'Report of the Senior Committee on Environmental, Safety, and Economic Aspects of Magnetic Fusion Energy'*, **UCRL-53766**, 1989.
8. H.W. Scholz and M. Zucchetti, Fus. Eng, Design, **29**, 219, 1995.
9. M.G. Sowerby and R.A. Forrest, *'A study of the environmental impact of fusion'*, **AERE R 13708**, 1990.

Activation Products From Fusion Structural Materials

E.T. Cheng

TSI Research, Inc.
225 Stevens Avenue, Suite 203
Solana Beach, CA 92075

May 1995

I. Introduction

Based on recent calculations for the ITER EDA investigations [1] and previous studies [2,3], principal neutron induced activation products were identified for the following candidate fusion structural materials: 316 Stainless Steel, Vanadium-alloy, Ferritic Steel (HT9), Reduced Activation Ferritic Steel (9CrWV), Inconel 625, Titanium-alloy (Ti-6Al-4V), and SiC. The identification of these principal activation products was based on calculations performed with these structural materials in a commercial or ITER - like experimental power reactor. All calculations were conducted with the REAC code and its associated cross section and decay libraries [4]. The important concerns for the activation products are: (a) safety related radiological hazard potential such as early dose during a reactor accident; (b) safety related decay heat; (c) maintenance related biological dose rate after shutdown; and waste management related long-lived radioactivity.

Neutron activation cross sections for which there are data deficiencies were reviewed [3,5,6], and highlighted.

II. Results

Table 1 shows the detailed list of contributing activation products for each alloying element constituting the respective fusion structural materials. Also listed are the compositions, abundance of isotopes in each natural element, main activation reactions leading to the production of contributing activation products, half-lives and decay modes, and corresponding activation related concerns.

Table 2 displays only the major contributing activation products for the respective fusion structural materials.

Table 3 shows the list of neutron activation reactions identified in Ref. 5 as those having cross section data deficiencies. Note that Table 3 lists only those relevant to fusion structural materials. Complete lists involving structural, breeder materials, and materials for general fusion applications were obtained in previous reviews [3,6]. The list concerning structural and breeder materials is given in Ref. 3 and reproduced as Table 4 in this report.

Acknowledgment

This work was supported by the U.S. Department of Energy, Office of Fusion energy, under Grant No. DE-FG03-92ER54137. This work was motivated by the suggestion and guidance from S.E. Berk of DOE/OFE.

References:

[1] These ITER EDA related calculations were performed primarily to support the safety study being conducted by G. Saji of ITER San Diego Co-Center and K. McCarthy, et al of INEL, during the period of April through November 1993.

[2] E.T. Cheng, "Activation Cross Sections for Safety and Environmental Assessment of Fusion Reactors," Proc. Specialists' Meeting on Neutron Activation Cross Sections for Fission and Fusion Energy Applications, ANL, U.S.A., 13-15 September 1989, p.29.

[3] E.T. Cheng and D.L. Smith, "Nuclear Data Needs and Status for fusion reactor technology," Proc. Intl. Conf. Nuclear Data for Science and Technology, 13-17 May 1991, Juelich, Germany, S.M. Qaim (ed.), Springer-Verlag (1992); p. 237.

[4] F.M. Mann, "REAC *3 Nuclear Data Libraries," ibid, p. 936.

[5] Summary report of the IAEA Specialists' Meeting on Comparison of Activation Cross Section Measurements and Experimental Techniques, Tokai Research Establishment, JAERI, Japan, 15-17 November 1993.

[6] E.T. Cheng, R.A. Forrest, J. Kopecky, F.M. Mann, "List of Neutron Activation Reactions Important for Fusion Power Plant Technology," BU Nuclear Energy, EAF-Doc-004, ECN Report, Petten, Holland, March 1994.

Table 1 Page 1

Table 1
D-T Fusion Activation Products from Neutron Interaction with Fusion Materials

Fusion Material	Alloy Elements (weight percent)	Natural Isotopes (percent abundance	Major Activated Nuclides	Main Activation Reactions	Half-Life and Decay Mode	Activation Product Concerns			
						Safety Radiolog. Hazard Potential	Safety: Decay Heat	Maintenance: Shutdown Dose Rate	Waste: Recycle and Disposal
SS316	Fe	Fe54	Fe55	Fe56(n,2n)	2.73y;ε	Low	Low	-	-
	(66.2)	(5.9)	Mn54	Fe54(n,p)	312d;ε	Low	Low	Low	-
		Fe56 (91.7)	Mn56	Fe56(n,p)	2.58h;β-	Low	Low	Low	-
		Fe57	Co60	Fe58(n,g)*	5.27y;β-	-	-	Low	-
		(2.1)	Mn53	Fe54(n,n'p)	3.7×10^{6}y;ε	-	-	Low	-
		Fe58 (0.28)	Fe60	Fe59(n,g) Co60(n,p)	1.5×10^{6} y;β-	-	-	-	Low
	Ni	Ni58	Co58	Ni58(n,p)	70.8d;ε	Low	Low	Low	-
	(13.9)	(68.1)	Co57	Ni58(n,n'p)	272d;ε	Low	Low	Low	-
		Ni60	Co60	Ni60(n,p)	5.27y;β	Low	Low	Low	-
		(26.2)	Fe55	Ni58(n,α)	2.73y;ε	Low	Low	-	-
		Ni61 (1.14) Ni62	Ni59	Ni58(n,g) Ni60(n,2n)	7.5×10^{4}y;ε	Low	-	Low	Low
		(3.63)	Fe60	Ni64(n,n'α)	1.5×10^{6}y;β-	-	-	-	Low
		Ni64 (0.93)	Ni63	Ni64(n,2n) Ni62(n,g)	100y;β-	-	-	-	Low
	Mo (2.5)	Mo92 (14.8) Mo94 (9.25) Mo95 (15.9)	Nb94	Mo94(n,p) Mo95(n,n'p)	2.0×10^{4}y β-	-	-	-	Low

D-T Fusion Activation Products from Neutron Interaction with Fusion Materials
(continued)

Fusion Material	Alloy Elements (weight percent)	Natural Isotopes (percent abundance)	Major Activated Nuclides	Main Activation Reactions	Half-Life and Decay Mode	Activation Product Concerns: Safety: Radiolog. Hazard Potential	Safety: Decay Heat	Maintenance: Shutdown Dose Rate	Waste: Recycle and Disposal
SS316	Mo	Mo96	Nb95	Mo95(n,p)	35.0d;β-	Low	-	Low	-
(cont.)	(2.5)	(167)	Tc99	Mo98(n,g)*	$2.1x10^5$y;β-	Low	Low	-	Low
	(cont.)	Mo97 (9.55)		Mo100(n,2n)*					
		Mo98	Tc98	Tc99(n,2n)	$4.2x10^6$y;β-	-	Low	-	Low
		(24.1)	Y88	Mo92(n,α)*	107d;β-	-	Low	-	Low
		Mo100	Mo93	Mo94(n,2n)	$3.5x10^3$y;ε	-	-	Low	Low
		(9.63)		Mo92(n,g)		-	-	Low	Low
	Nb	Nb93	Nb92m	Nb93(n,2n)	10.2d;ε	Low	Low	Low	-
	(0.05)	(100)	Nb94	Nb93(n,g)	$2.0x10^4$y;β-	Low	Low	Low	Low
			Nb92	Nb93(n,2n)	$3.5x10^7$y;ε	Low	Low	Low	Low
			Nb93m	Nb93(n,n')	16.1y;IT	-	Low	Low	-
			Y88	Nb93(n,n'α)*	107d;ε	-	Low	Low	-
	Cr	Cr50	Cr51	Cr50(n,g)	27.7d;ε	Low	Low	Low	-
	(16.3)	(435)		Cr52(n,2n)					
		Cr52 (83.8)							
		Cr53 (950)							
		Cr54 (2.37)							

Table 1 Page 3

D-T Fusion Activation Products from Neutron Interaction with Fusion Materials
(continued)

Fusion Material	Alloy Elements (weight percent)	Natural Isotopes (percent abundance)	Major Activated Nuclides	Main Activated Reaction	Half-Life and Decay Mode	Activation Product Concerns: Safety: Radiolog. Hazard Potential	Safety: Decay Heat	Maintenance: Shutdown Dose Rate	Waste: Recycle and Disposal
SS316	Co	Co59	Co60	Co59(n,g)	5.27y;β-	-	-	Low	-
(cont.)	(0.05)	(100)	Co58	Co59(n,2n)	70.8d;ε	Low	-	-	-
			Fe60	Co60(n,p)	1.5×10^6y;β-	-	-	-	Low
	Mn (2.0)	Mn55 (100)	Mn54	Mn55(n,2n)	312d;ε	Low	-	-	-

Table 1 Page 4

D-T Fusion Activation Products from Neutron Interaction with Fusion Materials
(continued)

Fusion Material	Alloy Elements (weight percent)	Natural Isotopes (percent abundance)	Major Activated Nuclides	Main Activated Reaction	Half-Life and Decay Mode	Activation Product Concerns: Safety: Radiolog. Hazard Potential	Safety: Decay Heat	Maintenance: Shutdown Dose Rate	Waste: Recycle and Disposal
V-alloy	V	V50	Sc48	V51(n,α)	43.7h;β-	Low	Low	Low	-
	(90)	(0.25)	V49	V50(n,2n)	338d;ε	Low	Low	-	-
		V51	Sc47	V51(n,n'α)	3.35d;β-	Low	Low	Low	-
		(99.75)	Sc46	V50(n,n'α)	83.8d;β-	-	Low	Low	-
			Ca45	V51(n,t)*	164d;β-	Low	-	-	-
	Cr	Cr50	Cr51	Cr50(n,g)	27.7d;ε	Low	Low	Low	-
	(5)	(4.35)		Cr52(n,2n)					
		Cr52							
		(83.8)							
		Cr53							
		(9.5)							
		Cr54							
		(2.37)							
	Ti	Ti46	Ca45	Ti48(n,α)	164d;β-	Low	-	-	-
	(5)	(8.0)	Sc48	Ti48(n,p)	43.7h;β-	-	Low	Low	-
		Ti47	Sc46	Ti46(n,p)	83.8d;β-	Low	Low	Low	-
		(7.3)	Ca47	Ti50(n,α)	4.54d;β-	Low	-	-	-
		Ti48	Ar42(K42)	Ca45(n,α)	32.9y;β-	-	-	Low	Low
		(73.8)	Sc47	Ti47(n,p)	3.35d;β-	Low	Low	-	-
		Ti49							
		(5.5)							
		Ti50							
		(5.4)							

Table 1 Page 5

D-T Fusion Activation Products from Neutron Interaction with Fusion Materials
(continued)

Fusion Material	Alloy Elements (weight percent)	Natural Isotopes (percent abundance)	Major Activated Nuclides	Main Activation Reaction	Half-Life and Decay Mode	Activation Product Concerns			
						Safety: Radiolog. Hazard Potential	Safety: Decay Heat	Mainenace: Shutdown Dose Rate	Waste: Recycle and Disposal
Impurities for V-alloy	Ag (300ppb)	Ag107 (51.8) Ag109 (48.2)	Ag108m	Ag109(n,2n) Ag107(n,g)	481y;ε	Low	-	-	Low
	Al (200ppm)	Al27 (100)	Na24	Al27(n,α)	15h;β-	Low	Low	Low	-
			Mg27	Al27(n,p)	9.46m;β-	-	Low	-	-
			Al26	Al27(n,2n)	7.4×10^5y;ε	-	-	Low	Low
			Na22	Al27(n,n'α)*	2.6y;ε	Low	-	Low	-
	Cd (200ppb)	Cd106 (1.25) Cd108 (0.89) Cd110 (12.49) Cd111 (12.8) Cd112 (24.1) Cd113 (12.2) Cd114 (28.7) Cd116 (7.49)	Ag108m	Cd108(n,p)	481y;ε	-	-	-	Low

D-T Fusion Activation Products from Neutron Interaction with Fusion Materials (continued)

Fusion Material	Alloy Element (weight percent)	Natural Isotopes (percent abundance)	Major Activated Nuclides	Main Activation Reaction	Half-Life and Decay Mode	Activation Product Concerns: Safety: Radiolog. Hazard Potential	Safety: Decay Heat	Maintenance: Shutdown Dose Rate	Waste: Recycle and Disposal
Impurities for V-alloy (cont.)	Co (200 ppb)	Co59 (100)	Co60	Co59(n,g)	5.27y;β-	-	-	Low	-
			Co58	Co59(n,2n)	70.8d;ε	Low	-	-	-
			Fe60	Co60(n,p)	1.5×10^6y;β-	-	-	-	Low
	Cu (5.0 ppm)	Cu63 (69.2)	Ni63	Cu63(n,p) Cu65(n,t)	100y;β-	-	-	-	Low
		Cu65 (30.8)	Cu64	Cu65(n,2n) Cu63(n,g)	12.7h;ε/β-	-	Low	-	-
			Cu66	Cu65(n,g)	5.10 min;β-	-	Low	-	-
			Co60	Cu63(n,α)	5.27y;β-	-	-	Low	-
			Cu62	Cu63(n,2n)	9.74m;ε	-	Low	Low	-
			Ni65	Cu65(n,p)	2.52h;β-	-	Low	-	-
	Dy (300 ppb)	Dy156 (0.06) Dy158 (0.10) Dy160 (2.34) Dy161 (18.9) Dy162 (25.5) Dy163 (24.9) Dy164 (28.2)	Tb158	Dy158(n,p)	180y;ε/β-	-	-	-	Low

Table 1 Page 7

D-T Fusion Activation Products from Neutron Interaction with Fusion Materials
(continued)

Fusion Material	Alloy Element (weight percent)	Natural Isotopes (percent abundance)	Major Activated Nuclides	Main Activation Reaction	Half-Life and Decay Mode	Activation Product Concerns: Safety: Radiolog. Hazard Potential	Safety: Decay Heat	Maintenance: Shutdown Dose Rate	Waste: Recycle and Disposal
Impurities for V-alloy (cont.)	Eu (100 ppb)	Eu151 (47.8) Eu153	Eu152	Eu153(n,2n)	13.5y;ε/β-	-	-	-	Low
				Eu151(n,g)		-	-	-	Low
		(82.2)	Eu150m	Eu151(n,2n)	150y;ε	-	-	-	Low
	Hf (5.6 ppm)	Hf174 (0.16) Hf176 (5.21)	Hf178m2	Hf179(n,2n) Hf178(n,n'α) Hf177(n,g)	31y;IT	Low	Low	Low	Low
		Hf177 (18.6)	Hf177m	Hf178(n,2n)	51.4m; IT	-	Low	Low	-
			Hf180m	Hf179(n,g)	5.5h; IT	-	-	Low	-
		Hf178 (27.3) Hf179 (13.6) Hf180 (35.1)	Hf181	Hf180(n,g)	42.4d;β-	-	-	Low	-
	Ho (100 ppb)	Ho165 (100)	Ho166m	Ho165(n,g)	1.2×10^3y;β-	-	-	-	-

D-T Fusion Activation Products from Neutron Interaction with Fusion Materials
(continued)

Fusion Material	Alloy Element (weight percent)	Natural Isotopes (percent abundance)	Major Activated Nuclides	Main Activation Reaction	Half-Life and Decay Mode	Activation Product Concerns			
						Safety: Radiolog. Hazard Potential	Safety: Decay Heat	Maintenance: Shutdon Dose Rate	Waste: Recycle and Disposal
Impuri-ties for V-alloy (cont.)	Mo (150 ppm)	Mo92 (14.8)	Nb94	Mo94(n,p) Mo95(n,n'p)	$2.0x10^4$y;β-	-	-	-	Low
		Mo94 (9.25)	Tc99	Mo98(n,p)*	$2.1x10^5$y;β-	-	-	-	Low
		Mo95 (15.9)	Mo93	Mo94(n,2n) Mo92(n,g)	$3.5x10^3$y;ε	-	-	-	Low
		Mo96 (16.7)							
		Mo97 (9.55)							
		Mo98 (24.1)							
		Mo100 (9.63)							
	Ni (3.0 ppm)	Ni58 (68.1)	Co60	Ni60(n,p) Ni61(n,n'p)	5.27y;β-	-	-	-	Low
		Ni60 (26.2)	Ni59	Ni58(n,g) Ni60(n,2n)	$7.5x10^4$y;ε	-	-	-	Low
		Ni61 (1.14)	Ni63	Ni62(n,g)	100y;β-	-	-	-	Low
		Ni62 (3.63)	Fe60	Ni64(n,2n) Ni64(n,n'α)	$1.5x10^6$y;β-	-	-	-	Low
		Ni64 (0.93)							

Table 1 Page 9

D-T Fusion Activation Products from Neutron Interaction with Fusion Materials
(continued)

Fusion Material	Alloy Element (weight percent)	Natural Isotopes (percent abundance)	Major Activated Nuclides	Main Activation Reaction	Half-Life and Decay Mode	Activation Product Concerns			
						Safety: Radiolog. Hazard Potential	Safety: Decay Heat	Maintenance: Shutdown Dose Rate	Waste: Recycle and Disposal
Impuri-	Nb	Nb93	Nb94	Nb93(n,g)	2.0×10^3y;β-	-	-	-	Low
ties for	(50 ppm)	(100)	Nb92m	Nb93(n,2n)	10.15d;ε	Low	-	-	-
V-alloy (cont.)	Tb (100 ppb)	Tb159 (100)	Tb158	Tb159(n,2n)	180y;β-	-	-	-	Low

D-T Fusion Activation Products from Neutron Interaction with Fusion Materials
(continued)

Fusion Material	Alloy Element (weight percent)	Natural Isotopes (percent abundance)	Major Activated Nuclides	Main Activation Reaction	Half-Life and Decay Mode	Activation Product Concerns			
						Safety: Radiolog. Hazard Potential	Safety: Decay Heat	Maintenance: Shutdown Dose Rate	Waste: Recycle and Disposal
Ferritic Steel (HT9)	Fe (85.0)	Fe54 (5.9)	Fe55	Fe56(n,2n)	2.73y;ε	Low	Low	-	-
			Mn54	Fe54(n,p)	312d;ε	Low	Low	Low	-
		Fe56 (91.7)	Mn56	Fe56(n,p)	2.58h;β-	-	Low	Low	-
		Fe57	Co60	Fe58(n,g)*	5.27y;β-	-	-	Low	-
		(2.1)	Mn53	Fe54(n,n'p)	3.7×10^6y;ε	-	-	-	Low
		Fe58 (0.28)	Fe60	Fe59(n,g) Co60(n,p)	1.5×10^6y;β-	-	-	-	Low
	Cr (11.5)	Cr50 (4.35) Cr52 (83.8) Cr53 (9.5) Cr54 (2.37)	Cr51	Cr50(n,g) Cr52(n,2n)	27.7d;ε	Low	Low	Low	-

Table 1 Page 11

D-T Fusion Activation Products from Neutron Interaction with Fusion Materials
(continued)

Fusion Material	Alloy Elements (weight percent)	Natural Isotopes (percent abundance)	Major Activated Nuclides	Main Activation Reactions	Half-Life and Decay Mode	Activation Product Concerns			
						Safety: Radiolog. Hazard Potential	Safety: Decay Heat	Maintenance: Shutdown Dose Rate	Waste: Recycle and Disposal
Ferritic Steel (HT-9) (cont.)	Ni (0.5)	Ni58 (68.1)	Co58	Ni58(n,p)	70.8d;ε	Low	Low	Low	–
			Co57	Ni58(n,n'p)	272d;ε	Low	Low	Low	–
		Ni60 (26.2)	Co60	Ni60(n,p)	5.27y;β	Low	Low	Low	–
			Fe55	Ni58(n,α)	2.73y;ε	Low	Low	–	–
		Ni61 (1.14)	Ni59	Ni58(n,g) Ni60(n,2n)	7.5×10^4y;ε	Low	–	Low	Low
		Ni62 (3.63)	Fe60	Ni64(n,n'α)	1.5×10^6y;β-	–	–	–	Low
		Ni64 (0.93)	Ni63	Ni64(n,2n) Ni62(n,g)	100y;β-	–	–	–	Low
	Mo (0.99)	Mo92 (14.8)	Nb94	Mo94(n,p) Mo95(n,n'p)	2.0×10^4y;β-	–	–	–	Low
		Mo94 (9.25)							
		Mo95 (15.9)							
		Mo96 (16.7)	Nb95	Mo95(n,p)	35.0d;β-	Low	–	Low	–
			Tc99	Mo98(n,g)* Mo100(n,2n)*	2.1×10^5y;β-	Low	Low	–	Low
		Mo97 (9.55)							
		Mo98 (24.1)	Tc98	Tc99(n,2n)	4.2×10^6y;β-	–	Low	–	Low
			Y88	Mo92(n,α)*	107d;β-	–	Low	–	Low
		Mo100 (9.63)	Mo93	Mo94(n,2n) Mo92(n,g)	3.5×10^3y;ε	–	–	Low	Low

D-T Fusion Activation Products from Neutron Interaction with Fusion Materials (continued)

Fusion Material	Alloy Elements (weight percent)	Natural Isotopes (percent abundance)	Major Activated Nuclides	Main Activation Reactions	Half-Life and Decay Mode	Activation Product Concerns: Safety: Radiolog. hazard Potential	Safety: Decay Heat	Maintenance: Shutdown Dose Rate	Waste: Recycle and Disposal
Ferritic Steel (HT-9) (cont.)	V (0.3)	V50 (0.25)	Sc48	V51(n,α)	43.7h;β-	Low	Low	Low	-
			V49	V50(n,2n)	338d;ε	Low	Low	-	-
		V51 (99.75)	Sc47	V51(n,n'α)	3.35d;β-	-	Low	Low	-
			Sc46	V50(n,n'α)	83.8d;β-	-	Low	Low	-
			Ca45	V51(n,t)*	164d;β-	Low	-	-	-
	Mn (0.55)	Mn55 (100)	Mn54	Mn55(n,2n)	312d;ε	Low	Low	Low	-
	W (0.5)	W180 (0.12)	W185	W186(n,2n) W184(n,g)	75.1d;β-	Low	Low	-	-
		W182 (26.3)	Ta182	W182(n,p) W183(n,n'p)	114d;β-	Low	Low	Low	-
		W183 (14.3)	Hf178m2	W182(n,n'α)	31y;IT	Low	-	Low	Low
			Hf182	W186(n,n'α)	$9x10^6$y;β-	Low	-	Low	Low
		W184 (30.7)	W181	W182(n,2n) W180(n,g)	121d;ε	Low	-	-	-
		W186 (28.6)	W187	W186(n,g)	23.7h;β-	Low	-	-	-
	Nb (500 ppm)	Nb93 (100)	Nb94	Nb93(n,g)	$2.0x10^3$y;β-	-	-	-	Low
			Nb92m	Nb93(n,2n)	10.15d;ε	Low	-	-	-

Table 1 Page 13

D-T Fusion Activation Products from Neutron Interaction with Fusion Materials
(continued)

Fusion Material	Alloy Elements (weight percent)	Natural Isotopes (percent abundance)	Major Activated Nuclides	Main Activation Reactions	Half-Life and Decay Mode	Activation Product Concerns			
						Safety: Radiolog. Hazard Potential	Safety: Decay Heat	Maintenance: Shutdown Dose Rate	Waste: Recycle and Disposal
Reduced Activation Ferritic Steel (9CrWV)	Fe (88.0)	Fe54 (5.9)	Fe55	Fe56(n,2n)	2.73y;ε	Low	Low	–	–
			Mn54	Fe54(n,p)	312d;ε	Low	Low	Low	–
		Fe56 (91.7)	Mn56	Fe56(n,p)	2.58h;β–	–	Low	Low	–
		Fe57 (2.1)	Co60	Fe58(n,g)*	5.27y;β–	–	–	Low	–
			Mn53	Fe54(n,n'p)	3.7×10^6y;ε	–	–	–	Low
		Fe58 (0.28)	Fe60	Fe59(n,g) Co60(n,p)	1.5×10^6y;β–	–	–	–	Low
	Cr (8.94)	Cr50 (4.35) Cr52 (83.8) Cr53 (9.5) Cr54 (2.37)	Cr51	Cr50(n,g) Cr52(n,2n)	27.7d;ε	Low	Low	Low	–
	Ni (100ppm)	Ni58 (68.1)	Co58	Ni58(n,p)	70.8d;ε	Low	Low	Low	–
			Co57	Ni58(n,n'p)	272d;ε	Low	Low	Low	–
		Ni60 (26.2)	Co60	Ni60(n,p)	5.27y;β–	Low	Low	Low	–
			Fe55	Ni58(n,α)	2.73y;ε	Low	Low	–	–
		Ni61 (1.14)	Ni59	Ni58(n,g) Ni60(n,2n)	7.5×10^4y;ε	Low	–	Low	Low
		(3.63)	Fe60	Ni64(n,n'α)	1.5×10^6y;β–	–	–	–	Low
		Ni64 (0.93)	Ni63	Ni64(n,2n) Ni62(n,g)	100y;β–	–	–	–	Low

D-T Fusion Activation Products from Neutron Interaction with Fusion Materials
(continued)

Fusion Material	Alloy Elements (weight percent)	Natural Isotopes (percent abundance)	Major Activated Nuclides	Main Activation Reactions	Half-Life and Decay Mode	Activation Product Concerns: Safety: Radiolog. Hazard Potential	Safety: Decay Heat	Maintenance: Shutdown Dose Rate	Waste: Recycle and Disposal
9CrWV (cont.)	Mo (10ppm)	Mo92 (14.8) Mo94 (9.25) Mo95 (15.9)	Nb94	Mo94(n,p) Mo95(n,n'p)	2.0×10^4y;β	-	-	-	Low
		Mo96 (167)	Nb95	Mo95(n,p)	35.0d;β-	Low	-	Low	-
		Mo97 (9.55)	Tc99	Mo98(n,g)* Mo100(n,2n)*	2.1×10^5y;β-	Low	Low	-	Low
		Mo98 (24.1)	Tc98	Tc99(n,2n)	4.2×10^6y;β-	-	Low	-	Low
			Y88	Mo92(h,α)*	107d;β-	-	Low	-	Low
		Mo100 (9.63)	Mo93	Mo94(n,2n) Mo92(n,g)	3.5×10^3y;ε	-	-	Low	Low
	V (0.25)	V50 (0.25)	Sc48	V51(n,α)	43.7h;β-	Low	Low	Low	-
			V49	V50(n,2n)	338d;ε	Low	Low	-	-
		V51 (99.75)	Sc47	V51(n,n'α)	3.35dβ-	-	Low	Low	-
			Sc46	V50(n,n'α)	8.38d;β-	-	Low	Low	-
			Ca45	V51(n,t)*	164d;β-	Low	-	-	-
	Mn (0.44)	Mn55 (100)	Mn54	Mn55(n,2n)	312d;ε	Low	-	-	-

Table 1 Page 15

D-T Fusion Activation Products from Neutron Interaction with Fusion Materials
(continued)

Fusion Material	Alloy Elements (weight percent)	Natural Isotopes (percent abundance)	Major Activated Nuclides	Main Activation Reactions	Half-Life and Decay Mode	Activation Product Concerns			
						Safety: Radiolog. Hazard Potential	Safety: Decay Heat	Maintenance: Shutdown Dose Rate	Waste: Recycle and Disposal
9CrWV (cont.)	Ta (777ppm)	Ta181 (100)	Ta182	Ta181(n,g)	114d;β	Low	Low	Low	-
	W (1.97)	W180 (0.12)	W185	W186(n,2n) W184(n,g)	75.1d;β	Low	Low	-	-
		W182 (26.3)	Ta182	W182(n,p) W183(n,n'p)	114d;β	Low	Low	Low	-
		W183 (14.3)	Hf178m2	W182(n,n'α)	31y;IT	Low	-	Low	Low
			Hf182	W186(n,n'α)	$9x10^6$y;β	Low	-	Low	Low
		W184 (30.7)	W181	W182(n,2n) W180(n,g)	121d;ε	Low	-	-	-
		W186 (28.6)	W187	W186(n,g)	23.7h;β-	Low	-	-	-
	Nb (<10ppm)	Nb93 (100)	Nb94	Nb93(n,g)	$2.0x10^4$y;β-	-	-	-	Low
			Nb92m	Nb93(n,2n)	10.15d;ε	Low	-	-	-

D-T Fusion Activation Products from Neutron Interaction with Fusion Materials
(continued)

Fusion Material	Alloy Elements (weight percent)	Natural Isotopes (percent abundance)	Major Activated Nuclides	Main Activation Reactions	Half-Life and Decay Mode	Activation Product Concerns: Safety: Radiolog. Hazard Potential	Safety: Decay Heat	Maintenance: Shutdown Dose Rate	Waste: Recycle and Disposal
Inconel 625									
	Ni	Ni58	Co58	Ni58(n,p)	70.8d;ε	Low	Low	Low	-
	(62.0)	(68.1)	Co57	Ni58(n,n'p)	272d;ε	Low	Low	Low	-
		Ni60	Co60	Ni60(n,p)	5.27y;β-	Low	Low	Low	-
		(26.2)	Fe55	Ni58(n,α)	2.73y;ε	Low	Low	-	-
		Ni61 (1.14)	Ni59	Ni58(n,g) Ni60(n,2n)	7.5×10^4y;ε	Low	-	Low	Low
		(3.63)	Fe60	Ni64(n,n'α)	1.5×10^6y;β-	-	-	-	Low
		Ni64 (0.93)	Ni63	Ni64(n,2n) Ni62(n,g)	100y;β-	-	-	-	Low
	Cr (21.5)	Cr50 (4.35) Cr52 (83.8) Cr53 (9.5) Cr54 (2.37)	Cr51	Cr50(n,g) Cr52(n,2n)	27.7d;ε	Low	Low	Low	-
	Nb	Nb93	Nb94	Nb93(n,g)	2.0×10^3y;β-	-	-	-	Low
	(1.8)	(100)	Nb92m	Nb93(n,2n)	10.15d;ε	Low	-	-	-

Table 1 Page 17

D-T Fusion Activation Products from Neutron Interaction with Fusion Materials
(continued)

Fusion Material	Alloy Elements (weight percent)	Natural Isotopes (percent abundance)	Major Activated Nuclides	Main Activation Reactions	Half-Life and Decay Mode	Activation Product Concerns: Safety: Radiolog. Hazard Potential	Safety: Decay Heat	Maintenance: Shutdown Dose Rate	Waste: Recycle and Disposal
Inconel 625 (cont.)	Mo (8.99)	Mo92 (14.8) Mo94 (9.25) Mo95 (15.9)	Nb94	Mo94(n,p) Mo95(n,n'p)	2.0×10^4y;β	-	-	-	Low
		Mo96 (16.7) Mo97 (9.55)	Nb95	Mo95(n,p)	35.0d;β-	Low	-	Low	-
			Tc99	Mo98(n,g)* Mo100(n,2n)*	2.1×10^5y;β-	Low	Low	-	Low
		Mo98 (24.1)	Tc98	Tc99(n,2n)	4.2×10^6y;β-	-	Low	-	Low
			Y88	Mo92(n,α)*	107d;β-	-	Low	-	Low
		Mo100 (9.63)	Mo93	Mo94(n,2n) Mo92(n,g)	3.5×10^3y;ε	-	-	Low	Low
	Ta (1.8)	Ta181 (100)	Ta182	Ta181(n,g)	114d;β	Low	Low	Low	-
	Fe (2.5)	Fe54 (5.9)	Fe55	Fe56(n,2n)	2.73y;ε	Low	Low	-	-
			Mn54	Fe54(n,p)	312d;ε	Low	Low	Low	-
		Fe56 (91.7)	Mn56	Fe56(n,p)	2.58h;β-	-	Low	Low	-
		Fe57 (2.1)	Co60	Fe58(n,g)*	5.27y;β-	-	-	Low	-
			Mn53	Fe54(n,n'p)	3.7×10^6y;ε	-	-	-	Low
		Fe58 (0.28)	Fe60	Fe59(n,g) Co60(n,p)	1.5×10^6y;β	-	-	-	Low

D-T Fusion Activation Products from Neutron Interaction with Fusion Materials
(continued)

Fusion Material	Alloy Elements (weight percent)	Natural Isotopes (percent abundance)	Major Activated Nuclides	Main Activation Reactions	Half-Life and Decay Mode	Activation Product Concerns: Safety: Radiolog. Hazard Potential	Safety: Decay Heat	Maintenance: Shutdown Dose Rate	Waste: Recycle and Disposal
Inconel 625 (cont.)	Co (0.5)	Co59 (100)	Co60	Co59(n,g)	5.27y;β-	Low	-	-	-
			Co58	Co59(n,2n)	70.8d;ε	Low	-	-	-
			Fe60	Co60(n,p)	1.5×10^6y;β-	-	-	-	Low
	Mn (0.27)	Mn55 (100)	Mn54	Mn55(n,2n)	312d;ε	Low	-	-	-
	Si (0.25)	Si28 (92.23)	Na24	Si28(n,np)*	15h;β-	Low	Low	Low	-
			Na22	Si28(n,np)*	2.6y;β-	Low	-	Low	-
		Si29 (4.67) Si30 (3.1)	Al26	Si28(n,np)*	7.4×10^5y;ε	-	-	-	Low
	Ti (0.25)	Ti46 (8.0)	Ca45	Ti48(n,α)	164d;β-	Low	-	-	-
			Sc48	Ti48(n,p)	43.7h;β-	-	Low	Low	-
		Ti47 (7.3)	Sc46	Ti46(n,p)	83.8d;β-	Low	Low	Low	-
			Sc47	Ti47(n,p)	3.35d;β-	Low	Low	-	-
		Ti48 (73.8) Ti49 (5.5) Ti50 (5.4)	Ar42(K42)	Ca45(n,α)	32.9y;β-	-	-	Low	Low
			Ca47	Ti50(n,α)	4.54d;β-	Low	-	-	-

Table 1 Page 19

D-T Fusion Activation Products from Neutron Interaction with Fusion Materials
(continued)

Fusion Material	Alloy Elements (weight percent)	Natural Isotopes (percent abundance)	Major Activated Nuclides	Main Activation Reactions	Half-Life and Decay Mode	Activation Product Concerns			
						Safety: Radiolog. Hazard Potential	Safety: Decay Heat	Maintenance: Shutdown Dose Rate	Waste: Recycle and Disposal
Inconel 625 (cont.)	Al (0.2)	Al27 (100)	Na24	Al27(n,α)	15h;β-	Low	Low	Low	-
			Mg27	Al27(n,p)	9.46m;β-	-	Low	-	-
			Al26	Al27(n,2n)	7.4×10^5y;ε	-	-	Low	Low
			Na22	Al27(n,n'α)	2.6y;ε	Low	-	Low	-

D-T Fusion Activation Products from Neutron Interaction with Fusion Materials
(continued)

Fusion Material	Alloy Elements (weight percent)	Natural Isotopes (percent abundance)	Major Activated Nuclides	Main Activation Reactions	Half-Life and Decay Mode	Activation Product Concerns: Safety: Radiolog. Hazard Potential	Safety: Decay Heat	Maintenance: Shutdown Dose Rate	Waste: Recycle and Disposal
Ti-6Al-4V	Ti	Ti46	Ca45	Ti48(n,α)	164d;β-	Low	-	-	-
	(90)	(8.0)	Sc48	Ti48(n,p)	43.7h;β-	-	Low	Low	-
		Ti47	Sc46	Ti46(n,p)	83.8d;β-	Low	Low	Low	-
		(7.3)	Sc47	Ti47(n,p)	3.35d;β-	Low	Low	-	-
		Ti48	Ar42(K42)	Ca45(n,α)	32.9y;β-	-	-	Low	Low
		(73.8)	Ca47	Ti50(n,α)	4.54d;β-	Low	-	-	-
		Ti49 (5.5)							
		Ti50 (5.4)							
	Al	Al27	Na24	Al27(n,α)	15h;β-	Low	Low	Low	-
	(6)	(100)	Mg27	Al27(n,p)	9.46m;β-	-	Low	-	-
			Al26	Al27(n,2n)	7.4×10^5y;ε	-	-	Low	Low
			Na22	Al27(n,n'α)	2.6y;ε	Low	-	Low	-
	V	V50	Sc48	V51(n,α)	43.7h;β-	Low	Low	Low	-
	(4)	(0.25)	V49	V50(n,2n)	338d;ε	Low	Low	-	-
		V51	Sc47	V51(n,n'α)	3.35d;β-	-	Low	Low	-
		(99.75)	Sc46	V50(n,n'α)	83.8d;β-	-	Low	Low	-
			Ca45	V51(n,t)*	164d;β-	Low	-	-	-

*indicates multi-step neutron reactions to reach the final activation products.

Table 1 Page 21

D-T Fusion Activation Products from Neutron Interaction with Fusion Materials
(continued)

Fusion Material	Alloy Elements (weight percent)	Natural Isotopes (percent abundance)	Major Activated Nuclides	Main Activation Reactions	Half-Life and Decay Mode	Activation Product Concerns			
						Safety: Radiolog. Hazard Potential	Safety: Decay Heat	Maintenance: Shutdown Dose Rate	Waste: Recycle and Disposal
SiC	Si	Si28		Si28(n,n'p)Al27					
	(70)	(92.2)	Na24	Al27(n,α)	15h;β-	Low	Low	Low	-
			Al26	Al27(n,2n)	7.2×10^5y;ε	-	-	Low	Low
			Na22	Al27(n,n'α)*	2.6y;ε	-	-	Low	-
			Al28	Si28(n,p)	2.24m;β-	Low	Low	-	-
		Si29 (4.67)	Al29	Si29(n,p)	6.56m;β-	Low	Low	-	-
		Si30	Mg27	Si30(n,α)	9.46m;β-	Low	Low	-	-
		(3.10)	Mg28	Si30(n,He3)	20.9h;β-	Low	Low	Low	-
	C (30)								

*indicates multi-step neutron reactions to reach the final activation products.

Table 2
D-T Fusion Activation Products from Neutron Interaction with Structural Materials

Fusion Material	Alloy Elements (weight percent)	Major Activated Nuclides	Main Activation Reactions	Half-Life and Decay Mode	Activation Product Concerns: Safety Radiolog. Hazard Potential	Safety: Decay Heat	Maintenance: Shutdown Dose Rate	Waste: Recycle and Disposal
SS316	Fe	Mn54	Fe54(n,p)	312d;ε	Low	Low	Low	-
	(66.2)	Mn56	Fe56(n,p)	2.58h;β-	Low	Low	Low	-
	Ni	Co60	Fe58(n,g)*	5.27y;β-	-	-	Low	-
	(13.9)	Co58	Ni58(n,p)	70.8d;ε	Low	Low	Low	-
	Mo	Co57	Ni58(n,n'p)	272d;ε	Low	Low	Low	-
	(2.5)	Co60	Ni60(n,p)	5.27y;β	Low	Low	Low	-
	Nb	Nb94	Mo94(n,p)	2.0×10^4y; β-	-	-	-	Low
	(0.05)		Mo95(n,n'p)					
	Cr		Nb93(n,g)	2.0×10^4y;β-	Low	Low	Low	Low
	(16.3)	Cr51	Cr50(n,g)	27.7d;ε	Low	Low	Low	-
			Cr52(n,2n)					
	Co	Co60	Co59(n,g)	5.27y;β-	-	-	Low	-
	(0.05)							
	Mn	Mn56	Mn55(n,g)	2.58h;β	Low	Low	Low	-
	(2.0)	Mn54	Mn55(n,2n)	312d;ε	Low	Low	Low	-

Table 2 page 2

D-T Fusion Activation Products from Neutron Interaction with Structural Materials
(continued)

Fusion Material	Alloy Elements (weight percent)	Major Activated Nuclides	Main Activated Reaction	Half-Life and Decay Mode	Activation Product Concerns			
					Safety: Radiolog. Hazard Potential	Safety: Decay Heat	Maintenance: Shutdown Dose Rate	Waste: Recycle and Disposal
V-alloy	V	Sc48	V51(n,α)	43.7h;β-	Low	Low	Low	-
	(90)	Sc47	V51(n,n'α)	3.35d;β-	Low	Low	Low	-
	Cr	Sc46	V50(n,n'α)	83.8d;β-	-	Low	Low	-
	(5)	Cr51	Cr50(n,g) Cr52(n,2n)	27.7d;ε	Low	Low	Low	-
	Ti	Ca47	Ti50(n,α)	4.54d;β-	Low	-	-	-
	(5)	Ar42(K42)	Ca45(n,α)	32.9y;β-	-	-	Low	Low
		Sc47	Ti47(n,p)	3.35d;β-	Low	-	-	-
Impurities for V-alloy	Ag (300ppb)	Ag108m	Ag109(n,2n)	481y;ε	Low	-	-	Low
	Al (200ppm)	Al26	Al27(n,2n)	7.4×10^5y;ε	-	-	Low	Low
	Cd (200ppb)	Ag108m	Cd108(n,p)	481y;ε	-	-	-	Low
	Co (200 ppb)	Co60	Co59(n,g)	5.27y;β-	Low	-	-	-
	Cu (5.0 ppm)	Ni63	Cu63(n,p)	100y;β-	-	-	-	Low
	Dy (300 ppb)	Tb158	Dy158(n,p)	180y;ε/β-	-	-	-	Low

Table 2 page 3

D-T Fusion Activation Products from Neutron Interaction with Structural Materials (continued)

Fusion Material	Alloy Element (weight percent)	Major Activated Nuclides	Main Activation Reaction	Half-Life and Decay Mode	Activation Product Concerns: Safety: Radiolog. Hazard Potential	Safety: Decay Heat	Maintenance: Shutdown Dose Rate	Waste: Recycle and Disposal
Impurities for V-alloy (continued)	Eu (100 ppb)	Eu152	Eu153(n,2n)	13.5y;ε/β-	-	-	-	Low
		Eu150m	Eu151(n,2n)	150y;ε	-	-	-	Low
	Hf (5.6 ppm)	Hf178m2	Hf179(n,2n)	31y;IT	Low	Low	Low	Low
	Ho (100 ppb)	Ho166m	Ho165(n,g)	1.2×10^{3}y;β-	-	-	-	Low
	Mo (150 ppm)	Nb94	Mo94(n,p) Mo95(n,n'p)	2.0×10^{4}y;β-	-	-	-	Low
		Tc99	Mo98(n,p)*	2.1×10^{5}y;β-	-	-	-	-
	Ni (3.0 ppm)	Co60	Ni60(n,p) Ni61(n,n'p)	5.27y;β-	-	-	-	Low
		Ni59	Ni58(n,g) Ni60(n,2n)	7.5×10^{4}y;ε	-	-	-	Low
		Ni63	Ni62(n,g) Ni64(n,2n)	100y;β-	-	-	-	Low
		Fe60	Ni64(n,n'α)	1.5×10^{6}y;β-	-	-	-	Low
	Nb (50 ppm)	Nb94	Nb93(n,g)	2.0×10^{3}y;β-	-	-	-	Low
		Nb92m	Nb93(n,2n)	10.15d;ε	Low	-	-	-
	Tb (100 ppb)	Tb158	Tb159(n,2n)	180y;β-	-	-	-	Low

Table 2 page 4

D-T Fusion Activation Products from Neutron Interaction with Structural Materials
(continued)

Fusion Material	Alloy Element (weight percent)	Major Activated Nuclides	Main Activation Reaction	Half-Life and Decay Mode	Activation Product Concerns: Safety: Radiolog. Hazard Potential	Safety: Decay Heat	Maintenance: Shutdown Dose Rate	Waste: Recycle and Disposal
Ferritic Steel (HT9)	Fe (85.0)	Fe55	Fe56(n,2n)	2.73y;ε	Low	Low	-	-
		Mn54	Fe54(n,p)	312d;ε	Low	Low	Low	-
		Mn56	Fe56(n,p)	2.58h;β-	-	Low	Low	-
		Co60	Fe58(n,g)*	5.27y;β-	-	-	Low	-
	Cr (11.5)	Cr51	Cr50(n,g) Cr52(n,2n)	27.7d;ε	Low	Low	Low	-
	Ni (0.5)	Co58	Ni58(n,p)	70.8d;ε	Low	Low	Low	-
		Co57	Ni58(n,n'p)	272d;ε	Low	Low	Low	-
		Co60	Ni60(n,p)	5.27y;β	Low	Low	Low	-
	Mo (0.99) V (0.3) Mn (0.55) W	Nb94	Mo94(n,p) Mo95(n,n'p)	2.0×10^4y;β-	-	-	-	Low
	(0.5)	Ta182	W182(n,p)	114d;β-	Low	Low	Low	-
		Hf178m2	W182(n,n'α)	31y;IT	Low	-	Low	Low
		W181	W182(n,2n) W180(n,g)	121d;ε	Low	-	-	-
		W187	W186(n,g)	23.7h;β-	Low	-	-	-
	Nb (500 ppm)	Nb94	Nb93(n,g)	2.0×10^3y;β-	-	-	-	Low

D-T Fusion Activation Products from Neutron Interaction with Structural Materials (continued)

Fusion Material	Alloy Elements (weight percent)	Major Activated Nuclides	Main Activation Reactions	Half-Life and Decay Mode	Activation Product Concerns: Safety: Radiolog. Hazard Potential	Safety: Decay Heat	Maintenance: Shutdown Dose Rate	Waste: Recycle and Disposal
Reduced	Fe	Fe55	Fe56(n,2n)	2.73y;ε	Low	Low	-	-
Activation	(88.0)	Mn54	Fe54(n,p)	312d;ε	Low	Low	Low	-
Ferritic		Mn56	Fe56(n,p)	2.58h;β-	-	Low	Low	-
Steel		Co60	Fe58(n,g)*	5.27y;β-	-	-	Low	-
(9CrWV)	Cr (8.94) Ni	Cr51	Cr50(n,g) Cr52(n,2n)	27.7d;ε	Low	Low	Low	-
	Mo (10ppm) V (0.25) Mn (0.44) Ta (777ppm)	Nb94	Mo94(n,p)	2.0×10^4y;β	-	-	-	Low
	W (1.97)	W185	W186(n,2n) W184(n,g)	75.1d;β	Low	Low	-	-
		Ta182	W182(n,p) W183(n,n'p)	114d;β	Low	Low	Low	-
		Hf178m2	W182(n,n'α)	31y;IT	Low	-	Low	Low
		W181	W182(n,2n) W180(n,g)	121d;ε	Low	-	-	-
		W187	W186(n,g)	23.7h;β-	Low	-	-	-
	Nb (<10ppm)	Nb94	Nb93(n,g)	2.0×10^4y;β-	-	-	-	Low

Table 2 page 6

D-T Fusion Activation Products from Neutron Interaction with Structural Materials (continued)

Fusion Material	Alloy Elements (weight percent)	Major Activated Nuclides	Main Activation Reactions	Half-Life and Decay Mode	Activation Product Concerns: Safety: Radiolog. Hazard Potential	Safety: Decay Heat	Maintenance: Shutdown Dose Rate	Waste: Recycle and Disposal
Inconel 625	Ni (62.0)	Co58	Ni58(n,p)	70.8d;ε	Low	Low	Low	-
		Co57	Ni58(n,n'p)	272d;ε	Low	Low	Low	-
		Co60	Ni60(n,p)	5.27y;β-	Low	Low	Low	-
	Cr (21.5)	Cr51	Cr50(n,g) Cr52(n,2n)	27.7d;ε	Low	Low	Low	-
	Nb (1.8)	Nb94	Nb93(n,g)	2.0×10^3y;β-	-	-	-	Low
		Nb92m	Nb93(n,2n)	10.15d;ε	Low	-	-	-
	Mo (8.99)	Nb94	Mo94(n,p) Mo95(n,n'p)	2.0×10^4y;β	-	-	-	Low
	Ta (1.8)	Ta182	Ta181(n,g)	114d;β	Low	Low	Low	-
	Fe (2.5)	Mn56	Fe56(n,p)	2.58h;β-	-	Low	Low	-
	Co (0.5)	Co60	Co59(n,g)	5.27y;β-	Low	-	-	-
	Mn (0.27)							
	Si (0.25)							
	Ti (0.25)							
	Al (0.2)							

Table 2 page 7

D-T Fusion Activation Products from Neutron Interaction with Structural Materials
(continued)

Fusion Material	Alloy Elements (weight percent)	Major Activated Nuclides	Main Activation Reactions	Half-Life and Decay Mode	Activation Product Concerns: Safety: Radiolog. Hazard Potential	Safety: Decay Heat	Maintenance: Shutdown Dose Rate	Waste: Recycle and Disposal
Ti-6Al-4V	Ti	Ca45	Ti48(n,α)	164d;β-	Low	-	-	-
	(90)	Sc48	Ti48(n,p)	43.7h;β-	-	Low	Low	-
		Sc46	Ti46(n,p)	83.8d;β-	Low	Low	Low	-
		Sc47	Ti47(n,p)	3.35d;β-	Low	Low	-	-
		Ar42(K42)	Ca45(n,α)	32.9y;β-	-	-	Low	Low
		Ca47	Ti50(n,α)	4.54d;β-	Low	-	-	-
	Al	Na24	Al27(n,α)	15h;β-	Low	Low	Low	-
	(6)	Al26	Al27(n,2n)	7.4×10^5y;ε	-	-	Low	Low
	V	Sc48	V51(n,α)	43.7h;β-	Low	Low	Low	-
	(4)	Sc47	V51(n,n'α)	3.35d;β-	-	Low	Low	-
		Sc46	V50(n,n'α)	83.8d;β-	-	Low	Low	-

*indicates multi-step neutron reactions to reach the final activation products.

Table 2 page 8

D-T Fusion Activation Products from Neutron Interaction with Structural Materials
(continued)

Fusion Material	Alloy Elements (weight percent)	Natural Isotopes (percent abundance)	Major Activated Nuclides	Main Activation Reactions	Half-Li and Decay Mode	Activation Product Concerns: Safety: Radiolog. Hazard Potential	Safety: Decay Heat	Maintenance: Shutdown Dose Rate	Waste: Recycle and Disposal
SiC	Si	Si28		Si28(n,n'p)Al27					
	(70)	(92.2)	Na24	Al27(n,α)	15h;β-	Low	Low	Low	-
			Al26	Al27(n,2n)	7.2×10^5y;ε	-	-	Low	Low
			Na22	Al27(n,n'α)*	2.6y;ε	-	-	Low	-
			Al28	Si28(n,p)	2.24m;β-	Low	Low	-	-
		Si29 (4.67)	Al29	Si29(n,p)	6.56m;β-	Low	Low	-	-
		Si30	Mg27	Si30(n,α)	9.46m;β-	Low	Low	-	-
		(3.10)	Mg28	Si30(n,He3)	20.9h;β-	Low	Low	Low	-
	C (30)								

*indicates multi-step neutron reactions to reach the final activation products.

Table 3
List of Neutron Reactions with Which there are Cross Sect' on Data Deficiencies for the Determination of Activation Concerns in Fusion Structural Materials

1. Fe58 (n,g) Fe59
   Needed for all iron-based structural materials. The energy range is from thermal to 1 MeV.

2. Cr50 (n,g) Cr51
   Needed for structural materials, such as 316SS and ferritic steel, containing significant amount of chromium. The energy range is from thermal to 1 MeV.

3. Ti50 (n,α) Ca47
   Needed for structural materials, such as vanadium-alloy and titanium-alloy, containing significant amount of titanium. This reaction is particularly important for early dose assessment. The energy range is from threshold to 14 MeV.

4. Ti48 (n,α) Ca45 and Ca45 (n,α) Ar42
   This 2-step reaction is important of V-5Ti-5Cr alloy. The energy range is from threshold to 14 MeV.

5. W (n,x) W181
   Production cross section for W181 from natural tungsten is needed for early dose analysis of the reduced activation ferritic steel. Two reactions are involved: W182 (n,2n) and W180 (n,g). The energy ranges are from threshold to 14 MeV, and from thermal to 1 MeV, respectively.

6. W186 (n,g) W187
   Production cross section for W187 from natural tungsten is needed for the reduced activation ferritic steel. The energy range is from thermal to 1 MeV.

7. Production cross sections for long-lived radioisotopes from alloying elements and impurities:

Ag109 (n,2n) Ag108m	Hf179 (n,2n) Hf178m2
Al27 (n,2n) Al26	Mo94 (n,p) Nb94
Cd108 (n,p) Ag108m	Mo98 (n,g) Mo99
Co59 (n,g) Co60	Ni (n,x) Ni59
Cu63 (n,p) Ni63	Ni (n,x) Ni63
Eu153 (n,2n) Eu152	Ni64 (n,n'α) Fe60
Eu151 (n,2n) Eu150m	Tb159 (n,2n) Tb158
Ho165 (n,g) Ho166m	W182 (n,n'α) Hf178m2

Energy ranges: (a) threshold reactions - from threshold to 14 MeV; (b) capture reactions - from thermal to 1 MeV.

Table 4

List of Neutron Activation Reactions
Whose Cross Sections are Considered Inadequate
(Reproduced from Ref. 3)

Ag-109(n,2n)Ag-108m; Ag-107(n,g)Ag-108m; Al-27(n,2n)Al-26;
Al-27(n,n'alpha)Na-23; Bi-209(n,g)Bi-210;
Bi-209(n,n'alpha)Tl-205; Tl-205(n,2n)Tl-204;
Ca-44(n,g)Ca-45; Ca-42(n,alpha)Ar-39; Ca-43(n,n'alpha)Ar-39;
Ca-40(n,2p)Ar-39; Co-59(n,g)Co-60; Cr-50(n,g)Cr-51;
Cu-63(n,p)Ni-63; Cu-65(n,t)Ni-63; Fe-58(n,g)Fe-59;
Fe-59(n,g)Fe-60; Fe-54(n,np)Mn-53; Hf-178(n,2n)Hf-177m;
Hf-177(n,g)Hf-178m2; Hf-179(n,g)Hf-180m; Hf-180(n,g)Hf-181;
Hg-204(n,2n)Hg-203; Tl-203(n,g)Tl-204; Hg-198(n,2n)Hg-197;
Hg-198(n,2n)Hg-197m; Hg-200(n,2n)Hg-199m; Hg-198(n,g)Hg-199m;
Hg-200(n,p)Au-200m; Hg-196(n,p)Au-196; Hg-196(n,n'p)Au-195;
Hg-196(n,alpha)Pt-193; Mg-25(n,np)Na-24; Mg-24(n,t)Na-22;
Mg-24(n,n'p)Na-23; Mg-26(n,g)Mg-27; Mo-95(n,p)Nb-95;
Mo-96(n,n'p)Nb-95; Mo-97(n,t)Nb-95; Mo-93(n,g)Mo-99;
Tc-99(n,2n)Tc-98; Tc-98(n,2n)Tc-97; Mo-92(n,alpha)Y-88;
Mo-92(n,g)Mo-93; Mo-94(n,2n)Mo-93; N-14(n,n'alpha)B-10;
Ni-60(n,t)Co-58; Ni-58(n,g)Ni-59; Ni-60(n,2n)Ni-59;
Ni-62(n,He-3)Fe-60; Ni-64(n,n'alpha)Fe-60; O-17(n,alpha)C-14;
O-18(n,n'alpha)C-14; Bi-209(n,2n)Bi-208; Pb-204(n,t)Tl-202;
Pb-206(n,alpha)Hg-203; Pb-207(n,n'alpha)Hg-203;
Pb-204(n,p)Tl-204; Pb-206(n,t)Tl-204; Re-185(n,g)Re186m;
Re-187(n,2n)Re-186m; Re-187(n,p)W-187; Re-187(n,alpha)Ta-184;
Re-185(n,alpha)Ta-182; Si-28(n,n'p)Al-27; Si-28(n,alpha)Mg-25;
Si-28(n,n'alpha)Mg-24; Ta-180(n,t)Hf-178m2; Ti-48(n,alpha)Ca-45;
Ti-46(n,n'alpha)Ca-42; V-50(n,n'alpha)Sc-46; V-51(n,t)Ca-45;
Sc-45(n,n'alpha)K-41; K-41(n,t)Ar-39; W-183(n,n'p)Ta-182;
W-184(n,t)Ta-182; W-182(n,n'alpha)Hf-178m2;
W-186(n,n'alpha)Hf-182; Zn-64(n,g)Zn-65; Zr-90(n,t)Y-88;
Zr-94(n,g)Zr-95; Zr-92(n,g)Zr-93; Zr-94(n,2n)Zr-93

Measurements of 14 MeV Neutron Cross-sections for the Production of Isomeric States in Hafnium Isotopes *)

B.H. Patrick, M.G. Sowerby, C.G. Wilkins and L.C. Russen

AEA Technology
Harwell
Didcot
Oxfordshire OX11 ORA
United Kingdom

*) presented by R.A. Forrest

1. Introduction

Fusion reactor systems operating on the (d,t) reaction will produce large numbers of neutrons which will, through nuclear reactions, produce activation products in material subjected to the neutron fluence. In particular, the irradiation by neutrons of the first wall of a power reactor system and structural materials in that vicinity could give rise to intense radioactivity. This is expected to result in radiation damage to the extent that the wall will probably have to be replaced every few years. There is clearly a great incentive to minimise the activity and the amount of radioactive waste generated. Also, if it can be reduced to a low level after a reasonable cooling time, the first wall material could be reused, with obvious economic benefits.

To address these problems the UK Fusion Programme initiated a search for suitable engineering materials for use in the first wall of a fusion power reactor. As activation would be an important criterion in selecting suitable elements, part of that Programme is devoted to the establishment of a nuclear data library and associated inventory code to enable activation to be calculated with sufficient accuracy. The neutron flux in a reactor will be such that sequential reactions in a given nucleus will be possible, driving the products well away from the stable region of the chart of the nuclides. For this reason, such a library must contain cross-sections for reactions in unstable isotopes as well as stable ones. To enable the search for low activity materials to be as comprehensive as possible, the nuclear data library also needs to be essentially complete; missing cross-sections could terminate a particular reaction path in calculations of activation, causing misleading conclusions to be reached regarding the suitability of some elements.

In studies of potential first wall materials, it was suggested that an alloy containing small quantities of tungsten and tantalum might have suitable activation properties. From an inspection of the chart of the nuclides in the region of these elements (see Figure 1) a possible problem was identified due to the presence of the 31-year isomeric state, ^{178m2}Hf. The production of significant numbers of nuclei in this state could lead to the first wall being active for many years, making reuse difficult to achieve and therefore raising a potential waste disposal problem. The situation is further complicated by the presence of a 25-day isomeric state, ^{179m2}Hf. This state could live long enough for an (n,2n) reaction to take place leading to the 31-year state in ^{178}Hf. This latter reaction is expected to have quite a high cross-section, consequently any ^{179m2}Hf formed would have a significant probability of being transformed into ^{178m2}Hf.

A search of the literature yielded no relevant measurements or theoretical calculations of cross-sections leading to the isomeric states in ^{178}Hf and ^{179}Hf, and the question then arose as to how reliable data could be derived. A solution to this problem came when the Lawrence Livermore National Laboratory (LLNL) offered to irradiate a package of materials, including tantalum, tungsten and hafnium, on the intense 14 MeV neutron generator, RTNS-II, to enable activation cross-sections to be measured.

2. Procedure

2.1 Sample Irradiation on RTNS-II

A package of 15 mm diameter foils of various materials was irradiated on the intense (d,t) neutron generator, RTNS-II, at LLNL in March 1987, on the x=0 axis close to the tritiated target. The accelerator produced 360 keV deuterons giving a maximum neutron energy of 15.6 MeV. The mean neutron energy was 14.8 MeV. The package was subjected to a fluence of about 10^{18} neutrons/cm^2 over a period of 11 days.

The materials consisted of one foil each of hafnium, tantalum, tungsten, titanium and a low-activation stainless steel, together with neutron fluence monitor foils of nickel, cobalt, gold, manganese and copper, the entire package being wrapped in thin aluminium foil. The package was approximately 6 mm thick, so that there was a significant flux gradient from front to back. Details of the materials are given in Table 1. The monitor foils were chosen because under irradiation by 14 MeV neutrons they produce, with accurately known cross-sections, γ-ray emitting isotopes with suitable half-lives. The package was to be returned to the UK after irradiation and as it was not clear how long shipment would take, short half-lives were ruled out as inappropriate. Care was taken to prevent any possibility of cross-contamination of the foils for which cross-sections were to be measured by ensuring that the foils of these materials were sandwiched between monitor foils.

As an independent check on the fluence, niobium foils were placed on the front and back of the package during the irradiation. The activity in these was measured at LLNL before the package was returned to the UK and the estimated neutron fluences were found to be in agreement with subsequent measurements using the monitor foils (see Section 4.1).

The time distribution of the neutron fluence during the 11-day irradiation period was measured at LLNL by recording the counts at regular intervals in a fission chamber placed some distance from the package. This enabled corrections to be made for decay of activation during the irradiation.

2.2 Measurement of Foil Activity

The activity of each foil was determined at intervals over a period of time using a Ge(Li) detector connected to a 4096-channel pulse height analyser system. The resulting (dead-time corrected) spectra were stored on a local VAX computer from which they were transferred to an IBM-PC compatible computer for subsequent data analysis.

The detector was mounted inside a lead castle into which the foil samples were placed for measurement. The distance of a foil from the detector was varied depending upon its activity to achieve a suitable count rate. The detector efficiency as a function of γ-ray energy had already been determined using standard sources mounted at 75 mm from the detector. When used with a foil

mounted at a distance other than this, an inverse square correction was applied to the efficiency data.

Detector energy calibration was carried out prior to spectrum collection using standard sources but, as will be explained in Section 3.2, independent energy (and resolution) calibration was carried out during later analysis of the spectra using the γ-ray lines produced by the foil samples.

3. Data Analysis

3.1 Spectrum Analysis

The stored spectra were analysed using the SABRE software package[1]. This suite of programs works by identifying γ-ray peaks in a spectrum. The intensity (I) or area of a given peak above the continuum background is proportional to the activity (a) of the isotope responsible according to the following expression:

$$a = \frac{I}{\varepsilon B} \quad Bq \qquad (1)$$

where:

ε = the efficiency of the detector at the energy of the γ-ray peak

B = the fractional abundance of the γ-ray line from the isotope

The SABRE software uses a peak search algorithm to locate all peaks above a predetermined threshold, determines the energy of the peak, its area and width. A gaussian fit is performed on each peak located in the spectrum to determine these three parameters; this technique even enables overlapping peaks to be measured.

3.2 Isotope Determination

Isotope identification is carried out with reference to a comprehensive γ-ray library. This computerised catalogue of γ-ray isotope lines is based on the GAMDAT-78 library[2]. It contains 2000 γ-emitting isotopes and lists over 12000 γ-ray energies. In the SABRE package there are two programs which use different approaches to carry out this type of analysis. The first of these, SPAN (SPectrum Analysis of unknown Nuclides), makes a general search of the γ-ray library for each peak it finds in the spectrum. Certain constraints may be applied to the candidate isotopes (e.g. half-life lower limit, atomic mass range etc.) but apart from this no other assumptions about the isotopes present are made. SPAN was therefore found to be useful when analysing the early sample foil spectra which contained large numbers of unknown γ-emitting isotopes.

The other program, SPIC (SPectrum analysis of Identified Components), performs a library directed search for peaks in a γ-ray spectrum. This was found to be most useful for analysing spectra for which the main isotopes present were well known. It works from a list of the isotopes of interest; each peak found is then compared against library entries for these few isotopes.

Both SPIC and SPAN require an energy calibrated γ-ray spectrum. The SABRE program, ENCAL, determines the calibration function. A rough energy calibration for the detector was carried out using standard sources (^{133}Ba, ^{57}Co, ^{60}Co and ^{54}Mn). ENCAL was used to obtain a more accurate calibration for each of the foil spectra in turn. Using the rough calibration as a starting point it searched the foil

spectrum for γ-ray peaks known to be present, and used these to determine the energy calibration. ENCAL also determined the resolution calibration (peak width versus energy) using all peaks in the spectrum; the resolution as a function of energy is used to help carry out the peak fitting in SPIC and SPAN.

Having located a peak in an energy (and resolution) calibrated spectrum, SPIC and SPAN calculate, for each candidate isotope assigned to the peak, the amount of the isotope present (expressed as an activity) using equation (1). When more than one isotope has been assigned to a given peak, selection of the correct one is often possible by looking for the presence of other γ-ray lines emitted by those isotopes (if they exist). Because each foil had been measured a number of times at intervals since the irradiation, confirmation of the identity of candidate isotopes could also be performed by determining the half-life from the rate of decay of the activity calculated from peaks in successive spectra.

This method was also used to combine the results of the successive measurements to obtain a more accurate overall determination of the activity of the isotope originally produced; a weighted least squares fit was performed on the activity versus time data to determine the activity produced at the time of the irradiation.

3.3 Fluence Determination

The neutron fluence was determined from measurements on the monitor foils of the activity of specific reaction products, the production cross-sections for which are well known. As detailed in Section 3.2, the amount of each reaction product in a given foil at the end of the irradiation was calculated from the successive measurements made on the foil by least squares fit and extrapolation.

Because the irradiation took place over a prolonged period (11 days) a correction was made for decay during the irradiation. Knowing the relative intensity of the neutron beam as a function of time throughout the irradiation (from half-hourly fission chamber measurements) it was possible to calculate in each half hour period, how much of a given isotope produced would have decayed (from knowledge of its half-life). Successive calculations of this kind were summed over the entire irradiation period to calculate the fraction that would have decayed by the end of the irradiation.

Having made the decay correction it was possible to calculate the neutron fluence (F) seen by each foil from the expression:

$$F = \frac{kaA}{mN\sigma} \qquad (2)$$

where:

k	=	a (known) constant
a	=	the activity of the reaction product isotope, calculated at the end of the irradiation
σ	=	the cross-section for the reaction producing the isotope
N	=	Avogadro's number
A	=	atomic mass of the target isotope
m	=	mass of the target isotope in the sample

To obtain the neutron fluence seen by each sample foil, the mean of the fluences seen by the two adjacent monitor foils was used.

3.4 Cross-Section Determination

Having determined the neutron fluence measured by the monitor foils, a similar method was used to calculate the cross-sections for the reactions producing the isotopes seen in the sample foils. As for the monitor foils, all isotope activities were extrapolated back to the time of the end of the irradiation from the several measurements that had been made on the foils. The same correction was made for decay during the period of the irradiation. The production cross-section was then calculated using the inverse of equation (2):

$$\sigma = \frac{kaA}{mNF} \qquad (3)$$

It should be noted that, as natural elements were used in the experiment, it is not strictly possible to obtain unique cross-sections in many cases as there are a number of reactions which could lead to the production of a given isotope. However, using a priori knowledge of 14-MeV cross-sections and being guided by theory, it is sometimes found that one cross-section dominates the route to a particular activity and it has been assumed that all the activity arises from this reaction.

3.5 Self-Absorption Correction

In addition to the correction for decay of the reaction product isotopes during the irradiation of the foils, a further correction factor was applied to the thicker foils (thicknesses 1 mm and above) to take into account the attenuation of the emitted γ-rays within the foil material. This (γ-ray energy dependent) correction factor is as follows:

$$C.F. = \frac{\ln T(E)}{1 - T(E)} \qquad (4)$$

where:

$T(E) = e^{-\mu x}$

and:

E = the γ-ray energy

μ = the linear absorption coefficient for the foil material (at energy E)

x = the foil thickness

The linear absorption coefficient for the foil material in question was obtained from standard data tables[3].

4. Results

4.1 Neutron Fluence Measurements

Table 2 shows the reactions in the monitor foils that were used to determine the neutron fluence. Nickel was the primary monitor material; the fluence results obtained from the 9 nickel foils distributed throughout the package were those used in all subsequent calculations of cross-sections in the main sample foils. The fluence measurements from thee other monitor materials were used simply as a check on the nickel results.

The fluence results are given in Table 3(a) and plotted as a function of position in the foil package in Figure 2. As expected, they show a gradual reduction in the fluence from the front to the back of the package. The results from the other monitor foils, including the two external niobium foils, generally agree with the nickel measurements.

To determine the fluence seen by a particular sample foil, the mean of the fluences measured by its two neighbouring monitor foils was used. Table 3(b) lists the fluence value used for each sample foil in the package.

4.2 Hafnium Foil Measurements

The activity of the hafnium foil was dominated for the first year after irradiation by the decay of ^{179m2}Hf and of ^{175}Hf (half-lives 25 days and 70 days respectively). Only after this activity had largely decayed away did the γ-rays from the 31-year isomeric state, ^{178m2}Hf begin to show clearly. Figure 3 shows a spectrum taken several weeks after the irradiation and Figure 4 is one taken two years later. Note particularly the spectra in the region 500-650 keV. In the earlier one, there is virtually no sign of peaks, while in the later one several peaks from the decay of ^{178m2}Hf are prominent.

Table 4(a) lists all of the significant γ-emitting isotopes identified in the 10 hafnium foil spectra that were taken. Some of these (^{95}Zr and ^{95}Nb) originated from reactions involving impurities in the foil samples and others were due to cross-contamination from neighbouring (nickel monitor) foils, in spite of the precautions taken. Cross-section results for reactions involving hafnium are given in Table 4(b). In deriving these, it has been assumed that the following cross-sections are zero at a mean neutron energy of 14.8 MeV:

$$^{178}\text{Hf}(n,n')^{178m2}\text{Hf}$$
$$^{178}\text{Hf}(n,\gamma)^{179m2}\text{Hf}$$
$$^{179}\text{Hf}(n,n')^{179m2}\text{Hf}$$

Cross-sections for the production of high-spin states arising from 14-Mev neutron-induced reactions in hafnium have been calculated by Chadwick and Young[4] using pre-equilibrium and compound nucleus theories. Considering the difficulties involved in doing the calculations and the assumptions which had to

be made, the agreement is remarkably good, as shown in Table 4(b).

4.3 Tungsten Foil Measurements

Table 5(a) lists the γ-emitting isotopes seen in the tungsten foil during the 9 measurements made on it since irradiation. Again, a number of these were due to cross-contamination by neighbouring nickel foils. Table 5(b) gives the cross-sections calculated for the tungsten activation products. Two possible reactions were identified as the potential source of both ^{182}Ta and ^{185}W. Because it was not possible to say whether, in these cases, a particular reaction dominated, cross-sections are given assuming that the stated reaction is solely responsible.

The isotope ^{178m2}Hf was not seen in any of the tungsten spectra, from which fact it was possible to put the upper limit of 9.7 μb to the reaction:

$$^{182}W(n,n\alpha)^{178m2}Hf$$

4.4 Tantalum Foil Measurements

Table 6 gives the results for the tantalum foil. Only two isotopes were seen in this sample and both of these were probably produced from reactions involving ^{181}Ta. The cross-section for the ^{181}Ta(n,p) reaction is given in the table.

4.5 Titanium Foil Measurements

Table 7(a) lists the isotopes seen in the titanium foil. All apart from one of these were due to contamination by the neighbouring nickel foil. As shown in Table 7(b), two possible reactions could have produced the ^{46}Sc. As in the case of the tungsten foil reactions, cross-sections are quoted in each case assuming a single production route.

4.6 Stainless Steel Foil Measurements

The results for the stainless steel foil are given in Tables 8(a) and 8(b). Cross-contamination of ^{46}Sc is seen originating from the titanium foil, which was immediately in front of the stainless steel foil in the sample package. Of the two isotopes produced by reactions in the steel constituents, the ^{54}Mn could arise from either of two reactions. Again, cross-sections are quoted assuming a single production route.

5. Conclusions

A comparison of the measured cross-sections with the corresponding theoretical ones shows a very good level of agreement. To calculate these small isomeric cross-sections to within a factor of about two compared with the measurements has to be viewed as remarkably satisfactory and provides some degree of confidence that such calculations can be used to obtain cross-section data of this type for improving fusion cross-section files.

6. Acknowledgements

The authors are grateful for the support of the UKAEA/EURATOM Fusion Association Programme while carrying out this work. They also wish to place on record their deep appreciation for the facilities provided by the Lawrence Livermore National Laboratory in irradiating the samples on RTNS-II. In particular, the co-operation of Dr D Heikkinen is gratefully acknowledged. Without their generous assistance, this experiment would still be a dream.

References

(1) Colvin, G G. Gamma ray analysis for Super-SABRE, a user's guide. Environmental and Medical Sciences internal report. July 1989.

(2) Erdtmann G and Soyka W. The radio-nuclide gamma-ray data file 'GAMDAT-78'. ISSN 04-769 (1978)

(3) Veigele, W J. Photon cross-sections from 0.1 keV to 1 MeV for elements Z=1 to Z=94. Atomic Data Tables 5 (1973) p.51-111.

(4) Chadwick M B and Young P G. Calculations of the Production Cross Sections of High-Spin Isomeric States in Hafnium. Nucl Sci and Eng 108 (1991) 117.

Table 1

Details of materials irradiated on RTNS-II

The foils, 15 mm diameter, were packaged in the order shown, sample number 1 being nearest to the neutron target.

Sample No.	Material	Thickness (mm)	Mass (g)
1	Ni	0.01	0.016
2	Cu	1.10	0.154
3	Au	0.005	0.017
4	Ni	0.01	0.015
5	Co	0.01	0.018
6	Mn/Ni*	0.05	0.060
7	Ni	0.01	0.016
8	Hf	1.00	2.386
9	Ni	0.01	0.017
10	W	1.00	3.170
11	Ni	0.01	0.016
12	Ta	1.00	2.884
13	Ni	0.01	0.015
14	Ti	0.10	0.075
15	SS**	0.14	0.188
16	Ni	0.01	0.016
17	Mn/Ni*	0.05	0.063
18	Co	0.01	0.018
19	Ni	0.01	0.016
20	Au	0.005	0.017
21	Cu	0.10	0.154
22	Ni	0.01	0.014

* 88% Mn, 12% Ni
** stainless steel

Table 2

Monitor Foils - Reactions Used

Foil Material			
Nickel	^{58}Ni	(n,p)	^{58}Co
	^{58}Ni	(n,pn)	^{57}Co
	^{60}Ni	(n,p)	^{60}Co
Copper	^{63}Cu	(n,α)	^{60}Co
Gold	^{197}Au	(n,2n)	^{196}Au
Cobalt	^{59}Co	(n,p)	^{59}Fe
	^{59}Co	(n,2n)	^{58}Co
Manganese	^{55}Mn	(n,2n)	^{54}Mn

Table 3

(a) Monitor Foils - Fluence Measurements

Nickel Foil Number	Measured Neutron Fluence (n/cm^2)
1	1.016×10^{18}
2	1.038×10^{18}
3	9.360×10^{17}
4	6.885×10^{17}
5	5.996×10^{17}
6	5.673×10^{17}
7	4.817×10^{17}
8	5.053×10^{17}
9	5.550×10^{17}

(b) Sample Foils - Fluence Values Used

Material	Neutron Fluence (n/cm^2)	Position of Material
Hafnium	$(8.12 \pm 0.57) \times 10^{17}$	Between Ni foils 3&4
Tungsten	$(6.44 \pm 0.45) \times 10^{17}$	Between Ni foils 4&5
Tantalum	$(5.83 \pm 0.41) \times 10^{17}$	Between Ni foils 5&6
Titanium	$(5.39 \pm 0.38) \times 10^{17}$	Between Ni foil 6 & SS
Stainless Steel (SS)	$(5.10 \pm 0.36) \times 10^{17}$	Between SS & Ni foil 7

Table 4

(a) Hafnium Foil - Gamma-emitting Isotopes

Isotope	Likely Origin
^{175}Hf	$^{176}Hf(n,2n)^{175}Hf$
$^{178m2}Hf$	$^{177}Hf(\bar{n},2\bar{n})^{178m2}Hf$
$^{179m2}Hf$	$^{180}Hf(n,2n)^{179m2}Hf$
^{173}Lu	$^{174}Hf(n,2n)^{173}Hf \rightarrow {}^{173}Lu$
^{95}Zr	from Zr impurity in Hf foil
^{95}Nb	decay product of ^{95}Zr
^{58}Co	} contamination from Ni foil
^{54}Mn	
^{60}Co	

(b) Hafnium Foil Reaction Cross-Sections

Reaction	Measured Cross-section (b)	Theoretical Cross-sections[4] (b)
$^{176}Hf(n,2n)^{175}Hf$	2.25 ± 0.25	
$^{179}Hf(n,2n)^{178m2}Hf$) $^{178}Hf(n,n')^{178m2}Hf$)	(6.75 ± 0.80) x 10^{-3}	2.95 x 10^{-3}
$^{180}Hf(n,2n)^{179m2}Hf$) $^{179}Hf(n,n')^{179m2}Hf$)	(2.92 ± 0.35) x 10^{-2}	1.31 x 10^{-2}

Table 5

(a) Tungsten Foil - Gamma-emitting Isotopes

Isotope	Likely Origin
^{181}Hf	^{184}W(n,α)^{181}Hf
^{182}Ta	^{182}W(n,p)^{182}Ta
	or ^{183}W(n,pn)^{182}Ta
^{185}W	^{186}W(n,2n)^{185}W
	or ^{184}W(n,γ)^{185}W
^{57}Co	} contamination from Ni foil
^{58}Co	
^{60}Co	
^{54}Mn	
^{59}Fe	

(b) Tungsten Foil Reaction Cross-Sections

Reaction	Cross-section (b)
^{184}W (n,α) ^{181}Hf	(1.02 ± 0.12) x 10^{-3}
^{182}W (n,p) ^{182}Ta	(7.21 ± 0.87) x 10^{-3} *
^{183}W (n,pn)^{182}Ta	(1.33 ± 0.16) x 10^{-2} *
^{186}W (n,2n) ^{185}W	1.77 ± 0.21 *

* Assumes this reaction is the only one responsible for the production of the measured isotope

Table 6

(a) Tantalum Foil - Gamma-emitting Isotopes

Isotope	Likely Origin
^{181}Hf	^{181}Ta (n,p) ^{181}Hf
^{182}Ta	^{181}Ta (n,γ) ^{182}Ta

(b) Tantalum Foil Reaction Cross-Sections

Reaction	Cross-section (b)
^{181}Ta (n,p) ^{181}Hf	$(4.20 \pm 0.50) \times 10^{-3}$

Table 7

(a) Titanium Foil - Gamma-emitting Isotopes

Isotope	Likely Origin
^{46}Sc	^{46}Ti (n,p) ^{46}Sc
	or ^{47}Ti (n,pn) ^{46}Sc
^{57}Co	} contamination from Ni foil
^{58}Co	
^{60}Co	
^{54}Mn	

(b) Titanium Foil Reaction Cross-Sections

Reaction	Cross-section (b)
^{46}Ti (n,p) ^{46}Sc	0.27 ± 0.03 *
^{47}Ti (n,pn) ^{46}Sc	0.31 ± 0.04 *

*Assumes this reaction is the only one responsible for the production of the measured isotope

Table 8

(a) Stainless Steel Foil - Gamma-emitting Isotopes

Isotope	Likely Origin
^{51}Cr	^{52}Cr (n,2n) ^{51}Cr
^{54}Mn	^{54}Fe (n,p) ^{54}Mn
	or ^{55}Mn (n,2n) ^{54}Mn
^{46}Sc	contamination from Ti foil

(b) Stainless Steel Foil Reaction Cross-Sections

Reaction	Cross-section (b)
^{52}Cr (n,2n) ^{51}Cr	0.42 ± 0.05
^{54}Fe (n,p) ^{54}Mn	0.41 ± 0.05 *
^{55}Mn (n,2n) ^{54}Mn	2.60 ± 0.31 *

* Assumes this reaction is the only one responsible for the production of the measured isotope

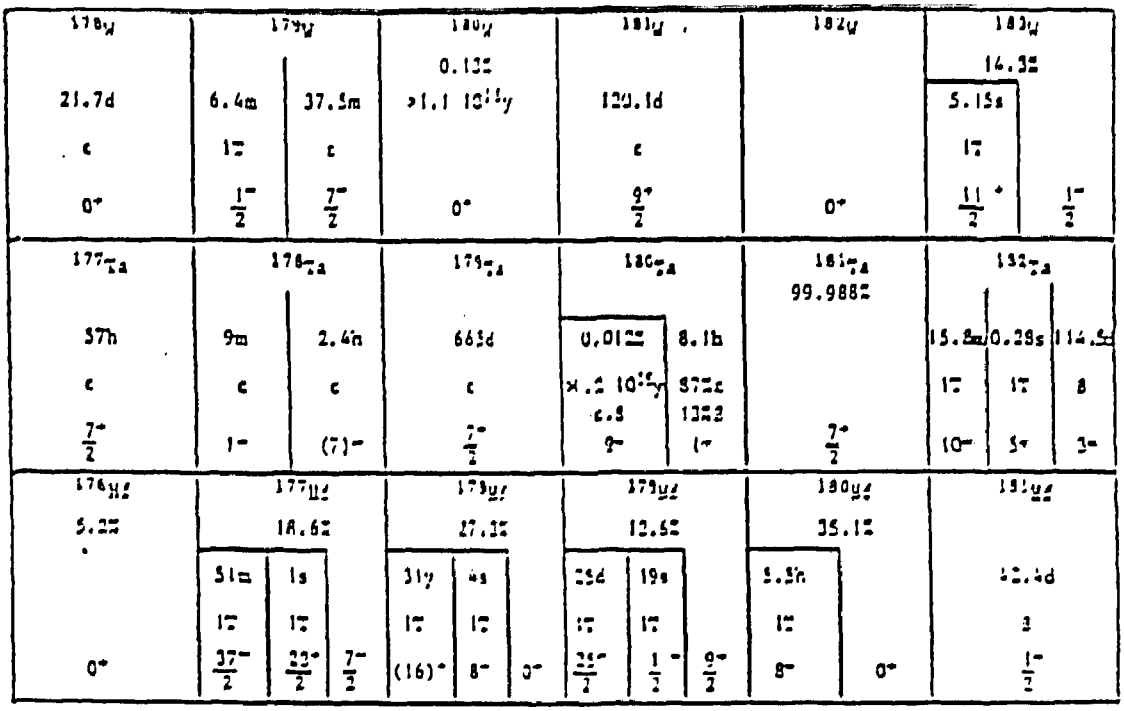

Fig 1. The chart of the nuclides in the region of tungsten, tantalum and hafnium.

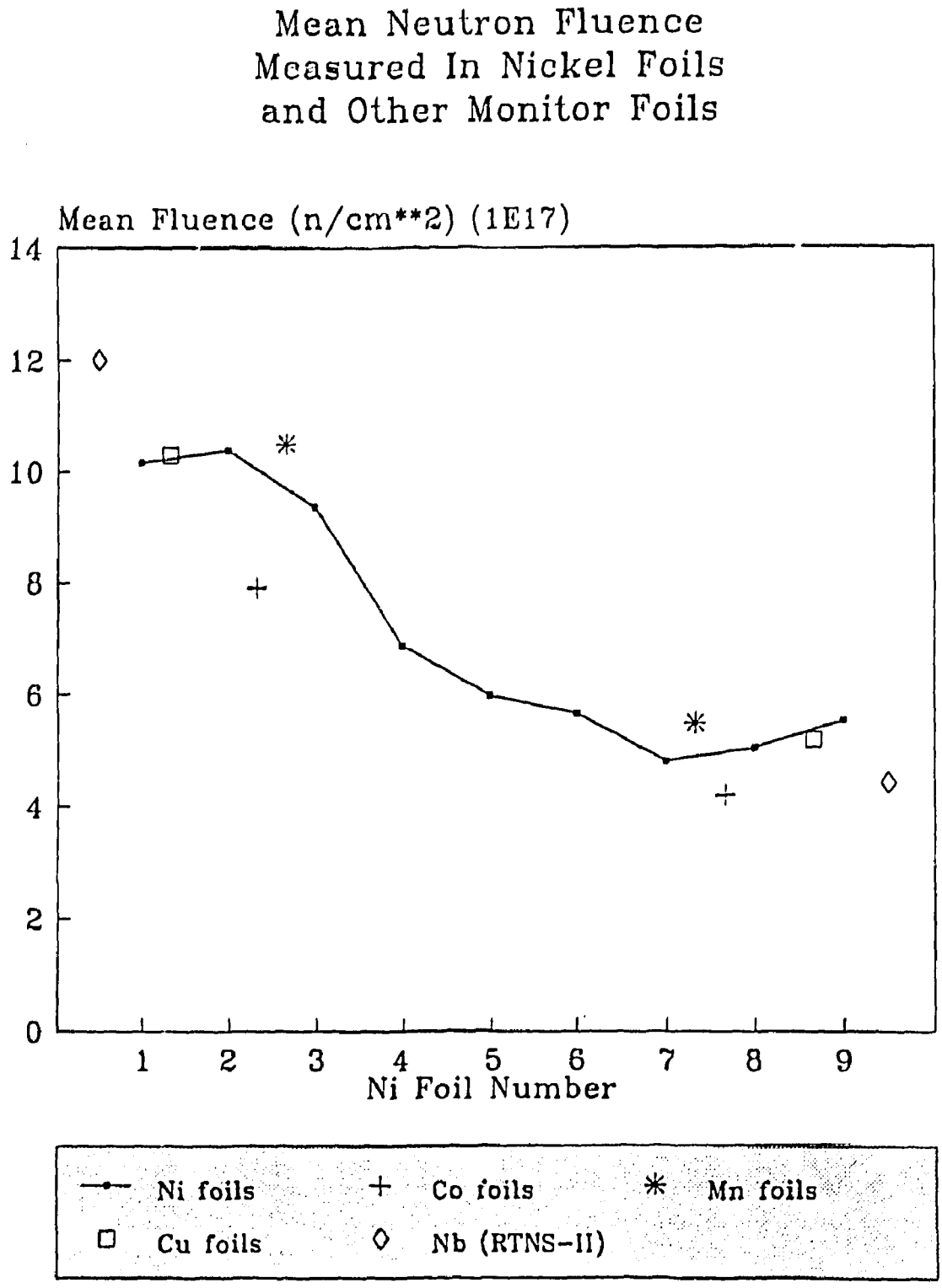

Fig 2. Mean neutron fluences measured with Ni, Co and Mn monitor foils

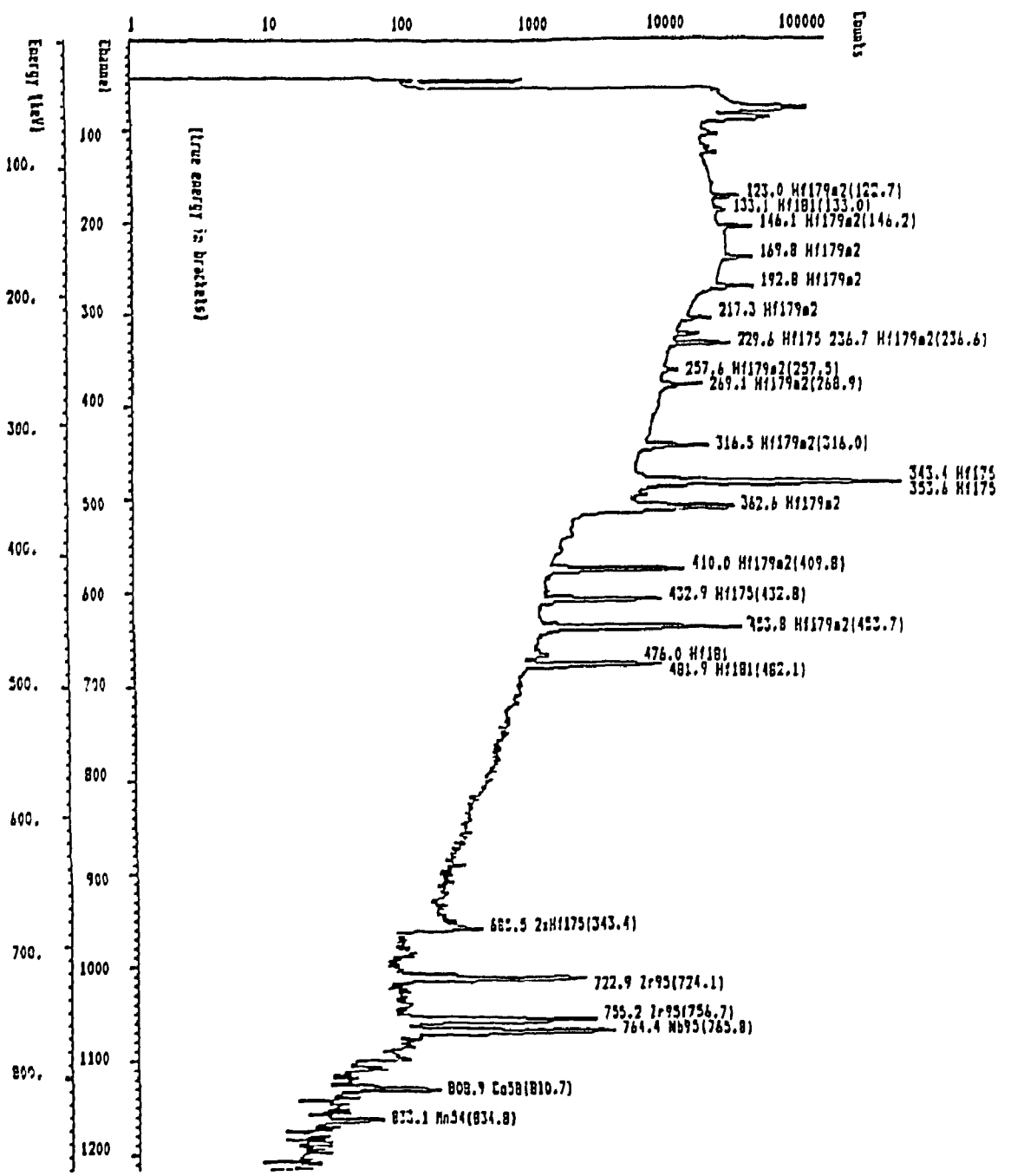

Fig 3. Hafnium foil spectrum taken six weeks after irradiation

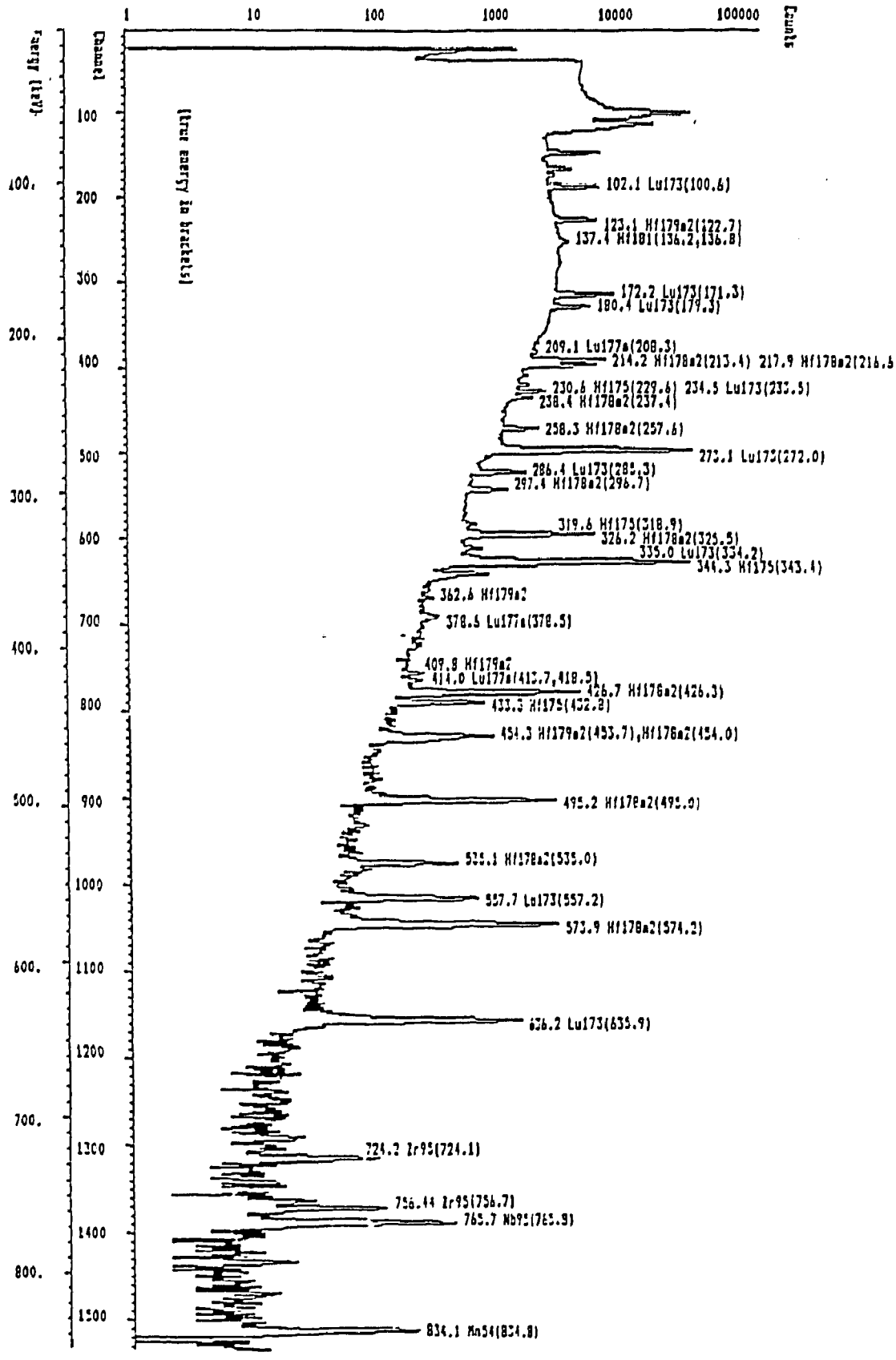

Fig 4. Hafnium foil spectrum taken two years after irradiation

Nuclear Data Section
International Atomic Energy Agency
P.O. Box 100
A-1400 Vienna
Austria

e-mail, INTERNET: SERVICES@IAEAND.IAEA.OR.AT
e-mail, BITNET: RNDS@IAEA1
fax: (43-1) 20607
cable: INATOM VIENNA
telex: 1-12645 atom a
telephone: (43-1) 2060-21710

online: TELNET or FTP: IAEAND.IAEA.OR.AT
username: IAEANDS for interactive Nuclear Data Information System
username: NDSOPEN for FTP file transfer